NEUROPHYSIOLOGICAL INVESTIGATION OF THE LATERAL PREFRONTAL CORTEX DURING THE TASK OF BINOCULAR FLASH SUPPRESSION

Dissertation

zur Erlangung des Grades eines

Doktors der Naturwissenschaften

der Mathematisch-Naturwissenschaftlichen Fakultät

und

der Medizinischen Fakultät

der Eberhard-Karls-Universität Tübingen

vorgelegt

von

Vishal Kapoor
aus New Delhi, India.

December - 2015

Tag der mündlichen Prüfung: 12th July 2016

Dekan der Math.-Nat. Fakultät: Prof. Dr. W. Rosenstiel

Dekan der Medizinischen Fakultät: Prof. Dr. I. B. Autenrieth

1. Berichterstatter: Prof. Dr. / PD Dr. / Dr. Nikos K. Logothetis

2. Berichterstatter: Prof. Dr. / PD Dr. / Dr. Andreas Bartels

3. Berichterstatter: Prof. Dr. / PD Dr. / Dr. Frank Bremmer

Prüfungskommission: Prof. Dr. Nikos K. Logothetis

Prof. Dr. Uwe Ilg

Prof. Dr. Laura Busse

Dr. Andreas Bartels

Erklärung / Declaration:

Ich erkläre, dass ich die zur Promotion eingereichte Arbeit mit dem Titel:

„ Neurophysiological investigation of the lateral prefrontal cortex during the task of binocular flash suppression “

selbständig verfasst, nur die angegebenen Quellen und Hilfsmittel benutzt und wörtlich oder inhaltlich übernommene Stellen als solche gekennzeichnet habe. Ich versichere an Eides statt, dass diese Angaben wahr sind und dass ich nichts verschwiegen habe. Mir ist bekannt, dass die falsche Abgabe einer Versicherung an Eides statt mit Freiheitsstrafe bis zu drei Jahren oder mit Geldstrafe bestraft wird.

I hereby declare that I have produced the work entitled “Neurophysiological investigation of the lateral prefrontal cortex during the task of binocular flash suppression”, submitted for the award of a doctorate, on my own (without external help), have used only the sources and aids indicated and have marked passages included from other works, whether verbatim or in content, as such. I swear upon oath that these statements are true and that I have not concealed anything. I am aware that making a false declaration under oath is punishable by a term of imprisonment of up to three years or by a fine.

Tübingen, den ....

Datum / Date Unterschrift /Signature

To badi mummy and nani ma, my grandmothers.

“If we ever reach the point where we think we thoroughly understand who we are and where we came from, we will have failed.”

Carl Sagan

Acknowledgements

‘My predominant feeling is one of gratitude’, wrote a kind soul Oliver Sacks on learning about his terminal cancer shortly before he passed away this year. My doctoral endeavor has been neither so grandiose, nor towards an end so grim. Nevertheless, it’s the feeling that consumes my mind at this moment of my life.

First and foremost I would like to thank my family. To my parents, you provided me with moral capacity, and taught me right from wrong. You gave me wings and the freedom of thought and feet, which kept me grounded to reality, a lesson, I found immensely valuable in my scientific journey.

I am especially grateful to my supervisor, Theofanis Panagiotaropoulos. Thank you for your invaluable guidance and advice through many years of my PhD research. Our collaboration was a great learning experience, teaching me the many details of scientific inquiry. Many thanks for the innumerable thoughtful and critical scientific discussions, and I shall always admire your patience with my endless questions. I experienced through this journey many hurdles, but I am glad that they could be overcome with your support.

I owe a deep sense of gratitude to Nikos Logothetis. Your infectious enthusiasm for science along with your relentless belief and support for pursuing scientific ambition made graduate research in this lab a truly wonderful experience. When I came here for an interview, I couldn’t meet you, but was told, ‘this is a place, where the only limitation is your own imagination’. As a boy travelling from thousands of kilometers away, it was a dream come true, when given an opportunity of pursuing a degree in such a laboratory. And in so many years of being here, it has been an unforgettable journey worthy of a book. And I believe that I have experienced what I heard the first time, I stepped into this building. Thank you for giving me this possibility and for making this a place for what it is, where flying creative imagination evolves into scientific reality.

I would also like to sincerely thank my committee members, Uwe Ilg and Andreas Bartels for their encouragement, time and valuable critique.

I am grateful to the scientific colleagues who also became friends and shared with me, not only their scientific critique but also the innumerable discussions about scientific life and beyond. I would especially like to thank Abhilash Dwarakanath, Ahalya Viswanathan, Ann-Catherine Zappe, Carsten Klein, Catherine Perrodin, Daniel Zaldivar, Elvira Fischer, Esther Florin, Frederico Azevedo, Hamed Bahmani, Kevin Whittingstall, Leonardo Azevedo, Mar Ubero, Masataka Watanabe, Michael Ortiz, Natalia Zaretskaya, Oxana Eschenko and Shervin Safavi. I would especially like to thank Michel Besserve for his guidance during the last period of my PhD work. The staff at the Department of physiology of cognitive processes was incredibly supportive and helpful, and my special thanks to Axel Oeltermann, Conchy Moya, Eduard Krampe and Joachim Werner. To my friends in Tuebingen and beyond, Ali, Amit, Anurag, Akshay, Ankita, Ashutosh, Avneesh, Gautam, Kirti, Manish, Mohit, Vikram, Varuna, Varun, Vishnu, the moments filled with laughter spent along your side kept me sane through difficult times. I would especially like to thank Roosa, for her love, support and advice on science and life.

And for the macaques, I cannot express enough gratitude for their irreplaceable sacrifice. Without them, such research would not see the light of the day and I solemnly vow to continue as before, to treat them with utmost respect, and care.

Finally, the scientific endeavor, although many a times a solitary journey is taken with maps meticulously cartographed by a generation of researchers through their scholarly work. It's on their shoulders; we stand with hope to peek at the road further ahead. To all of them, thank you for your toil and hardship in the physical and the mental laboratory and passing to the future, among others that one thing which gives true meaning to this life; the gift of knowledge.

To end, I sincerely apologize, in case I might have forgotten someone either due to the urgency of finalizing this thesis or the lapses of the very organ, I wish to understand. Thank you everybody, who participated with me in this journey.

CONTENTS

Abbreviations

BFS – Binocular Flash Suppression

BOLD – blood oxygen level dependent

FS – Flash Suppression

GFS – generalized flash suppression

LPFC – Lateral Prefrontal Cortex

LFP – Local Field Potential

MUA – Multi Unit Activity

NNMF – non negative matrix factorization

PSTH – peri stimulus time histogram

TuTe – Tube Tetrode

Abstract

Multistable visual phenomena, wherein unchanging sensory input elicits in an observer, perceptual fluctuations, have been instrumental in unravelling the neural correlates of conscious perception. Such paradigms, when combined with single unit recordings in macaques trained to report their perception, have allowed neurophysiologists to elucidate, if the cells in various regions of the brain are correlated with subjective experience or respond to the invariant retinal input. Results obtained from such an approach has so far revealed that the proportion of feature selective cells which fire in concordance with perception, increase as one progresses in the ventral visual pathway, with this fraction being up to 90% in the temporal lobe.

The next station in the ventral stream of vision is the lateral prefrontal cortex (LPFC), which has reciprocal connectivity with the inferotemporal cortex and displays responses which are selective for complex visual stimuli. However, it's not clear if this feature selective neural activity is just the result of sensory input or is related to subjective perception. Utilizing the task of binocular flash suppression (BFS), a psychophysical paradigm capable of dissociating perception from the retinal message, we probed the neural responses in the LPFC. The results revealed a robust perceptual modulation of both the spiking activity as well as high frequency gamma oscillations in this region of the brain. Even though single unit activity is robustly modulated according to perceptual content, a measure of effective functional connectivity between pairs of neurons, such as correlated variability could be revealing of interactions among neuronal populations during visual ambiguity. We therefore computed the spike count correlations across pairs of simultaneously recorded neurons during subjective visual perception. Interestingly, such interneuronal correlations among single units which preferred the same stimulus were close to zero during incongruent visual input, thus reflecting a modulation of the correlation structure during visual perception. Simulations with biophysically realistic networks suggested that the source of decorrelation was an active suppression of input fluctuations. This suggests that

such a decorrelated state might be critical for representation of conscious content during visual conflict.

These results together provide credence to the 'frontal lobe hypothesis' proposed by Crick and Koch, which suggested that the planning stages of the brain must have explicit access to the conscious visual percept so as to direct motor output. Such access is essential, if the LPFC needs to carry out one of its major function which is of cognitive control. Interestingly, when a control related signal, namely the modulation pattern of the beta band oscillations in the LPFC was analyzed, its modulation pattern was unchanged not only across monocular and incongruent visual stimulation but also during perceptual dominance and suppression. This suggests that a signal which is related to control processes is unaffected by local conscious or unconscious neural processing.

Lastly, we observed an enormous diversity among the patterns of single unit activity recorded in the LPFC and the neurons which displayed visual preference were just a minority. In order to elucidate, if there were any other patterns of activity which were related to the task, we clustered the neuronal responses using a non-negative matrix factorization (NNMF) method. This revealed five sequential dominant response patterns (or components) whose peaks were temporally distributed across various phases of the trial. A majority of the units with firing profiles similar to the patterns obtained, maintained their responses across monocular or incongruent stimulation suggesting that visual conflict did not affect their spiking modulation. Interestingly, an assessment of the effective functional connectivity across the pairs of neurons belonging to different temporally distributed components revealed that such correlated variability was maximum among units which were temporally coincident. However, we observed successive decorrelation as the pairs of units were chosen from temporally separated populations. This suggests a computational principle mediating a representation of sequential patterns of activity in the LPFC.

Together, the results presented in this thesis suggest a role for the LPFC in representation of conscious content. At the same time, we find that such a role of this

region is coexistent with other major functions typically attributed to this area, such as cognitive control or temporal encoding of task events through sequential neural activity.

1

Introduction

Earliest signs of life known to man on planet earth can be dated to 3.5 to 3.8 billion years ago (Awramik 1992, Schopf 1993, Mojzsis, Arrhenius et al. 1996). Thenceforth, evolution has been remarkable and guided life to develop from a simple primordial form to multicellular, self-reflecting, conscious social beings (Darwin 1859, Theobald 2010). An important property of life is its ability to detect and thus respond to environmental stimuli or cues. No matter the scale or cellular complexity of an organism, each one must interact with its environment (by environment here, I also include other members of the species). Among the earliest forms of such an interaction is phototaxis, which may be defined as displacement along a light vector or gradient, either towards the source of the light or away from it (Jekely 2009). The bridge from phototaxis to a phenomenon such as visual perception however remains unclear. When and why in the course of evolution, a motor action dependent on the detection of photons changed to interpretation and experiential qualia associated with the processing of complex visual input remains to be understood. Perhaps, one must first understand the mechanisms that bring about visual perception or visual awareness, which might provide clues on its evolutionary history.

This is especially important, since the sensory modality of vision is the dominant one among primates. With nearly 50 percent of the cerebral cortex of the macaque monkey and 30 percent of the cortical surface in humans involved in processing visual input, it seems apt to call us ‘visual animals’. Moreover, this network of brain areas is hierarchically organized and exhibits specialized functional properties (Werner and Chalupa 2004). Evolution has

endowed the visual system of primates the ability to transform photons of light bombarding the retinae into a phenomenal subjective experience. Although how this neural machinery brings about awareness remains to be understood, we do know that the various individual regions of the visual pathway display functional specialization and are sensitive to specific features in the visual environment (Werner and Chalupa 2004). We have come to learn about the anatomical and functional subdivisions as well as the properties of neurons in the visual system through systematic investigation of these brain regions in non-human primates. Indeed, the macaque visual system is the most suitable surrogate for such an investigation because of its similarity to that of human (Harwerth and Smith 1985).

It is therefore not surprising, that in a call to understand the 'neural correlates of consciousness', Crick and Koch thought that a fitting choice for exploring the physiological mechanisms underlying perception would be to investigate the primate visual system (Crick and Koch 1990). Evidently, scrutinizing the neural machinery which gives rise to visual perception could also provide insights into a more general understanding of awareness itself. Helmholtz similarly appreciated the importance of such a 'nervous mechanism' when he defined visual perception. He wrote 'The sensations aroused by light in the nervous mechanism of vision enable us to form conceptions as to the existence, form and position of external objects. These ideas are called visual perceptions (Helmholtz, Warren et al. 1968).'

However, a fundamental issue in the investigation of perception has been that it co-occurs with the concomitant sensory input which leads to it (an exception to this would be imagination, but here I refer to the kind of perception which results from an external sensory stimulus). Disentangling the two therefore is essential, if one wants to isolate the neural correlates of perception from those related to just the sensory input. This is where multistable stimuli (examples shown in Figure 1), are a potent tool in the arsenal of a neuroscientist aiming to understand the principles of perceptual organization (Attneave 1971). They elicit in the viewer, distinct perceptual interpretations without any changes in the retinal input, and thus allow the investigator to dissociate sensory input from the phenomenal percept.

A Necker Cube **B Face Vase Illusion**

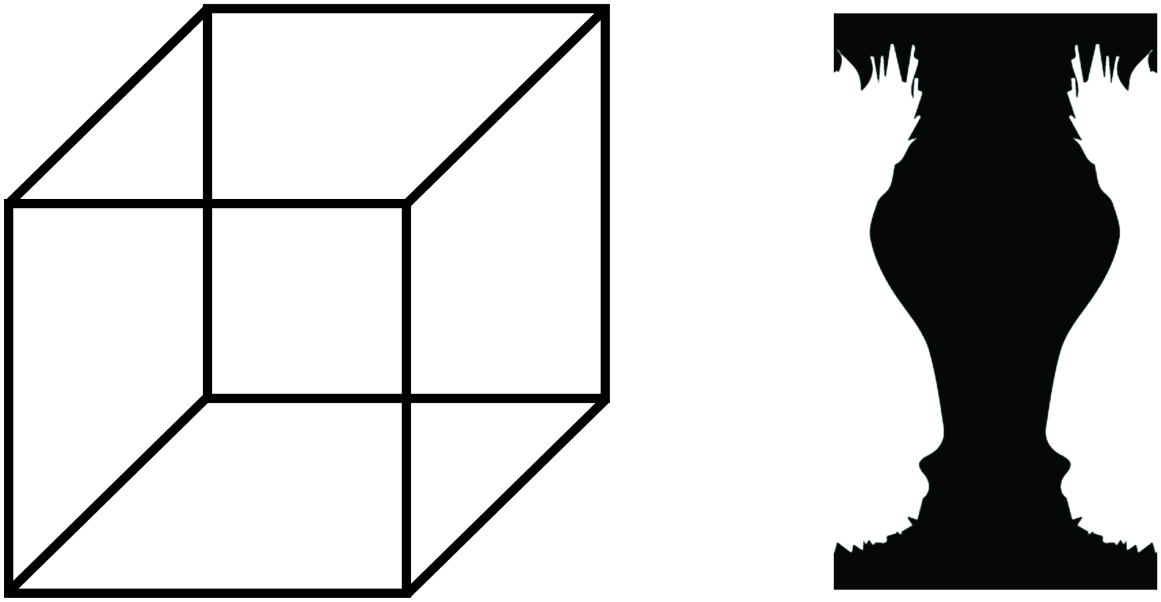

Figure 1.

Displayed are two examples of multistable figures, which when presented produce in the observer fluctuations of perception. A. Necker Cube (Necker 1832) and B. Modified version of the classic face vase illusion (Rubin 1915). (Adapted with permission from the monkey profile picture by Tracie Kaska)

One example of such a paradigm which has been exhaustively exploited for understanding the neurophysiological signals underlying visual perception is binocular rivalry (BR). It involves the simultaneous stimulation of corresponding retinal locations across the two eyes with dissimilar visual stimuli. When presented with such input, the observer typically experiences fluctuations in perception between the two visual stimuli. Although, Porta (Porta 1593) is attributed to the discovery of binocular rivalry, a first clear description of the phenomena (both contour and color rivalry) was provided by Dutour (Dutour 1760, Dutour 1763, O'Shea 1999, O'Shea 1999). Following these initial descriptions,

the first systematic study came from Sir Charles Wheatstone, who also invented the stereoscope, a device able of presenting distinct images to the two eyes (Wheatstone 1838). Describing his observations from experiencing rivalry between letters of the English alphabet, he wrote in a monograph (Wheatstone 1838), "*If a and b [which were letters S and A] are each presented at the same time to a different eye, the common border will remain constant, while the letter within it will change alternately from that which would be perceived by the right eye alone to that which would be perceived by the left eye alone. At the moment of change the letter which has just been seen breaks into fragments, while fragments of the letter which is about to appear mingle with them, and are immediately after replaced by the entire letter. It does not appear to be in the power of the will to determine the appearance of either of the letters, but the duration of the appearance seems to depend on causes which are under our control: thus if the two pictures be equally illuminated, the alternations appear in general of equal duration; but if one picture be more illuminated than the other, that which is less so will be perceived during a shorter time.*" With this succinct paragraph, Wheatstone illustrated the basic features of binocular rivalry, namely, the fluctuation of perception between the two stimuli, the piecemeal like pattern during phases of transition and finally the dependence of dominance durations of the two rivalling patterns on their relative stimulus strength.

Another interesting characteristic of the dominance and suppression durations observed during binocular rivalry is that they display sequential stochastic independence, that is the successive temporal durations during binocular rivalry are independent of the previous one (Fox and Herrmann 1967, Borselli.A, Allazett.A et al. 1972, Taylor and Aldridge 1974, Walker 1975). The distribution of visibility and invisibility durations can be fitted with a gamma function (Levelt 1967), parameters of which are remarkably similar across humans and macaques (Myerson 1981, Leopold and Logothetis 1996, Sheinberg and Logothetis 1997). The predominance of a pattern during binocular rivalry has been demonstrated to depend upon various stimulus properties, such as contrast (Mueller and Blake 1989), spatial frequency (Fahle 1982) or the brightness of the stimulus (Kaplan and Metlay 1964). Interestingly, such manipulation of so called low level properties of rivaling stimulus tends

to influence the duration for which it is suppressed, generally referred to as the Levelt's second law of binocular rivalry (Levelt 1965). On the other hand, manipulation of context, for example when one of the stimuli could be organized into a global meaningful pattern influences its dominance duration, leaving the suppression phases intact (Alais and Blake 1999). These two lines of evidence, wherein context and stimulus strength differentially influence the duration of dominance and suppression phases of a stimulus, indicate that they might be mediated by distinct neural processes (Blake and Logothetis 2002).

These interesting features of this phenomenon of binocular rivalry have motivated neurophysiologists to utilize it for investigation of visual regions of the brain in alert macaques. It is indeed ironical that a paradigm which instigates ambiguity in perception has been instrumental in enciphering its true neural correlates. Such tasks, when combined with physiology, has allowed neuroscientists to infer, if the neuronal activity elicited during the presentation of dichoptic stimuli is independent of animal's perception, and related to the external sensory input or if it undergoes dominance or suppression depending upon the subject's phenomenal experience. The activity of the latter kind is considered to be perceptually modulated and thus related to the subject's awareness of the stimulus. Several studies which have probed different areas of the primate visual system have provided the first clues into their relative contribution to the phenomena of visual perception.

The visual system of primates begins with the retina. The incoming sensory message from the retina is relayed to the lateral geniculate nucleus which does not display any temporal modulation among its single unit activity when alert monkeys are presented with incongruent visual input (Lehky and Maunsell 1996, Wilke, Mueller et al. 2009). Only a very small proportion of neurons (~20-25%) in the next region in the visual hierarchy, the primary visual cortex, respond to what the animal perceives during visual competition, with a majority of them firing in response to the incoming sensory message (Leopold and Logothetis 1996, Keliris, Logothetis et al. 2010). Moreover, a majority of the perceptually modulated neurons are binocular, thus refuting a theoretical claim once made about the competition during binocular rivalry being eye based and resolved through reciprocal

inhibition between population of monocular neurons present in V1 (Blake 1989). In extrastriate areas, such as V4/MT, the proportion of neurons which modulated their response according to the monkey's report during rivalry was higher at ~40 %. Surprisingly, certain neurons in both these regions responded with increasing their activity, when their preferred stimulus was suppressed (Logothetis and Schall 1989, Leopold and Logothetis 1996). These have been postulated as part of an inhibitory mechanism, which may be partially independent from the mechanism of perception (Logothetis 1998). In summary, these results indicate that suppression and dominance are mediated through populations of cells which are distributed across the visual hierarchy.

These perceptually modulated cells could mediate visual awareness, or instead be a reflection of stimulus selection which happens in higher visual regions of the brain. Therefore, it is essential to investigate the neuronal activity in higher visual centers in order to understand their status during visual conflict. In the first of such a study, neuronal activity was recorded in the temporal lobe, a region in the brain which is usually responsive to complex visual stimuli such as faces or objects (Logothetis, Pauls et al. 1995). Interestingly, it displayed the strongest perceptual modulation among the areas recorded in the visual stream. Specifically, 90 % of the cells which displayed visual selectivity were also perceptually modulated (Sheinberg and Logothetis 1997), indicating that this area represented a stage of processing, which was beyond the resolution of perceptual conflict (Logothetis 1998, Blake and Logothetis 2002).

The ventral visual pathway however continues beyond the temporal lobe. Visual responses selective to complex visual stimuli such as faces and objects have been recorded from the lateral prefrontal cortex (LPFC) (Pigarev, Rizzolatti et al. 1979, Rosenkilde, Bauer et al. 1981, Wilson, Scalaidhe et al. 1993, SP, Wilson et al. 1997), much like in the inferotemporal cortex to which it is reciprocally connected (Barbas 1988, Webster, Bachevalier et al. 1994, Borra, Ichinohe et al. 2010, Yeterian, Pandya et al. 2012). Interestingly, imaging studies have indicated a role for LPFC in mediating perceptual switches during visual competition (Lumer 1998, Lumer, Friston et al. 1998, Sterzer and

Kleinschmidt 2007, Zaretskaya, Thielscher et al. 2010, Knapen, Brascamp et al. 2011). Such a role is corroborated with data showing abnormal perceptual transitions in patients with lesions in the frontal lobe (Ricci and Blundo 1990, Meenan and Miller 1994, Windmann, Wehrmann et al. 2006).

While physiological evidence indicates that complex visual stimuli are processed in the LPFC, whether this activity is correlated with conscious perception during incongruent visual input, remained yet unexplored. One major aim of this thesis was to explore the feature selective neuronal activity in this region of the brain during visual competition. The 'frontal lobe' hypothesis, proposed by Crick and Koch hypothesized that the prefrontal cortex, wherein, planning for action is embedded, needs to have access to the explicit visual percept in order to control actions mediated through the motor cortices (Crick and Koch 1998). Therefore, probing the electrophysiological signals in the prefrontal cortex during visual competition is central to understanding the neural correlates of consciousness. The first study presented in chapter two of this thesis evaluated the modulation of neural signals in the LPFC during a task which instigated visual competition.

Although much has been learnt from investigation of single unit activity in various visual regions of the macaque brain (Logothetis 1998), an understanding of correlated variability or shared intrinsic noise among those recorded single units has not been analyzed during tasks that dissociate subjective perception from sensory stimulation. Such an evaluation is essential, since such fluctuations in neuronal discharges have been thought to influence population coding capacity (Zohary, Shadlen et al. 1994, Abbott and Dayan 1999, Sompolinsky, Yoon et al. 2001, Wilke and Eurich 2002, Averbeck, Latham et al. 2006, Averbeck and Lee 2006). The necessity for utilizing such analytical methods on the recorded physiological signals along with a review of the electrophysiology studies during multistable perceptual paradigms is summarized in chapter three. An assessment of interneuronal trial to trial discharge variability was carried out among the single unit activity recorded in the LPFC during presentation of ambiguous visual input. The results of this study are elaborated in the chapter four of this thesis.

In spite of physiological evidence supporting the representation of conscious content in the LPFC being reported (Panagiotaropoulos, Deco et al. 2012) (and also presented in chapter two of this thesis), a recent imaging study asserted that “frontal areas are associated with active report and introspection rather than with rivalry per se” (Frassle, Sommer et al. 2014). Such a conclusion was arrived at by a clever stimulus manipulation which allowed eliminating the need for manual report from subjects of their ongoing percept and instead decoding it from the pattern of their eye movements. In an opinion article(Safavi, Kapoor et al. 2014), which is summarized in chapter five of the thesis, we discuss the study, given the electrophysiological evidence for representation of perceptual content in the LPFC with a visual perception paradigm which also does not require the animals to report. In addition, we argue the importance of an integrative view, while reviewing the evidence on the role of prefrontal cortex in visual consciousness.

Interestingly, the ‘frontal lobe hypothesis’ (Crick and Koch 1998) mentioned earlier, was postulated while cognizant of the prefrontal cortex’s role in the temporal organization of behavior (Rao, Rainer et al. 1997, Fuster 2001, Miller and Cohen 2001, Fuster 2008). The successful execution of such a function necessitates integration of convergent sensory input (Chavis and Pandya 1976, Miller and Cohen 2001, Romanski 2012) and its subsequent retention for executing a goal directed motor act (Tanji and Hoshi 2008). Indeed, such a function of exerting cognitive control has been traditionally thought to be tightly bound to consciousness (Norman and Shallice 1986). Recent evidence, however, points out that the two processes might be functionally distinct, since subliminal, unconscious stimuli have been shown to influence control of action (van Gaal, de Lange et al. 2012, van Gaal and Lamme 2012). A signal pattern typically associated with cognitive control is beta band (~15-40 Hz) desynchronization, which consists of a disruption in the beta band oscillatory activity following the onset of a stimulus or execution of a voluntary motor act. This is immediately followed by a rebound of beta band activity as long as the stimulus input stays unchanged or a steady motor contraction is maintained (Sanes and Donoghue 1993, Pfurtscheller, Stancak et al. 1996, Donoghue, Sanes et al. 1998, Baker, Kilner et al. 1999, Gilbertson, Lalo et al. 2005, Jurkiewicz, Gaetz et al. 2006, O'Leary and Hatsopoulos 2006, Baker 2007, Siegel,

Warden et al. 2009, Engel and Fries 2010, Puig and Miller 2012, Kilavik, Zaepffel et al. 2013). Such constant beta band activity has been hypothesized to be an active process, supporting the maintenance of the current sensory, motor or cognitive set (Gilbertson, Lalo et al. 2005, Pogosyan, Gaynor et al. 2009, Swann, Tandon et al. 2009). Characterizing the pattern of such a control related signal during conscious or unconscious processing (as it happens, when a stimulus is perceptually dominant or suppressed during visual competition) would aid in elucidating dependencies between consciousness and control signals. Therefore, we evaluated these patterns in the LPFC during visual competition in sites which displayed robust perceptual modulation as judged from the multi-unit spiking responses. The results of this investigation are described in chapter six.

Further, the neuronal responses in the LPFC have been observed in many different paradigms such as those related to decision making, working memory, temporal sequencing of sensory input or motor action, reward expectation to mention a few (Tanji and Hoshi 2008). This versatility of responses observed in this region, most likely aids in the LPFC to subserve its function of temporal organization of behavior (Fuster 2008). Interestingly, while the diversity of responses we observed in the LPFC during ambiguous visual input was enormous, the units which discriminated the two visual stimuli utilized for eliciting visual competition were, however, a minority (results described in chapter two). We therefore wanted to understand and characterize the neuronal responses beyond those merely related to visual preference, and could be relevant to other aspects of the task. In a study presented in chapter seven, we developed a novel clustering approach for isolating dominant response profiles observed among the remaining majority of the neurons recorded.

Together, these studies provide the basis for a role of LPFC in conscious visual perception. They further elaborate on other functions which are typically attributed to the LPFC, which co-exist in this region in parallel with its role in representation of conscious visual input.

2

Neuronal discharges and gamma oscillations explicitly reflect visual consciousness in the lateral prefrontal cortex.

2.1 Motivation

Electrophysiological investigation of various visual areas in the primate brain has revealed a gradual increase in the percentage of cells whose spiking activity correlates with the subjective visual percept when the animal is presented with ambiguous visual input (Logothetis 1998, Leopold and Logothetis 1999). In earlier visual areas, like V1 and V2, only 20-25% of the single neurons recorded displayed increased electrical activity to their preferred visual stimulus when it was consciously perceived (Leopold and Logothetis 1996, Gail, Brinksmeyer et al. 2004, Keliris, Logothetis et al. 2010). In contrast, about 90% of the visually selective neurons recorded in the superior temporal sulcus and inferior temporal lobe (IT) fire in concurrence with the perceived stimulus (Sheinberg and Logothetis 1997). Similarly, neurons in the human medial temporal lobe were shown to be modulated by the phenomenal percept (Kreiman, Fried et al. 2002). The temporal lobe is reciprocally connected to the lateral prefrontal cortex (LPFC) (Barbas 1988, Webster, Bachevalier et al. 1994, Yeterian, Pandya et al. 2012), wherein single unit activity related to faces or complex visual stimuli has been previously observed (Pigarev, Rizzolatti et al. 1979, Wilson, Scalaidhe et al. 1993). We wondered if such feature selective neuronal responses observed in this

region would also correlate with the subjective percept. Therefore, we performed electrophysiological recordings in the LPFC during the task of binocular flash suppression (BFS), which allowed us to dissociate sensory input from phenomenal perception.

2.2 Methods

Single unit and local field potential (LFP) activity was recorded using twisted wire tetrodes from the LPFC of two rhesus macaques while they were engaged in the task of BFS (Lansing 1964, Wolfe 1984). The task consisted of trials which were divided across two conditions, namely the PA and flash suppression (FS). Each trial started with 300 millisecond presentation of the fixation spot in both eyes followed by one second of monocular stimulation with one pattern in one eye. During physical alternation (PA) trials, the first pattern was removed and another pattern was presented in the contralateral eye for one more second. In flash suppression (FS) trials, the stimulation with a new pattern in the contralateral eye was carried out without the removal of the stimulus presented first. Psychophysical evidence has shown that such stimulation results in the robust suppression of the first stimulus and perception of the pattern presented second (Wolfe 1984, Sheinberg and Logothetis 1997, Keliris, Logothetis et al. 2010). Evidently, the perception of the animal across the two trial types stays the same, albeit the underlying visual stimulation is different. Concomitant recording of feature selective neural activity can thus allow us to determine if the responses are related to perception or mere sensory input.

2.3 Results

We found that about 58% of the recorded single units which showed a preference to one of the two visual stimuli (as judged from the PA condition) used were also significantly modulated during FS. This proportion of perceptually modulated units increased to about

89% when the sites were chosen based on their discriminability across the two stimuli, as judged by the d prime index > 1 (see methods section in Appendix A.1).

Next, we analyzed the modulation of unsorted multiunit spiking activity in a similar way. In our data, 20% of the recorded sites displayed significant modulation during the PA condition. A large majority of these sites, about 70% maintained this preference and were significantly modulated during the FS condition. When only sites which displayed a d prime index > 1 were selected, the percentage of perceptually modulated sites increased to 92%. These proportions are very similar to the percentage of single units modulated by perception observed in the temporal lobe (Sheinberg and Logothetis 1997). We further observed that the latency of selective responses observed in all the sensory modulated sites during FS condition were delayed by approximately 60 milliseconds in comparison to the PA condition.

Finally, we aimed to characterize the modulations in synchronized neural activity as measured with power in the different frequency bands of the LFP. We found that in sites where the multiunit activity was selective in the PA condition, the high frequency LFP (> 50 Hz) also displayed a significant modulation during monocular presentation of the preferred pattern. Moreover, this was not significantly different from that during the BFS condition.

2.4 Conclusion

In summary, we show that the subjective visual percept is reflected in both the feature selective neuronal activity as well as power of high frequency oscillations in the LPFC.

3

Subjective visual perception: from local processing to emergent phenomena of brain activity.

3.1 Summary

Ambiguous visual stimuli provide a unique window into understanding the neural correlates of consciousness. Without a change in the visual input, they elicit in the observer, fluctuations of perception. An example of such a paradigm for instigating perceptual competition, binocular rivalry (and its variants such as binocular flash suppression (BFS) (Lansing 1964, Wolfe 1984) and generalized flash suppression (GFS) (Wilke, Logothetis et al. 2003)), has been an exquisite method for studying the neural correlates of conscious visual perception (Logothetis 1998, Blake and Logothetis 2002). It involves dichoptic stimulation to corresponding retinal locations with two distinct stimuli, which compete for dominance. Concomitant recording of neuronal activity displaying stimulus preference (as judged from a control condition where stimulation is singular and monocular and thus devoid of competition) has been utilized as a criterion for distinguishing if the response during visual competition is related to mere sensory input or perceptual experience (Logothetis 1998). Hence, a perceptually modulated cell is one which maintains its activity when its preferred stimulus is perceived, whereas a neuron which continues to respond, irrespective of whether its preferred stimulus is perceptually dominant or suppressed is considered to be sensory driven.

Such local recordings have so far been extremely beneficial in addressing several issues regarding perceptual awareness. To start, it was traditionally hypothesized that the conflict during binocular rivalry was resolved through competition in activity among pools of monocular neurons encoding the stimulus presented to the eye of origin (Blake 1989). Physiological probing of monocular neurons in the early visual areas however revealed that a majority of these neurons were not modulated by the ongoing percept (Leopold and Logothetis 1996, Keliris, Logothetis et al. 2010). Interestingly, only a small proportion of 20-25% of neurons were classified as being perceptually modulated indicating that the conscious visual percept might be mediated by a higher order cortical and a stimulus based representation.

Interestingly, neural activity in later regions in the ventral visual pathway correlated much better with visual perception. Specifically, in the superior temporal sulcus and inferotemporal cortex (IT), 90% of the neurons displaying visual preference were found to be modulated in concordance with the perceptual content (Sheinberg and Logothetis 1997). The next station in the visual hierarchy related to object recognition is the LPFC, which is reciprocally connected to IT (Barbas 1988, Webster, Bachevalier et al. 1994, Borra, Ichinohe et al. 2010, Yeterian, Pandya et al. 2012). A study as a part of this thesis found that a majority of units, (~ 60-90%, depending on the strength of the sensory preference) in this region are also perceptually modulated. Besides direct reciprocal connectivity between the temporal and prefrontal cortex, they are also connected indirectly through a subcortical pathway, which involves the pulvinar nucleus of the thalamus (Barbas, Henion et al. 1991, Webster, Bachevalier et al. 1993, Romanski, Giguere et al. 1997, Gutierrez, Cola et al. 2000, Contini, Baccarini et al. 2010). When the pulvinar was investigated during the paradigm of GFS, perceptual suppression was observed in 40% and 60% of the sites in the ventral and dorsal pulvinar, respectively (Wilke, Mueller et al. 2009). Three different but anatomically connected regions in the brain displaying robust activity in accordance with the conscious visual content indicates that perception is likely a phenomena mediated through a global network of areas.

Besides the spiking activity, an electrical signal which can be typically recorded with extracellular recordings is the local field potential (LFP), which is thought to reflect the synaptic input and dendritic processes (Mitzdorf 1985, Mitzdorf 1987, Logothetis 2003). Examination of LFP seems to resolve the dispute between the disparate results from spiking activity and functional imaging studies in areas like V1 and LGN during visual perception. A significant perceptual modulation is observed in the BOLD signal from these areas (Polonsky, Blake et al. 2000, Tong and Engel 2001, Lee and Blake 2002, Haynes, Deichmann et al. 2005, Haynes and Rees 2005, Lee, Blake et al. 2007). The high frequency gamma oscillations and spiking activity in these regions, however, display negligible modulation in concurrence with the subjective percept and instead, the power in low frequency LFPs is modulated more reliably with perception (Wilke, Logothetis et al. 2006, Maier, Wilke et al. 2008, Wilke, Mueller et al. 2009, Keliris, Logothetis et al. 2010). A study which combined both functional imaging and electrophysiology in the same animals during the paradigm of GFS, reported that both the BOLD as well as the low frequency LFP were modulated with perceptual suppression (Maier, Wilke et al. 2008). In comparison to this, one observes that perceptual suppression is reflected in the gamma band activity in the LPFC (Panagiotaropoulos, Deco et al. 2012), which might be a reflection of input it receives from the temporal lobe.

Besides the LFPs, slow and correlated variations in the activity of neuronal populations can also be detected in the spiking responses from neurons. The experimental work thus far has concentrated on the activity recorded from single neurons or single sites in order to assess the relative contribution of individual areas to perceptual awareness. The structure of correlated variability as measured with noise correlations has been shown to have an important influence on population coding (Zohary, Shadlen et al. 1994, Abbott and Dayan 1999, Sompolinsky, Yoon et al. 2001, Wilke and Eurich 2002, Averbeck, Latham et al. 2006, Averbeck and Lee 2006). One direction of future studies would be to simultaneously record multiple single neurons in a given area and understand their correlated variability during visual competition. A hypothesis interesting to investigate is whether fluctuations in

the structure of such noise correlations could be related to the spontaneous perceptual transitions observed during BR.

Finally, the perceptual transitions could also be a result of ongoing fluctuations in neural activity arising from spontaneous changes in mesoscopic brain state. With the advent of methods (for e.g., optical imaging, UTAH arrays) which are capable of measuring the spatiotemporal patterns of electrophysiological activity, prospective research could examine how such self-organized and dynamic intrinsic patterns are related not only to switches in perception, but could also represent periods of perceptual dominance and suppression.

4

Decorrelated discharge fluctuations in prefrontal microcircuits during visual consciousness.

4.1 Motivation

Probing the responses of single neuron in various visual regions of the brain during paradigms employing ambiguous visual stimulation (such as binocular rivalry) have aided in discerning the relative contributions of these different cortical areas to visual perception (Logothetis and Schall 1989, Leopold and Logothetis 1996, Sheinberg and Logothetis 1997, Keliris, Logothetis et al. 2010, Panagiotaropoulos, Deco et al. 2012). The neuronal population coding capacity however is thought to be severely influenced by effective functional connectivity between neurons, as represented by the structure of trial to trial spiking variability (Abbott and Dayan 1999, Sompolinsky, Yoon et al. 2001, Averbeck, Latham et al. 2006, Cohen and Kohn 2011). The structure of such interneuronal correlations during tasks which disentangle sensory input from visual perception could therefore provide insights into how a functional microcircuit organization affects the reliability of representation of conscious visual content among neuronal populations. In this study, we therefore measured the strength of these correlations among simultaneously recorded lateral prefrontal cortex (LPFC) neurons during the task of binocular flash suppression (BFS).

4.2 Methods

Electrophysiological activity was recorded from the LPFC of three rhesus macaques using twisted wire tetrodes, while they passively fixated during the paradigm of BFS (a description of the task is presented in the methods section of chapter 2). A second order statistical measure such as their pair wise spike count correlation coefficient (r_{sc}) was computed for pairs of neurons (Bair, Zohary et al. 2001) which showed similar or different stimulus selectivity as judged from their stimulus preference index (for details, refer to the methods section in Appendix A.3). This was calculated for the second half of a trial when perception was elicited with monocular presentation of a stimulus as in the physical alternation (PA) condition or during subjective perception while incongruent visual input was presented in the case of flash suppression (FS) trials.

Simulations were carried out with two biophysically realistic networks with distinct architectures. One network consisted of two excitatory neuronal populations selective to the two visual stimuli respectively utilized in the experiment and one inhibitory neuronal population. This network is characterized with cross inhibition and therefore competition between the two excitatory neuronal populations. The second network was similar to the first one; however it did not feature cross inhibition.

4.3 Results

In a study, which is also a part of this thesis, we report the existence of neurons which are reliably modulated in accordance to the content of visual perception (Panagiotaropoulos, Deco et al. 2012). In order to understand the structure of correlated variability across single units in the LPFC, we calculated noise correlations across simultaneously recorded neurons that displayed preference for the same stimulus during both physical alternation and flash suppression conditions in the second half of their trials. We observed that while monocular presentation of the preferred stimulus during PA led to

increased correlations, the subjective perception of the same stimulus during BFS led to a strong and significant decorrelation. Remarkably, these correlations observed during the period of subjective dominance in BFS were not significantly different from zero, suggesting a sparse encoding of perceptual content. Interestingly, this decorrelation was asymmetric, since we observed that the correlations did not change when the perceptual suppression of the stimulus during BFS was compared to the physical absence in PA. Further, this reduction in intrinsic noise was a network specific effect as single unit discharge variability was similar across the two different conditions.

In order to understand the mechanism of decorrelation, we considered a biophysically realistic spiking network that comprised of two selective excitatory neural populations, each of which encoded one of the two visual stimuli, undergoing competition arbitrated by an inhibitory population (Theodoni, Panagiotaropoulos et al. 2011). Although the simulated network for a set of parameters accounts for the experimentally observed correlations in PA, we observed increased correlations during BFS for both the dominant and suppressed populations contrary to the experimentally observed decorrelation. Instead, we found that a suppression of input fluctuations to the dominant population leads to a reduction in correlations without a change in the excitatory-inhibitory balance. Small decrease in the stimulus drive is however necessary to account for the marginally reduced firing rate observed during the FS condition. Next, we attempted to understand and simulate the similarity of correlations observed during perceptual suppression in FS or the physical absence of the stimulus in PA. Interestingly, a reduction of the input strength during perceptual suppression is required to maintain the correlations, so that they are equivalent to those obtained during stimulus absence in PA.

4.4 Conclusion

In summary, we show that subjective perception during the task of BFS in the LPFC is accompanied with near zero pair wise spike count variability, in comparison to monocular

presentation. This demonstrates a modulation of the correlation structure during processing of ambiguous visual input.

5

Is the frontal lobe involved in conscious perception?

5.1 Summary

Much research in neuroscience has been devoted to the scientific investigation of visual awareness, ever since a seminal paper from Crick and Koch (1990) incited researchers that 'the time is ripe for an attack on the neural basis of consciousness' (Crick and Koch 1990). However, it has been recently pointed out to exert caution while studying the neural correlates of consciousness in that one must carefully disentangle this activity from what could reflect the prerequisite or consequence of a subjective experience (Aru, Bachmann et al. 2012, de Graaf, Hsieh et al. 2012). For example, most paradigms used for studying sensory awareness typically ask the subjects to report their perception with a motor response. Such an action potentially requires introspection for monitoring the current perceptual state and can therefore be considered a consequence of the conscious experience. A recent study tried to eliminate such consequential processes by asking subjects to passively observe the ambiguous stimuli without reporting and decoded the current experiential state of the subject from their pattern of eye movements (Frassle, Sommer et al. 2014). Contrastive analysis to a condition, wherein the subjects reported their percept, led the authors to conclude that "frontal areas are associated with active report and introspection rather than with rivalry per se". However, soon after the study was published, it was pointed out that the BOLD activity in the right inferior frontal lobe and

right superior frontal lobe survived the contrastive analysis in their experiment (Zaretskaya and Narinyan 2014). Therefore, it does not completely rule out the entire prefrontal cortex from having a role in perception.

Moreover, a study carried out as a part of this thesis posits the representation of perceptual content in the LPFC of the macaque brain (Panagiotaropoulos, Deco et al. 2012). Interestingly, during the experiment, the animals passively fixated without any requirement of a behavioral report of their subjective percept. Even in the absence of any overt action to indicate what was perceived, we observed that the modulation of a large majority of feature selective neurons in the LPFC was in concordance with perceived stimulus. Together, this alludes to a role of prefrontal cortex in conscious awareness.

Although perceptually modulated neuronal activity has been observed by us and others in the prefrontal cortex (Libedinsky and Livingstone 2011, Panagiotaropoulos, Deco et al. 2012), an understanding of its mechanistic role in mediating perceptual organization is presently missing. We propose that in order to decipher of such a role of prefrontal cortex in awareness, we need to have a more integrative view on the evidence available thus far as well as versatility in our prospective research directions. Therefore, our future investigations should not only employ versatile experimental designs, but also diverse experimental techniques (e.g., fMRI, electrophysiology) which could allow observing neural dynamics at different spatial and temporal scales.

6

Desynchronization and rebound of beta oscillations during conscious and unconscious local neuronal processing in the macaque lateral prefrontal cortex.

6.1 Motivation

Oscillatory activity in the beta band has been linked to maintaining the current sensory motor set (Engel and Fries 2010). Specifically, it has been shown to be modulated during tasks which employ cognitive control. Control processes, although traditionally thought to be influenced by conscious perception, have now also been demonstrated to be influenced by unconscious stimuli (van Gaal, de Lange et al. 2012, van Gaal and Lamme 2012). However, the modulation of beta band activity during the processing of conscious or unconscious processing of stimulus input remains elusive. In a previous study, we found that the neural activity in certain sites in the lateral prefrontal cortex (LPFC) is correlated with conscious and unconscious processing (Panagiotaropoulos, Deco et al. 2012). In order to elucidate, how a signal attributed to cognitive control such as the beta band oscillations might be influenced by conscious or unconscious processing, we investigated its modulation in these specific prefrontal sites.

6.2 Methods

Electrophysiological recordings were performed in the LPFC of two rhesus macaques while they participated in a fixation task, whose trials were equally divided across two conditions, namely the physical alternation (PA) and flash suppression (FS) (details of the task are explained in section 2.2). The pattern preference of the total spiking activity recorded from a single site (multi unit activity or MUA) between the two stimuli was judged based on the responses during the PA trials. We analyzed the LFP activity for sites showing significant stimulus preference as well as from sites where spontaneous, resting-state activity was recorded.

6.3 Results

Examining the power spectral density of the LFP activity recorded during spontaneous, resting state (10-30 min) revealed that there was a peak in the beta frequency range, between 15 to 30 Hz. Therefore, further analysis focused on this frequency band. Specifically, we analyzed the modulation of the beta band in sites where feature selective MUA was detected. Interestingly, during PA trials, monocular visual stimulation resulted in an abrupt desynchronization of the rhythmic beta band oscillations. This was followed by a rebound of synchronous beta band activity ~400 milliseconds after onset of the visual stimulus. In PA trials, after one second of stimulation with a monocular stimulus, it was removed and a second pattern was presented in the contralateral eye. This resulted in a new decrease of power in the beta band, which was followed by a rebound ~400 milliseconds after the onset of this second input. Interestingly, such a pattern was observed irrespective of whether the current input was preferred or non-preferred (as judged from the MUA).

Next, in order to understand the dynamics of beta band activity during conscious perception or perceptual suppression, we focused our analysis on the FS condition. Irrespective of whether the preferred stimulus for the given site was perceived or suppressed, and therefore the local spiking activity was dominant or repressed, the beta oscillations in the site presented a modulation pattern very similar to that observed in the PA condition; that is, there was an initial desynchronization which was later followed by a recovery of the beta power. Visual competition thus had no effect on the pattern of beta band modulation in comparison to the PA.

6.4 Conclusion

Our results indicate that a control related signal, such as the beta band oscillations as studied here under control free conditions not only remains unaffected by local neuronal or perceptual dominance and suppression, but coexists independently from contemporaneous conscious and unconscious neuronal representations.

7

Sequential patterns of neuronal activity in the lateral prefrontal cortex during the task of binocular flash suppression

7.1 Motivation

Electrophysiological investigation of the lateral prefrontal cortex (LPFC) during the task of binocular flash suppression (BFS) revealed a population of perceptually modulated neurons (Panagiotaropoulos, Deco et al. 2012). However, feature selective neuronal population formed a minority of the single units recorded during the task. In this study, we wanted to characterize any other task related activity in the firing profiles of the remaining majority of the recorded units.

7.2 Methods

We utilized the method of non-negative matrix factorization (NNMF) (Paatero and Tapper 1994, Lee and Seung 1999) for identifying the major patterns of activity among non-feature preferring neurons recorded during the task of binocular flash suppression. In addition, spike count correlations (method described in chapter 4) were assessed for simultaneously recorded neurons whose activity was similar to the different patterns obtained with nnmf.

7.3 Results

Five major profiles of activity, whose peak was temporally distributed across the various phases of a trial, were characterized with nnmf. Specifically, we obtained response profiles, two of which displayed ramping up or ramping down while two others displayed increases in amplitude during the presentation of the first and the second stimulus respectively. The fifth profile peaked around the switch from the first pattern to the second. Further, a majority of the neurons with activity similar to different patterns, responded similarly across different stimulus conditions, that is the physical alternation (PA) and the flash suppression (FS).

Interestingly, when the neurons sorted according to the latency of their peak amplitude were plotted, it revealed that the peaks of different single units were distributed across the entire duration of the trial and such a distribution pattern was similar for different stimulus conditions.

In order to assess effective functional connectivity across neurons whose profiles were similar to components which were distributed across temporal windows, we calculated noise correlations between them. The correlations were highest for the pair of neurons, which belonged to the same component, that is, those displaying a similar response profile. Interestingly, we observed that this correlation steadily decreased as a function of temporal distance between the peaks of the patterns to which the constituents of the pair of single units belonged. Moreover a similar pattern was observed when the condition of PA and FS were analyzed individually, thus displaying its independence from the nature of the visual input. Surprisingly, this decrease was specific for positive noise correlations. The negative noise correlations did not show any difference as a function of temporal distance.

7.4 Conclusion

Our results show the existence of sequential activity patterns among single units during the task of BFS which does not require any mnemonic demands related to the order of the stimuli presented. Interestingly, their correlated variability demonstrated that it was higher for neurons which were temporally more similar than neurons which were not. This was similar across both PA and FS conditions, thus demonstrating that such a process is likely represented independently from the one mediating conscious visual perception.

8

Development of tube tetrodes and a multi-tetrode drive for deep structure electrophysiological recordings in the macaque brain.

8.1 Motivation

Unravelling the mechanisms mediating brain function requires investigation of the electrical signal underlying it (Scanziani and Hausser 2009). Electrophysiology has thus been a tool of choice for the neurophysiologist in this endeavor since Galvani's description of 'animal electricity' (Galvani 1791). The technique has progressed from the recording of the first action potential (Hodgkin and Huxley 1939), to more recently, probing of the physiological signal from several neurons simultaneously (Pine 2006). Twisted wire tetrode (TWT) has especially been instrumental in this regard with both the number and quality of isolation of single neurons from the recorded signal (Gray, Maldonado et al. 1995, Harris, Henze et al. 2000). Hence, they have been extensively used for extracellular electrophysiology (Buzsaki 2004). A limitation of its weak tensile strength and an issue of tip splaying during chronic implantation (Jog, Connolly et al. 2002) have, however, both hindered its use in deep brain electrophysiology. We wanted to utilize TWT for recordings in the temporal lobe of the macaque brain and therefore developed tetrodes with improved tensile strength and an electrode drive for accessing the temporal lobe.

8.2 Methods

Standard methods were used for fabrication of TWTs (Nguyen, Layton et al. 2009). We conferred strength to them by developing a simple laboratory technique for inserting them inside beveled, deburred and cleaned 35 gauge stainless steel tubes (outer diameter – 0.005 inches, inner diameter – 0.002 inches, 304SS, welded and drawn, hard temper, Vita needle, MA, USA). We call these tube tetrodes (TuTes). After electroplating them with gold, these TuTes were then loaded onto a custom built multi-tetrode, which allowed them to be driven independently of each other.

Electrophysiological investigation of the temporal lobe of one rhesus macaque implanted with a ball and socket recording chamber (Schiller and Koerner 1971, Logothetis, Pauls et al. 1995, Sheinberg and Logothetis 1997) was carried out utilizing the TuTes loaded on to the multi-tetrode drive. Single unit isolation from the recorded signal was carried out with customized algorithms which utilized the first three components of the recorded waveforms as features (Tolias, Ecker et al. 2007). Visual inspection of the resulting clusters performed using Klusters (Lynn Hazan, Buzsáki lab, Rutgers, Newark NJ) revealed that one could achieve reliable isolation of single unit with TuTes.

8.3 Results

Neural recordings with TuTes were carried out while the animal was engaged in a simple fixation task. Each trial started with 300 millisecond long presentation of the fixation spot in both eyes. During half of the trials, this was followed by monocular stimulation of a face stimulus for 1000 milliseconds after which a checkerboard pattern was presented in the contralateral eye for another 1000 milliseconds. These trials were randomly intermixed with the rest half of the trials, in which the order of the stimuli was reversed. We observed visually responsive single unit activity preferring the face or the checkerboard pattern. Similarly, visual responsiveness was also observed in the multiunit activity.

Power spectral density estimation of the recorded LFP signal demonstrated that most of the power was concentrated in the lower frequencies (1-4 Hz). Further, the magnitude of the LFP power displayed an inverse relationship with temporal frequency, hence following the power law, a characteristic typical of the LFP signal (Bedard, Kroger et al. 2006).

8.4 Conclusion

We developed a fabrication procedure for a novel kind of tetrode, the TuTe, which are especially useful for deep brain electrophysiology because of their stiffness in comparison to the conventional TWTs. Further, their thin diameter of ~0.127 mm makes them about 10-20 % in size, when compared to the cannulae, which have been utilized in recent studies for probing neural activity in deeper regions of the brain (Erickson and Desimone 1999, Erickson, Jagadeesh et al. 2000, Skaggs, McNaughton et al. 2007, Santos, Opris et al. 2012, Thome, Erickson et al. 2012).

9

Discussion and Conclusions

9.1 Prefrontal cortex and visual awareness - spiking activity and gamma oscillations

Previous studies investigating the relative contribution of various brain regions to visual perception have compared the magnitude of feature selective neuronal modulation with that observed during monocular, competition free sensory stimulation (Logothetis 1998). These studies revealed that the majority of spiking activity in early sensory areas such as V1/V2 followed the sensory input rather than the phenomenal percept (Leopold and Logothetis 1996, Keliris, Logothetis et al. 2010). On the other hand, majority of the feature selective spiking activity among the single units recorded in the temporal lobe are correlated with the subjective percept (Sheinberg and Logothetis 1997, Kreiman, Fried et al. 2002). We therefore investigated the next hierarchical region, which is reciprocally connected to the temporal lobe and thought to be the culmination of the ventral visual pathway, namely the lateral prefrontal cortex (LPFC) (Barbas 1988, Webster, Bachevalier et al. 1994, Borra, Ichinohe et al. 2010, Yeterian, Pandya et al. 2012). We found that both the spiking activity and the power of high frequency local field potential oscillations are modulated in concurrence to animal's perception. Our results posit that LPFC together with the temporal lobe could act as a cortico-cortical network for mediating visual awareness. Our results, however, do not allow us to conclude about the direction of this perceptual information flow. Reciprocal connectivity between the two regions could mediate this in

either direction. Interestingly, the pulvinar nucleus of the thalamus is connected to both the temporal lobe and the LPFC and could provide a subcortical (Barbas, Henion et al. 1991, Webster, Bachevalier et al. 1993, Romanski, Giguere et al. 1997, Contini, Baccarini et al. 2010) indirect route of communication. This hypothesis is given credence from the recordings in the dorsal pulvinar, which found that 60% of the recorded sites displayed perceptual modulation (Wilke, Mueller et al. 2009).

Although a suggestion that synchronous gamma band activity could mediate visual awareness was made more than two decades ago (Crick and Koch 1990), experimental evidence for the same in macaque cortex had been lacking. Our findings, showing that high frequency LFPs in the LPFC reflect subjective visual perception, provide the first experimental evidence of such a physiological substrate in the macaque brain. Moreover, our findings add credence to the 'frontal lobe hypothesis' (Crick and Koch 1998), which suggested that the planning stages of the brain such as the prefrontal cortex must have direct access to conscious representations in order to mediate motor action. Finally, a conglomerate of brain regions (LPFC and temporal lobe) with an explicit representation of perceptual content posits consciousness as an emergent phenomenon mediated through diverse neuronal populations.

9.2 Correlated discharges and population coding of perceptual content

The next study presented in the thesis investigated how the structure of correlations across pairs of neurons recorded in the LPFC is modulated by incongruent visual stimulation. We found limited range correlation between neuronal pairs with similar stimulus preference during monocular presentation of their preferred stimulus. Interestingly, during visual competition, there was an active decorrelation across these pairs of single units thus inducing a different structure of correlations.

Next, we focused on determining the source of this decorrelation. Cross inhibition across neuronal pools representing competing stimuli is an integral part of theoretical models explaining perceptual bistability (Moreno-Bote, Rinzel et al. 2007, Shpiro, Moreno-Bote et al. 2009, Theodoni, Panagiotaropoulos et al. 2011, Pastukhov, Garcia-Rodriguez et al. 2013) and a decrease in correlations could occur via an increase in inhibition (Renart, de la Rocha et al. 2010). The simulations however suggested that cross inhibition was not the source of decorrelation, instead, it was mediated through an asymmetric suppression of input fluctuations. This is similar to recent studies attributing input fluctuations responsible for noise correlations (Ecker, Berens et al. 2014, Goris, Movshon et al. 2014).

A key question in binocular rivalry research is to elucidate a mechanism of the transitions in perception. Theoretical models have proposed noise as a driving force for alternations between two attractor-percepts (Moreno-Bote, Rinzel et al. 2007, Shpiro, Moreno-Bote et al. 2009, Panagiotaropoulos, Kapoor et al. 2013, Pastukhov, Garcia-Rodriguez et al. 2013). We observed that weak correlated noise (not significantly different from zero) accompanies subjective perception during BFS. It must be noted here that the paradigm of BFS utilized by us did not allow us to directly study perceptual transitions. However, the simulations showed that a low correlation regime did not allow an induction of switches in perception when BFS was followed by BR and an increased correlated variability led to a detrimental state for flash suppression. This suggests that a decorrelated state could be functionally beneficial for perceptual stabilization. This leads to a prediction that an increase in strength of correlations could be involved in perceptual transitions. This change could be because of a common input fluctuation, for example a low frequency component of the LFP such as the slow cortical potential, which was recently suggested to play a role in consciousness (He and Raichle 2009).

It remains to be seen, however, if such a decorrelation mechanism during visual competition is a feature unique to an association area such as the LPFC or if similar active suppression of correlated noise could be a phenomenon observed universally in other areas of the visual system.

9.3 Prefrontal cortex – beyond visual perception – beta band oscillations and cognitive control

Experiments as a part of this thesis (Panagiotaropoulos, Deco et al. 2012) and other studies (Lumer 1998, Sterzer and Kleinschmidt 2007, Gaillard, Dehaene et al. 2009, Dehaene and Changeux 2011, Libedinsky and Livingstone 2011) have demonstrated a role for LPFC in mediating conscious visual perception. This provides support to the 'frontal lobe hypothesis' that the planning stages of the brain (such as the prefrontal cortex) must have access to explicitly encoded visual information (Crick and Koch 1998). Such access would facilitate this region of the brain to carry out other major functions attributed to it which is of cognitive control and temporal organization of behavior (Luria 1969, Goldman-Rakic, Bates et al. 1992, Miller 1999, White and Wise 1999, Miller 2000, Miller and Cohen 2001, Wallis, Anderson et al. 2001, Fuster 2008, Tanji and Hoshi 2008, Swann, Tandon et al. 2009, Buschman, Denovellis et al. 2012). Many research studies have addressed these processes independently. In a study detailed in chapter 6, it was investigated how a control related signal, such as the beta band oscillations, is influenced by conscious or unconscious processing of visual input. The results showed a robust modulation of beta band oscillatory activity in reference to the sensory input. This was characterized by a brief visual stimulus-induced desynchronization followed by a rebound of beta band activity which has been reported previously (Siegel, Warden et al. 2009, Puig and Miller 2012). This modulation in the beta band activity did not display any stimulus preference in sites where multi-unit spiking activity was selective for one of the two stimuli utilized in the study. Such a lack of selectivity in the beta band has been traditionally suggested to reflect diffuse neuromodulatory input (Belitski, Gretton et al. 2008, Magri, Schridde et al. 2012). The similarity in the pattern of modulation of beta band activity across the two different stimuli and task conditions (PA and FS) suggests a common source of such an input to the LPFC.

Although the task did not feature a condition which tested specifically for cognitive control, the observation of an unspecific disruption of the intrinsic control related signal such as the beta rhythm points during PA and FS, or dominance and suppression indicates

of its independence from cortical networks underlying conscious perception. Future work involving a task which could delineate conscious perception and cognitive control with concurrent electrophysiological investigation of the prefrontal cortex could provide valuable insights into the relationship between these cognitive processes.

9.4 Sequential patterns of neuronal activity in the LPFC

We observed robust perceptual suppression of feature selective neuronal activity in the LPFC during the task of BFS. However, the percentage of cells which displayed stimulus preference was a minority (Panagiotaropoulos, Deco et al. 2012). Moreover, there was considerable diversity among the recorded neuronal responses during such a simple passive fixation paradigm. In order to characterize this diversity, we employed a novel procedure, namely the non-negative matrix factorization (NNMF) (Paatero and Tapper 1994, Lee and Seung 1999), for clustering peristimulus time histograms (PSTH) of the neurons, to identify the most prominent patterns of activity present in the data. Such methodology, which allows the isolation of dominant patterns present in the data, is a necessity, as electrophysiological methods progress towards recording the activity of several hundred neurons or sites simultaneously (Pine 2006, Miller and Wilson 2008).

Decomposition of the PSTH's (with NNMF) obtained from neurons recorded during the task led us to identify five major patterns of activity which were sequential and distributed across the trial. Two of these patterns were restricted to the first or the second half of trial, thus time locked to the presentation of the first or the second visual pattern. Such temporal order related activity has previously been observed in the LPFC, especially in paradigms which required monkeys to memorize the sequence of sensory input so as to execute an appropriate motor response (Ninokura, Mushiake et al. 2003, Ninokura, Mushiake et al. 2004, Inoue and Mikami 2006, Berdyyeva and Olson 2010). Interestingly, the BFS task does not pose any mnemonic demands, but such patterns were still observed. The other temporal patterns, with ramping up or ramping down profile, could also be

related to the passage of elapsed time or reward expectation, correlates of which have been reported in the LPFC (Leon and Shadlen 1999, Roesch and Olson 2003, Berdyyeva and Olson 2011). Taken together, the different patterns of responses could be attributed to the different temporal events associated with the task. Such a representation in the LPFLC would be essential for mediating its role in the temporal organization of behavior (Tanji and Hoshi 2008).

In order to understand the interactions among the different subpopulations of neurons which were similar to the temporally distinct patterns obtained with nnmf, we calculated the spike count correlation between them. Interestingly, we observed that the correlations were highest among neurons with a similar temporal profile. A previous report also found high correlations among neurons with similar 'time tuning' in the CA1 region of the rodent (Modi, Dhawale et al. 2014). Moreover, strong correlations have been shown among neurons with similar response types (Komiyama, Sato et al. 2010). In addition, the correlations successively reduced among populations of neurons whose profiles were temporally separated. This indicates reduced effective functional connectivity among neurons which were temporally separated. Interestingly, this pattern of reduction was observed only among positive correlations, while the structure of negative correlations stayed similar across temporally divergent populations. Similar divergence among positive and negative correlations has been reported among the neurons recorded from the primary visual cortex. Specifically, positive correlation decreased exponentially as a function of the difference in the orientation preference between the cells, while the negative correlations displayed a uniform distribution (Chelaru and Dragoi 2014). It is striking that such a correspondence in the correlation structure is observed across different regions of the brain among neurons involved in representation of rather different neural processes. It makes one wonder if such a neural architecture could be perhaps a more generic computational principle employed by the brain.

Finally, such temporally contingent neuronal activity was similar across PA and FS conditions signifying that such a signal is unaffected by ambiguous visual input. Moreover, it co-exists with the representation of conscious visual content in the LPFC.

10

Outlook and future investigations

The work described in this thesis shows that feature selective neuronal activity explicitly reflects conscious visual content in the LPFC (Panagiotaropoulos, Deco et al. 2012). Thus, there are at least two areas in the brain which display such robust sensitivity to perceptual suppression, the second being the inferotemporal cortex (Sheinberg and Logothetis 1997). It currently remains unclear, if the nature of interactions between these two regions of the brain wherein population of neurons are modulated in concurrence with visual perception. Most interestingly, it is not yet known in which of the two areas does the cellular activity representing the result of perceptual selection during ambiguous input can be detected first. The modulation observed in the second region could then reflect a read out of this due to its reciprocal connectivity. Alternatively, the resolution of competition could appear simultaneously in two regions of the brain and could be mediated through dynamic interactions. This is best studied through population recordings in these two areas simultaneously. In order to study this, the first steps of developing a recording methodology, which allows us to access the temporal lobe with tetrodes was carried out. This is presented in chapter 8 of this thesis, wherein we developed novel tetrodes (called tube tetrodes), which are stronger and stiffer than conventional twisted wire tetrodes, allowing us to measure neuronal signals deep in the brain. In order to transport these tetrodes to the temporal lobe through a ball and socket chamber, a multi-tetrode microdrive system was also developed. Experimental validation of these TuTes showed that

they can detect reliable single unit activity from the temporal lobe in the macaque brain (Kapoor, Krampe et al. 2013).

Further, such electrophysiological recordings would be most insightful when carried out with paradigms which utilize free flowing binocular rivalry for instigating competition, wherein transitions in perception are stochastic and internally driven in comparison to the paradigm of binocular flash suppression, where such a transition is induced externally due to the nature of visual stimulation. The random nature of transitions shall aid in judging the chronology of neuronal activity across the two regions during perceptual changes and elucidate where one can observe the 'first switch' in perceptual modulation.

While most research with respect to understanding neurophysiology of multistable phenomena (including that described in this thesis) has focused on single unit activity or local field potential in limited regions of the cortex with single electrodes, the mesoscopic patterns of brain state during conscious visual perceptions remain currently unexplored. Therefore, another important research direction is to understand the state of cortical regions as represented by spatiotemporal patterns of activity with dense electrophysiology recordings during incongruent visual stimulation. This approach has also been proposed in a review, which has been detailed in Chapter three.

Recently it has been pointed out that in order to elucidate the true neural correlates of consciousness, it is essential to dissociate it from potential confounding cognitive components such as attention, working memory or expectation, which can be the result of reporting strategies utilized in various experimental designs (Aru, Bachmann et al. 2012, de Graaf, Hsieh et al. 2012, Tsuchiya, Wilke et al. 2015). In order to manage this, researchers now begin to rely on paradigms which do not require the subjects to report their perception and the subjective dominance or suppression is instead decoded from eye movements, pupil diameter or reliably controlled through subtle stimulus manipulations (Tsuchiya, Wilke et al. 2015). Therefore, future research could rely on such surrogate measures for the assessment of a subject's perceptual experience, with concurrent physiological investigation of different visual regions of the macaque brain.

To conclude, neural correlates of visual awareness have been observed not just in a single isolated node in the brain but in multiple regions displaying perceptual modulation to various degrees, with their activity most likely being orchestrated through dynamic interactions with each other. Therefore, most remarkable insights shall probably come to light from probing several regions in the brain simultaneously during visual competition, while we continue this Sherlockian investigative journey towards the pursuit of physiological underpinnings of conscious perception.

11

References

Abbott, L. F. and P. Dayan (1999). "The effect of correlated variability on the accuracy of a population code." Neural Comput **11**(1): 91-101.

Alais, D. and R. Blake (1999). "Grouping visual features during binocular rivalry." Vision Res **39**(26): 4341-4353.

Aru, J., T. Bachmann, W. Singer and L. Melloni (2012). "Distilling the neural correlates of consciousness." Neurosci Biobehav Rev **36**(2): 737-746.

Attneave, F. (1971). "Multistability in perception." Sci Am **225**(6): 63-71.

Averbeck, B. B., P. E. Latham and A. Pouget (2006). "Neural correlations, population coding and computation." Nat Rev Neurosci **7**(5): 358-366.

Averbeck, B. B. and D. Lee (2006). "Effects of noise correlations on information encoding and decoding." J Neurophysiol **95**(6): 3633-3644.

Awramik, S. M. (1992). "The oldest records of photosynthesis." Photosynth Res **33**(2): 75-89.

Bair, W., E. Zohary and W. T. Newsome (2001). "Correlated firing in macaque visual area MT: time scales and relationship to behavior." J Neurosci **21**(5): 1676-1697.

Baker, S. N. (2007). "Oscillatory interactions between sensorimotor cortex and the periphery." Curr Opin Neurobiol **17**(6): 649-655.

Baker, S. N., J. M. Kilner, E. M. Pinches and R. N. Lemon (1999). "The role of synchrony and oscillations in the motor output." Exp Brain Res **128**(1-2): 109-117.

Barbas, H. (1988). "Anatomic organization of basoventral and mediodorsal visual recipient prefrontal regions in the rhesus monkey." J Comp Neurol **276**(3): 313-342.

Barbas, H., T. H. Henion and C. R. Dermon (1991). "Diverse thalamic projections to the prefrontal cortex in the rhesus monkey." J Comp Neurol **313**(1): 65-94.

Bedard, C., H. Kroger and A. Destexhe (2006). "Does the 1/f frequency scaling of brain signals reflect self-organized critical states?" Physical Review Letters **97**(11).

Belitski, A., A. Gretton, C. Magri, Y. Murayama, M. A. Montemurro, N. K. Logothetis and S. Panzeri (2008). "Low-frequency local field potentials and spikes in primary visual cortex convey independent visual information." J Neurosci **28**(22): 5696-5709.

Berdyyeva, T. K. and C. R. Olson (2010). "Rank signals in four areas of macaque frontal cortex during selection of actions and objects in serial order." J Neurophysiol **104**(1): 141-159.

Berdyyeva, T. K. and C. R. Olson (2011). "Relation of ordinal position signals to the expectation of reward and passage of time in four areas of the macaque frontal cortex." J Neurophysiol **105**(5): 2547-2559.

Blake, R. (1989). "A neural theory of binocular rivalry." Psychol Rev **96**(1): 145-167.

Blake, R. and N. Logothetis (2002). "Visual competition." Nat Rev Neurosci **3**(1): 13-21.

Borra, E., N. Ichinohe, T. Sato, M. Tanifuji and K. S. Rockland (2010). "Cortical connections to area TE in monkey: hybrid modular and distributed organization." Cereb Cortex **20**(2): 257-270.

Borselli.A, Allazett.A, Bartolin.B, A. Rinesi and A. Demarco (1972). "Reversal Time Distribution in Perception of Visual Ambiguous Stimuli." Kybernetik **10**(3): 139-&.

Buschman, T. J., E. L. Denovellis, C. Diogo, D. Bullock and E. K. Miller (2012). "Synchronous oscillatory neural ensembles for rules in the prefrontal cortex." Neuron **76**(4): 838-846.

Buzsaki, G. (2004). "Large-scale recording of neuronal ensembles." Nat Neurosci **7**(5): 446-451.

Chavis, D. A. and D. N. Pandya (1976). "Further observations on corticofrontal connections in the rhesus monkey." Brain Res **117**(3): 369-386.

Chelaru, M. I. and V. Dragoi (2014). "Negative Correlations in Visual Cortical Networks." Cereb Cortex.

Cohen, M. R. and A. Kohn (2011). "Measuring and interpreting neuronal correlations." Nature Neuroscience **14**(7): 811-819.

Contini, M., M. Baccarini, E. Borra, M. Gerbella, S. Rozzi and G. Luppino (2010). "Thalamic projections to the macaque caudal ventrolateral prefrontal areas 45A and 45B." Eur J Neurosci **32**(8): 1337-1353.

Crick, F. and C. Koch (1990). "Toward a neurobiological theory of consciousness." Seminars in the Neurosciences **2**: 263-275.

Crick, F. and C. Koch (1998). "Consciousness and neuroscience." Cereb Cortex **8**(2): 97-107.

Darwin, C. (1859). On the origin of species by means of natural selection, or, The preservation of favoured races in the struggle for life. London, John Murray

de Graaf, T. A., P. J. Hsieh and A. T. Sack (2012). "The 'correlates' in neural correlates of consciousness." Neurosci Biobehav Rev **36**(1): 191-197.

Dehaene, S. and J. P. Changeux (2011). "Experimental and theoretical approaches to conscious processing." Neuron **70**(2): 200-227.

Donoghue, J. P., J. N. Sanes, N. G. Hatsopoulos and G. Gaal (1998). "Neural discharge and local field potential oscillations in primate motor cortex during voluntary movements." J Neurophysiol **79**(1): 159-173.

Dutour, E.-F. (1760). "Discussion d'une question d'optique [Discussion on a question of optics]." l'Académie des Sciences. Mémoires de Mathématique et de physique présentés par Divers Savants **3**: 514-530.

Dutour, E.-F. (1763). "Addition au Mémoire intitulé, Discussion d'une question d'Optique, imprimé dans le troisième Volume des Mémoires des Savan[t]s Étrangers, pages 514 & suivantes. [Addition to the Memoir entitled, Discussion on a question of Optics printed in the third Volume of Memoirs of Foreign Scientists, pages 514 and following]." Academie des Sciences. Mémoires de Mathématique et Physique Préséntes par Divers Savants **4**: 499-511.

Ecker, A. S., P. Berens, R. J. Cotton, M. Subramaniyan, G. H. Denfield, C. R. Cadwell, S. M. Smirnakis, M. Bethge and A. S. Tolias (2014). "State dependence of noise correlations in macaque primary visual cortex." Neuron **82**(1): 235-248.

Engel, A. K. and P. Fries (2010). "Beta-band oscillations--signalling the status quo?" Curr Opin Neurobiol **20**(2): 156-165.

Erickson, C. A. and R. Desimone (1999). "Responses of macaque perirhinal neurons during and after visual stimulus association learning." J Neurosci **19**(23): 10404-10416.

Erickson, C. A., B. Jagadeesh and R. Desimone (2000). "Clustering of perirhinal neurons with similar properties following visual experience in adult monkeys." Nat Neurosci **3**(11): 1143-1148.

Fahle, M. (1982). "Binocular rivalry: suppression depends on orientation and spatial frequency." Vision Res **22**(7): 787-800.

Fox, R. and J. Herrmann (1967). "Stochastic Properties of Binocular Rivalry Alternations." Perception & Psychophysics **2**(9): 432-436.

Frassle, S., J. Sommer, A. Jansen, M. Naber and W. Einhauser (2014). "Binocular rivalry: frontal activity relates to introspection and action but not to perception." J Neurosci **34**(5): 1738-1747.

Fuster, J. M. (2001). "The prefrontal cortex--an update: time is of the essence." Neuron **30**(2): 319-333.

Fuster, J. M. (2008). Chapter 8 - Overview of Prefrontal Functions: The Temporal Organization of Action. The Prefrontal Cortex (Fourth Edition). J. M. Fuster. San Diego, Academic Press**:** 333-385.

Fuster, J. M. (2008). The prefrontal cortex. Amsterdam ; Boston, Academic Press/Elsevier.

Gail, A., H. J. Brinksmeyer and R. Eckhorn (2004). "Perception-related modulations of local field potential power and coherence in primary visual cortex of awake monkey during binocular rivalry." Cereb Cortex **14**(3): 300-313.

Gaillard, R., S. Dehaene, C. Adam, S. Clemenceau, D. Hasboun, M. Baulac, L. Cohen and L. Naccache (2009). "Converging intracranial markers of conscious access." PLoS Biol **7**(3): e61.

Galvani, L. (1791). Aloysii Galvani De viribus electricitatis in motu musculari commentarius. Bononiae, Ex Typographia Instituti Scientiarum.

Gilbertson, T., E. Lalo, L. Doyle, V. Di Lazzaro, B. Cioni and P. Brown (2005). "Existing motor state is favored at the expense of new movement during 13-35 Hz oscillatory synchrony in the human corticospinal system." J Neurosci **25**(34): 7771-7779.

Goldman-Rakic, P. S., J. F. Bates and M. V. Chafee (1992). "The prefrontal cortex and internally generated motor acts." Curr Opin Neurobiol **2**(6): 830-835.

Goris, R. L., J. A. Movshon and E. P. Simoncelli (2014). "Partitioning neuronal variability." Nat Neurosci **17**(6): 858-865.

Gray, C. M., P. E. Maldonado, M. Wilson and B. McNaughton (1995). "Tetrodes markedly improve the reliability and yield of multiple single-unit isolation from multi-unit recordings in cat striate cortex." J Neurosci Methods **63**(1-2): 43-54.

Gutierrez, C., M. G. Cola, B. Seltzer and C. Cusick (2000). "Neurochemical and connectional organization of the dorsal pulvinar complex in monkeys." J Comp Neurol **419**(1): 61-86.

Harris, K. D., D. A. Henze, J. Csicsvari, H. Hirase and G. Buzsaki (2000). "Accuracy of tetrode spike separation as determined by simultaneous intracellular and extracellular measurements." Journal of Neurophysiology **84**(1): 401-414.

Harwerth, R. S. and E. L. Smith, 3rd (1985). "Rhesus monkey as a model for normal vision of humans." Am J Optom Physiol Opt **62**(9): 633-641.

Haynes, J. D., R. Deichmann and G. Rees (2005). "Eye-specific effects of binocular rivalry in the human lateral geniculate nucleus." Nature **438**(7067): 496-499.

Haynes, J. D. and G. Rees (2005). "Predicting the stream of consciousness from activity in human visual cortex." Curr Biol **15**(14): 1301-1307.

He, B. J. and M. E. Raichle (2009). "The fMRI signal, slow cortical potential and consciousness." Trends Cogn Sci **13**(7): 302-309.

Helmholtz, H. v., R. M. Warren and R. P. Warren (1968). Helmholtz on perception, its physiology, and development. New York,, Wiley.

Hodgkin, A. L. and A. F. Huxley (1939). "Action potentials recorded from inside a nerve fibre." Nature **144**: 710-711.

Inoue, M. and A. Mikami (2006). "Prefrontal activity during serial probe reproduction task: encoding, mnemonic, and retrieval processes." J Neurophysiol **95**(2): 1008-1041.

Jekely, G. (2009). "Evolution of phototaxis." Philos Trans R Soc Lond B Biol Sci **364**(1531): 2795-2808.

Jog, M. S., C. I. Connolly, Y. Kubota, D. R. Iyengar, L. Garrido, R. Harlan and A. M. Graybiel (2002). "Tetrode technology: advances in implantable hardware, neuroimaging, and data analysis techniques." Journal of Neuroscience Methods **117**(2): 141-152.

Jurkiewicz, M. T., W. C. Gaetz, A. C. Bostan and D. Cheyne (2006). "Post-movement beta rebound is generated in motor cortex: evidence from neuromagnetic recordings." Neuroimage **32**(3): 1281-1289.

Kaplan, I. T. and W. Metlay (1964). "Light Intensity and Binocular Rivalry." J Exp Psychol **67**: 22-26.

Kapoor, V., E. Krampe, A. Klug, N. K. Logothetis and T. I. Panagiotaropoulos (2013). "Development of tube tetrodes and a multi-tetrode drive for deep structure electrophysiological recordings in the macaque brain." J Neurosci Methods **216**(1): 43-48.

Keliris, G. A., N. K. Logothetis and A. S. Tolias (2010). "The role of the primary visual cortex in perceptual suppression of salient visual stimuli." J Neurosci **30**(37): 12353-12365.

Kilavik, B. E., M. Zaepffel, A. Brovelli, W. A. MacKay and A. Riehle (2013). "The ups and downs of beta oscillations in sensorimotor cortex." Exp Neurol **245**: 15-26.

Knapen, T., J. Brascamp, J. Pearson, R. van Ee and R. Blake (2011). "The role of frontal and parietal brain areas in bistable perception." J Neurosci **31**(28): 10293-10301.

Komiyama, T., T. R. Sato, D. H. O'Connor, Y. X. Zhang, D. Huber, B. M. Hooks, M. Gabitto and K. Svoboda (2010). "Learning-related fine-scale specificity imaged in motor cortex circuits of behaving mice." Nature **464**(7292): 1182-1186.

Kreiman, G., I. Fried and C. Koch (2002). "Single-neuron correlates of subjective vision in the human medial temporal lobe." Proc Natl Acad Sci U S A **99**(12): 8378-8383.

Lansing, R. W. (1964). "Electroencephalographic Correlates of Binocular Rivalry in Man." Science **146**(3649): 1325-1327.

Lee, D. D. and H. S. Seung (1999). "Learning the parts of objects by non-negative matrix factorization." Nature **401**(6755): 788-791.

Lee, S. H. and R. Blake (2002). "V1 activity is reduced during binocular rivalry." J Vis **2**(9): 618-626.

Lee, S. H., R. Blake and D. J. Heeger (2007). "Hierarchy of cortical responses underlying binocular rivalry." Nat Neurosci **10**(8): 1048-1054.

Lehky, S. R. and J. H. Maunsell (1996). "No binocular rivalry in the LGN of alert macaque monkeys." Vision Res **36**(9): 1225-1234.

Leon, M. I. and M. N. Shadlen (1999). "Effect of expected reward magnitude on the response of neurons in the dorsolateral prefrontal cortex of the macaque." Neuron **24**(2): 415-425.

Leopold, D. A. and N. K. Logothetis (1996). "Activity changes in early visual cortex reflect monkeys' percepts during binocular rivalry." Nature **379**(6565): 549-553.

Leopold, D. A. and N. K. Logothetis (1999). "Multistable phenomena: changing views in perception." Trends Cogn Sci **3**(7): 254-264.

Levelt, W. J. (1965). On Binocular Rivalry. PhD, Institute of Perception.

Levelt, W. J. (1967). "Note on the distribution of dominance times in binocular rivalry." Br J Psychol **58**(1): 143-145.

Libedinsky, C. and M. Livingstone (2011). "Role of prefrontal cortex in conscious visual perception." J Neurosci **31**(1): 64-69.

Logothetis, N. K. (1998). "Single units and conscious vision." Philos Trans R Soc Lond B Biol Sci **353**(1377): 1801-1818.

Logothetis, N. K. (2003). "The underpinnings of the BOLD functional magnetic resonance imaging signal." J Neurosci **23**(10): 3963-3971.

Logothetis, N. K., J. Pauls and T. Poggio (1995). "Shape representation in the inferior temporal cortex of monkeys." Curr Biol **5**(5): 552-563.

Logothetis, N. K. and J. D. Schall (1989). "Neuronal Correlates of Subjective Visual-Perception." Science **245**(4919): 761-763.

Lumer, E. D. (1998). "A neural model of binocular integration and rivalry based on the coordination of action-potential timing in primary visual cortex." Cereb Cortex **8**(6): 553-561.

Lumer, E. D., K. J. Friston and G. Rees (1998). "Neural correlates of perceptual rivalry in the human brain." Science **280**(5371): 1930-1934.

Luria, A. R. (1969). Frontal lobe syndromes. Handbook of Clinical Neurology. P. Vinken and G. Bruyn, North Holland**:** 2--725.

Magri, C., U. Schridde, Y. Murayama, S. Panzeri and N. K. Logothetis (2012). "The amplitude and timing of the BOLD signal reflects the relationship between local field potential power at different frequencies." J Neurosci **32**(4): 1395-1407.

Maier, A., M. Wilke, C. Aura, C. Zhu, F. Q. Ye and D. A. Leopold (2008). "Divergence of fMRI and neural signals in V1 during perceptual suppression in the awake monkey." Nat Neurosci **11**(10): 1193-1200.

Meenan, J. P. and L. A. Miller (1994). "Perceptual flexibility after frontal or temporal lobectomy." Neuropsychologia **32**(9): 1145-1149.

Miller, E. K. (1999). "The prefrontal cortex: complex neural properties for complex behavior." Neuron **22**(1): 15-17.

Miller, E. K. (2000). "The prefrontal cortex and cognitive control." Nat Rev Neurosci **1**(1): 59-65.

Miller, E. K. and J. D. Cohen (2001). "An integrative theory of prefrontal cortex function." Annu Rev Neurosci **24**: 167-202.

Miller, E. K. and M. A. Wilson (2008). "All my circuits: using multiple electrodes to understand functioning neural networks." Neuron **60**(3): 483-488.

Mitzdorf, U. (1985). "Current source-density method and application in cat cerebral cortex: investigation of evoked potentials and EEG phenomena." Physiol Rev **65**(1): 37-100.

Mitzdorf, U. (1987). "Properties of the evoked potential generators: current source-density analysis of visually evoked potentials in the cat cortex." Int J Neurosci **33**(1-2): 33-59.

Modi, M. N., A. K. Dhawale and U. S. Bhalla (2014). "CA1 cell activity sequences emerge after reorganization of network correlation structure during associative learning." Elife **3**: e01982.

Mojzsis, S. J., G. Arrhenius, K. D. McKeegan, T. M. Harrison, A. P. Nutman and C. R. Friend (1996). "Evidence for life on Earth before 3,800 million years ago." Nature **384**(6604): 55-59.

Moreno-Bote, R., J. Rinzel and N. Rubin (2007). "Noise-induced alternations in an attractor network model of perceptual bistability." J Neurophysiol **98**(3): 1125-1139.
Mueller, T. J. and R. Blake (1989). "A fresh look at the temporal dynamics of binocular rivalry." Biol Cybern **61**(3): 223-232.
Myerson, J. M., F.M.; Allman, J.M. (1981). "Binocular rivalry in macaque monkeys and humans: A comparative study in perception." BEHAVIOUR ANALYSIS LETTERS **1**(3): 149-159.
Necker, L. A. (1832). "LXI. Observations on some remarkable optical phænomena seen in Switzerland; and on an optical phænomenon which occurs on viewing a figure of a crystal or geometrical solid." Philosophical Magazine Series 3 **1**(5): 329-337.
Nguyen, D. P., S. P. Layton, G. Hale, S. N. Gomperts, T. J. Davidson, F. Kloosterman and M. A. Wilson (2009). "Micro-drive array for chronic in vivo recording: tetrode assembly." J Vis Exp(26).
Ninokura, Y., H. Mushiake and J. Tanji (2003). "Representation of the temporal order of visual objects in the primate lateral prefrontal cortex." J Neurophysiol **89**(5): 2868-2873.
Ninokura, Y., H. Mushiake and J. Tanji (2004). "Integration of temporal order and object information in the monkey lateral prefrontal cortex." J Neurophysiol **91**(1): 555-560.
Norman, D. A. and T. Shallice (1986). Attention to action: willed and automatic control of behavior. Consciousness and Self-Regulation. R. J. S. Davidson, G.E.; Shapiro, D. New York, Plenum Press. **4:** 1-14.
O'Leary, J. G. and N. G. Hatsopoulos (2006). "Early visuomotor representations revealed from evoked local field potentials in motor and premotor cortical areas." J Neurophysiol **96**(3): 1492-1506.
O'Shea, R. P. (1999). "Translation of Dutour (1760)."
O'Shea, R. P. (1999). "Translation of Dutour (1763)."
Paatero, P. and U. Tapper (1994). "Positive Matrix Factorization - a Nonnegative Factor Model with Optimal Utilization of Error-Estimates of Data Values." Environmetrics **5**(2): 111-126.

Panagiotaropoulos, T. I., G. Deco, V. Kapoor and N. K. Logothetis (2012). "Neuronal discharges and gamma oscillations explicitly reflect visual consciousness in the lateral prefrontal cortex." Neuron **74**(5): 924-935.

Panagiotaropoulos, T. I., V. Kapoor, N. K. Logothetis and G. Deco (2013). "A common neurodynamical mechanism could mediate externally induced and intrinsically generated transitions in visual awareness." PLoS One **8**(1): e53833.

Pastukhov, A., P. E. Garcia-Rodriguez, J. Haenicke, A. Guillamon, G. Deco and J. Braun (2013). "Multi-stable perception balances stability and sensitivity." Front Comput Neurosci **7**: 17.

Pfurtscheller, G., A. Stancak, Jr. and C. Neuper (1996). "Post-movement beta synchronization. A correlate of an idling motor area?" Electroencephalogr Clin Neurophysiol **98**(4): 281-293.

Pigarev, I. N., G. Rizzolatti and C. Scandolara (1979). "Neurons responding to visual stimuli in the frontal lobe of macaque monkeys." Neurosci Lett **12**(2-3): 207-212.

Pine, J. (2006). A History of MEA Development. Advances in Network Electrophysiology. M. Taketani and M. Baudry, Springer US**:** 3-23.

Pogosyan, A., L. D. Gaynor, A. Eusebio and P. Brown (2009). "Boosting cortical activity at Beta-band frequencies slows movement in humans." Curr Biol **19**(19): 1637-1641.

Polonsky, A., R. Blake, J. Braun and D. J. Heeger (2000). "Neuronal activity in human primary visual cortex correlates with perception during binocular rivalry." Nat Neurosci **3**(11): 1153-1159.

Porta, J. B. (1593). De refractione. Optices parte. Libri novem., Naples: Salviani.

Puig, M. V. and E. K. Miller (2012). "The role of prefrontal dopamine D1 receptors in the neural mechanisms of associative learning." Neuron **74**(5): 874-886.

Rao, S. C., G. Rainer and E. K. Miller (1997). "Integration of what and where in the primate prefrontal cortex." Science **276**(5313): 821-824.

Renart, A., J. de la Rocha, P. Bartho, L. Hollender, N. Parga, A. Reyes and K. D. Harris (2010). "The asynchronous state in cortical circuits." Science **327**(5965): 587-590.

Ricci, C. and C. Blundo (1990). "Perception of ambiguous figures after focal brain lesions." Neuropsychologia **28**(11): 1163-1173.

Roesch, M. R. and C. R. Olson (2003). "Impact of expected reward on neuronal activity in prefrontal cortex, frontal and supplementary eye fields and premotor cortex." J Neurophysiol **90**(3): 1766-1789.

Romanski, L. M. (2012). Convergence of Auditory, Visual, and Somatosensory Information in Ventral Prefrontal Cortex. The Neural Bases of Multisensory Processes. M. M. Murray and M. T. Wallace. Boca Raton (FL).

Romanski, L. M., M. Giguere, J. F. Bates and P. S. Goldman-Rakic (1997). "Topographic organization of medial pulvinar connections with the prefrontal cortex in the rhesus monkey." J Comp Neurol **379**(3): 313-332.

Rosenkilde, C. E., R. H. Bauer and J. M. Fuster (1981). "Single cell activity in ventral prefrontal cortex of behaving monkeys." Brain Res **209**(2): 375-394.

Rubin, E. (1915). Synsoplevede figurer, studier i psykologisk analyse. København og Kristiania,, Gyldendal, Nordisk forlag.

Safavi, S., V. Kapoor, N. K. Logothetis and T. I. Panagiotaropoulos (2014). "Is the frontal lobe involved in conscious perception?" Front Psychol **5**: 1063.

Sanes, J. N. and J. P. Donoghue (1993). "Oscillations in local field potentials of the primate motor cortex during voluntary movement." Proc Natl Acad Sci U S A **90**(10): 4470-4474.

Santos, L., I. Opris, J. Fuqua, R. E. Hampson and S. A. Deadwyler (2012). "A novel tetrode microdrive for simultaneous multi-neuron recording from different regions of primate brain." J Neurosci Methods **205**(2): 368-374.

Scanziani, M. and M. Hausser (2009). "Electrophysiology in the age of light." Nature **461**(7266): 930-939.

Schiller, P. H. and F. Koerner (1971). "Discharge characteristics of single units in superior colliculus of the alert rhesus monkey." J Neurophysiol **34**(5): 920-936.

Schopf, J. W. (1993). "Microfossils of the Early Archean Apex chert: new evidence of the antiquity of life." Science **260**: 640-646.

Sheinberg, D. L. and N. K. Logothetis (1997). "The role of temporal cortical areas in perceptual organization." Proc Natl Acad Sci U S A **94**(7): 3408-3413.

Shpiro, A., R. Moreno-Bote, N. Rubin and J. Rinzel (2009). "Balance between noise and adaptation in competition models of perceptual bistability." J Comput Neurosci **27**(1): 37-54.

Siegel, M., M. R. Warden and E. K. Miller (2009). "Phase-dependent neuronal coding of objects in short-term memory." Proc Natl Acad Sci U S A **106**(50): 21341-21346.

Skaggs, W. E., B. L. McNaughton, M. Permenter, M. Archibeque, J. Vogt, D. G. Amaral and C. A. Barnes (2007). "EEG sharp waves and sparse ensemble unit activity in the macaque hippocampus." J Neurophysiol **98**(2): 898-910.

Sompolinsky, H., H. Yoon, K. Kang and M. Shamir (2001). "Population coding in neuronal systems with correlated noise." Phys Rev E Stat Nonlin Soft Matter Phys **64**(5 Pt 1): 051904.

SP, O. S., F. A. Wilson and P. S. Goldman-Rakic (1997). "Areal segregation of face-processing neurons in prefrontal cortex." Science **278**(5340): 1135-1138.

Sterzer, P. and A. Kleinschmidt (2007). "A neural basis for inference in perceptual ambiguity." Proc Natl Acad Sci U S A **104**(1): 323-328.

Swann, N., N. Tandon, R. Canolty, T. M. Ellmore, L. K. McEvoy, S. Dreyer, M. DiSano and A. R. Aron (2009). "Intracranial EEG reveals a time- and frequency-specific role for the right inferior frontal gyrus and primary motor cortex in stopping initiated responses." J Neurosci **29**(40): 12675-12685.

Tanji, J. and E. Hoshi (2008). "Role of the lateral prefrontal cortex in executive behavioral control." Physiol Rev **88**(1): 37-57.

Taylor, M. M. and K. D. Aldridge (1974). "Stochastic-Processes in Reversing Figure Perception." Perception & Psychophysics **16**(1): 9-27.

Theobald, D. L. (2010). "A formal test of the theory of universal common ancestry." Nature **465**(7295): 219-222.

Theodoni, P., T. I. Panagiotaropoulos, V. Kapoor, N. K. Logothetis and G. Deco (2011). "Cortical microcircuit dynamics mediating binocular rivalry: the role of adaptation in inhibition." Front Hum Neurosci **5**: 145.

Thome, A., C. A. Erickson, P. Lipa and C. A. Barnes (2012). "Differential effects of experience on tuning properties of macaque MTL neurons in a passive viewing task." Hippocampus **22**(10): 2000-2011.

Tolias, A. S., A. S. Ecker, A. G. Siapas, A. Hoenselaar, G. A. Keliris and N. K. Logothetis (2007). "Recording chronically from the same neurons in awake, behaving primates." J Neurophysiol **98**(6): 3780-3790.

Tong, F. and S. A. Engel (2001). "Interocular rivalry revealed in the human cortical blind-spot representation." Nature **411**(6834): 195-199.

Tsuchiya, N., M. Wilke, S. Frassle and V. A. Lamme (2015). "No-Report Paradigms: Extracting the True Neural Correlates of Consciousness." Trends Cogn Sci.

van Gaal, S., F. P. de Lange and M. X. Cohen (2012). "The role of consciousness in cognitive control and decision making." Front Hum Neurosci **6**: 121.

van Gaal, S. and V. A. Lamme (2012). "Unconscious high-level information processing: implication for neurobiological theories of consciousness." Neuroscientist **18**(3): 287-301.

Walker, P. (1975). "Stochastic Properties of Binocular Rivalry Alternations." Perception & Psychophysics **18**(6): 467-473.

Wallis, J. D., K. C. Anderson and E. K. Miller (2001). "Single neurons in prefrontal cortex encode abstract rules." Nature **411**(6840): 953-956.

Webster, M. J., J. Bachevalier and L. G. Ungerleider (1993). "Subcortical connections of inferior temporal areas TE and TEO in macaque monkeys." J Comp Neurol **335**(1): 73-91.

Webster, M. J., J. Bachevalier and L. G. Ungerleider (1994). "Connections of inferior temporal areas TEO and TE with parietal and frontal cortex in macaque monkeys." Cereb Cortex **4**(5): 470-483.

Werner, J. S. and L. M. Chalupa (2004). The visual neurosciences. Cambridge, Mass., MIT Press.

Wheatstone, C. (1838). "Contributions to the Physiology of Vision. Part the First. On Some Remarkable, and Hitherto Unobserved, Phenomena of Binocular Vision." Philosophical Transactions of the Royal Society of London **128**: 371-394.

White, I. M. and S. P. Wise (1999). "Rule-dependent neuronal activity in the prefrontal cortex." Exp Brain Res **126**(3): 315-335.

Wilke, M., N. K. Logothetis and D. A. Leopold (2003). "Generalized flash suppression of salient visual targets." Neuron **39**(6): 1043-1052.

Wilke, M., N. K. Logothetis and D. A. Leopold (2006). "Local field potential reflects perceptual suppression in monkey visual cortex." Proc Natl Acad Sci U S A **103**(46): 17507-17512.

Wilke, M., K. M. Mueller and D. A. Leopold (2009). "Neural activity in the visual thalamus reflects perceptual suppression." Proc Natl Acad Sci U S A **106**(23): 9465-9470.

Wilke, S. D. and C. W. Eurich (2002). "Representational accuracy of stochastic neural populations." Neural Comput **14**(1): 155-189.

Wilson, F. A., S. P. Scalaidhe and P. S. Goldman-Rakic (1993). "Dissociation of object and spatial processing domains in primate prefrontal cortex." Science **260**(5116): 1955-1958.

Windmann, S., M. Wehrmann, P. Calabrese and O. Gunturkun (2006). "Role of the prefrontal cortex in attentional control over bistable vision." J Cogn Neurosci **18**(3): 456-471.

Wolfe, J. M. (1984). "Reversing ocular dominance and suppression in a single flash." Vision Res **24**(5): 471-478.

Yeterian, E. H., D. N. Pandya, F. Tomaiuolo and M. Petrides (2012). "The cortical connectivity of the prefrontal cortex in the monkey brain." Cortex **48**(1): 58-81.

Zaretskaya, N. and M. Narinyan (2014). "Introspection, attention or awareness? The role of the frontal lobe in binocular rivalry." Front Hum Neurosci **8**: 527.

Zaretskaya, N., A. Thielscher, N. K. Logothetis and A. Bartels (2010). "Disrupting parietal function prolongs dominance durations in binocular rivalry." Curr Biol **20**(23): 2106-2111.

Zohary, E., M. N. Shadlen and W. T. Newsome (1994). "Correlated neuronal discharge rate and its implications for psychophysical performance." Nature **370**(6485): 140-143.

12

List of papers and statement of contributions

12.1 Panagiotaropoulos TI*****, Deco G*****, **Kapoor V** and Logothetis NK (June-2012). **Neuronal discharges and gamma oscillations explicitly reflect visual consciousness in the lateral prefrontal cortex.** *Neuron* 74(5) 924–935.

T.I. Panagiotaropoulos and N.K. Logothetis designed the study. V. Kapoor and T.I. Panagiotaropoulos performed the electrophysiology experiments and data collection. T.I. Panagiotaropolous performed the analysis with contributions from G.Deco and V.Kapoor. V.Kapoor trained an animal and collected and analyzed behavioral psychophysical data. T.I. Panagiotaropoulos, V.Kapoor, G.Deco and N.K. Logothetis participated in the discussion and evaluation of the results. T.I. Panagiotaropoulos wrote the first draft of the manuscript and all the authors gave feedback on the manuscript.

12.2 Panagiotaropoulos TI, **Kapoor V** and Logothetis NK (March-2014). **Subjective visual perception: from local processing to emergent phenomena of brain activity.** *Philosophical Transactions of the Royal Society London B* **369(1641)** 1-13.

T.I. Panagiotaropoulos and V.Kapoor discussed the results of previous publications in order to put them into context with our current findings. T.I. Panagiotaropoulos wrote the first

draft of the manuscript. V. Kapoor and N.K. Logothetis provided comments and feedback on the manuscript.

12.3 Panagiotaropoulos TI*****, Theodoni P*****, **Kapoor V***, Deco G, Logothetis NK. **Decorrelated discharge fluctuations in prefrontal microcircuits during visual consciousness.** (* - equal contribution) (Manuscript under preparation)

V.Kapoor and T.I. Panagiotaropoulos conducted the electrophysiology experiments and collected the data. T.I. Panagiotaropoulos performed the noise correlation analysis with contributions from V.Kapoor. Y. Theodoni and G.Deco contributed to the simulation work. T.I. Panagiotaropoulos, V.Kapoor, P.Theodoni, G.Deco and N.K. Logothetis participated in the discussion and evaluation of the results. T.I. Panagiotaropoulos wrote the first draft of the manuscript with feedback from all other authors.

12.4 Safavi S*****, **Kapoor V***, Logothetis NK and Panagiotaropoulos TI (September-2014). **Is the frontal lobe involved in conscious perception?** *Frontiers in Psychology* 5(1063) 1-2. (* - equal contribution)

V.Kapoor, S.Safavi and T.I. Panagiotaropoulos discussed the goal and layout of the opinion article. V.Kapoor and S.Safavi wrote the first draft of the manuscript. T.I. Panagiotaropoulos and N.K. Logothetis gave feedback and comments on the manuscript.

12.5 Panagiotaropoulos TI, **Kapoor V** and Logothetis NK (September -2013). **Desynchronization and rebound of beta oscillations during conscious and unconscious local neuronal processing in the macaque lateral prefrontal cortex.** *Frontiers in Psychology* 4(603) 1-10.

V.Kapoor and T.I. Panagiotaropoulos conducted the experiments. T.I. Panagiotaropoulos performed the analysis. T.I. Panagiotaropoulos, V.Kapoor and N.K. Logothetis participated in the discussion and evaluation of results. T.I. Panagiotaropoulos wrote the first draft of the manuscript. V.Kapoor and N.K. Logothetis gave comments and feedback on the manuscript.

12.6 **Kapoor V,** Besserve M, Logothetis NK, Panagiotaropoulos TI. **Sequential neuronal activity in the lateral prefrontal cortex during the task of binocular flash suppression.** (Manuscript under preparation)

V.Kapoor and T.I. Panagiotaropoulos designed the study. V.Kapoor analyzed the data with contributions from M. Besserve. V.Kapoor, T.I. Panagiotaropoulos, M.Besserve and N.K. Logothetis participated in discussion and evaluation of the results. V.Kapoor wrote the first draft of the manuscript with contributions on the methods section from M. Besserve. T.I. Panagiotaropoulos, M.Besserve and N.K. Logothetis provided comments and feedback on the manuscript.

12.7 **Kapoor V,** Krampe E, Klug A, Logothetis NK and Panagiotaropoulos TI (May-2013). **Development of tube tetrodes and a multi-tetrode drive for deep structure electrophysiological recordings in the macaque brain.** *Journal of Neuroscience Methods* 216(1) 43–48.

V.Kapoor and T.I. Panagiotaropoulos designed the study. V.Kapoor and E.Krampe standardized the procedures for development of tetrodes. V.Kapoor and A.Klug developed the multi-tetrode drive. T.I. Panagiotaropoulos supervised these developments. V.Kapoor and T.I. Panagiotaropoulos conducted the experiments. V.Kapoor analyzed the data. V.Kapoor, T.I. Panagiotaropoulos and N.K. Logothetis participated in the discussion and evaluation of results. V.Kapoor wrote the first draft of the manuscript. T.I. Panagiotaropoulos and N.K. Logothetis gave feedback on the manuscript.

Appendix

A.1 Neuronal discharges and gamma oscillations explicitly reflect visual consciousness in the lateral prefrontal cortex.

"Before brains there was no color and no sound in the universe, nor was there any flavor or aroma and probably little sense and no feeling or emotion."

Roger Sperry, "Problems outstanding in the evolution of brain function"

Neuron
Article

Neuronal Discharges and Gamma Oscillations Explicitly Reflect Visual Consciousness in the Lateral Prefrontal Cortex

Theofanis I. Panagiotaropoulos,[1,5,*] Gustavo Deco,[2,3,5] Vishal Kapoor,[1] and Nikos K. Logothetis[1,4]
[1]Department of Physiology of Cognitive Processes, Max Planck Institute for Biological Cybernetics, 72076 Tübingen, Germany
[2]Center for Brain and Cognition, Computational Neuroscience Group, Department of Information and Communications Technologies
[3]Institució Catalana de la Recerca i Estudis Avançats
Universitat Pompeu Fabra, Barcelona 08010, Spain
[4]Division of Imaging Science and Biomedical Engineering, University of Manchester, Manchester M13 9PT, UK
[5]These authors contributed equally to this work
*Correspondence: theofanis.panagiotaropoulos@tuebingen.mpg.de
DOI 10.1016/j.neuron.2012.04.013

SUMMARY

Neuronal discharges in the primate temporal lobe, but not in the striate and extrastriate cortex, reliably reflect stimulus awareness. However, it is not clear whether visual consciousness should be uniquely localized in the temporal association cortex. Here we used binocular flash suppression to investigate whether visual awareness is also explicitly reflected in feature-selective neural activity of the macaque lateral prefrontal cortex (LPFC), a cortical area reciprocally connected to the temporal lobe. We show that neuronal discharges in the majority of single units and recording sites in the LPFC follow the phenomenal perception of a preferred stimulus. Furthermore, visual awareness is reliably reflected in the power modulation of high-frequency (>50 Hz) local field potentials in sites where spiking activity is found to be perceptually modulated. Our results suggest that the activity of neuronal populations in at least two association cortical areas represents the content of conscious visual perception.

INTRODUCTION

The neural signature of visual consciousness can be detected in the electrical activity of multiple cortical areas across the visual hierarchy, during tasks that permit a dissociation of purely sensory stimulation from subjective perception. Binocular rivalry (BR) and binocular flash suppression (BFS) are extensively used paradigms of such ambiguous stimulation in which two disparate visual patterns, presented at corresponding parts of the two retinas, compete for access to perceptual awareness.

Electrophysiological recordings combined with BR and/or BFS showed a stronger correlation between conscious visual perception and neuronal activity in higher association areas of the cortex. In the primary visual cortex (V1) and visual area V2, only 14% of the recorded sites and 20%–25% of single units fired more when a preferred stimulus was consciously perceived (Gail et al., 2004; Keliris et al., 2010; Leopold and Logothetis, 1996). In cortical areas V4 and MT, single unit activity (SUA) was also weakly correlated with perceptual dominance since only 25% of the recorded population was found to discharge in consonance with the perceptual dominance of a preferred stimulus (Leopold and Logothetis, 1996; Logothetis and Schall, 1989; Maier et al., 2007). Interestingly, V4 and MT showed significant traces of nonconscious stimulus processing since a fraction of the perceptually modulated selective neurons (13% and 20%, respectively) fired more when their preferred stimulus was perceptually suppressed. In striking contrast, almost 90% of the recorded units in the superior temporal sulcus (STS) and inferior temporal (IT) cortex reflected the phenomenal perception of a preferred stimulus (Sheinberg and Logothetis, 1997). Similar results were obtained from recordings in the human medial temporal lobe (MTL), where two thirds of the sensory selective neurons fired more during the phenomenal perception of their preferred stimulus (Kreiman et al., 2002). Furthermore, nonconscious stimulus processing was absent in human MTL and macaque STS/IT cortex, where none of the modulated cells consistently fired more during the perceptual suppression of a preferred stimulus.

These findings led to the hypothesis that perceptually modulated activity in early, extrastriate cortical areas reflects competitive interactions mediating image segmentation, figure-ground segregation, and perceptual grouping, mechanisms that give rise to perceptual organization and, therefore, subjective visual perception (Blake and Logothetis, 2002; Logothetis, 1998). In contrast, perceptually modulated activity in the temporal lobe represents a final stage of cortical processing, beyond the resolution of ambiguities in the sensory environment, where neural activity explicitly represents the content of visual consciousness (Blake and Logothetis, 2002; Logothetis, 1998). However, the temporal cortex is not the final endpoint of the ventral visual processing stream. The STS/IT cortex is reciprocally connected to visual areas of the lateral prefrontal cortex (LPFC) (Barbas, 1988; Borra et al., 2010; Webster et al., 1994; Yeterian et al., 2012) where neuronal activity, including single units, is also

known to respond selectively to faces and complex visual objects similar to the perceptually modulated cells found in the STS/IT cortex (Pigarev et al., 1979; Ó Scalaidhe et al., 1997, 1999; Tsao et al., 2008). Thus, an intriguing question is whether such feature-selective neuronal activity in the LPFC correlates with phenomenal perception under conditions introducing perceptual ambiguity.

Previous studies provided strong evidence supporting a role for the LPFC in spontaneously induced perceptual alternations. For example, patients with widespread prefrontal cortex lesions show abnormal perceptual transitions during bistable perception (Meenan and Miller, 1994; Ricci and Blundo, 1990; Windmann et al., 2006; but see Valle-Inclán and Gallego, 2006). In addition, human functional magnetic resonance imaging (fMRI) studies repeatedly revealed an increase in the blood-oxygenation-level-dependent (BOLD) signal of the inferior prefrontal gyrus during endogenously triggered perceptual alternations compared to purely sensory stimulus transitions (Lumer et al., 1998; Sterzer and Kleinschmidt, 2007; Zaretskaya et al., 2010). More recently, a direct neuronal correlate of perceptual transitions was identified in the firing rate modulation of neurons in the macaque frontal eye fields, which predicted perceptual alternations during the bistable paradigm of motion-induced blindness (Libedinsky and Livingstone, 2011). Although these findings undoubtedly demonstrate a crucial contribution of the LPFC in perceptual transitions, no studies have yet been undertaken to examine perceptual modulation of feature selective neural activity in the LPFC during incongruent visual input. This is particularly important since the maintenance of feature-selective neuronal activity under conditions of visual ambiguity is thought to be a prerequisite for visual consciousness, allowing and reflecting explicit neural processing of the perceived stimulus (Crick and Koch, 1998, 2003).

Here we studied whether spiking activity and local field potentials (LFPs) in the LPFC represent the perceptual dominance of a preferred stimulus during 1 s of visual ambiguity externally induced by BFS. Our results show that feature-selective spiking activity and the power of high-frequency gamma oscillations in the LPFC largely reflect the content of subjective visual perception. Some weak traces, compared to primary and secondary sensory areas, of nonconscious stimulus processing were also observed in the spiking activity during the perceptual dominance of a nonpreferred stimulus.

RESULTS

BFS

We recorded simultaneously neuronal discharges and LFPs in the LPFC of two alert macaques during a passive fixation task that included randomly interleaved trials of physical alternation and BFS. BFS constitutes a highly controlled variant of BR that has been extensively used to dissociate subjective visual perception from purely sensory stimulation (Kreiman et al., 2002; Maier et al., 2007; Sheinberg and Logothetis, 1997; Wolfe, 1984). The BFS (“perceptual”) trials, as well as the physical (“sensory”) alternation of the visual stimuli that was used as a control condition, are depicted in Figure 1. Every trial starts with the presentation of a fixation spot in both eyes that is binocularly fused and remains on until the end of the trial. In both sensory (Figure 1A, upper panel, “Physical alternation”) and perceptual (Figure 1A, lower panel, “Flash suppression”) trials, a fixation spot was presented for 300 ms followed by monocular stimulation with the same visual pattern (a polar checkerboard in the paradigm presented in the figure). In perceptual trials, 1 s after stimulus onset, a disparate visual pattern (here, a monkey face) is suddenly flashed to the corresponding part of the contralateral eye. It has been repeatedly shown that, in both humans and monkeys, the flashed stimulus remains dominant for at least 1,000 ms, robustly suppressing the perception of the contralaterally presented visual pattern that is still physically present (Wolfe, 1984; Sheinberg and Logothetis, 1997; Keliris et al., 2010). We provide additional behavioral evidence for the robust suppression elicited by our paradigm in Figure S1, available online. The mean dominance time of the flashed stimulus was almost 2 s for a separate monkey that was trained to report BFS after the end of our electrophysiological recordings. Thus, in perceptual trials, a visual competition period dissociating sensory stimulation from perception is externally induced for at least 1,000 ms. During this period, the newly presented image is perceptually dominant while the initially presented visual pattern is perceptually suppressed despite its physical presence in the retina (Figure 1A, middle panel). In sensory trials, the same visual patterns physically alternate between the two eyes, resulting in a visual percept identical to the perceptual condition but this time without any concurrent visual competition (Figure 1A, upper panel). Specifically, after 1 s of visual stimulation, the initially presented pattern is removed and immediately followed by the presentation of the disparate pattern in the contralateral eye.

SUA in the LPFC Follows Phenomenal Perception during BFS

We recorded the spiking activity from 211 recording sites (n = 577 cells) in the LPFCs of two alert monkeys. We focused our analysis on cells exhibiting feature-selective spiking activity, detected during the monocular presentation of two disparate stimuli in physical alternation trials. We examined whether significant sensory feature selectivity was maintained, eliminated, or reversed during subjective visual perception of the same visual patterns (i.e., during BFS). In addition, we studied whether feature selectivity was developed during BFS across sensory nonselective units.

We found that 19% of the total sample of recorded cells (n = 110/577) exhibited a statistically significant preference (i.e., they fired more) for one of the two monocularly presented stimuli in the physical alternation condition (Wilcoxon rank-sum test, $p < 0.05$). Our results show that 58% of the single units showing such a significant sensory preference in the physical alternation condition were also significantly modulated during BFS (n = 64/110; Figure 2A). During BFS, almost all of these units (n = 61/64, or 95%) maintained the same stimulus preference that was observed during monocular physical alternation, indicating only weak traces of nonconscious stimulus processing (Figure 2A). The magnitude of perceptual modulation for sensory modulated units shows that SUA in the LPFC follows phenomenal perception much more efficiently than SUA in lower visual

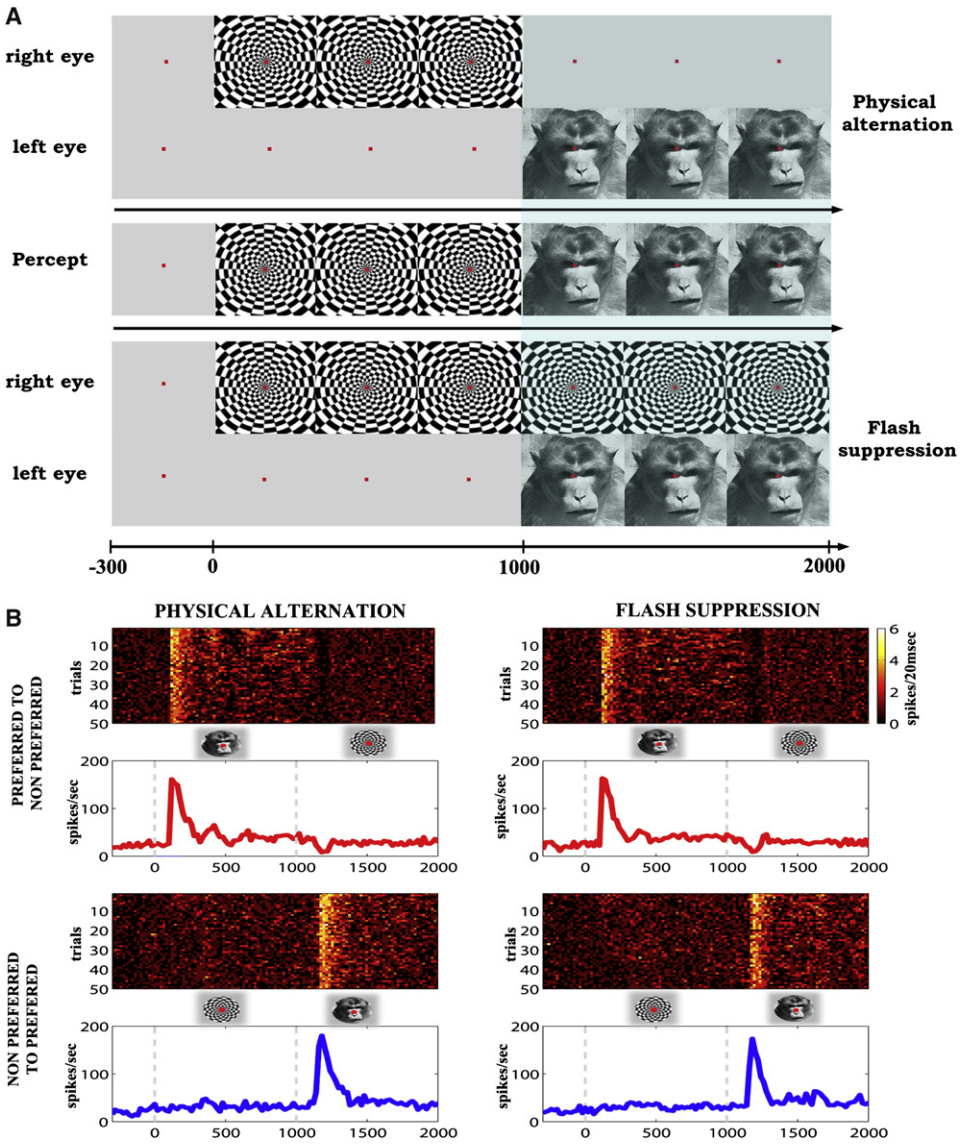

Figure 1. Behavioral Task and Typical Single Unit Modulation

(A) Physical alternation (upper panel) and BFS (lower panel) paradigm. For psychophysical measurements demonstrating the duration of perceptual suppression, see also Figure S1.

(B) Example raster plots (in 20 ms time bins) and mean discharge responses for a single unit showing a strong preference for a monkey face during both physical alternation (left panel) and BFS (right panel). Stimuli insets depict the perceived visual pattern.

areas. Specifically, we found that the mean magnitude of perceptual modulation across all 110 sensory modulated units was significantly decreased compared to their mean sensory modulation (54% of sensory modulation; $d'_{\text{sensory SUA}} = 0.46 \pm 0.06$ and $d'_{\text{perceptual SUA}} = 0.25 \pm 0.07$, Wilcoxon rank-sum test $p < 0.001$; Figure 2A). However, albeit significantly reduced compared to monocular stimulation, the magnitude of the observed modulation is much higher than the respective modulation of sensory tuned single units during BFS in V1 (reported to be 15% of sensory modulation; see Keliris et al., 2010). At the same time, these findings show that the percentage of both sensory and perceptually modulated LPFC cells is considerably smaller (almost 60%) than the respective percentage (almost 90%) found in STS/IT (Sheinberg and Logothetis, 1997) but very similar to the percentage of perceptually modulated cells found in the human MTL during BFS (67%; Kreiman et al., 2002).

This relative discrepancy between STS/IT and LPFC could be attributed to two different reasons. First, it is possible that perceptual modulation reaches a maximum in intermediate cortical areas (like STS/IT) and is lower in the LPFC or the MTL (Crick and Koch, 1998; Kreiman et al., 2002). The second reason is related to the magnitude of selectivity of the single units under study. Cells with stronger modulation during monocular stimulation could be much more prone to retain this modulation under

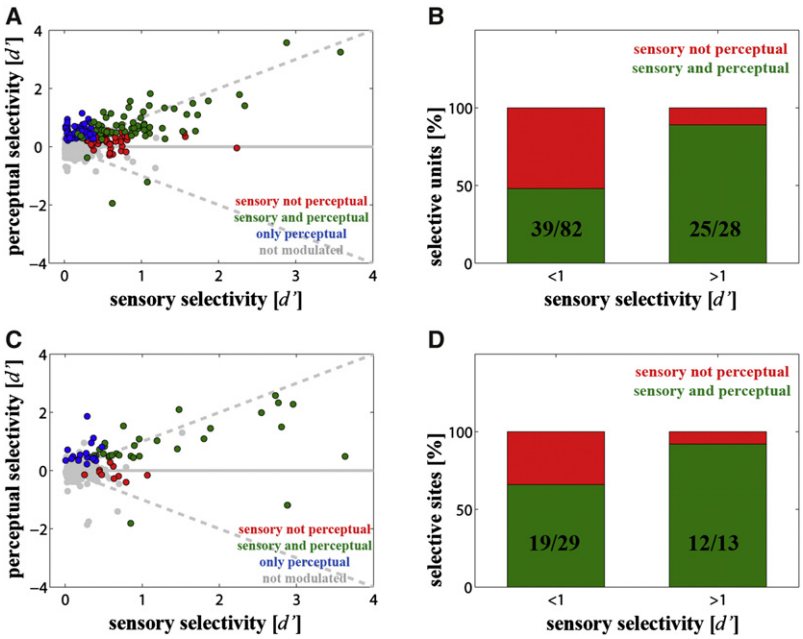

Figure 2. Sensory versus Perceptual Modulation of Neuronal Discharges

(A) Scatterplot of sensory versus perceptual preference (d′) for all 577 recorded single units. Grey dots represent single units showing no significant modulation in either of the two conditions. Green dots represent units showing significant modulation during both physical alternation and BFS. Red dots represent units that showed only significant sensory preference. Blue dots depict single units that exhibited significant modulation only during the BFS condition. Only 5% of the sensory modulated units (green dots, n = 3/64) fired more when their preferred stimulus was perceptually suppressed (represented here by a negative d′ value). The large majority of perceptually modulated single units followed phenomenal perception. For typical examples of perceptually modulated single units, see Figure S2.

(B) Significant modulation during both physical alternation and BFS is more likely for units showing high sensory selectivity ($d' > 1$).

(C) Same as (A) for MUA. Here, each point represents the sensory versus perceptual selectivity (d′) of the summed, local spiking activity within a cortical site. The spiking activity in the large majority of sensory modulated sites followed the phenomenal perception of a preferred stimulus.

(D) Same as (B) for MUA. Perceptual modulation is more likely for units showing stronger sensory selectivity (d′ > 1). Insets in bars in (B) and (D) show the ratio: number of sensory and perceptually modulated/number of sensory modulated cells.

BFS. Sheinberg and Logothetis (1997) took particular care to record from STS/IT cells with very strong sensory modulation, while the single unit population in our study shows a higher variability in the degree of sensory modulation. Indeed, we observed that, when units with very high sensory modulation were selected ($d'_{\text{sensory SUA}} > 1$), the percentage of significantly sensory and perceptually modulated units in the LPFC increased to the levels reported for the STS/IT cortex (Figure 2B). Specifically, 89% (n = 25/28) of sensory modulated single units were found to be significantly modulated during BFS when $d'_{\text{sensory SUA}} > 1$. Only 4% of these units (n = 1/25) reversed their preference during BFS (analysis of variance [ANOVA], Stimulus × Condition interaction effect, $p < 0.05$).

Furthermore, when our statistical criteria were more conservative and the p values of the firing rate differences in the physical alternation condition were corrected for multiple comparisons, the percentage of single units found to be both sensory and perceptually modulated further increased. Specifically, when we performed a multiple comparison correction of the firing rate differences in the physical alternation condition using the false discovery rate (FDR) method (Benjamini and Hochberg, 1995), we found that 76% of the single units were significantly modulated during both physical alternation and BFS (n = 48/63, $q < 0.05$). Almost all of these perceptually modulated cells (n = 46/48, 96%) maintained the same stimulus preference during BFS. Therefore, FDR correction decreased the total number of neurons (n = 63/577, or 11% of the total sample) found to be sensory modulated. However, the proportion of sensory modulated neurons found to maintain their selectivity during BFS was higher (75%) compared to the percentage obtained in the initial analysis, performed without multiple comparisons correction (58%). These results place the perceptual responses of feature-selective single units in the LPFC closer to the modulation observed in STS/IT and MTL, where the large majority of sensory modulated cells retain their preference during subjective visual perception (Kreiman et al., 2002; Sheinberg and Logothetis, 1997), than to V1/V2, V4, and MT, where the majority of sensory modulated cells are not perceptually modulated. Moreover, in contrast to LPFC and the temporal cortex, 20%–50% of the perceptually modulated cells in striate/extrastriate areas reverse their selectivity and fire more when their preferred stimulus is perceptually suppressed (Keliris et al., 2010; Leopold and Logothetis, 1996; Logothetis and Schall, 1989).

Monocular switching between preferred and nonpreferred visual patterns resulted in large modulations of the mean spiking activity that lasted for the total duration of visual stimulation (Figure 3A). Following monocular, sensory stimulus alternation from a nonpreferred to a preferred pattern, spiking activity increased and peaked at approximately 200 ms following the stimulus switch. In trials where a stimulus switch to a nonpreferred visual pattern followed monocular stimulation of the contralateral eye with a preferred stimulus, firing rate decreased. The difference in the mean population firing rate elicited by stimulation with a preferred and a nonpreferred visual pattern was significantly higher than zero for the total duration of visual stimulation following the stimulus switch (running Wilcoxon signed-rank test, $p < 0.05$, for all time points examined; Figures 3C and 3D).

The mean population discharge response during subjective visual perception of the same stimuli showed a very similar pattern (Figure 3B). During BFS, perceptual dominance of a preferred stimulus resulted in a significant increase of the mean population firing rate, similar to the increase observed

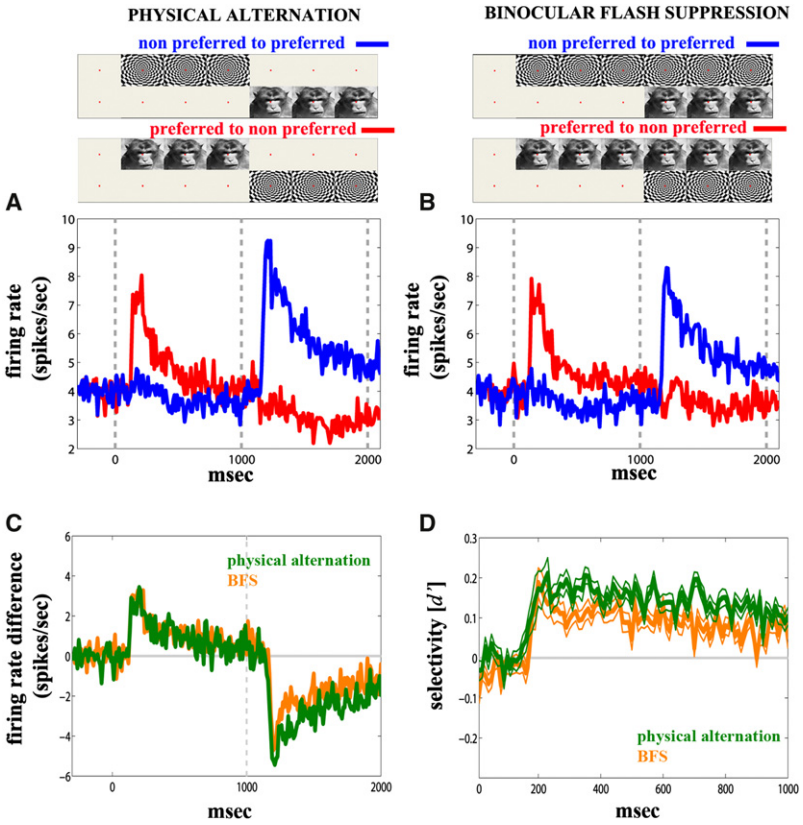

Figure 3. Mean SUA Population Response during Physical Alternation and BFS

(A) Mean population SUA averaged across units showing significant sensory modulation during physical alternation. Blue curve depicts the mean SUA when visual stimulation starts from a nonpreferred stimulus followed by switching to a preferred visual pattern. Red curve depicts the mean SUA when visual stimulation starts with a preferred pattern followed by switching to a nonpreferred stimulus in the contralateral eye.

(B) Same as (A) for BFS. Perceptual dominance of a preferred stimulus (blue, t = 1,001–2,000 ms) results in increased spiking activity similar to that observed during physical alternation of the same stimuli. When the same stimulus is perceptually suppressed (red, t = 1,001–2,000), the mean SUA remains suppressed.

(C) Mean firing rate difference (nonpreferred − preferred) averaged across all significantly sensory modulated units during physical alternation (green curve) and BFS (orange curve) for the whole duration of visual stimulation. The mean firing rate difference was lower during BFS compared to physical alternation but still significantly higher than zero from t = 1,001–2,000 (running Wilcoxon signed-rank test, $p < 0.05$ for all time points examined).

(D) Mean sensory (green curve) and perceptual (orange curve) ± SEM (thin lines) selectivity (d′) following a physical or perceptual stimulus transition. The magnitude of selectivity during BFS was high, albeit lower than the selectivity observed during physical alternation. Selectivity exhibited adaptation during the perceptual dominance of a preferred pattern but lasted for almost the whole second of visual competition. Firing rate difference (C) and d′ (D) were computed for 10 ms time bins.

during physical alternation, despite the physical presence of a nonpreferred pattern in the contralateral eye that was now perceptually suppressed. In a similar fashion, a pattern identical to the physical alternation was obtained when a preferred stimulus was perceptually suppressed (see Figures 1B and S2 for typical examples of modulated neurons). Although spiking activity was not suppressed to the full extent that was observed during monocular stimulation with a nonpreferred visual pattern (see red curves in Figures 3A and 3B and compare the green/orange curves in Figure 3C), we did not observe any significant differences in the magnitude of this suppression. In particular, only three time bins showed a significantly higher firing rate during the suppression of a preferred stimulus compared to the respective monocular condition (running Wilcoxon signed-rank test, $p < 0.05$). Overall, the SUA pattern shows that the magnitude of SUA perceptual modulation observed in the LPFC is very similar to the magnitude reported in temporal areas (Kreiman et al., 2002; Sheinberg and Logothetis, 1997) during BFS and BR. Similar mean population firing rate patterns were observed when our analysis was focused only on the 63 single units that survived the FDR correction.

We also found that 9% of the total number of sampled neurons (n = 54/577) significantly modulated their mean firing rate only during the BFS trials (Wilcoxon rank-sum test, $p < 0.05$; Figure 2A). The existence of such, purely perceptually modulated, cells has been previously reported in other cortical areas during paradigms like BFS and BR. In our LPFC recordings, the frequency of recording from such neurons appeared to be much higher (46% of the total number of modulated cells during the BFS condition; n = 54/118) than the respective percentage observed in cortical areas lower in the visual hierarchy, like V1 (10%, n = 10/104; Keliris et al., 2010), V4 (30%, n = 8/26; Leopold and Logothetis, 1996), and MT (26%, n = 12/46; Logothetis and Schall, 1989). However, encountering such cells is most likely the result of weak and variable stimulus preferences. In our data, when interaction effects (Stimulus × Condition) were explicitly tested using an ANOVA, only 2% of cells (n = 10/577) were found to be significantly modulated ($p < 0.05$) only during BFS.

MUA in the LPFC Follows Phenomenal Perception during BFS

We also studied whether local cortical processing reflected in the local population spiking activity within a prefrontal cortical site could represent subjective visual perception. When non-sorted multiunit spiking activity was examined (MUA, i.e., the sum of the spikes recorded from a tetrode before spike sorting), we found further evidence that the spiking activity of neuronal populations in the LPFC follows reliably phenomenal perception.

Our results show that 20% of the total number of recorded sites (n = 42/211) were significantly modulated during physical alternation (Wilcoxon rank-sum test, $p < 0.05$). In the large majority of these sites, MUA was also found to be significantly modulated during BFS (n = 31/42, or 74%). During BFS, sensory preference was retained in 94% (n = 29/31) of these sites, and in

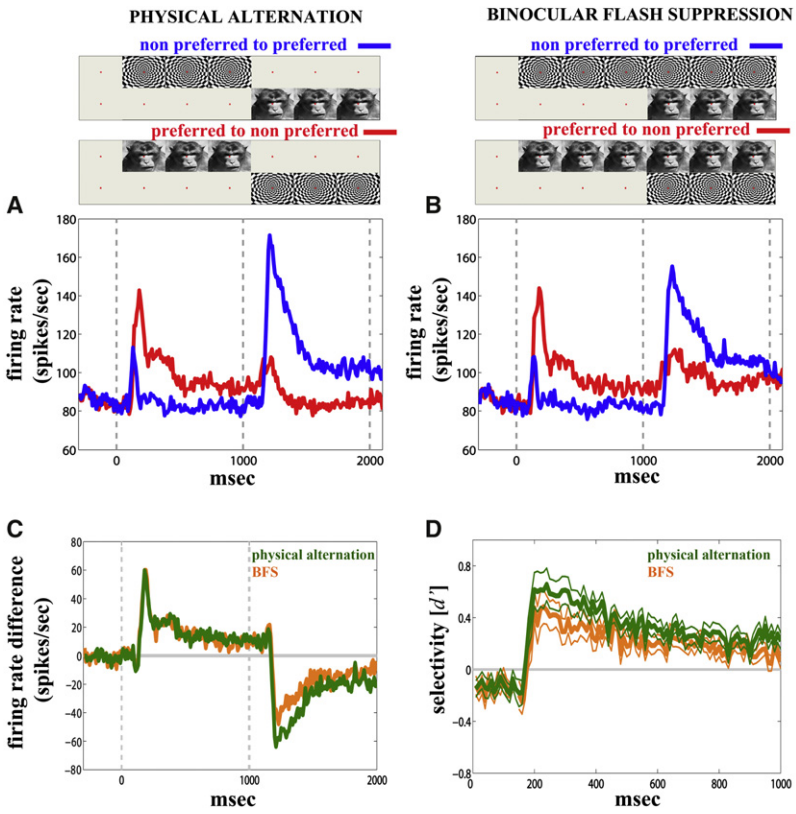

Figure 4. Mean MUA Population Response during Physical Alternation and BFS

(A) Mean MUA population response during physical alternation, averaged across sites where spiking activity showed significant sensory modulation. Activity reflects monocular stimulus transitions between preferred and nonpreferred visual patterns (similar to Figure 3A).

(B) Same as (A) for BFS. Modulation of local spiking activity is largely retained during subjective visual perception.

(C) Mean firing rate difference (nonpreferred − preferred) during physical alternation (green curve) and BFS (orange curve) averaged across all sensory modulated units for the whole duration of visual stimulation. The mean firing rate difference was lower during BFS (orange) compared to physical alternation (green) but still significantly higher than zero (running Wilcoxon signed-rank test, $p < 0.05$ for all time points examined).

(D) Sensory versus perceptual selectivity during the last second of visual stimulation. Perceptual modulation was reduced compared to physical alternation but remained above zero for most of the duration of visual competition. Firing rate difference (C) and d′ (D) were computed for 10 ms time bins. See also Figures S3 and S4.

only 6% of the sites (n = 2/31), neuronal discharges were found to reverse their preference and increased their firing rate when a preferred stimulus was perceptually suppressed (ANOVA, Stimulus × Condition interaction effect, $p < 0.05$). We compared the magnitude of sensory and perceptual modulation for the 42 MUA sites found to be significantly modulated during physical alternation (Figure 2C). We found that MUA modulation during BFS was significantly decreased and reached 56% of the modulation observed during physical stimulus alternation ($d'_{\text{sensory MUA}} = 1.1 \pm 0.14$ and $d'_{\text{perceptual MUA}} = 0.62 \pm 0.13$, Wilcoxon rank-sum test $p = 0.019$). Both distributions were significantly different from zero (t test, $p < 10^{-9}$ for $d'_{\text{sensory MUA}}$, $p < 10^{-6}$ for $d'_{\text{perceptual MUA}}$), thus indicating that the level of mean perceptual modulation was also adequate to distinguish between preferred and nonpreferred stimuli during subjective perception. Similar to SUA, we found that in cases where MUA exhibited a particularly strong sensory modulation ($d'_{\text{sensory MUA}} > 1$), the percentage of perceptually modulated recording sites was even higher. In such strongly modulated cases, 92% of the sensory selective recording sites (n = 12/13) were also significantly modulated during BFS (Figure 2D). Only one (or 8%) of these recording sites was found to increase its firing rate during the perceptual suppression of its preferred visual pattern (ANOVA, Stimulus × Condition interaction effect, $p < 0.05$). These results were not different following an FDR correction of the initially obtained p values for the MUA physical modulation. Specifically, 23 of the initial 42 sensory modulated sites survived the multiple comparisons correction ($q < 0.05$), and 21/23 sites retained the same stimulus preference during BFS. Finally, similar to purely perceptual modulations observed for SUA, the MUA in 17 recording sites was found to be significantly modulated during BFS but not during the physical alternation of the same visual patterns (Wilcoxon rank-sum test, $p < 0.05$; Figure 2C). However, when an ANOVA was used, only six sites showed a significant ($p < 0.05$) interaction effect.

The MUA perceptual modulation observed in the LPFC is significantly higher than the respective modulation observed in V1 during BR, where only 30% of the sensory modulated MUA sites were also found to be perceptually modulated (Gail et al., 2004). Moreover, in more than half of these modulated V1 sites, firing rate increased when a preferred stimulus was perceptually suppressed. Thus, our results show that the sum of LPFC spiking activity measured on a local scale reflects accurately the outcome of subjective visual perception.

Figure 4A depicts the mean MUA activity averaged across the 42 sensory modulated sites during physical alternation. MUA dramatically increased following a monocular switch to a preferred stimulus while it decreased when a preferred stimulus was physically removed and replaced from a nonpreferred pattern (Figure 4A). The mean MUA rate pattern obtained for BFS was remarkably similar to that for physical alternation (Figure 4B). We note that, although MUA activity closely follows phenomenal perception when a preferred stimulus is dominant, we observed an absence of suppression in the spiking activity when the preferred stimulus undergoes perceptual suppression (cf. the red curves in Figures 4A and 4B and the green/orange curves in Figure 4C). In 30% of the 10-ms-wide time bins used to average spiking activity following the onset of flash suppression, the mean MUA activity was found to be significantly higher during the perceptual dominance of a nonpreferred stimulus, compared

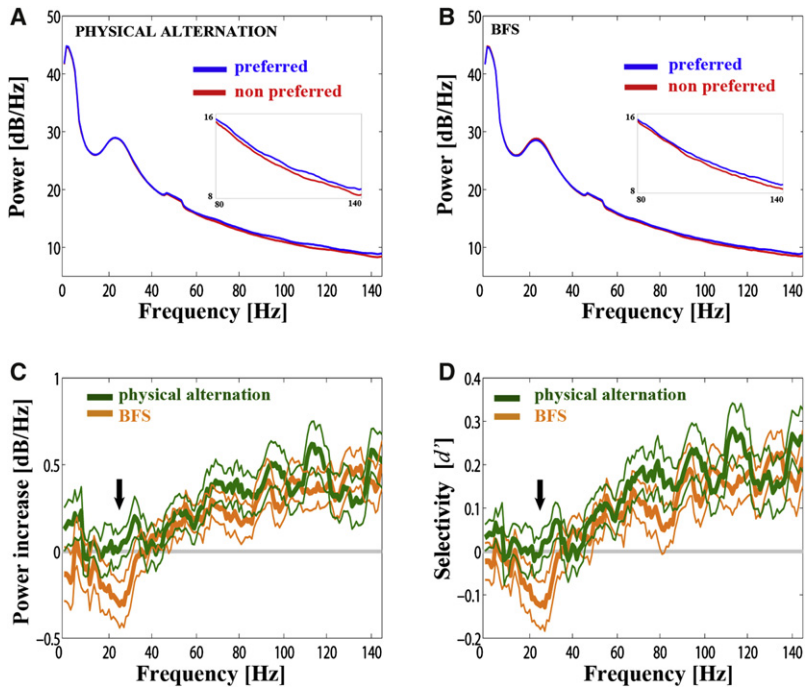

Figure 5. Mean LFP Modulation for All Recorded Sites with Significant Sensory Modulation

(A) Mean power spectra for a period of 1,000 ms following a stimulus switch (t = 1,001–2,000 ms) across all sites showing significant MUA modulation during physical alternation. Note the dominant LPFC beta rhythm (15–35 Hz) appearing as a distinct peak in the power spectra. When a preferred (determined by using MUA modulation as a criterion) stimulus was perceived (blue) oscillatory power in the high frequency gamma range (here, 50–140 Hz) was higher compared to the mean power during the monocular presentation of a nonpreferred pattern (red). No effect is observed in the beta band. Spectral power peak in 50 Hz reflects power line noise.

(B) Same as (A) for BFS. Oscillatory power in the high-frequency range was increased when a preferred stimulus was perceptually dominant (blue) compared to the respective power when the same stimulus was perceptually suppressed (red). LFP power in frequencies between 15 and 30 Hz decreased when a preferred (by the MUA and high-frequency LFP power) stimulus was perceptually dominant compared to the power measured during its perceptual suppression. Insets in (A) and (B) are magnified plots of the high-frequency spectral differences.

(C) Quantification of the mean power difference, observed in (A) and (B), between preferred and nonpreferred stimulus for physical alternation (green curve, mean [thick lines] ± SEM [thin lines]) and BFS (orange curve, mean [thick lines] ± SEM [thin lines]). For frequencies higher than 50 Hz, oscillatory power was higher when a preferred stimulus was perceived without significant difference between purely sensory stimulation and BFS. In frequencies between 15 and 30 Hz, there is a trend of oscillatory power to decrease during the perceptual dominance of a preferred stimulus in BFS (black arrow).

(D) Same as (C), using the d′ as a measure of LFP power modulation. Similar to (C), there are no remarkable differences in the modulation of high frequencies between physical alternation and BFS. Intermediate frequencies (15–30 Hz) decrease during the perceptual dominance of a preferred stimulus (black arrow). See also Figure S5.

to monocular stimulation with a nonpreferred pattern. This result shows that, despite perceptual suppression and robust modulation of spiking activity during the dominance of a preferred stimulus, weak traces of nonconscious stimulus processing are still observed in the LPFC, in particular when the sum of spiking activity in local sites is examined (see also Figure S3). It would be of great interest to monitor the dynamics of this activity during spontaneous perceptual alternations and determine whether these intrinsically driven changes in the perceptual state are correlated with changes in the subliminal process reported in this study.

Finally, we observed a significant difference in the sensory and perceptual selectivity latencies across all sensory modulated sites, with perceptual preference arising approximately 60 ms later compared to physical alternation ($latency_{sensory\ MUA}$ = 169 ± 20 ms; $latency_{perceptual\ MUA}$ = 223 ± 23 ms; Wilcoxon signed-rank test $p = 0.018$; Figure S4).

For both SUA and MUA, we did not find a significant prevalence of preference for one of the two stimuli used. In the past, face selective and complex pattern selective cells have both been described in the inferior convexity of the macaque PFC (Ó Scalaidhe et al., 1997, 1999).

LFP Power Modulation during Subjective Visual Perception in the LPFC

We further studied whether synchronized neural activity in the LPFC, as measured in the power of LFPs recorded from a cortical site, reflected subjective visual perception. We focused our analysis on LFP signals recorded at the 42 sites where MUA was found to be sensory selective. The LFP power spectra in the LPFC show a distinctive pattern, with high oscillatory power in low (1–8 Hz) but also in intermediate frequencies between 15–35 Hz, classically defined as the "beta" band (Figures 5A and 5B). We observed that high frequencies that had low spectral power were more consistently modulated. We found that high-frequency (>50 Hz) oscillatory power exhibited relatively modest but significant sensory preference for the same visual pattern preferred by MUA (Figure 5A). Specifically, we observed a significant, albeit modest, mean power increase in all frequencies above 50 Hz during monocular, sensory stimulation with a preferred stimulus, compared to visual stimulation with a nonpreferred pattern (running Wilcoxon signed-rank test, $p < 0.05$) while lower frequencies (<50 Hz) were not significantly modulated ($p > 0.05$). The mean power modulation across the same recording site for frequencies higher than 50 Hz was very similar during BFS and, most important, not significantly different from the modulation observed during physical alternation. Therefore, the overall magnitude and pattern of high-frequency modulation during conscious perception was remarkably similar to the pattern observed during monocular sensory stimulation.

To eliminate the possibility of spectral contamination of the gamma LFP power from the low frequency components of spike waveforms (Bair et al., 1994; Liu and Newsome, 2006; Pesaran et al., 2002; Ray and Maunsell, 2011; Zanos et al., 2011) we computed the power spectrum of the recorded MUA spike trains

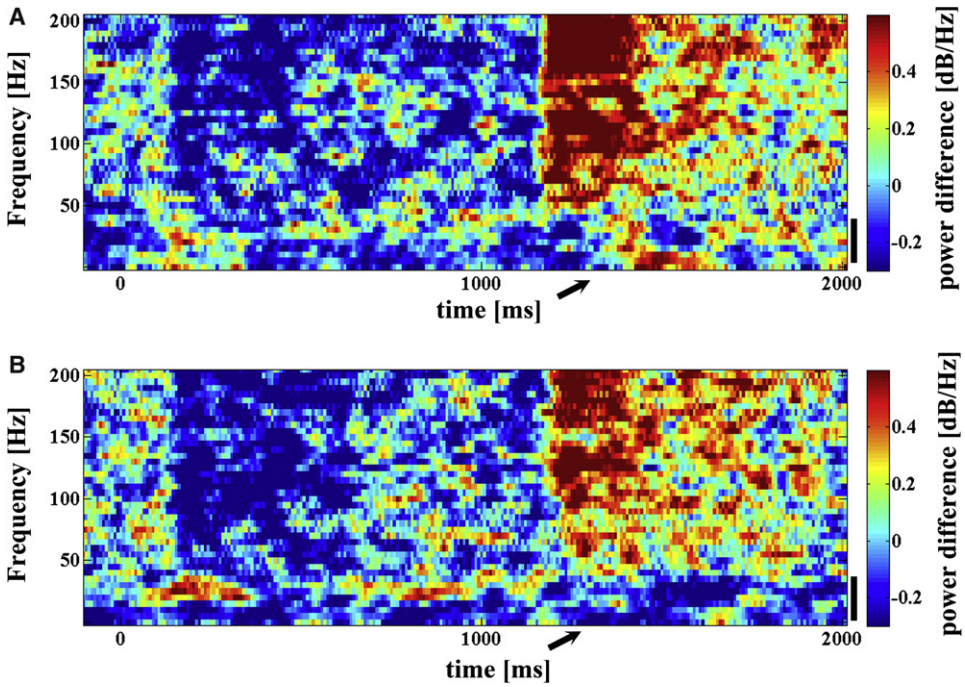

Figure 6. Time-Frequency LFP Modulation

(A) Time-frequency plot during physical alternation, averaged across the population of significantly sensory modulated sites. The average (across trials) spectrogram of each recording site for preferred to nonpreferred transitions was subtracted from the respective spectrogram obtained for nonpreferred to preferred transitions.

(B) Same as (A) during BFS. High-frequency modulation was retained during almost one second of subjective visual perception. In addition, 15–30 Hz power slightly decreased during the perceptual dominance of a preferred pattern specifically during BFS, as indicated by arrows in (A) and (B). See also Figure S6.

for each condition/trial and compared the MUA spectral selectivity to the respective selectivity of the LFP for each recording site. We found that the power spectral density (PSD) of the MUA signal in the LFP frequency range is negligible compared to the PSD of the LFP signal (see Figure S5 and Supplemental Information). Most important, the differences in the PSD selectivity are minimal and they do not seem adequate to explain the magnitude of the respective selectivity of the gamma LFP signal in the frequency range we examined (up to 140 Hz). Therefore, the gamma LFP spectral power most likely reflects components of neural activity that are not observed when the MUA spectral power is taken into account. The analog filtering ("LFP board") used in our recordings was recently shown to be insensitive to spectral contamination when nontemporal measures of the LFPs (such as the tuning of the spectral power) are used (Zanos et al., 2011). Indeed, we further tested the effect of importing our recorded spike trains to our recording system and measured the effects on the LFP channel. We found that our hardware filtering did not permit any detectable effects in the LFP channel. A more detailed analysis of the relationship between gamma LFPs and spiking activity is beyond the scope of this study. However, future experiments should definitely exploit the comparison of BFS to sensory stimulation as a paradigm that could potentially dissociate spiking activity from high-frequency LFPs.

Interestingly, we observed a trend for a BFS-specific power modulation between 15 and 30 Hz (i.e., in the cortical rhythm that, apart from the low frequencies, appears to dominate the LPFC power spectra). During the perceptual dominance of a preferred (by the MUA and high-frequency LFP power) visual pattern (Figures 5B–5D), 15–30 Hz LFP power decreased. In striking contrast, oscillatory power in the same frequency range during physical alternation was not modulated (Figures 5A, 5C, and 5D). The difference in the 15-30 Hz LFP power sensitivity between sensory stimulation and BFS was statistically significant ($d'_{\text{sensory LFP}} = 0.02 \pm 0.03$, $d'_{\text{perceptual LFP}} = -0.11 \pm 0.04$; $p < 0.03$). The effect is due to a small (0.3 dB/Hz) but significant power decrease when a preferred stimulus is perceived under BFS. Although this result shows a trend for desynchronization in the beta band, statistical significance disappears following a Bonferroni correction for multiple comparisons.

The power modulation of high frequencies (50–200 Hz) lasts for the whole duration of the trial and follows the modulation of spiking activity (Figure 6A). The same pattern is observed during BFS (Figure 6B) where perceptual modulation between 50 and 200 Hz lasts for most of the duration of ambiguous stimulation (i.e., t = 1,001–2,000 ms). The marked drop in 15–30 Hz power during the perceptual dominance of a preferred stimulus can be observed for the same period that high-frequency power increases and also lasts for most of the trial duration. The observed LFP power modulations are not due to any possible transient effects observed immediately following the stimulus switch/flash. Spectral power analysis of the same data for the last 500 ms of the trials showed that both high- and intermediate-frequency

modulations were identical to the results obtained when the whole duration of the trial is taken into account (Figure S6).

DISCUSSION

Mechanisms like image segmentation, figure-ground segregation, and perceptual grouping mediate perceptual organization and, therefore, subjective visual perception (Pomerantz and Kubovy, 1986; Logothetis, 1998). During ambiguous visual stimulation, the competitive interactions underlying these mechanisms are believed to be reflected in the neural responses observed in lower and intermediate cortical areas, where considerable activity is elicited during the perceptual suppression of a preferred stimulus (Gail et al., 2004; Keliris et al., 2010; Leopold and Logothetis, 1996; Logothetis and Schall, 1989; Maier et al., 2007; Wilke et al., 2006). In striking contrast, other studies indicated that conscious visual perception is explicitly represented in the spiking activity of the primate temporal lobe, an association cortical area (Kreiman et al., 2002; Sheinberg and Logothetis, 1997). Here, we dissociated sensory stimulation from ambiguous visual perception and studied the neural correlates of visual awareness in the macaque LPFC, one step further in the visual hierarchy. We found a robust representation of phenomenal perception by spiking activity (very similar to the temporal lobe) and high-frequency (>50 Hz) LFPs.

Explicit Representation of Visual Awareness by Neuronal Discharges in the LPFC

Comparing the magnitude of feature-selective neuronal modulation during subjective visual perception with the respective magnitude during purely sensory stimulation has been extensively used to study the relative contribution of different cortical areas to visual consciousness. Spiking activity and gamma oscillations in V1/V2 are generally found to exhibit small perceptual modulation in a variety of ambiguous perception tasks (Keliris et al., 2010; Leopold and Logothetis, 1996; Logothetis and Schall, 1989; Wilke et al., 2006). However, despite the fact that the output of V1/V2 (reflected in spiking activity) is largely unaffected by the perceptual state, low-frequency LFPs are found to be more consistently modulated (Keliris et al., 2010; Maier et al., 2007; Wilke et al., 2006), potentially explaining human fMRI results showing significant perceptual modulation of the BOLD signal in V1 during BR (Lee et al., 2005; Haynes and Rees, 2005; Lee and Blake, 2002; Polonsky et al., 2000; Tong and Engel, 2001). Sparse evidence suggests that modulation of low-frequency LFPs in V1 during ambiguous perception is temporally delayed (Gail et al., 2004; Maier et al., 2007), indicating that V1 BOLD modulation could reflect feedback from higher, perceptually modulated, cortical areas (and/or top-down attentional effects; see Watanabe et al., 2011). Indeed, neuronal discharges in the macaque and human temporal lobe (STS/IT for macaque, MTL for human) during ambiguous visual stimulation represent subjective perception in an all-or-none manner (Kreiman et al., 2002; Sheinberg and Logothetis, 1997). Therefore, perceptual modulation in the temporal cortex was proposed to reflect a stage of cortical processing where visual ambiguity has already been resolved and neural activity reflects phenomenal perception rather than the retinal, sensory input.

Our findings show that spiking activity and the power of high-frequency LFPs in the macaque LPFC, a cortical area reciprocally and monosynaptically connected to the temporal lobe (Barbas, 1988; Borra et al., 2010; Webster et al., 1994; Yeterian et al., 2012), also reflect subjective visual perception in a manner close to all-or-none. In particular, we observed that the magnitude of SUA and MUA perceptual modulation in the macaque LPFC is significantly higher than the respective magnitude in lower visual cortical areas during BFS/BR (Gail et al., 2004; Keliris et al., 2010; Leopold and Logothetis, 1996; Logothetis and Schall, 1989) and largely follow phenomenal perception. Therefore, the results presented in this study suggest that the LPFC and temporal cortex could consist a corticocortical network critically involved in explicit processing of stimulus awareness. Assuming a feed-forward scheme, it is possible that perceptually related activity is transferred from the STS/IT to the LPFC through the well-described anatomical connections between these two areas. However, these connections are reciprocal, indicating that the direction of perceptual modulation flow could as well follow the opposite direction (i.e., from the LPFC to the IT/STS cortex). Our results did not allow us to draw any solid conclusions regarding the flow of perceptual information. We observed, however, that the mean SUA and MUA perceptual latencies started to become significant at approximately 220 ms following the stimulus flash, thus looking very similar to the latency reported by Sheinberg and Logothetis (1997) for STS/IT cortex. Perceptual information flow between STS/IT and LPFC could also follow a transthalamic pathway, since both cortical areas connect to the pulvinar nucleus of the thalamus (Barbas et al., 1991; Contini et al., 2010; Romanski et al., 1997; Webster et al., 1993). Interestingly, perceptual modulation of spiking activity is surprisingly high in the dorsal pulvinar (which receives mostly afferents from the frontal cortex), where MUA activity in 60% of the recorded sites is modulated during generalized flash suppression but absent in the lateral geniculate nucleus during BR (Lehky and Maunsell, 1996; Wilke et al., 2009).

Future experiments employing simultaneous electrophysiological recordings in the temporal cortex and LPFC during BR of BFS could (a) allow monitoring of perceptual latencies and directed functional connectivity and thus hint at the direction of interareal perceptual information flow and (b) elucidate which features of functional connectivity between these two cortical areas are related to the emergence of conscious visual perception.

Weak Traces of Nonconscious Stimulus Processing in the LPFC

Interestingly, we observed some weak traces of nonconscious stimulus processing in the pattern of the mean MUA responses during the perceptual dominance of a nonpreferred stimulus. Specifically, the mean spiking activity was not suppressed but instead was slightly increased, compared to monocular stimulation with the same, nonpreferred stimulus. The magnitude of this spiking activity was still significantly lower than the respective magnitude of the discharge response when a preferred stimulus was perceptually dominant. However, the maintenance of a, higher than the sensory condition, firing rate during the suppression of a preferred stimulus could reflect an ongoing subliminal process related to the nonconscious processing of a preferred

visual pattern in the LPFC. Most likely, the effect we report here is not due to working memory, since we found that spiking activity is robustly suppressed when the preferred stimulus is not physically present. Rather, this result could be more related to a subliminal mechanism of nonconscious processing that coexists with the dominant mechanism of explicit, conscious processing in the LPFC and resembles the recently demonstrated activation of the inferior frontal cortex during the presentation of an unconscious no-go stimulus in human fMRI and electroencephalogram (EEG) studies (van Gaal et al., 2008, 2010). It is likely that spontaneous fluctuations in such residual, subliminal activity might be tightly related to the spontaneous perceptual alternations observed in BR.

Perceptual Modulation of LFPs in the LPFC

We also observed that high-frequency (>50 Hz) LFPs in the LPFC reflect subjective visual perception, while power in the beta frequency band (15–30 Hz) exhibited a tendency to decrease during the phenomenal perception of a preferred stimulus. Despite the fact that synchronous neural activity in the gamma frequency range has been suggested to mediate visual awareness (Crick and Koch, 1990), no evidence has been found until now for significant gamma modulation during conscious visual perception in the macaque cortex. Our findings suggest that this is most likely because LFPs have been studied in sensory cortices where perceptual modulation is generally weak but not in association cortices where neural activity appears to be more correlated to phenomenal perception. Indeed, both the power and interelectrode coherence of high-frequency oscillations in lower visual areas are not significantly modulated during perceptual suppression (Gail et al., 2004; Keliris et al., 2010; Maier et al., 2007; Wilke et al., 2006; but see Fries et al. [1997, 2002] for some opposite results in studies with strabismic cats). Thus, to our knowledge, our findings provide the first concrete indication that high-frequency oscillations reflect conscious perception in the macaque cortex. However, this correlate is not located in a primary sensory area such as V1 but in a higher association area such as the LPFC, in sites where spiking activity also reflects conscious perception. High-frequency oscillations in the gamma range have indeed been associated to conscious processing in a plethora of noninvasive human EEG and magnetoencephalography studies (for an extensive review, see Dehaene and Changeux, 2011). In a recent study employing visual masking, gamma power was increased and beta decreased during conscious processing, particularly in the frontal cortex, a result remarkably similar to our findings (Gaillard et al., 2009). An increase in the gamma power accompanied by long-distance gamma synchrony was also observed in frontotemporal and parieto-occipital electrodes approximately 200 ms after the presentation of a Mooney face but not when the face was inverted and, thus, not recognized (Rodriguez et al., 1999). Interestingly, in the same study phase, desynchronization coexisted with above average gamma activity.

"Frontal Lobe Hypothesis" and Global Networks Mediating Conscious Perception

In conclusion, our findings support the "frontal lobe hypothesis" of conscious visual perception (Crick and Koch, 1998), suggesting that the neural correlates of consciousness (NCC) should be related to explicit neural activity with direct access to planning stages of the brain, like the prefrontal cortex. In fact, our results demonstrate that the NCC are embedded in the LPFC, a cortical area having direct connections to premotor and motor cortices, thus with direct access to motor output. However, the fact that neural activity in two cortical areas (LPFC and temporal cortex) reflects phenomenal perception in an all-or-none manner supports the view that consciousness is not localized in a unique cortical area but, rather, is an emergent property of global networks of neuronal populations (Blake and Logothetis, 2002).

EXPERIMENTAL PROCEDURES

Electrophysiological Recordings and Stimulus Presentation

The cranial headpost, scleral eye coil, and recording chamber were implanted in two monkeys under general anesthesia using aseptic and sterile conditions. The recording chamber (18 mm in diameter) was centered stereotaxically above the LPFC (centered toward the inferior convexity of the LPFC, defined as the area anterior to the arcuate and ventral to the principal sulcus) based on high-resolution MR anatomical images collected in a vertical 4.7 T scanner with a 40-cm-diameter bore (Biospec 47/40c; Bruker Medical, Ettlingen, Germany).

We used custom-made tetrodes made from Nichrome wire and electroplated with gold to decrease the impedances below 1 MΩ. We recorded LFP signals by filtering the raw voltage signal using analog band bass filtering (high-pass set at 1 Hz and low-pass at 475 Hz) and digitized at 2 kHz (12 bits). MUA was defined as the events detected in the high-pass analog filtered signal (0.6–6 kHz) that exceeded a predefined threshold (typically, 25μV) on any tetrode channel. The 0.6–6 kHz recorded signal was sampled at 32 kHz and digitized at 32 kHz (12 bits). The recorded signals were stored using the Cheetah data acquisition system (Neuralynx, Tucson, AZ, USA). We identified single units by employing a spike-sorting method using the first three principal components of the recorded waveforms as features (a method previously described in Tolias et al., 2007). Eye movements were monitored online and stored for offline analysis using the QNX-based acquisition system (QNX Software Systems Ltd.) and Neuralynx. Visual stimuli were displayed using a dedicated graphics workstation (TDZ 2000; Intergraph Systems, Huntsville, AL, USA) with a resolution of 1,280 × 1,024 and a 60 Hz refresh rate, running an OpenGL-based stimulation program. All procedures were approved by the local authorities (Regierungspräsidium Tübingen, Tübingen, Germany) and were in full compliance with the guidelines of the European Community (EUVD 86/609/EEC) for the care and use of laboratory animals.

Behavioral Task and Data Analysis

Before the beginning of each data set, a number of visual stimuli was presented, and, based on the MUA response, a preferred stimulus that could drive neuronal activity better was contrasted to a nonpreferred stimulus that induced less robust responses. In most of our experiments, we found that the stimuli depicted in Figure 1 elicited robustly selective responses. Stimuli were foveally presented with a typical size of 2°–3°.

In both BFS and physical alternation trials, a fixation spot (size, 0.2°; fixation window, ±1°) is presented for 300 ms (t = −300–0 ms), followed by the same visual pattern (a polar checkerboard in the paradigm presented in Figure 1) to one eye (t = 1–1,000 ms). In BFS trials (Figure 1A, "Flash suppression"), 1 s after stimulus onset, a disparate visual pattern (here, a monkey face) is suddenly flashed to the corresponding part of the contralateral eye. The flashed stimulus remains on for 1,000 ms (t = 1,001–2,000 ms), robustly suppressing the perception of the contralaterally presented visual pattern, which is still physically present. In the physical alternation trials (Figure 1A, "Physical alternation"), the same visual patterns are physically alternating between the two eyes, resulting in a visual percept identical to the perceptual condition (Figure 1, middle panel) but this time without any underlying visual competition. At the end of each trial and after a brief, stimulus free, fixation period (100–300 ms), a drop of juice was used as a reward for maintaining fixation.

To further confirm the efficiency of flash suppression to induce perceptual suppression, we trained a different monkey to report BFS by pulling levers for the two different stimuli used in our recordings. Whenever a stimulus was dominant, the monkey had to keep the lever pulled and then release it and pull the other lever to report a perceptual switch. We recorded the time following the onset of flash suppression that the monkey released the lever for the flashed stimulus, thus indicating the occurrence of a perceptual switch.

To determine the contribution of LPFC in visual awareness, we compared the "sensory" stimulus preference during physical alternation to the "perceptual" stimulus preference for each single unit and recording site during BFS. Similar sensory and perceptual stimulus preference indicates that sensory modulated units/sites continue to follow the perception of a preferred stimulus during rivalrous stimulation (BFS). We computed a preference index for each unit/site and each condition (physical alternation, $d'_{\text{sensory SUA/MUA}}$; and BFS, $d'_{\text{perceptual SUA/MUA}}$) as following:

$$d' = \frac{\mu_{\text{preferred}} - \mu_{\text{non preferred}}}{\sqrt{(var_{\text{preferred}} + var_{\text{non preferred}})/2}},$$

where $\mu_{\text{preferred}}$ and $\mu_{\text{non preferred}}$ are the mean discharge responses to the preferred and the nonpreferred visual patterns from t = 1,001–2,000 ms and $\sqrt{(var_{\text{preferred}} + var_{\text{non preferred}})/2}$ is the pooled variance of the two response distributions during the same time window. A positive d′ in both conditions indicates units/sites that retained their preference in the BFS, while a negative d′ in the BFS condition indicates units/sites that fired more when their preferred stimulus was perceptually suppressed. Statistically significant modulations for each unit/site were identified by using a Wilcoxon rank-sum test to compare the two response distributions (consisting of the total number of spike counts from t = 1,001–2,000 for the preferred and the nonpreferred stimuli, across all trials). Where appropriate, p values were corrected (and converted to q values) using the FDR method (Benjamini & Hochberg (1995)).

The PSD of the raw LFP signals from t = 1,001 to t = 2,000 ms was estimated using the multitaper method (Thomson, 1982). This method uses linear or nonlinear combinations of modified periodograms to estimate the PSD. These periodograms are computed using a sequence of orthogonal tapers (windows in the frequency domain) specified from the discrete prolate spheroidal sequences. Selectivity of spectral power was computed using the d′ for narrow frequency bins of 1 Hz ($d'_{\text{sensory LFP}}$ and $d'_{\text{perceptual LFP}}$) for sites where MUA exhibited significant sensory selectivity. Time frequency analysis was carried out by computing a spectrogram in each trial using overlapping (94%) 256 ms windows and then averaged across all trials.

SUPPLEMENTAL INFORMATION

Supplemental Information includes six figures and Supplemental Experimental Procedures and can be found with this article online at doi:10.1016/j.neuron.2012.04.013.

ACKNOWLEDGMENTS

This study was supported by the Max Planck Society. We thank Drs. Andreas Tolias, Christoph Kayser, Kevin Whittingstall, and Michel Besserve for helpful discussions and comments on a previous version of the manuscript. Joachim Werner and Axel Oeltermann provided excellent technical support.

Accepted: April 3, 2012
Published: June 6, 2012

REFERENCES

Bair, W., Koch, C., Newsome, W., and Britten, K. (1994). Power spectrum analysis of bursting cells in area MT in the behaving monkey. J. Neurosci. *14*, 2870–2892.

Barbas, H. (1988). Anatomic organization of basoventral and mediodorsal visual recipient prefrontal regions in the rhesus monkey. J. Comp. Neurol. *276*, 313–342.

Barbas, H., Henion, T.H., and Dermon, C.R. (1991). Diverse thalamic projections to the prefrontal cortex in the rhesus monkey. J. Comp. Neurol. *313*, 65–94.

Benjamini, Y., and Hochberg, Y. (1995). Controlling the false discovery rate: a practical and powerful approach to multiple testing. J. Roy. Statist. Soc. Ser. B (Methodological). *57*, 289–300.

Blake, R., and Logothetis, N.K. (2002). Visual competition. Nat. Rev. Neurosci. *3*, 13–21.

Borra, E., Ichinohe, N., Sato, T., Tanifuji, M., and Rockland, K.S. (2010). Cortical connections to area TE in monkey: hybrid modular and distributed organization. Cereb. Cortex *20*, 257–270.

Contini, M., Baccarini, M., Borra, E., Gerbella, M., Rozzi, S., and Luppino, G. (2010). Thalamic projections to the macaque caudal ventrolateral prefrontal areas 45A and 45B. Eur. J. Neurosci. *32*, 1337–1353.

Crick, F., and Koch, C. (1990). Some reflections on visual awareness. Cold Spring Harb. Symp. Quant. Biol. *55*, 953–962.

Crick, F., and Koch, C. (1998). Consciousness and neuroscience. Cereb. Cortex *8*, 97–107.

Crick, F., and Koch, C. (2003). A framework for consciousness. Nat. Neurosci. *6*, 119–126.

Dehaene, S., and Changeux, J.P. (2011). Experimental and theoretical approaches to conscious processing. Neuron *70*, 200–227.

Fries, P., Roelfsema, P.R., Engel, A.K., König, P., and Singer, W. (1997). Synchronization of oscillatory responses in visual cortex correlates with perception in interocular rivalry. Proc. Natl. Acad. Sci. USA *94*, 12699–12704.

Fries, P., Schröder, J.H., Roelfsema, P.R., Singer, W., and Engel, A.K. (2002). Oscillatory neuronal synchronization in primary visual cortex as a correlate of stimulus selection. J. Neurosci. *22*, 3739–3754.

Gail, A., Brinksmeyer, H.J., and Eckhorn, R. (2004). Perception-related modulations of local field potential power and coherence in primary visual cortex of awake monkey during binocular rivalry. Cereb. Cortex *14*, 300–313.

Gaillard, R., Dehaene, S., Adam, C., Clémenceau, S., Hasboun, D., Baulac, M., Cohen, L., and Naccache, L. (2009). Converging intracranial markers of conscious access. PLoS Biol. *7*, e61.

Haynes, J.D., and Rees, G. (2005). Predicting the stream of consciousness from activity in human visual cortex. Curr. Biol. *15*, 1301–1307.

Keliris, G.A., Logothetis, N.K., and Tolias, A.S. (2010). The role of the primary visual cortex in perceptual suppression of salient visual stimuli. J. Neurosci. *30*, 12353–12365.

Kreiman, G., Fried, I., and Koch, C. (2002). Single-neuron correlates of subjective vision in the human medial temporal lobe. Proc. Natl. Acad. Sci. USA *99*, 8378–8383.

Lee, S.H., and Blake, R. (2002). V1 activity is reduced during binocular rivalry. J. Vis. *2*, 618–626.

Lee, S.H., Blake, R., and Heeger, D.J. (2005). Traveling waves of activity in primary visual cortex during binocular rivalry. Nat. Neurosci. *8*, 22–23.

Lehky, S.R., and Maunsell, J.H. (1996). No binocular rivalry in the LGN of alert macaque monkeys. Vision Res. *36*, 1225–1234.

Leopold, D.A., and Logothetis, N.K. (1996). Activity changes in early visual cortex reflect monkeys' percepts during binocular rivalry. Nature *379*, 549–553.

Libedinsky, C., and Livingstone, M. (2011). Role of prefrontal cortex in conscious visual perception. J. Neurosci. *31*, 64–69.

Liu, J., and Newsome, W.T. (2006). Local field potential in cortical area MT: stimulus tuning and behavioral correlations. J. Neurosci. *26*, 7779–7790.

Logothetis, N.K. (1998). Single units and conscious vision. Philos. Trans. R. Soc. Lond. B Biol. Sci. *353*, 1801–1818.

Logothetis, N.K., and Schall, J.D. (1989). Neuronal correlates of subjective visual perception. Science *245*, 761–763.

Lumer, E.D., Friston, K.J., and Rees, G. (1998). Neural correlates of perceptual rivalry in the human brain. Science *280*, 1930–1934.

Maier, A., Logothetis, N.K., and Leopold, D.A. (2007). Context-dependent perceptual modulation of single neurons in primate visual cortex. Proc. Natl. Acad. Sci. USA *104*, 5620–5625.

Meenan, J.P., and Miller, L.A. (1994). Perceptual flexibility after frontal or temporal lobectomy. Neuropsychologia *32*, 1145–1149.

Ó Scalaidhe, S.P., Wilson, F.A., and Goldman-Rakic, P.S. (1997). Areal segregation of face-processing neurons in prefrontal cortex. Science *278*, 1135–1138.

Ó Scalaidhe, S.P., Wilson, F.A., and Goldman-Rakic, P.S. (1999). Face-selective neurons during passive viewing and working memory performance of rhesus monkeys: evidence for intrinsic specialization of neuronal coding. Cereb. Cortex *9*, 459–475.

Pesaran, B., Pezaris, J.S., Sahani, M., Mitra, P.P., and Andersen, R.A. (2002). Temporal structure in neuronal activity during working memory in macaque parietal cortex. Nat. Neurosci. *5*, 805–811.

Pigarev, I.N., Rizzolatti, G., and Scandolara, C. (1979). Neurons responding to visual stimuli in the frontal lobe of macaque monkeys. Neurosci. Lett. *12*, 207–212.

Polonsky, A., Blake, R., Braun, J., and Heeger, D.J. (2000). Neuronal activity in human primary visual cortex correlates with perception during binocular rivalry. Nat. Neurosci. *3*, 1153–1159.

Pomerantz, J.R., and Kubovy, M. (1986). Theoretical approaches to perceptual organization: simplicity and likelihood principles. In Handbook of Perception and Human Performance, Vol. 2: Cognitive Processes and Performance, K.R. Boff, L. Kaufman, and J.P. Thomas, eds. (New York: John Wiley & Sons), 36-1–36-46.

Ray, S., and Maunsell, J.H. (2011). Different origins of gamma rhythm and high-gamma activity in macaque visual cortex. PLoS Biol. *9*, e1000610.

Ricci, C., and Blundo, C. (1990). Perception of ambiguous figures after focal brain lesions. Neuropsychologia *28*, 1163–1173.

Rodriguez, E., George, N., Lachaux, J.P., Martinerie, J., Renault, B., and Varela, F.J. (1999). Perception's shadow: long-distance synchronization of human brain activity. Nature *397*, 430–433.

Romanski, L.M., Giguere, M., Bates, J.F., and Goldman-Rakic, P.S. (1997). Topographic organization of medial pulvinar connections with the prefrontal cortex in the rhesus monkey. J. Comp. Neurol. *379*, 313–332.

Sheinberg, D.L., and Logothetis, N.K. (1997). The role of temporal cortical areas in perceptual organization. Proc. Natl. Acad. Sci. USA *94*, 3408–3413.

Sterzer, P., and Kleinschmidt, A. (2007). A neural basis for inference in perceptual ambiguity. Proc. Natl. Acad. Sci. USA *104*, 323–328.

Thomson, D.J. (1982). Spectrum estimation and harmonic-analysis. Proc. IEEE *70*, 1055–1096.

Tolias, A.S., Ecker, A.S., Siapas, A.G., Hoenselaar, A., Keliris, G.A., and Logothetis, N.K. (2007). Recording chronically from the same neurons in awake, behaving primates. J. Neurophysiol. *98*, 3780–3790.

Tong, F., and Engel, S.A. (2001). Interocular rivalry revealed in the human cortical blind-spot representation. Nature *411*, 195–199.

Tsao, D.Y., Schweers, N., Moeller, S., and Freiwald, W.A. (2008). Patches of face-selective cortex in the macaque frontal lobe. Nat. Neurosci. *11*, 877–879.

Valle-Inclán, F., and Gallego, E. (2006). Chapter 13 Bilateral frontal leucotomy does not alter perceptual alternation during binocular rivalry. Prog. Brain Res. *155*, 235–239.

van Gaal, S., Ridderinkhof, K.R., Fahrenfort, J.J., Scholte, H.S., and Lamme, V.A. (2008). Frontal cortex mediates unconsciously triggered inhibitory control. J. Neurosci. *28*, 8053–8062.

van Gaal, S., Ridderinkhof, K.R., Scholte, H.S., and Lamme, V.A. (2010). Unconscious activation of the prefrontal no-go network. J. Neurosci. *30*, 4143–4150.

Watanabe, M., Cheng, K., Murayama, Y., Ueno, K., Asamizuya, T., Tanaka, K., and Logothetis, N. (2011). Attention but not awareness modulates the BOLD signal in the human V1 during binocular suppression. Science *334*, 829–831.

Webster, M.J., Bachevalier, J., and Ungerleider, L.G. (1993). Subcortical connections of inferior temporal areas TE and TEO in macaque monkeys. J. Comp. Neurol. *335*, 73–91.

Webster, M.J., Bachevalier, J., and Ungerleider, L.G. (1994). Connections of inferior temporal areas TEO and TE with parietal and frontal cortex in macaque monkeys. Cereb. Cortex *4*, 470–483.

Wilke, M., Logothetis, N.K., and Leopold, D.A. (2006). Local field potential reflects perceptual suppression in monkey visual cortex. Proc. Natl. Acad. Sci. USA *103*, 17507–17512.

Wilke, M., Mueller, K.M., and Leopold, D.A. (2009). Neural activity in the visual thalamus reflects perceptual suppression. Proc. Natl. Acad. Sci. USA *106*, 9465–9470.

Windmann, S., Wehrmann, M., Calabrese, P., and Güntürkün, O. (2006). Role of the prefrontal cortex in attentional control over bistable vision. J. Cogn. Neurosci. *18*, 456–471.

Wolfe, J.M. (1984). Reversing ocular dominance and suppression in a single flash. Vision Res. *24*, 471–478.

Yeterian, E.H., Pandya, D.N., Tomaiuolo, F., and Petrides, M. (2012). The cortical connectivity of the prefrontal cortex in the monkey brain. Cortex *48*, 58–81.

Zanos, T.P., Mineault, P.J., and Pack, C.C. (2011). Removal of spurious correlations between spikes and local field potentials. J. Neurophysiol. *105*, 474–486.

Zaretskaya, N., Thielscher, A., Logothetis, N.K., and Bartels, A. (2010). Disrupting parietal function prolongs dominance durations in binocular rivalry. Curr. Biol. *20*, 2106–2111.

Neuron, Volume *74*

Supplemental Information

Neuronal Discharges and Gamma Oscillations Explicitly Reflect Visual Consciousness in the Lateral Prefrontal Cortex

Theofanis I. Panagiotaropoulos, Gustavo Deco, Vishal Kapoor, and Nikos K. Logothetis

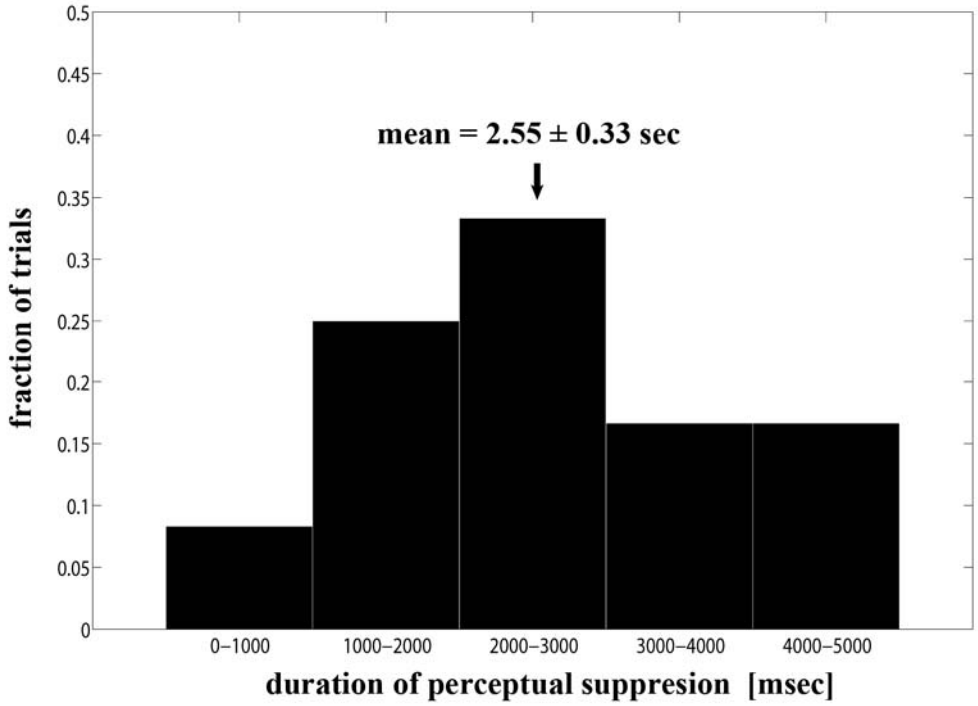

Figure S1, related to Figure 1

Distribution of lever release times following the onset of the flashed stimulus. Lever release indicates that the flashed stimulus is not dominant due to a subsequent spontaneous perceptual stimulus alternation. Similar to previous reports, our behavioral data show that flash suppression is effective for at least 2 seconds, given a conservative estimate of 500ms delay between the actual occurrence of the perceptual switch and the behavioral report.

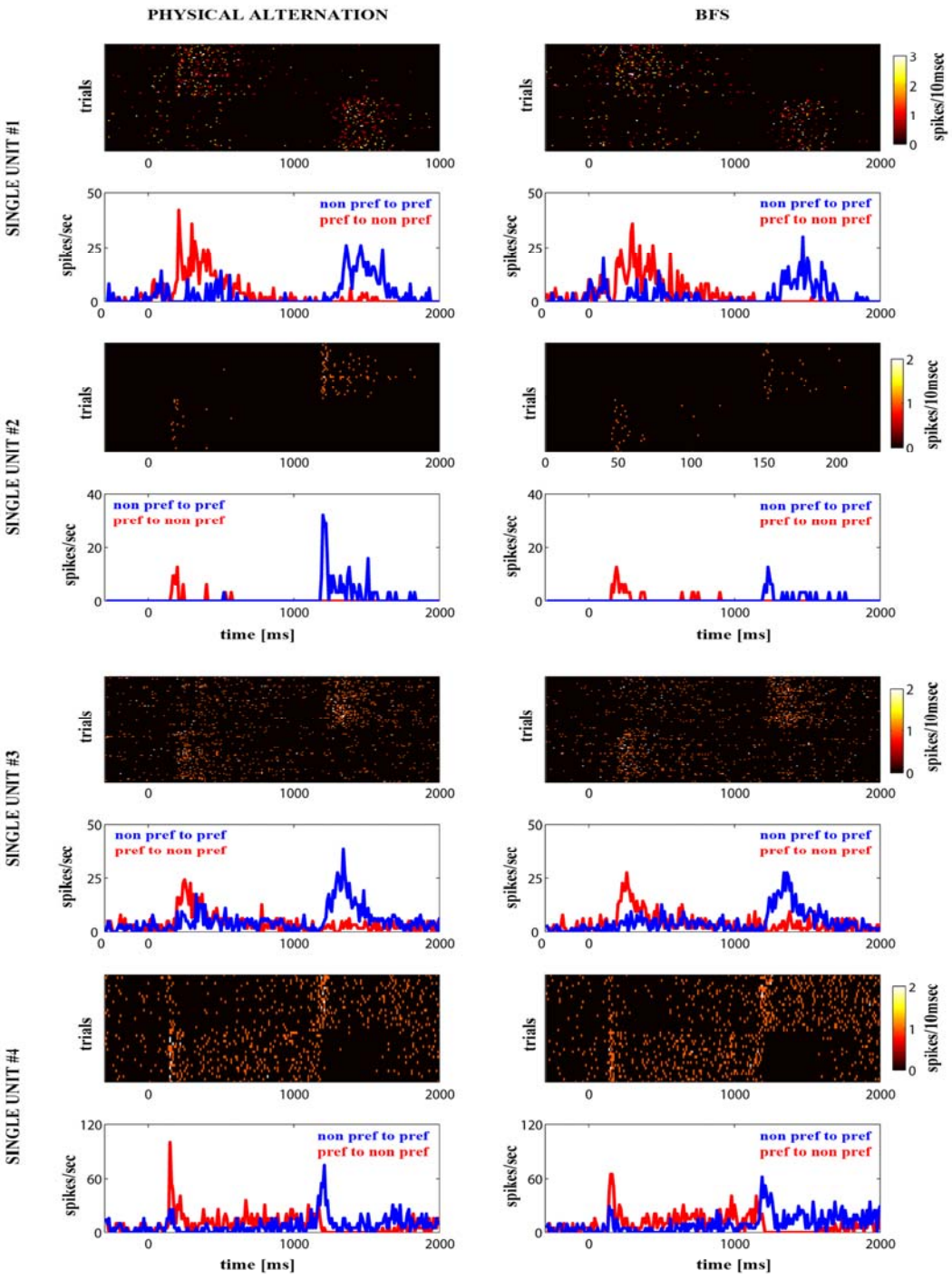

Figure S2, related to Figure 2

Typical examples of raster plots and mean SUA modulations during physical alternation and BFS. All units presented here followed phenomenal perception during BFS. Raster plots group trials across the two conditions (non preferred to preferred vs. preferred to non preferred).

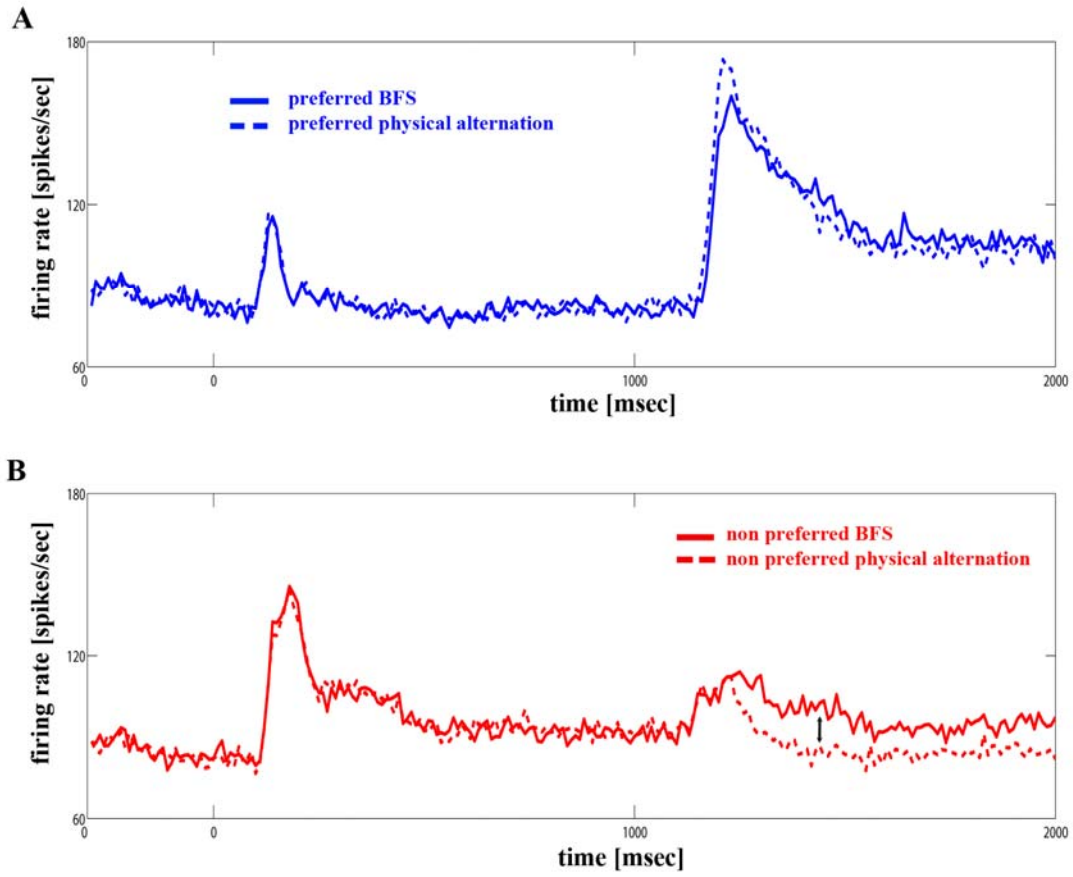

Figure S3, related to Figure 4

Traces of non conscious stimulus processing in MUA responses**.** (A) No differences in MUA responses were observed when a preferred stimulus was perceptually dominant during BFS compared to monocular physical stimulation. However, MUA responses were not suppressed during the perceptual suppression of a preferred stimulus (B).

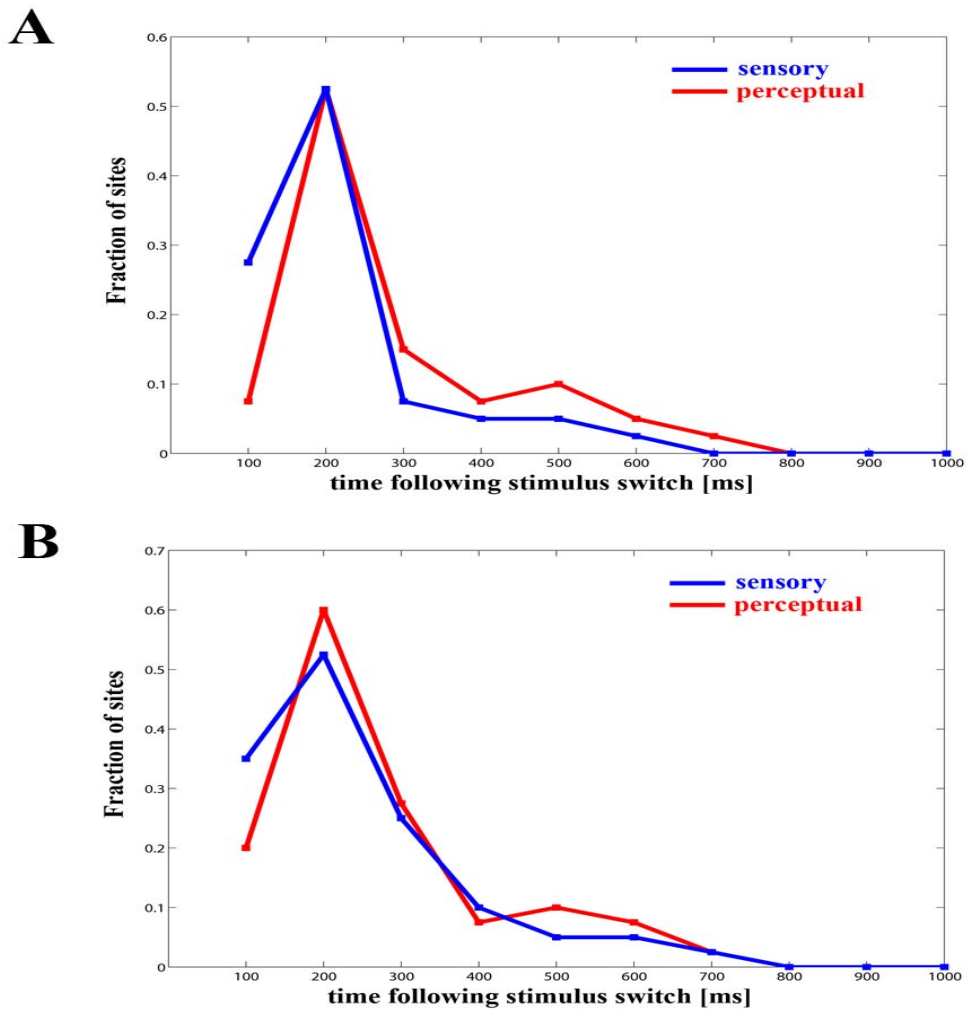

Figure S4

Distribution of sensory and perceptual MUA latencies for all significantly sensory (A) and perceptually (B) modulated sites. For each recording site we computed the first 10ms time bin in which a significant preference was observed. The latency of perceptual preference was significantly increased compared to the emergence of sensory preference (Wilcoxon signed-rank test, p=0.018). Almost 30% of the recording sites exhibited significant sensory selectivity during the first 100ms following stimulus switch. This early sensory component was replaced by preferences arising later during BFS. In more than 50% of the recording sites sensory and perceptual preference arises between 100-200ms following the stimulus switch or flash, respectively.

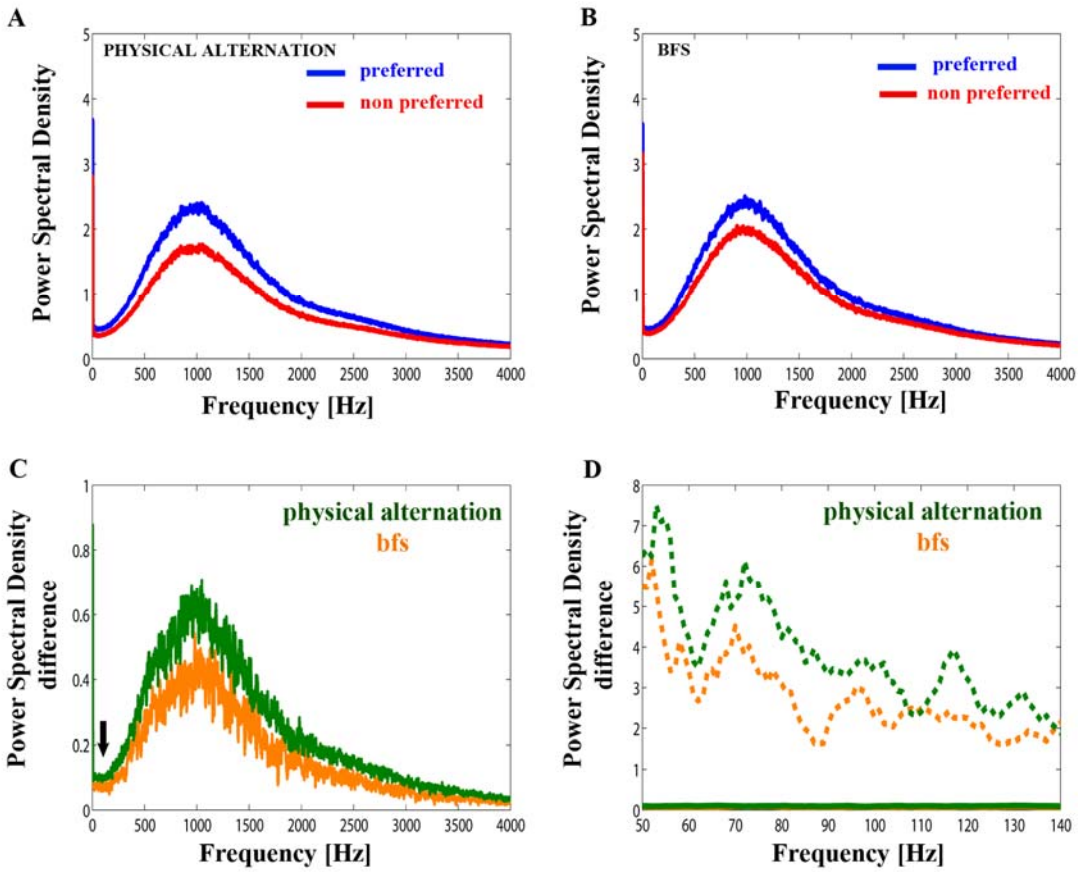

Figure S5, related to Figure 5

Spectral analysis of the reconstructed MUA signal extended to the gamma LFP frequency range. The mean power spectral density (PSD) of the MUA is higher between approximately 600 and 2000Hz, due to spiking activity, also reflecting the differences between the experimental conditions reported in the main text (A and B). However, for lower frequencies, particularly in the relevant range that overlaps with the gamma LFP's (50-140Hz) the PSD of the MUA signal is negligible and more than an order of a magnitude smaller compared to the magnitude of the LFP signal (A,B and C (black arrow)). The selectivity of this signal is also minimal, at least for frequencies up to 140Hz, and therefore is not adequate to explain the selectivity magnitude of the LFP signal (C and magnification of the low frequencies (50-140Hz) in D). Very similar results were obtained when the recorded spikes were imported in the recording system and the same spectral analysis was performed.

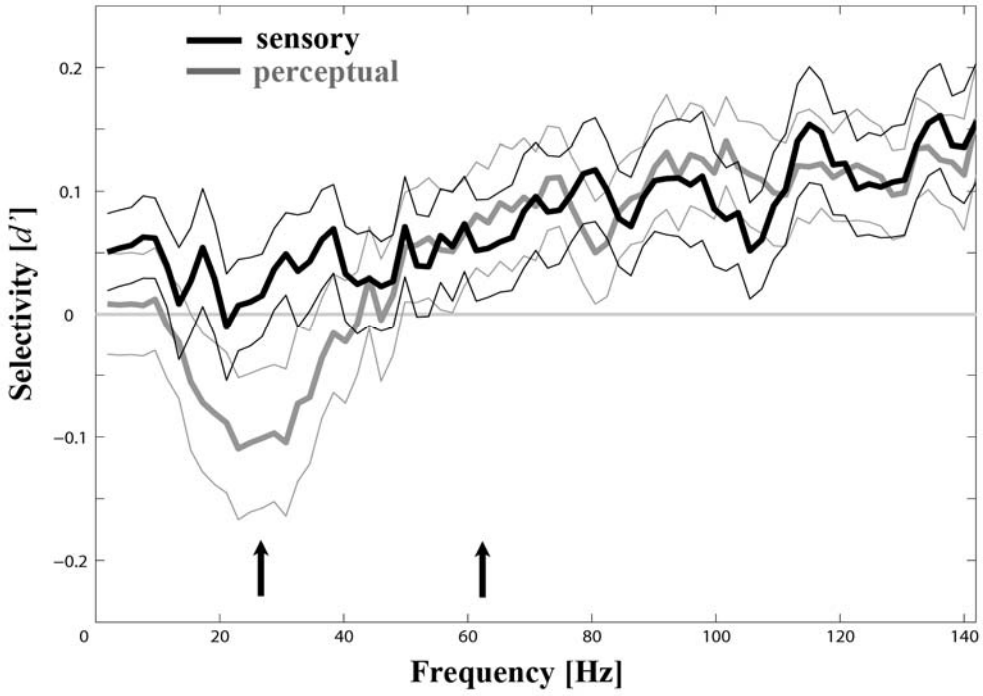

Figure S6, related to Figure 6

Power selectivity as a function of frequency for all sensory modulated recording sites during the last 500 ms of visual stimulation (*t* = 1501-2000 ms). High frequency (>60Hz) power followed phenomenal perception. This effect was accompanied by a drop in the spectral power for frequencies between 15-30 Hz. Arrows point at a) significant differences for 15-30 Hz and b) the frequency above which significant preference was observed for high frequencies.

SUPPLEMENTAL TEXT

Spectral Contamination of the LFP Signals

The high frequency power of the LFP spectrum ("gamma" band) could be prone to artifacts due to spectral contamination from the low frequency components of the action potential waveforms. This is a point been discussed extensively in recent studies (Zanos et al., 2011; Ray and Maunsell 2011; Liu and Newsome, 2006; Pesaran et al., 2002). This important methodological problem is now addressed and discussed in detail in the revised manuscript. Specifically, we used two different methods to show that spectral contamination from spikes is minimal in our LFP data and therefore it doesn't affect the validity of our result regarding the perceptual modulation of gamma oscillatory power:

a) Our recording method didn't allow us to record the full, broadband signal. Spikes and LFP's were split due to the analog/hardware filtering of our recording system (Neuralynx). The LFP signal (from 1 to 475Hz) was continuously recorded at 2kHz. The high pass filtered signal (between 0.6-6 kHz) was recorded at 32 kHz but only the spike waveforms (all the events that crossed a predefined threshold) were collected. Therefore, the rest of the high frequency signal (background noise) between the spikes was not recorded. To reconstruct the continuous high frequency signal we used gaussian noise (-10dB to mean spike amplitude) to fill in the gaps between the collected spike waveforms. This was deemed necessary since using only the spike waveforms is not the best approach to estimate spectral power. It is known that apart from the shape of the spike waveforms, the temporal structure of the spike train is likely to contain considerable power in the lower frequencies (Bair et al., 1994). We then measured for each condition/trial the power spectrum of this reconstructed signal and compared it to the power spectrum obtained for the low frequency (1 to 140Hz) LFP signals for the same conditions/trials in the same electrode. We compared the mean sensory and perceptual selectivity pattern and magnitude to determine the contribution of the spiking signal to the gamma power selectivity reported in Figure 5 of the main text. Our analysis shows that the power spectral density (PSD) selectivity of the MUA

spiking activity (before converting to a logarithmic scale) follows a completely different pattern than the pattern observed in the LFP. Specifically we find that the power spectrum of the MUA spike trains shows some selectivity for all frequencies between 1-140 Hz, however the magnitude of this selectivity is much different from the pattern observed in the LFP's. Although we can't totally exclude the contribution of spiking activity to the LFP signal, our analysis shows that the spectral contamination from spikes in our LFP recordings is minimal.

b) The reconstructed spiking signal was also introduced in the LFP board of our recording system to measure potential effects in the LFP spectrum. We used the reconstructed signal described in the previous paragraph to create waveform audio files (.wav) that were subsequently imported in the LFP channel of the Neuralynx recording system through a sound card output plugged to the preamplifier. The output of the sound card was approximately between 500 and 1000mV which, after amplitude adjustment to match the observed, during the experiments, waveforms in the display resulted in a signal of 0.3 - 0.6 mV imported in the Neuralynx input. We recorded the effect of this signal to the power of the recorded LFP channel for randomly selected datasets. This method returned identical results to the results presented in Figure S5 showing that spectral contamination from spikes is negligible.

Relation of BFS to Binocular Rivalry

Most of the existing psychophysical evidence suggests that the properties of suppression during binocular flash suppression (BFS) are basically identical with those observed in the perceptual suppression stochastically experienced during free-running binocular rivalry (BR). The bulk of evidence is coming indeed from psychophysical studies in humans, which show that the strength and time course of suppression and its all-or-none character are all the same in BR and BFS. Nonetheless

there is also physiological evidence which shows that BR and BFS drive equally strongly the neurons of STS/IT cortex (Sheinberg et al., 1997).

The similarity in the properties of BR and BFS was first discussed in detail in the original study describing the phenomenon of flash suppression (Wolfe, 1984). It is well known that the simultaneous presentation of a grating in one eye and a blank field in the other eye results in a state of continuous perceptual dominance of the eye being stimulated with the grating (Blake and Camisa, 1978). Specifically, when test flashes of short duration were delivered to the suppressed eye detection of the flashes was significantly impaired compared to the delivery of test flashes to the dominant eye. Thus, detection thresholds in the suppressed eye stimulated with the blank field are elevated similar to the elevation of the detection thresholds in the eye suppressed during binocular rivalry (Fox and Check, 1968). This striking similarity in the elevation of detection thresholds suggests that the rivalry mechanism is active during the initial monocular stimulation. Furthermore, previous findings have also shown that if the initial stimulus duration is less than 150ms then a simultaneous flash of disparate patterns in each eye results in fusion of these patterns and not perceptual suppression of one of them (Wolfe, 1983). Thus, the rivalry mechanism requires a minimum of 150ms of visual stimulation of either eye to become active. In our paradigm, 1000ms of initial monocular stimulation guarantee that a period of perceptual dominance has been well established.

According to these findings, the initial monocular stimulation with a polar checkerboard in both physical alternation and BFS conditions (see for example Figure 1A) will reduce sensitivity of the contralateral eye that will be suppressed and trigger the activation of perceptual dominance. In physical alternation the reversal in visual stimulation will lead to a reversal of perceptual dominance and suppression. The initially suppressed eye will now become dominant while the initially dominant eye will become suppressed. Since stimulus offset following a period of monocular stimulation does not affect the dominance of the stimulated eye (Leguire and Fox, 1979) the only reason for the observed reversal in dominance is the impact of the newly presented stimulus which is well above detection

threshold. In that case the animal will perceive the only visual pattern that is presented due to the suppression of the blank field. However, the reversal observed during physical alternation is purely sensory in the sense that no disparate visual pattern is suppressed and thus no "pattern rivalry" is induced. Similarly, the flashed stimulus during BFS consists a powerful, above threshold, visual pattern that is able to reverse suppression of the eye that was previously stimulated with a blank field and at the same time induce contralateral suppression for 1000ms in the eye that was previously dominant and is still stimulated with the originally presented pattern (thus resulting in a brief period of rivalry between disparate visual patterns).

A profound difference between these two paradigms of perceptual suppression is that perceptual alternations in BR are spontaneously generated while in BFS they are externally triggered. However, the above findings as well as findings from recent studies show that dominance and suppression in BFS and BR could potentially be attributed to the same underlying mechanism. Specifically, Tsuchiya et al. (2006) found no additive effect in the depth of suppression when BFS was added to spontaneous BR, thus suggesting a common mechanism. Furthermore, Nichols and Wilson (2009) suggested that any observed differences in the depth of suppression between BFS and BR could be ascribed to differences in the temporal characteristics of the resulting activations. Although some differences in the suppression could exist (like different suppression depth in chromatic channels for BR and BFS (Ooi and Loop, 1994) the same suppression mechanism could operate in a different manner.

Last but not least, the neural responses during BR and BFS in the inferior temporal cortex were found to be remarkably similar (Sheinberg and Logothetis, 1997) further supporting our argument that the neural correlates of BFS could be extrapolated to draw conclusions about perceptual dominance and suppression in binocular rivalry. In addition to the inferior temporal cortex, recent results from our lab (Keliris et al., 2010) show that in V1 the percent of perceptually modulated neurons during BFS is also similar to the respective percent found during BR (Leopold and Logothetis, 1996).

SUPPLEMENTAL REFERENCES

Blake R, Camisa J (1978). Is binocular vision always monocular? Science *200*, 1497-9.

Fox R, Check R (1968). Detection of motion during binocular rivalry suppression. J Exp Psychol. *78*, 388-95.

Nichols DF, Wilson HR (2009). Effect of transient versus sustained activation on interocular suppression. Vision Res 49:102-14.

Ooi TL, Loop MS. (1994). Visual suppression and its effect upon color and luminance sensitivity. Vision Res *34*, 2997-3003.

Tsuchiya N, Koch C, Gilroy LA, Blake R (2006). Depth of interocular suppression associated with continuous flash suppression, flash suppression, and binocular rivalry. J Vis 6:1068-78.

Wolfe, J.M. (1983). Influence of spatial frequency, luminance, and duration on binocular rivalry and abnormal fusion of briefly presented dichoptic stimuli. Perception *12*, 447-56.

A.2 Subjective visual perception: from local processing to emergent phenomena of brain activity.

"To say that an animal responds to sensory stimuli may not be the most natural and efficient way to describe behaviour. Rather, it appears that animals most of the time react to situations, to opponents or things which they actively isolate from their environment. Situations, things, partners or opponents are, in a way, the terms of behaviour. It is legitimate, therefore, to ask what phenomena correspond to them in the internal activity of the brain, or, in other words: how are the meaningful chunks of experience 'represented' in the brain?"

Valentino Braitenberg, "Cell assemblies in the cerebral cortex"

PHILOSOPHICAL TRANSACTIONS OF THE ROYAL SOCIETY B

rstb.royalsocietypublishing.org

Review

Cite this article: Panagiotaropoulos TI, Kapoor V, Logothetis NK. 2014 Subjective visual perception: from local processing to emergent phenomena of brain activity. *Phil. Trans. R. Soc. B* **369**: 20130534.
http://dx.doi.org/10.1098/rstb.2013.0534

One contribution of 13 to a Theme Issue 'Understanding perceptual awareness and its neural basis'.

Subject Areas:
neuroscience, physiology, behaviour

Keywords:
neural correlates of consciousness, electrophysiology, single units, local field potentials, oscillations, spatio-temporal patterns

Author for correspondence:
Theofanis I. Panagiotaropoulos
e-mail: theofanis.panagiotaropoulos@tuebingen.mpg.de

Subjective visual perception: from local processing to emergent phenomena of brain activity

Theofanis I. Panagiotaropoulos[1], Vishal Kapoor[1] and Nikos K. Logothetis[1,2]

[1]Department of Physiology of Cognitive Processes, Max-Planck-Institute for Biological Cybernetics, Tübingen 72076, Germany
[2]Division of Imaging Science and Biomedical Engineering, University of Manchester, Manchester M13 9PT, UK

The combination of electrophysiological recordings with ambiguous visual stimulation made possible the detection of neurons that represent the content of subjective visual perception and perceptual suppression in multiple cortical and subcortical brain regions. These neuronal populations, commonly referred to as the *neural correlates of consciousness*, are more likely to be found in the temporal and prefrontal cortices as well as the pulvinar, indicating that the content of perceptual awareness is represented with higher fidelity in higher-order association areas of the cortical and thalamic hierarchy, reflecting the outcome of competitive interactions between conflicting sensory information resolved in earlier stages. However, despite the significant insights into conscious perception gained through monitoring the activities of single neurons and small, local populations, the immense functional complexity of the brain arising from correlations in the activity of its constituent parts suggests that local, microscopic activity could only partially reveal the mechanisms involved in perceptual awareness. Rather, the dynamics of functional connectivity patterns on a mesoscopic and macroscopic level could be critical for conscious perception. Understanding these emergent spatio-temporal patterns could be informative not only for the stability of subjective perception but also for spontaneous perceptual transitions suggested to depend either on the dynamics of antagonistic ensembles or on global intrinsic activity fluctuations that may act upon explicit neural representations of sensory stimuli and induce perceptual reorganization. Here, we review the most recent results from local activity recordings and discuss the potential role of effective, correlated interactions during perceptual awareness.

1. Introduction

In the—not so remote—past, arguments in favour of a scientific approach to the problem of consciousness were met with skepticism. Arguably, a major hindrance was the first-person perspective of conscious experience that prohibited a quantitative approach to a process that is inherently subjective. However, in the psychological tradition, it was gradually realized that ambiguous stimuli could penetrate into features of conscious experience that are intersubjective and repeatable [1]—such as periods of subjective perceptual dominance and suppression as well as spontaneous perceptual alternations—and therefore used to unravel the general mechanisms mediating the instantaneous content of conscious perception [2,3].

Almost simultaneously with the first experimental study that combined ambiguous visual stimulation with extracellular electrophysiological recordings in the non-human primate brain [4], Crick & Koch [5] suggested that narrowing down and simplifying the search for the mechanisms of consciousness by studying the neural correlates of subjective perception in a single sensory modality could provide valuable insights into the mechanisms underlying all aspects of conscious processing. This proposal led to an explosion in the number of studies using multistable visual stimuli such as the Necker cube (figure 1*a*), Rubin's face-vase illusion (figure 1*b*), binocular rivalry (BR) (figure 1*c*), structure-from-motion

Royal Society Publishing

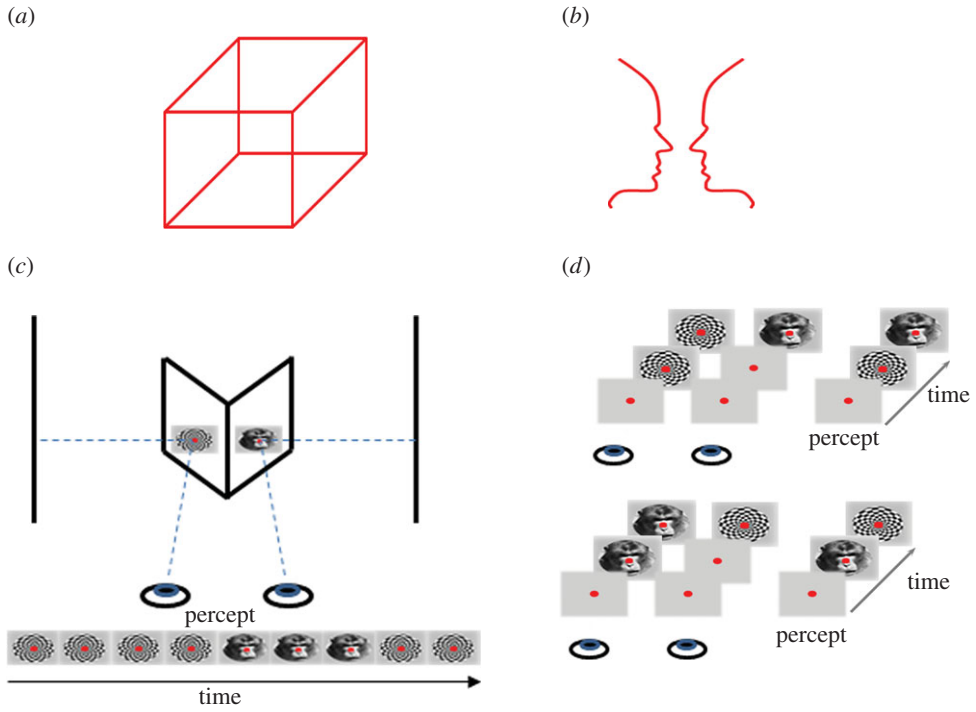

Figure 1. Paradigms of ambiguous visual stimulation used to study subjective perception. (*a*) Necker cube. Two possible interpretations of the cube are randomly switching back and forth in perception. The surface of the cube that appears in front suddenly retrieves to the back and disappears from perception only to be replaced by the perception of the surface that was previously not visible, in the back of the cube. Within a given temporal window, only one surface is consciously perceived, a phenomenon reflecting the struggle of the visual system to conclude on a unique conscious interpretation of the visual stimulus. (*b*) The face-vase illusion. Similar to the Necker cube two faces or a vase are continuously alternating in perception. (*c*) Binocular rivalry (BR). When two disparate visual patterns (here a face and a checkerboard) are continuously presented through a stereoscope in corresponding parts of the two retinas, ambiguity drives visual perception to fluctuate between the two competing stimuli although these stimuli remain unchanged. Periods of stimulus dominance are followed by perceptual suppression in an unpredictable manner, characterized by stochastic temporal dynamics. (*d*) Binocular flash suppression (BFS). Here, perceptual suppression is externally induced by a stimulus flash. Specifically, a stimulus is presented in one of the eyes and after one second, a second stimulus is flashed on the contralateral eye resulting in the perceptual suppression of the originally presented pattern (upper panel). In electrophysiological recordings, by changing the order of stimulus presentation, it is possible to detect the pattern of neuronal activity during the perceptual dominance or suppression of a preferred stimulus (lower panel). (Online version in colour.)

(SFM), etc., which, instead of having a unique interpretation, are characterized by multiple (at least two) perceptual solutions and therefore provide an excellent method for studying the neural mechanisms of subjective, conscious perception (figure 1) [3,6].

In BR (figure 1*c*), probably the most extensively used paradigm, each retina is stimulated with a different visual pattern, both occupying corresponding receptive fields. These conditions of sensory ambiguity elicit visual competition and the content of perception starts to fluctuate between each stimulus in a spontaneous and stochastic manner revealing the dynamic nature of neural phenomena that mediate perceptual alternations [6]. Therefore, each of the competing stimuli enters periods of *perceptual dominance* and *suppression*, gaining access to perceptual awareness or being suppressed and therefore momentarily disappearing from conscious perception. These states of perceptual dominance and suppression can also be studied using other forms of externally induced suppression of stimulus visibility like binocular flash suppression (BFS) [7] (figure 1*d*), generalized flash suppression (GFS) [8] (figure 2*a*) or motion-induced blindness (MIB) [12] that exploit the saliency of an external stimulus flash to induce the temporary invisibility of a target stimulus. However, continuous BR is unique for deciphering the mechanisms underlying the endogenously generated transitions between the competing stimuli [6].

The neural correlates of perceptual dominance and suppression during visual rivalry are currently conceptualized to involve competing neuronal ensembles, each one holding an explicit representation of a competing sensory stimulus. Specifically, the activity dominance or suppression of each ensemble is thought to mediate the respective dominance or suppression of the encoded stimulus during subjective perception. The detection of such modulations has been the focus of the quest for the *neural correlates of consciousness* which are believed to reflect the minimal set of such neural responses that are both *necessary* and *sufficient* for conscious perception. When extracellular electrophysiological recordings in the non-human primate brain were combined with visual rivalry, such perceptually modulated neurons were detected across a plethora of visual brain areas. However, robustly modulated neurons that followed reliably the dominance or suppression of their preferred stimulus were less likely to be found in early, sensory cortical and thalamic areas but more likely in higher-order, association cortical areas and thalamic nuclei. Specifically, competitive forces in early visual areas are strong enough to prohibit inferring the consciously perceived or suppressed stimulus from the observation of neural responses, since firing rates are high for both the dominant and the suppressed pattern. However, in association areas competition has been resolved and neural responses reflect reliably the dominance or suppression of a preferred stimulus. As a result, it is currently believed that the increased strength of competitive interactions between neurons in early, sensory visual areas is related to processes occurring before the resolution of visual rivalry has been

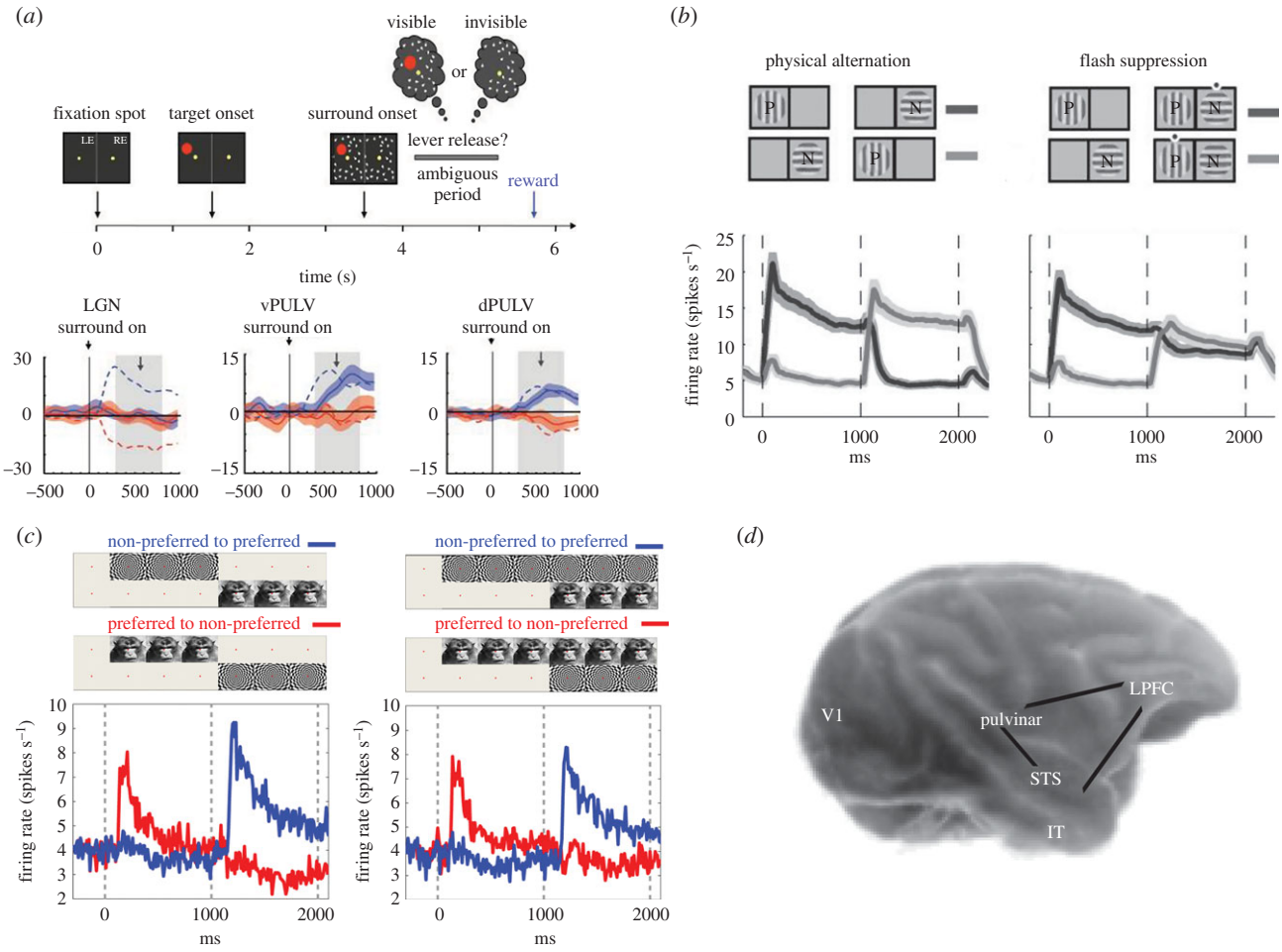

Figure 2. (*a*) In the paradigm of generalized flash suppression (GFS) a salient surround pattern induces perceptual suppression of a target (red dot) stimulus. Monkeys released a lever whenever the target stimulus was invisible. MUA increasing (blue solid lines) or decreasing (red solid lines) in response to perceptual suppression were found in dorsal and ventral pulvinar but not in LGN. Responses to physical stimulus disappearance are depicted with dashed lines (adapted from [9]). (*b*) Mean SUA responses to monocular physical alternation (left) and BFS (right) in V1 for preferred and non-preferred orientations of grating stimuli. In the right plot, the modulation of responses during flash suppression ($t = 1000-2000$) represents only a tiny fraction of the monocular, purely sensory, stimulation response (left plot) (adapted from [10]). (*c*) Mean SUA responses to monocular physical alternation (left) and BFS (right) in the LPFC. The modulation during BFS (right plot) is close to the modulation observed during perception without visual competition (left plot) (adapted from [11]). (*d*) Suggested corticothalamic network (LPFC-STS/IT-pulvinar) where subjective coding of perceptual dominance and suppression resembles the responses observed without any underlying visual competition. The pulvinar is depicted on the surface of the cortex for illustration purposes.

achieved, while the outcome of this processing and thus the content of conscious perception is reflected in association areas [6].

The major focus of this review is on studies undertaken in the non-human primate brain. The non-human primate studies are relevant to human consciousness due to the similarity of psychophysical measures in paradigms of bistable perception between humans and macaques and the evolutionary closeness between the macaque and human visual system. In §2, we provide the most recent overview of the current state of knowledge on the electrophysiological correlates of perceptual awareness, which derives almost exclusively from monitoring local activity. However, scrutinizing local activity by employing single-unit, single-electrode recordings lacks sufficient spatial resolution to reveal emergent phenomena such as mesoscopic and macroscopic patterns of electrophysiological activity whose dynamics have been proposed to be critical for the emergence of conscious perception [13–21]. Based on findings from local activity recordings, in §3 we discuss how population coding and dynamic systems theory, that emphasize the value of tracking simultaneously the activity of large populations of neurons within and across different areas, could contribute to a deeper understanding and refining of the mechanisms mediating perceptual awareness.

2. Locally recorded activity during conscious perception

In intracortical, extracellular recordings, a single electrode picks up the mean extracellular field potential (mEFP) which is the aggregate electrical activity generated by a local neuronal population. In the high-frequency range of the mEFP signal (approx. 0.6–6 kHz) it is possible to detect action potentials that typically cross a voltage threshold of 20–30 µV and reflect the discharge activity of a local neuronal ensemble within a radius of 140–300 µm around the electrode tip [22–24]. The total number of action potentials (spikes) recorded from a single electrode is commonly referred to as the multi-unit spiking activity (MUA), while similar spike waveforms detected in this band-passed signal are assumed to originate from the same single unit (single unit activity—SUA). Since this locally recorded spiking activity reflects the output of neurons within a local site, tracking local spiking activity during paradigms of

subjective visual perception reveals the output of a local population and therefore the degree of explicit neuronal coding during periods of perceptual dominance and suppression.

Such local recordings of neuronal discharge activity during ambiguous visual stimulation helped to address five important issues in perceptual awareness. These are (a) The debate regarding the nature of competition during BR (i.e. monocular versus binocular neurons), (b) the identification of a network of brain regions where neuronal activity is more likely to reflect the content of perceptual awareness, (c) the profile of neural activity during perceptual suppression of a preferred stimulus across the visual processing hierarchy, (d) the neurodynamical mechanisms of perceptual transitions and (e) the role of subthreshold signals (local field potentials). These topics are presented in detail in the following sections.

(a) Local discharge activities resolve interocular versus stimulus feature competition during rivalrous perception

Some indirect evidence from psychophysical experiments implied that competition during BR could be instantiated in the brain as a competition between the mean discharge activities of two pools of monocular neurons, suggesting a model of interocular competition that mediates perceptual awareness [25,26]. In this model, monocular pools of neurons are the rivaling components, and their competition for activity dominance gives rise to the respective alternations subjectively experienced as alternations between the two stimuli presented in each eye. The interocular competition model underlines the importance of perceptual suppression between sensory-driven inputs originating in different monocular channels and not between representations of stimuli that are independent of the eye of origin [6,26,27]. Therefore, the direct experimental validation of this model using electrophysiological recordings could shed light on an elementary question, which is whether rivalry has a purely sensory substrate, involving competition between monocular inputs and dominance or suppression of monocular information, or if it involves a competition between stimulus representations that are not necessarily bound to the eye of origin. Single electrode recordings have the necessary spatial resolution to detect ocular dominance columns and monocular neurons and they were used to address this fundamental question.[1]

In the retinogeniculate visual pathway, the lateral geniculate nucleus (LGN), a thalamic nucleus that is the first relay structure where visual input is processed before reaching the primary visual cortex (V1), contains neurons that respond to sensory input presented to a particular eye. If a strictly interocular competition model was valid, inhibition during BR could already be manifested in the activity of monocularly driven single units in this subcortical area of the visual pathway. However, electrophysiological recordings failed to reveal any effect of BR on the firing rates of monocular neurons in the LGN [28]. The absence of LGN spiking activity modulation during BR indicates that perceptual suppression is still undetectable in this stage of visual processing. This conclusion was confirmed by more recent experiments showing that neuronal discharge activity in the LGN is totally unaffected by perceptual suppression, even when stimulus invisibility is induced through other forms of perceptual illusions seen by both eyes, such as the GFS paradigm [9].

Further evidence against the interocular competition model in BR came from recordings in V1 and V2 which showed that only 14% of MUA and 20–25% of SUA in these regions significantly increase their firing rate when a preferred stimulus is consciously perceived and decrease their firing rate when the same stimulus is perceptually suppressed [10,29,30]. None of these studies found a larger contribution of monocular neurons or monocularly driven MUA in the rather weak traces of perceptual modulation during rivalrous perception. In fact, the overall trend suggests that most of the neurons and MUA sites that followed phenomenal perception in these primary and secondary sensory areas were binocular since they were driven equally well by both eyes. The results of these studies indicate that monocular channel information in LGN or V1 does not reflect the outcome of competitive interactions during BR and therefore the content of conscious visual perception could be a higher-order cortical representation related to the activity of binocularly driven, feature-selective neurons.

(b) Local discharge activities reveal a global network of explicit coding during perceptual awareness

Apart from arguments against a dominant influence of monocular information, SUA/MUA recordings revealed the low probability of LGN and V1 neurons reflecting the content of conscious perception (figure 2*a*,*b*), as well as the small magnitude of perceptual modulation in the discharge rates in these areas compared with monocular stimulation (i.e. without visual competition). Supporting the findings of V1 extracellular recordings during BR, a study in the same cortical area using bistable SFM stimuli found that only 20% of the neurons follow the content of subjective perception [31], while V1 and V2 neurons were not responsive to perceptual suppression induced by GFS [32,33] or MIB [34]. Such dissociation between neuronal activity in primary visual cortex and consciousness is also supported by other results showing that disparity-selective neurons in V1 are able to differentiate between local depth cues even in the absence of conscious stereopsis perception [35].

Although recordings during ambiguous stimulation in the primary visual cortex did not show any obvious temporal differences (i.e. early versus late components) in the amplitude of perceptual modulation between perceptual dominance and suppression (e.g. [29]), a late onset (more than 100 ms) component of spiking activity in V1 was found to be suppressed specifically when figure–ground segregation failed to be consciously perceived [36]. This finding indicates a mixture of activity in V1 where the initial transient responses are more related to sensory, stimulus-driven, modulation while the delayed response component correlates more to consciously perceived effects of perceptual organization, reflected in the segmentation between figure and ground [37]. This divergence of neural responses in V1 has been suggested to underlie an initial feed-forward sweep of activity which does not discriminate between conscious and non-conscious processing, and a later feedback loop that is related to conscious processing.

These findings suggest that neuronal activity in V1 despite being *necessary* is not *sufficient* for perceptual awareness since it does not represent a reliable and explicit neural correlate of subjective perception or perceptual suppression [38–40].[2] On the contrary, hints from psychophysics (reviewed in

[27]) or the potential extrastriate, feedback source of the delayed component in V1 activity [41] indicate that later areas in the visual hierarchy could provide a more explicit correlate of conscious perception.

Indeed, more reliable correlates of subjective visual perception were found in extrastriate and higher-order association cortical areas. Specifically, in hierarchically intermediate cortical areas V4 and middle temporal (MT) cortex where neurons are also tuned to stimulus features such as orientation and direction of motion, SUA and MUA were modulated in accordance with the perceptual dominance and suppression of a preferred stimulus substantially more than in V1. However, even in this processing stage competitive forces between the rivaling populations were particularly strong, resulting in roughly 25–60% of the recorded neurons following the phenomenal perception of a preferred visual stimulus in paradigms such as BR, BFS or SFM [4,30,31,42–44]. Most interestingly, in MT the strength of perceptual modulation appears to be influenced by factors like the context of stimulus competition which, when taken into account, could boost perceptual modulation to 70–90% of the recorded neurons [42].

One step further in the visual processing hierarchy, the superior temporal sulcus (STS) and the inferior temporal (IT) cortices are the target of afferent projections from intermediate areas V4 and MT, and the source of efferent, feedback projections to V1. Neurons in this large cortical expanse exhibit preference for higher-order stimuli such as faces and complex objects. Electrophysiological recordings during BR and BFS in the temporal cortex demonstrated that almost 90% of the recorded units in STS and IT cortex reflect the phenomenal perception of a preferred stimulus [45]. Although not directly comparable to the temporal cortex, very similar responses were collected from recordings in the human medial temporal lobe (MTL) where almost 70% of feature selective neurons fired more during the phenomenal perception of their preferred stimulus during BFS [46]. Most importantly, the magnitude of firing rate modulation during ambiguous stimulation in these temporal areas is very similar to the magnitude observed during stimulation without any underlying stimulus competition, in striking contrast to the miniscule perceptual modulation in V1 which represents only a tiny fraction of the unambiguous sensory responses.

These findings indicate that neurons in the temporal lobe reflect the outcome of processes mediating perceptual awareness, where ambiguities and competition in the sensory input have been resolved and neural activity represents explicitly the content of subjective perception [6,27,45]. However, these temporal areas are not the final processing stage in the ventral visual stream that is involved in object perception [47]. Temporal cortical regions are reciprocally connected through monosynaptic connections with visually modulated areas of the lateral prefrontal cortex (LPFC) [48–51] where single units respond to faces and complex visual objects similarly to cells recorded in the temporal cortex [52–54]. Therefore, an intriguing question is whether the content of conscious perception is represented with the same magnitude in the LPFC. In a recent study, we found that the large majority of single units (approx. 60–90%, depending on the original strength of sensory modulation) and local MUA (approx. 75–95%) in the LPFC reflect the perceptual dominance and suppression of a preferred stimulus during 1 s of ambiguous stimulation externally induced by BFS [11] (figure 2*c*). It is also probable that in the prefrontal cortex there is some functional specialization of the mechanisms involved in subjective perception since the feature selective modulated units during BFS were mostly found in the inferior convexity of the LPFC, while neuronal correlates of perceptual transitions unrelated to stimulus preference were identified in the discharge rate modulation of single units in the macaque frontal eye fields, which predicted perceptual alternations during the paradigm of MIB [55].

These studies support the 'frontal lobe hypothesis' [38,39], suggesting that the neural correlates of conscious perception should have access to brain areas related to planning and decision making, such as the prefrontal cortex, in critical position to affect motor behaviour. In particular, our BFS study [11] showed conscious perception-related activity in the LPFC during passive fixation—that is without any planning, memory, decision making or motor component contaminating neural activities. Therefore, the current evidence strongly suggests that LPFC spiking activity reflects a relatively reliable correlate of conscious perception and not a consequence as proposed recently by Aru *et al*. [56]. However, findings indicating that unconsciously triggered control is feasible [57] and involves the prefrontal cortex [58,59] indicate that conscious prefrontal processing is not a prerequisite for control processes (see also [60]). Therefore, the 'frontal lobe hypothesis' has to be re-evaluated.

In summary, electrophysiological recordings during ambiguous visual stimulation suggest that neurons in the temporal and prefrontal cortices reflect perceptual dominance and suppression much more robustly than the respective neurons in striate and extrastriate cortical areas. Interestingly, temporal and prefrontal areas are reciprocally connected, not only through corticocortical monosynaptic connections, but also indirectly through a subcortical pathway involving the higher-order, pulvinar thalamic nucleus [61–65]. It is thus not surprising that during GFS the magnitude of perceptual modulation of discharge activity in the pulvinar, which receives afferents from the frontal and temporal cortices, is not only detectable compared to LGN, but also close to the magnitude observed in the temporal and prefrontal cortices [9]. Specifically, 40% and 60% of the recorded sites in the ventral and dorsal pulvinar, respectively, reflect perceptual suppression. The somewhat lower perceptual modulation of spiking activity in the ventral pulvinar could be associated to the stronger connectivity of this part of the pulvinar with the primary visual cortex [65] where the correlates of awareness are weak. In contrast, dorsal areas of the pulvinar communicate mainly with association cortical areas.

These results suggest that prefrontal and temporal areas of the cortex as well as the pulvinar could form a cortico-thalamo-cortical network that represents reliably the content of subjective visual perception and reflects perceptual suppression (figure 2*d*). Most importantly, these findings demonstrate that explicit, conscious processing and perceptual suppression are not localized in a unique cortical area but they should rather be conceptualized as an emergent property of a global network involving at least two cortical areas (i.e. temporal and prefrontal cortices) and the pulvinar thalamic nucleus. It has been suggested that due to the absence of a well-defined parcellation of the cortical topography in the pulvinar, rival populations in the cortex could be in competition to recruit thalamic elements in order to outlast each other in activity [66]. In the context of subjective perception, it is possible that when neuronal populations in prefrontal and temporal visual areas are in a dominant state during BR,

long-range binding through the pulvinar results in a beneficial state that outlasts the suppressed, rival cortical populations. In the future, simultaneous recordings in IT, prefrontal cortex and the pulvinar could reveal dynamic interareal interactions that mediate both perceptual dominance and suppression states as well as spontaneous perceptual alternations. The identification of this network of explicit encoding and perceptual suppression during subjective visual perception could help to elaborate and constrain models studying access to consciousness that emphasize the importance of recurrent corticothalamic networks forming a global functional workspace as a necessary condition for conscious perception [67–69]. Studies using electroencephalography (EEG) and magnetoencephalography (MEG) techniques have already started revealing such macroscopically observed, global functional networks that involve coherent activity between frontal, temporal, parietal and occipital areas predicting conscious perception or perceptual alternations during ambiguous stimulation [13,14,16,19,20,70]. Both findings from local, single electrode electrophysiological recordings and EEG/MEG could guide simultaneous *intracortical* recordings which would allow fine spatial resolution and analysis of coherent structures for stimulus-specific spiking activity which is not feasible in EEG/MEG measurements.

(c) Local discharge activities suggest two modes of non-conscious processing during perceptual suppression

Neural processing of a preferred stimulus could also continue during its subjective invisibility. The magnitude of SUA and MUA firing when a preferred stimulus is perceptually suppressed could therefore indicate the strength of non-conscious processing during perceptual suppression. In some cases, this processing is strong enough to induce a complete reversal of the monocularly induced discharge patterns, resulting in higher firing rate when the preferred stimulus is suppressed compared to the respective rate when the same stimulus is dominant. The spatial extent of this type of processing appears to be constrained in striate and extrastriate areas. On the other hand, weaker traces of ongoing but rather residual neural processing during perceptual suppression can be found in almost all areas of the cortical hierarchy as far as in the LPFC. Therefore, although weak, traces of continuous processing during perceptual suppression appear to be present in both sensory and association areas, indicating that explicit, conscious coding and ongoing non-conscious processing during perceptual suppression could coexist within the same cortical network.

More specifically, V1, V4 and V5 (MT) showed significant evidence for the first mode of non-conscious processing during perceptual suppression, since in these areas a fraction of the perceptually modulated selective neurons and MUA (approx. 20–50%) increase their firing rate when their preferred stimulus is perceptually suppressed [4]. In these areas, the particularly strong response profile during perceptual suppression could indicate that some neurons or local populations are more sensitive to non-conscious processing during perceptual suppression compared with processing during perceptual dominance. It has also been suggested that this mode of non-conscious processing during perceptual suppression reflects the perturbation of processes involved in perceptual grouping through feed-forward and feedback connections between different visual areas [27].

In striking contrast, such strong non-conscious stimulus processing during perceptual suppression is nearly absent in the spiking activity of both human MTL and macaque STS/IT cortex where none of the modulated cells consistently fired more during the perceptual suppression of a preferred stimulus [45,46]. Similarly, in the LPFC only a small percentage of SUA and MUA (approx. 5%) were modulated during the perceptual suppression of a preferred stimulus [11]. However, in both the prefrontal and temporal cortices the firing rate of the recorded populations during perceptual suppression of a preferred stimulus is slightly elevated compared to physical removal of the same stimulus (see, for example, the LPFC spiking response in figure 2*c* and the modulation during perceptual suppression in [45, fig. 5]). This firing pattern might reflect a second mode of non-conscious processing during the course of perceptual suppression with residual characteristics that can still be detected in association cortical areas, even after visual competition has been resolved.

These findings from BR and BFS are in accordance with other studies of conscious perception using paradigms of visual masking and show that non-conscious processing of visual signals can be detected all the way up to the prefrontal cortex (for a review, see [59,67]).

(d) Mean local discharge rates and neurodynamical mechanisms of perceptual transitions

Although the SUA and MUA electrophysiological studies revealed the pattern of neuronal discharge activity across different brain areas during stable states of perceptual dominance and suppression, it is still not clear what the mechanism is that underlies a spontaneous switch in the dominant activity and therefore a spontaneous perceptual alternation during BR. This is a key issue since the underlying mechanism could reflect the processes allowing access of a particular content to consciousness. Most of the work on this question has been performed in theoretical models using methods of computational neuroscience where different neurodynamical mechanisms have been proposed to mediate the competition dynamics between the rivaling neuronal pools, involving features such as adaptation, cross-inhibition and noise [26,71–86].

The vast majority of these models examine two possible mechanisms that could be responsible for an alternation in the dominance between antagonistic neuronal populations, as observed in BR. The first alternation mechanism is *adaptation-driven* with cross-inhibition between the two competing pools, and assumes that a slow adaptation process resulting in fatigue of the discharge activity in the dominant pool results in a subsequent decrease of cross-inhibition. The cross-inhibition decrease leads to a disinhibition of the suppressed population which can take over the competition, becoming active and inactivating the originally dominant population [26,71,73,76–79,82–86]. The potential importance of adaptation in BR is well supported by psychophysical studies showing a gradual decrease in the strength of a dominant stimulus and an increase in the probability of a perceptual switch as a function of increasing dominance duration [7,71]. This indirect psychophysical evidence for the significance of adaptation is confirmed by electrophysiological observations in the temporal and prefrontal cortices, which reveal a gradual adaptation of the mean population discharge response during the perceptual dominance of a preferred stimulus [11,45].

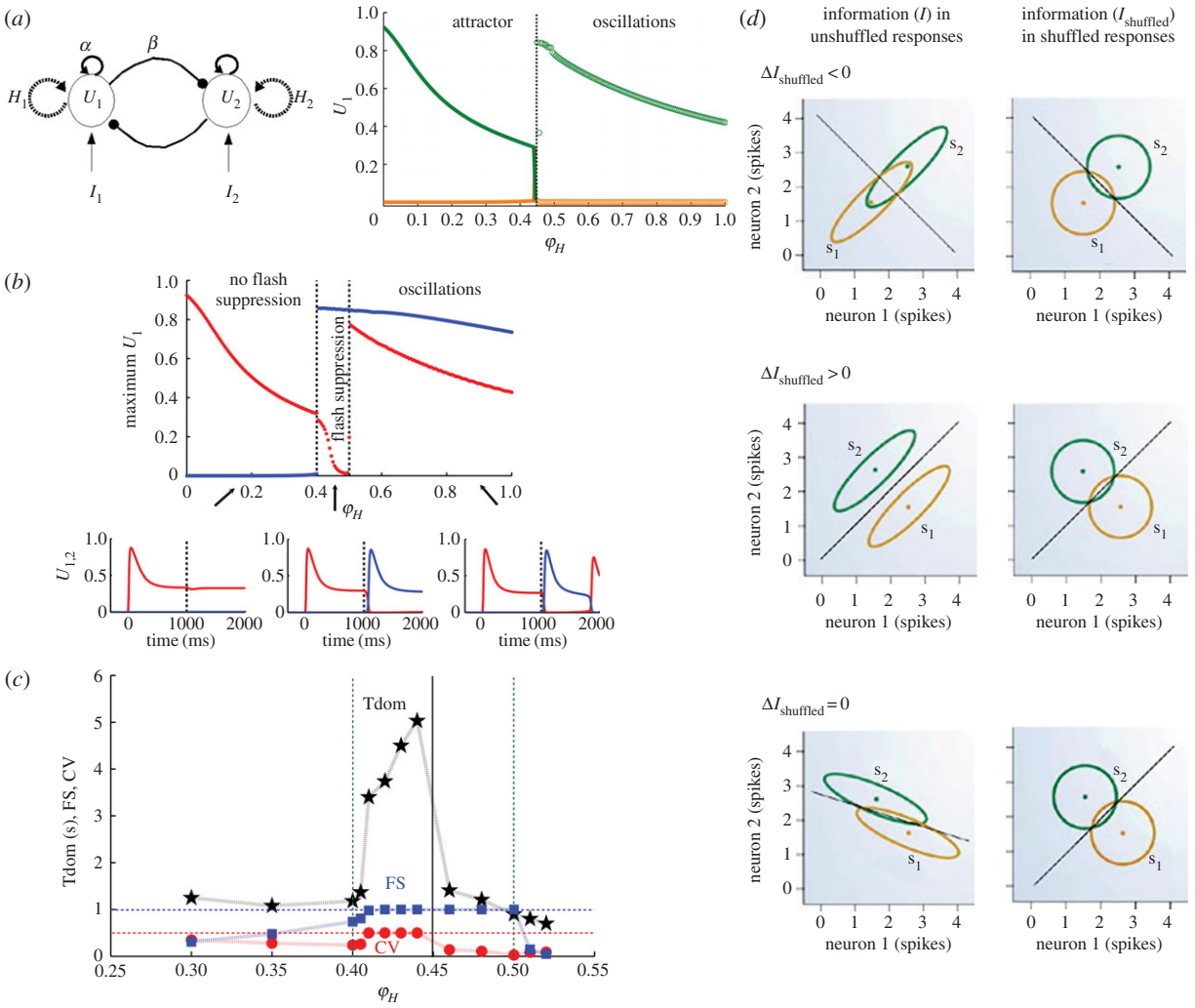

Figure 3. (*a*) Left: Schematic of the unified noise and adaptation competition model. U_i denotes the population rate on each competing neuronal population *i*. I_i denotes the external visual input on each population. Mutual inhibitory connections β are represented by filled circles and recurrent excitatory connections α by arrows. The recurrent dashed arrows on each population symbolize a slow adaptation process (rate frequency adaptation), where the adaptation variable is denoted by H_i on each population *i*. Right: Bifurcation analysis of the noise-free dynamic system as a function of the strength of the adaptation process (φ_H). A bifurcation from a bistable ('attractor') regime to an oscillatory ('oscillations') regime occurs at 0.45. Left of the bifurcation, a double-branched bistable region (solid lines) emerges. The upper (green) and lower (orange) branches correspond to the high and low activity of the dominant and suppressed population, respectively. Right of the bifurcation, an oscillatory region emerges. In this region, the maximum and the minimum (green and orange circles) of the populations' activity during rivalry periodic oscillations are shown. (*b*) Bifurcation analysis of BFS simulation. Upper panel: Flash suppression dynamic range of the competition neuronal model for the noise free case. Flash suppression is characterized by plotting the maximum value of the populations' activity (U_1 in red and U_2 in blue) during the last second of the simulations. Flash suppression corresponds to the region where only the second flashed population U_2 shows high activity and the first stimulated population U_1 is suppressed. Lower panel: Temporal evolution of the populations' firing rate activity U_1 (red) and U_2 (blue) for progressively stronger levels of adaptation (black arrows). Only the type of simulated neuronal behaviour observed in the region labelled 'flash suppression' is similar to the electrophysiological observations in the LPFC. (*c*) Flash suppression (FS), BR dominance time (Tdom) and BR coefficient of variation (CV) as a function of the adaptation level φ_H and with a level of noise σ optimized for each point such that the FS index (number of effective trials/100) is maximal and the CV is as near to 0.5 as possible. There is only one dynamic region where the model is consistent with experimental constraints; that is the narrow, noise-driven, region just before the bifurcation at 0.45. (*d*) Statistical features such as correlated variability could affect population coding. Here, $\Delta I_{\text{shuffled}}$ is a measure of the effect of spike count correlations on the amount of information in a population code. Ellipses represent 95% confidence intervals of the response distributions while the diagonal lines show the optimal decision boundary between stimulus 1 and stimulus 2. The larger the overlap of the ellipses the less information is contained in the population code. Correlations affect ΔI differentially depending on the similarity of the tuning between the two units. During ambiguous stimulation such statistical relationships in the firing of the competing populations could be relevant for perceptual dominance, suppression and perceptual transitions (adapted from [89]).

The second mechanism is known as *noise-driven* and assumes that the underlying neurodynamical system is bi-stable. Here, noise is the main source inducing a transition between the two states (minima), by causing a jump over the barrier (maximum) separating the two stable attractors of the system [71,73,75,78,81–83,85,87]. In these theoretical models when noise is absent, alternations are impossible since the system relaxes indefinitely in one of the two attractors that represent the two possible states of perceptual dominance. The most important evidence for the role of noise in perceptual transitions is the stochastic temporal dynamics of the perceptual transitions observed during BR.

Recent theoretical work suggests that both adaptation and noise operating in a fine balance induce the stochastic properties of perceptual transitions observed in BR [71,83–85,88]. In a recent study [88], we attempted to constrain a mean-field reduced model of rivalrous perception (figure 3*a*, left) with the mean population response observed in the LPFC during

BFS by detecting in which space of a bifurcation separating noise from adaptation regimes (figure 3*a*, right) the neuronal and behavioural correlates of BFS and BR overlap. Our simulations showed that the mean population discharge pattern observed during externally induced perceptual alternations (BFS) in the LPFC can be obtained only in a narrow region around the bifurcation separating a noise-driven, attractor regime from an adaptation-driven, oscillatory regime (figure 3*b*). Therefore, it is probable that neither noise nor adaptation forces alone have a primary, crucial role in externally induced (BFS) perceptual switches. The population discharge pattern observed in the LPFC during BFS could be the result of either adaptation or noise alone. However, the fact that all BR and BFS experimental constraints (psychophysical and electrophysiological, respectively) overlap in a narrow region before the bifurcation (figure 3*c*) provides the first electrophysiologically constrained indication that a noise-driven attractor mechanism might be active during spontaneous perceptual transition in BR.

The mechanism that is validated by the mean discharge response during BFS, implies that adaptation progressively decreases the stability of the perceptually dominant state [83], but just until a critical point where the state becomes unstable. Therefore, adaptation is not enough to induce a transition without the dominant influence of noise which drives the alternation even before the dominant state becomes unstable.

The neuronal responses used to constrain this model were recorded from the macaque LPFC where they reflect reliably the content of conscious visual perception [11]. Therefore, the results and the interpretation of this modelling study are under the assumption that the dynamics of competition at this stage of cortical processing, acting between explicit representations of neuronal activity, is the critical factor for perceptual transitions. Indeed, the human prefrontal cortex is also involved in the temporal dynamics of perceptual alternations during subjective perception as evidenced in patients with prefrontal cortex lesions showing substantial 'freezing' of alternations [90–92]. However, a dominant role for the prefrontal cortex during perceptual transitions remains to be experimentally confirmed. In this context, a much needed study is to record electrophysiological activity in the prefrontal cortex during BR to exclude the possibility that distinct neural mechanisms support dominance and suppression in different paradigms.

(e) Local field potentials and perceptual awareness

In contrast to spiking activity, the local field potential (LFP) is a component of the extracellular field potential that is much slower (approx. 0.1–200 Hz) than spiking activity, and is believed to reflect excitatory and inhibitory postsynaptic potentials and therefore synaptic input and dendritic processing [93–95] within a radius between 500 µm up to several millimetres around the tip of the recording electrode. Thus, although recorded locally, LFP reflects the integration of signals across a larger area compared to MUA and represents more the input and local processing than the output of a local population. Therefore, studying local LFPs in combination with MUA could contribute to our understanding of the specific computations and input–output transformations performed in a given cortical or thalamic area during subjective perception, for example, revealing modulations that are detected in the input and local processing, but not in the output of a brain region.

Indeed, LFP recordings during perceptual suppression seem to resolve a dispute between electrophysiological studies and functional magnetic resonance imaging (fMRI) studies regarding the modulation of LGN and V1 during perceptual awareness. In particular, a number of fMRI studies show significant perceptual modulation in the blood-oxygen-level-dependent (BOLD) signal in LGN and V1 during BR [96–101]. High-frequency (gamma) oscillations in LGN and V1/V2 exhibit negligible perceptual modulation in BR and GFS, similar to spiking activity [9,10,29,32,33].[3] This finding is not surprising since high-frequency ('gamma') LFP power is affected mostly by local discharge activity, while low frequencies reflect mainly neuromodulatory processes [104–106]. However, the power of low-frequency LFPs is more consistently modulated [9,10,29,32,33] and a study that combined fMRI with electrophysiological recordings during GFS found that suppression is indeed reflected in the BOLD and low-frequency LFPs (5–30 Hz), but not in spiking activity and high-frequency LFPs [33]. Furthermore, the modulation of LFPs in V1 appears to be laminar dependent, with supragranular layers being more modulated than infragranular grey matter [107]. This result may indicate that modulation of low-frequency LFPs and BOLD signal in V1 is either due to feedback input from extrastriate cortex where perceptual suppression modulates spiking activity, or due to modulatory signals of subcortical origin. However, the fact that low-frequency LFPs are more likely to reflect processes performed in a larger spatial scale compared to high-frequency LFPs, indicates that the modulation observed during perceptual suppression is most probably non-specific, targeting indiscriminately dominant and suppressed populations.

By contrast, in association cortical areas such as the LPFC the power of high-frequency gamma oscillations was more consistently modulated in sites where MUA also followed subjective stimulus visibility [11]. Therefore, the modulation of gamma LFPs in the LPFC could reflect fairly local input originating from modulated populations in the temporal cortex. On the other hand, beta (15–30 Hz) oscillations in the LPFC exhibited a different, distinctive pattern characterized by desynchronization followed by rebound of activity regardless of the local dominance or suppression of the local neuronal populations and therefore independent of conscious or unconscious processing. Beta oscillations have been suggested to reflect control processes in the frontal cortex and this dissociation between beta LFPs and local processing of conscious perception may underlie a similar dissociation between control functions and consciousness [60].

In a sense, a locally recorded LFP reflects an emergent signal arising from non-linear synaptic and dendritic operations corresponding to integration of inputs in a local site (with differences in the spatial resolution of the signal depending on the frequency examined). Therefore, locally recorded LFP is a signal that reflects the complexity and dynamics of local computations occurring within a few millimetres of the electrode tip and represents the only mesoscopic intracortical signal that has been so far examined with extracellular recordings during perceptual awareness. In §3, we discuss the potential involvement of more complex, emergent patterns of discharge and oscillatory activity of neural populations in conscious perception.

3. Correlated activity and self-organization processes

(a) Correlated neuronal activity and population coding in perceptual awareness

Apart from the LFPs, slow and correlated fluctuations in the activity of neuronal populations can also be detected in the coherence of discharges across neurons. These spike-to-spike coherence measures have been associated with the magnitude of correlated variability or noise across neuronal populations [108]. So far, in every single electrophysiological study of visual awareness, the spiking activity of single units and recorded sites has been studied in isolation and the difference in the magnitude of their averaged firing rate during perceptual dominance and suppression was the measure used to infer the relative contribution of a given cortical area in perceptual awareness. However, due to the probabilistic characteristics of neuronal coding, statistical features such as the magnitude and structure of noise could have important consequences for population coding [89,109–113]. Therefore, measuring and assessing the effects of correlated noise within and between the competing neuronal pools could impose significant constraints on stimulus coding during subjective visual perception.

Specifically, the total amount of noise in a neuronal ensemble can be described by the covariance matrix that includes both individual and interneuronal, correlated, variability [113]. Interneuronal variability is commonly referred to as 'noise correlation' and its impact on neuronal information processing has been studied extensively in a plethora of processes such as stimulus drive [114], neuronal adaptation [115,116], perceptual discrimination [117], attention [108, 118–120], perceptual and associative learning [121,122] and behavioural context [123]. In these studies, correlations were shown to be detrimental, beneficial or not relevant to the efficiency of population codes, depending on their structure and magnitude. In general, for neuronal populations that have similar tuning (or 'signal correlation'), correlations are believed to be detrimental since pooling neuronal responses is not able to average out common noise fluctuations. By contrast, correlations are thought to be beneficial for neuronal populations with opposite tuning (figure 3*d*).

It is therefore important for future electrophysiological studies investigating visual consciousness to record simultaneously from multiple neurons and compare the variability in neuronal discharges during visual rivalry to the respective variability during perception without any underlying visual competition in order to re-evaluate the efficiency of population signal averaging, that is currently thought to encode the content of perceptual awareness, particularly in higher-order cortical areas [38,39]. For example, these measurements could either reinforce the current belief that V1 is indifferent to subjective visibility or reveal properties of neuronal coding that are not reflected in the discharge rate but rather in more fine population properties such as the noise entropy [124] which could potentially represent dominance and suppression. In a similar fashion, for association cortical and thalamic areas, where firing rates reflect dominance and suppression, it is necessary to study how visual competition affects neuronal variability and therefore population coding during subjective perception in order to confirm their role in explicit coding during conscious perception.

Most importantly, it is probable that spontaneous fluctuations of correlated firing within and between competing ensembles (for example, spontaneous transitions from correlated to decorrelated states) could be related to spontaneous perceptual transitions. It would be particularly interesting to associate both theoretically and experimentally such intrinsic neurophysiological fluctuations of coherent population activity to the theoretical concept of noise used in computational models of spontaneous perceptual transitions.

Recently, a role for ongoing fluctuations of cortical activity in conscious perception was indeed detected in functional imaging studies that found a relationship between stimulus awareness and prestimulus ongoing fluctuations of the BOLD signal [125,126]. However, the spatial resolution of fMRI is not adequate to reveal fluctuations within each antagonistic ensemble as well as between them and uncover the role of such population-specific fluctuations in determining the perceptual outcome. On the contrary, due to limitations in the spatio-temporal resolution of fMRI, these BOLD fluctuations may be more related to ultra-low-frequency (less than 0.1 Hz) fluctuations that span neuronal populations regardless of their tuning and feature-specific properties.

(b) Mesoscopic spatio-temporal activity patterns as internal context and a potential role in perceptual reorganization

The endogenously generated perceptual transitions observed in paradigms of multistable perception reflect a, yet unknown, mechanism of state transitions in brain activity. Until now the focus of research has been on the dynamics of competition between rivaling pools of feature selective neurons. However, it has been suggested that the source of this perceptual reorganization process might be independent of the dynamics of antagonistic ensembles and rather reflect a general mechanism underlying perceptual selection that induces the transitions in feature-specific neuronal populations only as a secondary effect [127]. This selection mechanism has been described as a form of involuntary exploratory attention shifting [127] and could be related to ongoing fluctuations of neural activity [125,126] and association areas such as the prefrontal cortex where both BOLD and electrophysiological signals reflect perceptual transitions [55,128] and have a crucial role in representing internal contextual and motivational states assumed to result in perceptual reorganization [127].

Indeed, contextual influences on subjective perception have been well-documented psychophysically (for a review, see [129]) but there is a lack of electrophysiological studies examining how internal context is associated with perceptual reorganization. A candidate neural substrate of internal context could be provided by spatio-temporal patterns of electrophysiological activity whose intrinsic dynamics could offer a link between the state transitions observed in ongoing brain activity and spontaneous perceptual transitions [21,130,131]. The theoretical framework for such state transitions is well established [15,17], and pioneering work by Walter J. Freeman has revealed the dominant role of nonlinear mesoscopic brain dynamics in creating a context for external stimulation (for a review, see [131]). The availability of optical imaging and multielectrode extracellular recording methods (e.g. Utah arrays, tetrode arrays) has already demonstrated the existence of such complex spatio-temporal patterns (travelling waves, spiral waves, etc.) in the mammalian brain both *in vitro* and *in vivo* (figure 4) [132–134]. The spontaneous transitions between different

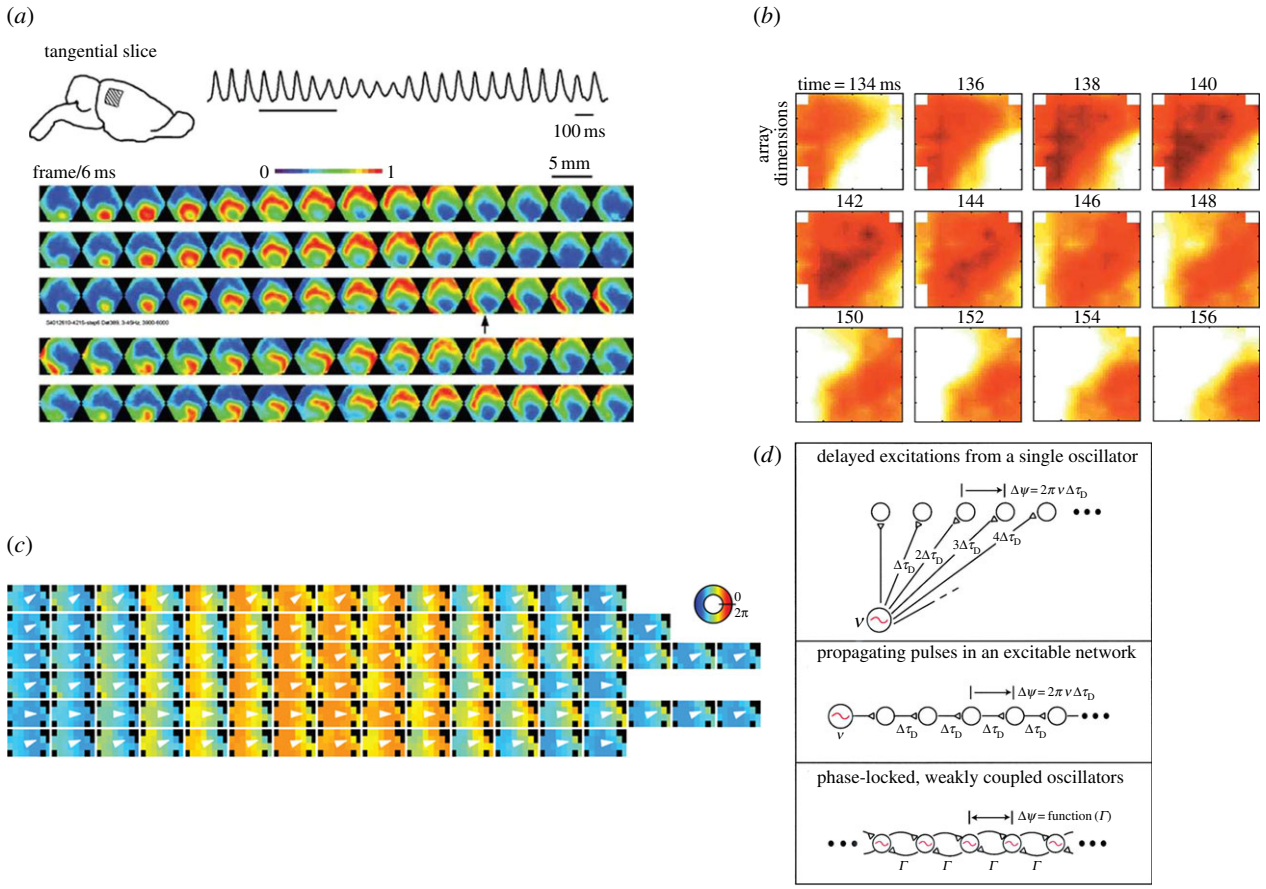

Figure 4. (*a*) Mesoscopic patterns observed *in vitro* using voltage sensitive dyes (VSDs) in the rat visual cortex. A planar wave in the upper pannel is replaced by a spiral wave starting a few frames after the frame marked with an arrow (adapted from [132]). (*b*) Spatio-temporal patterns can be frequency-specific as in the motor cortex where beta oscillations are organized as travelling waves of propagating activity (adapted from [133]). (*c*) In the rat hippocampus frequency-specific travelling waves can be observed in the theta LFP band [134]. (*d*) Phase differences resulting in propagating spatio-temporal patterns can be explained as delayed excitations resulting from a single oscillator, propagating pulses in an excitable network or stable, phase-locked differences between weakly coupled oscillators. Spontaneous changes in the effective interactions between oscillators could result in state transitions between different patterns that might be of great computational value and we hypothesize that they could also be involved in spontaneous transitions in perceptual awareness (adapted from [135]).

mesoscopic patterns are believed to occur due to changes in the effective connectivity of the spatially extended coupled oscillators and could be of great computational significance [135–137]. It is an essential step to perform such invasive recordings of spatio-temporal activity during perceptual awareness tasks and examine how the dynamics of effective connectivity leading to self-organized activity patterns are related to the dynamics of perceptual dominance, perceptual suppression and perceptual reorganization.

4. Conclusion

Although local recordings of electrophysiological activity advanced our understanding of perceptual awareness, they also confirmed that the underlying mechanisms involve multiple areas and populations across the brain. In particular, neurons in higher cortical (LPFC, IT/STS) and thalamic (pulvinar) association areas are more heavily involved in coding explicitly the contents of consciousness and could therefore form a global network of explicit coding, associated to concepts involving a global neuronal workspace in conscious perception. Future efforts should concentrate on understanding the role of functional interactions and spatio-temporal patterns formed by the activity of neuronal populations within and across these areas but also in areas where SUAs are seemingly not correlated to subjective perception. Such studies, along with the development of more elaborate paradigms that disentangle different stages in conscious perception [56] could further enhance our understanding of the mechanisms mediating the emergence of visual consciousness.

Funding statement. This research was supported by the Max Planck Society.

Endnotes

[1]The issue of interocular competition has been thoroughly presented in the past in another review published in this journal [27], where additional evidence against the interocular competition model coming from psychophysical experiments was discussed. Here, we review additional electrophysiological studies that were undertaken later and elucidated further this debate.

[2]For a detailed review of the evidence supporting the necessity but against the sufficiency of V1 for conscious perception, see [37].

[3]Some opposite evidence is provided by Fries *et al.* [102] showing that perceptual dominance but not suppression is accompanied by gamma synchronization in the striate cortex of strabismic cats. The discrepancy between the study of Fries and the negative findings from recordings in the macaque striate cortex could reflect species differences, the effect of strabismus or the different methods used to assess gamma synchronization. Specifically, while in all the macaque studies the absolute band limited gamma power was used, Fries *et al.* employed spike field coherence measures to quantify synchronization. However, LFP–LFP coherence [29] and spike-to-spike synchrony in V1 were also not modulated during subjective perception or texture segregation [103]. Future studies could resolve this issue by performing more detailed analysis of synchronized spiking in the brain during conscious perception.

References

1. Velmans M. 1993 A reflexive science of consciousness. *Ciba Found. Symp.* **174**, 81–91.
2. Attneave F. 1971 Multistability in perception. *Sci. Am.* **225**, 63–71. (doi:10.1038/scientificamerican1271-62)
3. Panagiotaropoulos TI, Logothetis NK. 2013 Multistable visual perception as a gateway to the neural correlates of phenomenal consciousness. The scope and limits of neuroscientific analysis. In *The handbook of experimental phenomenology: visual perception of shape, space and appearance* (ed. L Albertazzi), pp. 119–144. New York, NY: Wiley.
4. Logothetis NK, Schall JD. 1989 Neuronal correlates of subjective visual perception. *Science* **245**, 761–763. (doi:10.1126/science.2772635)
5. Crick F, Koch C. 1990 Towards a neurobiological theory of consciousness. *Semin. Neurosci.* **2**, 263–275.
6. Blake R, Logothetis N. 2002 Visual competition. *Nat. Rev. Neurosci.* **3**, 13–21. (doi:10.1038/nrn701)
7. Wolfe JM. 1984 Reversing ocular dominance and suppression in a single flash. *Vis. Res.* **24**, 471–478. (doi:10.1016/0042-6989(84)90044-0)
8. Wilke M, Logothetis NK, Leopold DA. 2003 Generalized flash suppression of salient visual targets. *Neuron* **39**, 1043–1052. (doi:10.1016/j.neuron.2003.08.003)
9. Wilke M, Mueller KM, Leopold DA. 2009 Neural activity in the visual thalamus reflects perceptual suppression. *Proc. Natl Acad. Sci. USA* **106**, 9465–9470. (doi:10.1073/pnas.0900714106)
10. Keliris G, Logothetis NK, Tolias AS. 2010 The role of the primary visual cortex in perceptual suppression of salient visual stimuli. *J. Neurosci.* **30**, 12 353–12 365. (doi:10.1523/?JNEUROSCI.0677-10.2010)
11. Panagiotaropoulos TI, Deco G, Kapoor V, Logothetis NK. 2012 Neuronal discharges and gamma oscillations explicitly reflect visual consciousness in the lateral prefrontal cortex. *Neuron* **74**, 924–935. (doi:10.1016/j.neuron.2012.04.013)
12. Bonneh YS, Cooperman A, Sagi D. 2001 Motion-induced blindness in normal observers. *Nature* **411**, 798–801. (doi:10.1038/35081073)
13. Cosmelli D, David O, Lachaux JP, Martinerie J, Garnero L, Renault B, Varela F. 2004 Waves of consciousness: ongoing cortical patterns during binocular rivalry. *Neuroimage* **23**, 128–140. (doi:10.1016/j.neuroimage.2004.05.008)
14. Doesburg SM, Green JJ, McDonald JJ, Ward LM. 2009 Rhythms of consciousness: binocular rivalry reveals large-scale oscillatory network dynamics mediating visual perception. *PLoS ONE* **4**, e6142. (doi:10.1371/journal.pone.0006142)
15. Haken H. 2004 *Synergetic computers and cognition*, 2nd edn. Berlin, Germany: Springer.
16. Hipp JF, Engel AK, Siegel M. 2011 Oscillatory synchronization in large scale networks predicts perception. *Neuron* **69**, 387–396. (doi:10.1016/j.neuron.2010.12.027)
17. Kelso JAS. 2012 Multistability and metastability: understanding dynamic coordination in the brain. *Phil. Trans. R. Soc. B* **367**, 906–918. (doi:10.1098/rstb.2011.0351)
18. Melloni L, Singer W. 2010 Distinct characteristics of conscious experience are met by large-scale neuronal synchronization. In *New horizons in the neuroscience of consciousness* (eds EK Perry, D Collerton, FEN LeBeau, H Ashton), pp. 17–28. Amsterdam, The Netherlands: John Benjamins.
19. Srinivasan R, Russell DP, Edelman GM, Tononi G. 1999 Increased synchronization of neuromagnetic responses during conscious perception. *J. Neurosci.* **19**, 5435–5448.
20. Tononi G, Srinivasan R, Russell DP, Edelman GM. 1998 Investigating neural correlates of conscious perception by frequency-tagged neuromagnetic responses. *Proc. Natl Acad. Sci. USA* **95**, 3198–3203. (doi:10.1073/pnas.95.6.3198)
21. Varela FJ. 1999 The specious present: a neurophenomenology of time consciousness. In *Naturalizing phenomenology: issues in contemporary phenomenology and cognitive science* (eds J Petitot, FJ Varela, J-M Roy, B Pachoud), pp. 266–314. Stanford, CA: Stanford University Press.
22. Henze DA, Borhegyi Z, Csicsvari J, Mamiya A, Harris KD, Buszaki G. 2000 Intracellular features predicted by extracellular recordings in the hippocampus *in vivo*. *J. Neurophysiol.* **94**, 479–490.
23. Gray JM, Maldonado PE, Wilson M, McNaughton B. 1995 Tetrodes markedly improve the reliability and yield of multiple single-unit isolation from multi-unit recordings in cat striate cortex. *J. Neurosci. Methods* **63**, 43–54. (doi:10.1016/0165-0270(95)00085-2)
24. Logothetis NK. 2008 What we can do and what we cannot do with fMRI. *Nature* **453**, 869–878. (doi:10.1038/nature06976)
25. Blake R, Westendorf D, Overton R. 1979 What is suppressed during binocular rivalry? *Perception* **9**, 223–231. (doi:10.1068/p090223)
26. Blake R. 1989 A neural theory of binocular rivalry. *Psychol. Rev.* **96**, 145–167. (doi:10.1037/0033-295X.96.1.145)
27. Logothetis NK. 1998 Single units and conscious vision. *Phil. Trans. R. Soc. Lond. B* **353**, 1801–1818. (doi:10.1098/rstb.1998.0333)
28. Lehky SR, Maunsell JHR. 1996 No binocular rivalry in the LGN of alert macaque monkeys. *Vis. Res.* **36**, 1225–1234. (doi:10.1016/0042-6989(95)00232-4)
29. Gail A, Brinksmeyer HJ, Eckhorn R. 2004 Perception-related modulations of local field potential power and coherence in primary visual cortex of awake monkey during binocular rivalry. *Cereb. Cortex* **14**, 300–313. (doi:10.1093/cercor/bhg129)
30. Leopold DA, Logothetis NK. 1996 Activity changes in early visual cortex reflect monkeys' percepts during binocular rivalry. *Nature* **379**, 549–553. (doi:10.1038/379549a0)
31. Grunewald A, Bradley DC, Andersen RA. 2002 Neural correlates of structure-from-motion perception in macaque V1 and MT. *J. Neurosci.* **22**, 6195–6207.
32. Wilke M, Logothetis NK, Leopold DA. 2006 Local field potential reflects perceptual suppression in monkey visual cortex. *Proc. Natl Acad. Sci. USA* **103**, 17 507–17 512. (doi:10.1073/pnas.0604673103)
33. Maier A, Wilke M, Aura C, Zhu C, Ye FQ, Lepold DA. 2008 Divergence of fMRI and neural signals in V1 during perceptual suppression in the awake monkey. *Nat. Neurosci.* **11**, 1193–1200. (doi:10.1038/nn.2173)
34. Libedinsky C, Savage T, Livingstone M. 2009 Perceptual and physiological evidence for a role for early visual areas in motion-induced blindness. *J. Vis.* **9**, 14. 1–10. (doi:10.1167/9.1.14)
35. Cumming BG, Parker AJ. 1997 Responses of primary visual cortical neurons to binocular disparity without depth perception. *Nature* **389**, 280–283. (doi:10.1038/38487)
36. Supèr H, Spekreijse H, Lamme VA. 2001 Two distinct modes of sensory processing observed in monkey primary visual cortex (V1). *Nat. Neurosci.* **4**, 304–310. (doi:10.1038/85170)
37. Lamme VAF. 2000 The role of primary visual cortex (V1) in visual awareness. *Vis. Res.* **40**, 1507–1521. (doi:10.1016/S0042-6989(99)00243-6)
38. Crick F, Koch C. 1995 Are we aware of neural activity in primary visual cortex? *Nature* **375**, 121–123. (doi:10.1038/375121a0)
39. Crick F, Koch C. 1998 Consciousness and neuroscience. *Cereb. Cortex* **8**, 97–107. (doi:10.1093/cercor/8.2.97)
40. Leopold DA. 2012 Primary visual cortex: awareness and blindsight. *Annu. Rev. Neurosci.* **35**, 91–109. (doi:10.1146/annurev-neuro-062111-150356.)
41. Lamme VAF, Roelfsema PR. 2000 The distinct modes of vision offered by feedforward and recurrent processing. *Trends Neurosci.* **23**, 571–579. (doi:10.1016/S0166-2236(00)01657-X)
42. Maier A, Logothetis NK, Leopold DA. 2007 Context-dependent perceptual modulation of single neurons in primate visual cortex. *Proc. Natl Acad. Sci. USA* **104**, 5620–5625. (doi:10.1073/pnas.0608489104)
43. Bradley DC, Chang GC, Andersen RA. 1998 Encoding the three-dimensional structure-from-motion by primate area MT neurons. *Nature* **392**, 714–717. (doi:10.1038/33688)
44. Dodd JV, Krug K, Cumming BG, Parker AJ. 2001 Perceptually bistable three-dimensional figures evoke high choice probabilities in cortical area MT. *J. Neurosci.* **21**, 4809–4821.
45. Sheinberg DL, Logothetis NK. 1997 The role of temporal cortical areas in perceptual organization. *Proc. Natl Acad. Sci. USA* **94**, 3408–3413. (doi:10.1073/pnas.94.7.3408)
46. Kreiman G, Fried I, Koch C. 2002 Single-neuron correlates of subjective vision in the human medial

temporal lobe. *Proc. Natl Acad. Sci. USA* **99**, 8378–8383. (doi:10.1073/pnas.072194099)

47. Ungerleider LG, Haxby JV. 1994 What and where in the human brain. *Curr. Opin. Neurobiol.* **4**, 157–165. (10.1016/0959-4388(94)90066-3)
48. Barbas H. 1988 Anatomic organization of basoventral and mediodorsal visual recipient prefrontal regions in the rhesus monkey. *J. Comp. Neurol.* **276**, 313–342. (doi:10.1002/cne.902760302)
49. Borra E, Ichinohe N, Sato T, Tanifuji M, Rockland KS. 2010 Cortical connections to area TE in monkey: hybrid modular and distributed organization. *Cereb. Cortex* **20**, 257–270. (doi:10.1093/cercor/bhp096)
50. Webster MJ, Bachevalier J, Ungerleider LG. 1994 Connections of inferior temporal areas TEO and TE with parietal and frontal cortex in macaque monkeys. *Cereb. Cortex* **4**, 470–483. (doi:10.1002/cne.903340111)
51. Yeterian EH, Pandya DN, Tomaiuolo F, Petrides M. 2012 The cortical connectivity of the prefrontal cortex in the monkey brain. *Cortex* **48**, 58–81. (doi:10.1016/j.cortex.2011.03.004)
52. Pigarev IN, Rizzolatti G, Scandolara C. 1979 Neurons responding to visual stimuli in the frontal lobe of macaque monkeys. *Neurosci. Lett.* **12**, 207–212. (doi:10.1016/0304-3940(79)96063-4)
53. Scalaidhe SP, Wilson FA, Goldman-Rakic PS. 1999 Face-selective neurons during passive viewing and working memory performance of rhesus monkeys: evidence for intrinsic specialization of neuronal coding. *Cereb. Cortex* **9**, 459–475. (doi:10.1093/cercor/9.5.459)
54. Wilson FA, Scalaidhe SP, Goldman-Rakic PS. 1993 Dissociation of object and spatial processing domains in primate prefrontal cortex. *Science* **260**, 1955–1958. (doi:10.1126/science.8316836)
55. Libedinsky C, Livingstone M. 2011 Role of prefrontal cortex in conscious visual perception. *J. Neurosci.* **31**, 64–69. (doi:10.1523/JNEUROSCI.3620-10.2011)
56. Aru J, Bachmann T, Singer W, Melloni L. 2012 Distilling the neural correlates of consciousness. *Neurosci. Biobehav. Rev.* **36**, 737–746. (doi:10.1016/j.neubiorev.2011.12.003)
57. van Gaal S, deLange FP, Cohen MX. 2012 The role of consciousness in cognitive control and decision making. *Front. Hum. Neurosci.* **6**, 121. (doi:10.3389/fnhum.2012.00121)
58. van Gaal S, Ridderinkhof KR, Scholte HS, Lamme VA. 2010 Unconscious activation of the prefrontal no-go network. *J. Neurosci.* **30**, 4143–4150. (doi:10.1523/JNEUROSCI.2992-09.2010)
59. van Gaal S, Lamme VA. 2012 Unconscious high-level information processing: implication for neurobiological theories of consciousness. *Neuroscientist* **18**, 287–301. (doi:10.1177/1073858411404079)
60. Panagiotaropoulos TI, Kapoor V, Logothetis NK. 2013 Desynchronization and rebound of beta oscillations during conscious and unconscious local neuronal processing in the macaque lateral prefrontal cortex. *Front. Psychol.* **4**, 603. (doi:10.3389/fpsyg.2013.00603)
61. Barbas H, Henion TH, Dermon CR. 1991 Diverse thalamic projections to the prefrontal cortex in the rhesus monkey. *J. Comp. Neurol.* **313**, 65–94. (doi:10.1002/cne.903130106)
62. Contini M, Baccarini M, Borra E, Gerbella M, Rozzi S, Lupino G. 2010 Thalamic projections to the macaque caudal ventrolateral prefrontal areas 45A and 45B. *Eur. J. Neurosci.* **32**, 1337–1353. (doi:10.1111/j.1460-9568.2010.07390.x)
63. Romanski LM, Giguere M, Bates JF, Goldman-Rakic PS. 1997 Topographic organization of medial pulvinar connections with the prefrontal cortex in the rhesus monkey. *J. Comp. Neurol.* **379**, 313–332. (doi:10.1002/(SICI)1096-9861(19970317)379:33.0.CO;2-6)
64. Webster MJ, Bachevalier J, Ungerleider LG. 1993 Subcortical connections of inferior temporal areas TE and TEO in macaque monkeys. *J. Comp. Neurol.* **335**, 73–91. (doi:10.1002/cne.903350106)
65. Gutierrez C, Cola MG, Seltzer B, Cusick C. 2000 Neurochemical and connectional organization of the dorsal pulvinar complex in monkeys. *J. Comp. Neurol.* **419**, 61–86. (10.1002/(SICI)1096-9861(20000327)419:1<61::AID-CNE4>3.0.CO;2-I)
66. Shipp S. 2003 The functional logic of cortico-pulvinar connections. *Phil. Trans. R. Soc. Lond. B* **358**, 1605–1624. (doi:10.1098/rstb.2002.1213)
67. Dehaene S, Changeux JP. 2011 Experimental and theoretical approaches to conscious processing. *Neuron* **70**, 200–227. (doi:10.1016/j.neuron.2011.03.018)
68. Baars BJ, Franklin S, Ramsoy TZ. 2013 Global workspace dynamics: cortical 'binding and propagation' enables conscious contents. *Front. Psychol.* **4**, 200. (doi:10.3389/fpsyg.2013.00200)
69. Llinas RR, Ribary U, Contreras D, Pedroarena C. 1998 The neuronal basis for consciousness. *Phil. Trans. R. Soc. Lond. B* **353**, 1841–1849. (doi:10.1098/rstb.1998.0336)
70. Gaillard R, Dehaene S, Adam C, Clémenceau S, Hasboun D, Baulac M, Cohen L, Naccache L. 2009 Converging intracranial markers of conscious access. *PLoS Biol.* **7**, e61. (doi:10.1371/journal.pbio.1000061)
71. Alais D, Cass J, O'Shea RP, Blake R. 2010 Visual sensitivity underlying changes in visual consciousness. *Curr. Biol.* **20**, 1362–1367. (doi:10.1016/j.cub.2010.06.015)
72. Bialek W, DeWeese M. 1995 Random switching and optimal processing in the perception of ambiguous signals. *Phys. Rev. Lett.* **74**, 3077–3080. (doi:10.1103/PhysRevLett.74.3077)
73. Brascamp JW, van Ee R, Noest AJ, Jacobs RH, van den Berg AV. 2006 The time course of binocular rivalry reveals a fundamental role of noise. *J. Vis.* **6**, 1244–1256. (doi:10.1167/6.11.8)
74. Freeman AW. 2005 Multistage model for binocular rivalry. *J. Neurophysiol.* **94**, 4412–4420. (doi:10.1152/jn.00557.2005)
75. Kim Y, Grabowecky M, Suzuki S. 2006 Stochastic resonance in binocular rivalry. *Vis. Res.* **46**, 392–406. (doi:10.1016/j.visres.2005.08.009)
76. Lago-Fernandez L, Deco G. 2002 A model of binocular rivalry based on competition in IT. *Neurocomputing* **44**, 503–507. (doi:10.1016/S0925-2312(02)00408-3)
77. Laing CR, Chow CC. 2002 A spiking neuron model for binocular rivalry. *J. Comput. Neurosci.* **12**, 39–53. (doi:10.1023/A:1014942129705)
78. Lankheet MJ. 2006 Unraveling adaptation and mutual inhibition in perceptual rivalry. *J. Vis.* **6**, 304–310. (doi:10.1167/6.4.1)
79. Lehky S. 1987 A stable multivibrator model of binocular rivalry. *Perception* **17**, 215–228. (doi:10.1068/p170215)
80. Lumer ED. 1998 A neural model of binocular integration and rivalry based on the coordination of action-potential timing in primary visual cortex. *Cereb. Cortex* **8**, 553–561. (doi:10.1093/cercor/8.6.553)
81. Moreno-Bote R, Rinzel J, Rubin N. 2007 Noise-induced alternations in an attractor network model of perceptual bistability. *J. Neurophysiol.* **98**, 1125–1139. (doi:10.1152/jn.00116.2007)
82. Shpiro A, Curtu R, Rinzel J, Rubin N. 2007 Dynamical characteristics common to neuronal competition models. *J. Neurophysiol.* **97**, 462–473. (doi:10.1152/jn.00604.2006)
83. Shpiro A, Moreno-Bote R, Rubin N, Rinzel J. 2009 Balance between noise and adaptation in competition models of perceptual bistability. *J. Comput. Neurosci.* **27**, 37–54. (doi:10.1007/s10827-008-0125-3)
84. Theodoni P, Panagiotaropoulos TI, Kapoor V, Logothetis NK, Deco G. 2011 Cortical microcircuit dynamics mediating binocular rivalry: the role of adaptation in inhibition. *Front. Hum. Neurosci.* **5**, 145. (doi:10.3389/fnhum.2011.00145)
85. van Ee R. 2009 Stochastic variations in sensory awareness are driven by noisy neuronal adaptation: evidence from serial correlations in perceptual bistability. *J. Opt. Soc. Am. A Opt. Image Sci. Vis.* **26**, 2612–2622. (doi:10.1364/JOSAA.26.002612)
86. Wilson HR. 2003 Computational evidence for a rivalry hierarchy in vision. *Proc. Natl Acad. Sci. USA* **100**, 14 499–14 503. (doi:10.1073/pnas.2333622100)
87. Kramers HA. 1940 Brownian motion in a field of force and the diffusion model of chemical reactions. *Physicas* **7**, 284–304. (doi:10.1016/S0031-8914(40)90098-2)
88. Panagiotaropoulos TI, Kapoor V, Logothetis NK, Deco G. 2013 A common neurodynamical mechanism could mediate externally induced and intrinsically generated transitions in visual awareness. *PLoS ONE* **8**, e53833. (doi:10.1371/journal.pone.0053833)
89. Averbeck BB, Latham PE, Pouget A. 2006 Neural correlations population coding and computation. *Nat. Rev. Neurosci.* **7**, 358–366. (doi:10.1038/nrn1888)
90. Meenan JP, Miller LA. 1994 Perceptual flexibility after frontal or temporal lobectomy. *Neuropsychologia* **32**, 1145–1149. (doi:10.1016/0028-3932(94)90159-7)
91. Ricci C, Blundo C. 1990 Perception of ambiguous figures after focal brain lesions. *Neuropsychologia* **28**, 1163–1173. (doi:10.1016/0028-3932(90)90052-P)

92. Windmann S, Wehrmann M, Calabrese P, Güntürkün O. 2006 Role of the prefrontal cortex in attentional control over bistable vision. *J. Cogn. Neurosci.* **18**, 456–471. (doi:10.1162/jocn.2006.18.3.456)
93. Mitzdorf U. 1985 Current-source density method and application in cat cerebral cortex: investigation of evoked potentials and EEG phenomena. *Physiol. Rev.* **65**, 37.
94. Mitzdorf U. 1987 Properties of the evoked potential generators: current-source density analysis of visually evoked potentials in the cat cortex. *Int. J. Neurosci.* **33**, 33–59. (doi:10.3109/00207458708985928)
95. Logothetis NK. 2003 The underpinnings of the BOLD functional magnetic resonance imaging signal. *J. Neurosci.* **23**, 3963–3971.
96. Haynes JD, Deichmann R, Rees G. 2005 Eye-specific effects of binocular rivalry in the human lateral geniculate nucleus. *Nature* **438**, 496–499. (doi:10.1038/nature04169)
97. Haynes JD, Rees G. 2005 Predicting the stream of consciousness from activity in the human visual cortex. *Curr. Biol.* **15**, 1201–1207. (doi:10.1016/j.cub.2005.06.026)
98. Lee SH, Blake R. 2002 V1 activity is reduced during binocular rivalry. *J. Vis.* **2**, 618–626. (doi:10.1167/1.3.448)
99. Lee SH, Blake R, Heeger DJ. 2007 Hierarchy of cortical responses underlying binocular rivalry. *Nat. Neurosci.* **10**, 1048–1054. (doi:10.1038/nn1939)
100. Polonsky A, Blake R, Braun J, Heeger DJ. 2000 Neuronal activity in human primary visual cortex correlates with perception during binocular rivalry. *Nat. Neurosci.* **3**, 1153–1159. (doi:10.1038/80676)
101. Tong F, Engel SA. 2001 Interocular rivalry revealed in the human cortical blind-spot representation. *Nature* **411**, 195–199. (doi:10.1038/35075583)
102. Fries P, Roelfsema PR, Engel AK, König P, Singer W. 1997 Synchronization of oscillatory responses in visual cortex correlates with perception in interocular rivalry. *Proc. Natl Acad. Sci. USA* **94**, 12 699–12 704. (doi:10.1073/pnas.94.23.12699)
103. Lamme VA, Spekreijse H. 1998 Neuronal synchrony does not represent texture segregation. *Nature* **396**, 362–366. (doi:10.1038/24608)
104. Belitski A, Gretton A, Magri A, Murayama Y, Montemurro MA, Logothetis NK, Panzeri S. 2008 Low-frequency local field potentials and spikes in primary visual cortex convey independent visual information. *J. Neurosci.* **28**, 5696–5709. (doi:10.1523/JNEUROSCI.0009-08.2008)
105. Magri C, Schridde U, Murayama Y, Panzeri S, Logothetis NK. 2012 The amplitude and timing of the BOLD signal reflects the relationship between local field potential power at different frequencies. *J. Neurosci.* **32**, 1395–1407. (doi:10.1523/JNEUROSCI.3985-11.2012)
106. Steriade M. 2006 Grouping of brain rhythms in corticothalamic systems. *Neuroscience* **137**, 1087–1106. (doi:10.1016/j.neuroscience.2005.10.029)
107. Maier AV, Aura CJ, Leopold DA. 2007 Laminar differences in perceptual modulation of V1 local field potentials. In *Program No. 451.12. Neuroscience Meeting Planner*. San Diego, CA: Society for Neuroscience.
108. Mitchell JF, Sundberg KA, Reynolds JH. 2009 Spatial attention decorrelates intrinsic activity fluctuations in macaque area V4. *Neuron* **63**, 879–888. (doi:10.1016/j.neuron.2009.09.013)
109. Abbott LF, Dayan P. 1999 The effect of correlated variability on the accuracy of a population code. *Neural Comput.* **11**, 91–101. (doi:10.1162/089976699300016827)
110. Sompolinsky H, Yoon H, Kang K, Shamir M. 2001 Population coding in neuronal systems with correlated noise. *Phys. Rev. E Stat. Nonlin. Soft Matter Phys.* **64**, 051904. (doi:10.1103/PhysRevE.64.051904)
111. Wilke SD, Eurich CW. 2002 Representational accuracy of stochastic neural populations. *Neural Comput.* **14**, 155. (doi:10.1162/089976602753284482)
112. Zohary E, Shadlen MN, Newsome WT. 1994 Correlated neuronal discharge rate and its implications for psychophysical performance. *Nature* **370**, 140–143. (doi:10.1038/370140a0)
113. Averbeck BB, Lee D. 2006 Effects of noise correlations on information encoding and decoding. *J. Neurophysiol.* **95**, 3633–3644. (doi:10.1152/jn.00919.2005)
114. Kohn A, Smith MA. 2005 Stimulus dependence of neuronal correlation in primary visual cortex of the macaque. *J. Neurosci.* **25**, 3661–3673. (doi:10.1523/JNEUROSCI.5106-04.2005)
115. Adibi M, McDonald JS, Clifford CW, Arabzadeh E. 2013 Adaptation improves neural coding efficiency despite increasing correlations in variability. *J. Neurosci.* **33**, 2108–2120. (doi:10.1523/JNEUROSCI.3449-12.2013)
116. Gutnisky DA, Dragoi V. 2008 Adaptive coding of visual information in neural populations. *Nature* **452**, 220–224. (doi:10.1038/nature06563)
117. Romo R, Hernández A, Zainos A, Salinas E. 2003 Correlated neuronal discharges that increase coding efficiency during perceptual discrimination. *Neuron* **38**, 649–657. (doi:10.1016/S0896-6273(03)00287-3)
118. Cohen MR, Maunsell JHR. 2009 Attention improves performance primarily by reducing interneuronal correlations. *Nat. Neurosci.* **12**, 1594–1600. (doi:10.1038/nn.2439)
119. Herrero JL, Gieselmann MA, Sanayei M, Thiele A. 2013 Attention-induced variance and noise correlation reduction in macaque V1 is mediated by NMDA receptors. *Neuron* **78**, 729–739. (doi:10.1016/j.neuron.2013.03.029)
120. Poort J, Roelfsema PR. 2009 Noise correlations have little influence on the coding of selective attention in area V1. *Cereb. Cortex* **19**, 543–553. (doi:10.1093/cercor/bhn103)
121. Gu Y, Liu S, Fetsch CR, Yang Y, Fok S, Sunkara A, DeAngelis GC, Angelaki DE. 2011 Perceptual learning reduces interneuronal correlations in macaque visual cortex. *Neuron* **71**, 750–761. (doi:10.1016/j.neuron.2011.06.015)
122. Jeanne JM, Sharpee TO, Gentner TQ. 2013 Associative learning enhances population coding by inverting interneuronal correlation patterns. *Neuron* **78**, 352–363. (doi:10.1016/j.neuron.2013.02.023)
123. Cohen MR, Newsome WT. 2008 Context-dependent changes in functional circuitry in visual area MT. *Neuron* **60**, 162–173. (doi:10.1016/j.neuron.2008.08.007)
124. Ecker AS, Berens P, Tolias AS, Bethge M. 2011 The effect of noise correlations in populations of diversely tuned neurons. *J. Neurosci.* **31**, 14 272–14 283. (doi:10.1523/JNEUROSCI.2539-11.2011)
125. Hesselmann G, Kell CA, Eger E, Kleinschmidt A. 2008 Spontaneous local variations in ongoing neural activity bias perceptual decisions. *Proc. Natl Acad. Sci. USA* **105**, 10 984–10 989. (doi:10.1073/pnas.0712043105)
126. Hesselmann G, Kell CA, Kleinschmidt A. 2008 Ongoing activity fluctuations in hMT+ bias the perception of coherent visual motion. *J. Neurosci.* **28**, 14 481–14 485. (doi:10.1523/JNEUROSCI.4398-08.2008)
127. Leopold DA, Logothetis NK. 1999 Multistable phenomena: changing views in perception. *Trends Cogn. Sci.* **3**, 254–264. (doi:10.1016/S1364-6613(99)01332-7)
128. Lumer ED, Friston KJ, Rees G. 1998 Neural correlates of perceptual rivalry in the human brain. *Science* **280**, 1930–1934. (doi:10.1126/science.280.5371.1930)
129. Klink PC, van Wezel RJ, van Ee R. 2012 United we sense, divided we fail: context-driven perception of ambiguous visual stimuli. *Phil. Trans. R. Soc. B* **367**, 932–941. (doi:10.1098/rstb.2011.0358)
130. Cosmelli DJ, Lachaux JP, Thompson E. 2007 *Neurodynamical approaches to consciousness*. In *Cambridge handbook of consciousness* (eds PD Zelazo, M Moscovitch, E Thompson), pp. 731–774. Cambridge, UK: Cambridge University Press.
131. Freeman WJ. 2000 Mesoscopic neurodynamics: from neuron to brain. *J. Physiol. Paris* **94**, 303–322. (doi:10.1016/S0928-4257(00)01090-1)
132. Wu JY, Huang X, Zhang C. 2008 Propagating waves of activity in the neocortex: what they are, what they do. *Neuroscientist* **14**, 487–502. (doi:10.1177/1073858408317066)
133. Rubino D, Robbins KA, Hatsopoulos NG. 2006 Propagating waves mediate information transfer in the motor cortex. *Nat. Neurosci.* **9**, 1549–1557. (doi:10.1038/nn1802)
134. Lubenov EV, Siapas AG. 2009 Hippocampal theta oscillations are travelling waves. *Nature* **459**, 534–539. (doi:10.1038/nature08010)
135. Ermentrout GB, Kleinfeld D. 2001 Traveling electrical waves in cortex: insights from phase dynamics and speculation on a computational role. *Neuron* **29**, 33–44. (doi:10.1016/S0896-6273(01)00178-7)
136. Kenet T, Bibitchkov D, Tsodyks M, Grinvald A, Arieli A. 2003 Spontaneously emerging cortical representations of visual attributes. *Nature* **425**, 954–956. (doi:10.1038/nature02078)
137. Tsodyks M, Kenet T, Grinvald A, Arieli A. 1999 Linking spontaneous activity of single cortical neurons and the underlying functional architecture. *Science* **286**, 1943–1946. (doi:10.1126/science.286.5446.1943)

A.3 Decorrelated discharge fluctuations in prefrontal microcircuits during visual consciousness.

"...one of the strongest motives that lead men to art and science is escape from everyday life with its painful crudity and hopeless dreariness, from the fetters of one's own ever-shifting desires. A finely tempered nature longs to escape from the personal life into the world of objective perception and thought."

Albert Einstein, "Principles of Research address"

Decorrelated discharge fluctuations in prefrontal microcircuits during visual consciousness

Theofanis I. Panagiotaropoulos [1, 6, 7, 9], Panagiota Theodoni [2, 3, 9*], Vishal Kapoor [1, 8, 9], Gustavo Deco[2, 4], & Nikos K. Logothetis[1, 5]

1. Max-Planck-Institute for Biological Cybernetics, Department of Physiology of Cognitive Processes, 72076 Tübingen, Germany.
2. Center for Brain and Cognition, Computational Neuroscience Group, Department of Information and Communications Technologies, Universitat Pompeu Fabra, 08010 Barcelona, Spain.
3. Centre de Recerca Matemàtica, Campus de Bellatera, 08193 Bellatera (Barcelona), Spain.
4. Institució Catalana de la Recerca i Estudis Avançats, Universitat Pompeu Fabra, 08010 Barcelona, Spain.
5. Imaging Science and Biomedical Engineering, University of Manchester, Manchester M13 9PL, UK.
6. Centre for Systems Neuroscience, University of Leicester, Great Britain
7. Institute of Psychiatry, Psychology and Neuroscience, King's College London, Great Britain.
8. Graduate School of Neural and Behavioral Sciences, International Max Planck Research School, Eberhard-Karls University of Tübingen, 72074 Tübingen, Germany.
9. These authors contributed equally to this work.

Key words: prefrontal cortex, noise correlations, spiking network, visual consciousness.

SUMMARY

Single neuron discharges in association cortices represent the content of consciousness during subjective visual perception. However, it is currently unknown if emergent properties of intra-areal functional connectivity patterns like the structure of interneuronal firing correlations constrain the population coding accuracy. Here we show that in the macaque lateral prefrontal cortex (LPFC), subjective perception is accompanied by extremely weak – zero assuming sparse coding – pairwise correlations reflecting a beneficial structure compared to significant correlations during perception without a subjective component. Biophysically realistic simulations suggest that the source of decorrelation during subjective perception is not local cross-inhibition between antagonistic ensembles but active suppression of input fluctuations. Furthermore, the decorrelated state is tightly associated to the discharge rate representation of subjective perception suggesting that suppression of input fluctuations is critical for conscious content coding. Our results provide the first insights into the structure and underlying mechanisms of correlated fluctuations during visual consciousness.

INTRODUCTION

Ambiguous visual stimulation has the astonishing capacity to disentangle the content of conscious perception from sensory input. Such a well described psychophysical paradigm is binocular rivalry (BR) in which two disparate visual stimuli presented at corresponding parts of the two retinas compete for access to awareness and, as a result of this competition, enter successive phases of perceptual dominance and suppression [1]. Under such ambiguous conditions, the subjective perceptual dominance of a visual stimulus is conceptualized to be physiologically supported by an assembly of neurons with similar stimulus preference that dominates over a competing, suppressed, population through the dominance of its averaged firing rate [2-3].

Indeed, studies combining rivalrous visual stimulation with electrophysiology in the macaque brain suggest that perceptual competition involves two rivaling stimuli representations embedded in two distinct neuronal assemblies that are tuned to each visual pattern and battle for activity dominance [4-7]. These populations can be detected across the visual cortical hierarchy but their discharge activity is more likely to reflect the content of conscious perception in association cortical areas like the temporal and prefrontal cortex [6-9].

Until now, these neurons were studied in isolation. Their averaged rate across repeated epochs of subjective perceptual dominance or suppression of their preferred stimulus was compared to the respective average rate during perception or physical absence of the same stimulus without any underlying visual competition, to infer the relative contribution of a given cortical area in visual consciousness. However, from a theoretical point of view, functional connectivity features like the structure of interneuronal trial-to-trial discharge variability could severely influence population coding capacity [10-13]. Specifically, fluctuations in neuronal

discharge responses to repeated presentations of the same stimulus are thought to be the consequence of intrinsically generated noise [14]. The total amount of noise, or noise entropy, in a neuronal ensemble is captured in the population covariance matrix that describes the magnitude of both individual and interneuronal, correlated, fluctuations [11, 15]. The latter component is commonly called spike count - or noise - correlations (r_{sc}) and its impact on information coding has been studied experimentally in sensory [16-19] and cognitive [20-26] processing. In these studies correlations were found to be detrimental, beneficial or irrelevant to the fidelity of population codes, depending on their structure, magnitude and the assumptions employed by decoding algorithms that read out ensemble activity.

In general, a so-called limited range correlation structure - where correlations are stronger for similarly tuned neurons - is detrimental for population coding since the signal enhancement from averaging neuronal responses is constrained by correlated noise fluctuations [27-29]. In contrast, strong correlations across neurons with opposite tuning could be beneficial for stimulus coding [10-11, 21]. Therefore, the structure of interneuronal correlations during subjective visual perception could reveal how functional microcircuit organization affects the fidelity of conscious representations, particularly in association areas where a population average is currently believed to represent more reliably the content of consciousness compared to primary sensory areas [3, 8-9].

Here we determined the structure of LPFC correlations during visual rivalry by measuring their magnitude within and between dominant and suppressed neuronal pools. Our results reveal a beneficial, decorrelated state during subjective visual perception compared to perception without any underlying stimulus competition. Considering a biophysically realistic spiking network comprising two neural populations with or without cross-inhibition we find that cross-inhibition is not the source of decorrelation during visual consciousness. Rather, active

suppression of input fluctuations induces the decorrelated prefrontal state.

RESULTS

Induction of perceptual dominance and suppression

We dissected dominant and suppressed states of LPFC neurons during visual consciousness by combining binocular flash suppression (BFS), a well-controlled variant of BR stimulation that dissociates subjective perception from sensory input [6-7, 30], with extracellular tetrode recordings in alert macaques. The effects of subjective perceptual dominance and suppression of a preferred stimulus on intrinsic noise in BFS were compared to the effects of corresponding non-subjective perceptual states during monocular physical alternation (PA) of the same stimuli.

In PA (Fig. 1A-B), each trial starts with the presentation of a fixation spot in both eyes that is binocularly fused and remains on until the end of the trial. In Fig. 1A, after 300ms of stimulus-free fixation (t = 0-300ms) a polar checkerboard is monocularly presented for 1000ms (t = 301-1300ms) and then removed and followed by a monkey face stimulus presented in the contralateral eye for 1000ms (t = 1301-2300ms). In half of the PA trials the order of stimulus presentation is reversed (Fig. 1B). In both PA conditions visual perception is non-subjective since a unique pattern stimulates the visual system during each trial phase. The normalized difference in the mean firing rate of each recorded unit between monocular stimulation with a face and a checkerboard from t = 1301-2300ms was used to estimate a non-subjective neuronal stimulus preference index (SPI_{PA}).

In BFS trials (Fig. 1C-D), one second following the first stimulus onset (i.e. at t = 1301ms), the same disparate visual patterns - as in PA - are flashed to the contralateral eye. The

flashed stimuli remain on for 1000ms (t = 1301-2300ms), robustly suppressing the perception of contra laterally presented stimuli that are still physically present (compare Fig. 1C to 1A and 1D to 1B). During this period the newly presented pattern is perceptually dominant while the initially presented stimulus becomes perceptually suppressed [6-7].The maintenance of stimulus preference under subjective conditions, suggestive of a conscious representation, was determined by calculating the stimulus preference index during BFS (SPI_{BFS}).

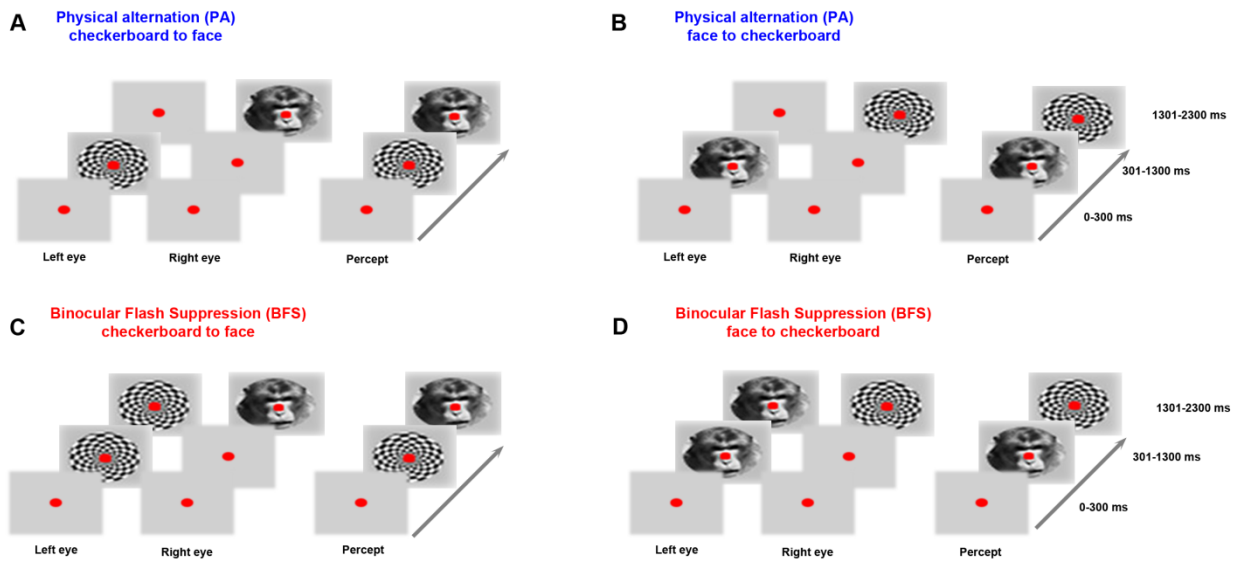

Figure 1

Physical alternation (PA) and Binocular Flash Suppression (BFS)

Monocular PA between two disparate stimuli (checkerboard and face) was used to determine the sensory stimulus preference of all recorded neurons (A and B). In (A), monocular stimulation with a polar checkerboard during the first second of the trial is followed by stimulation of the contralateral eye with a face. In (B) the order of stimulus presentation is reversed. For each recorded neuron, the normalized difference in the mean discharge rate between the two stimuli in

A and B during t =1301-2300ms was used to estimate the baseline, non-subjective, stimulus preference index (*SPI*).

In BFS (C and D) the initially presented stimulus was not removed but remained in place to be suppressed by the second stimulus flash. Therefore, depending on the sensory preference of each recorded neuron (determined in PA trials) BFS trials allowed to study discharge activity during the dominance or suppression of a preferred stimulus.

Discharge responses and second order statistics during subjective and non-subjective perception

The profile of a typical pair of simultaneously recorded units exhibiting same stimulus preference in PA and BFS is shown in Fig. 2. Both cells were recorded from the same tetrode (Fig. 2A-B) and were extremely well isolated (false assignment rate $p < 0.005\%$ for both units, for spike sorting methods and quantitative evaluation of single unit isolation see ref. **31**). During PA both neurons fired more during monocular presentation of a polar checkerboard pattern compared to monocular stimulation with a monkey face (neuron 1: $SPI_{PA} = 0.34$, neuron 2: $SPI_{PA} = 0.51$; Fig. 2C, upper panel). The averaged discharge response of this pair in PA trials during t = 1301-2300ms as assessed by the mean geometric spike count rate ($geo\,\overline{x}_{sc}$) was 5.47 ± 0.47 Hz (mean ± SEM) for the preferred and 1.79 ± 0.3 Hz for the non-preferred stimulus (Wilcoxon signed rank test, $p < 10^{-8}$). Although reduced in strength, each neuron retained the same stimulus preference during BFS (neuron 1: $SPI_{BFS} = 0.12$, neuron 2: $SPI_{BFS} = 0.34$; Fig. 2C). As a result, the pairwise discharge response during subjective perceptual dominance remained stronger compared to perceptual suppression ($geo\,\overline{x}_{\text{sc BFSpref}} = 6.58 \pm 0.45$ Hz vs. $geo\,\overline{x}_{\text{sc BFSnonpref}} = 4.04 \pm 0.35$ Hz; Wilcoxon signed rank test, $p < 10^{-4}$).

We estimated the shared discharge variability of this pair by computing for t = 1301-2300ms the trial by trial spike count correlations (r_{sc}) in each condition. During subjective perceptual dominance r_{sc} was dramatically reduced, compared to perception of the same stimulus without visual competition ($r_{sc\ PApref}$ = 0.45 t-test, p = 0.001 vs. $r_{sc\ BFSpref}$ = 0.11 t-test, p = 0.48; reduction 78%, Fig. 2D). In contrast, correlated firing during perceptual suppression of the preferred stimulus resulted in a modest reduction (27%) of correlated firing compared to physical absence of the same stimulus ($r_{sc\ PAnonpref}$ = 0.33 t-test, p = 0.02 vs. $r_{sc\ BFSnonpref}$ = 0.24 t-test, p=0.1).

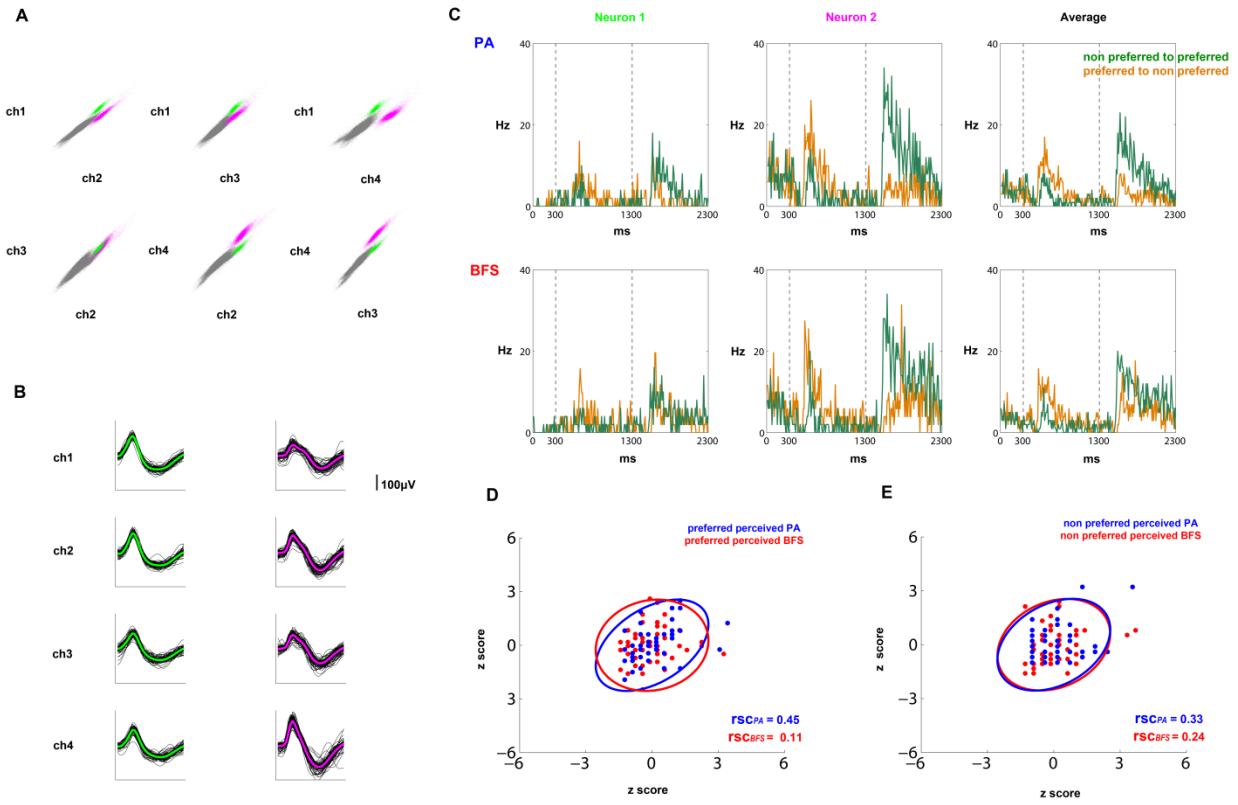

Figure 2

Example of a simultaneously recorded neuronal pair in the LPFC.

(A) Scatter plots depicting the amplitude of the first principal component of the recorded waveforms for all possible pairwise channel combinations (channels 1-4). The gray cluster represents background, multiunit activity (non – sorted spikes) while the colored clusters represent the two sorted single units.

(B) Waveforms of the two isolated single units depicted in A. For each tetrode channel the mean waveform is overlaid on a sample of 100 waveforms. The advantage of tetrodes is clear since recording for example the waveforms only in channel 3 would result in merging the two single units.

(C) Mean responses of neurons 1 (first column) and 2 (second column) depicted in A and B during PA (first row) and BFS (second row). Both neurons exhibited the same stimulus preference (for a polar checkerboard) in both PA and BFS. Specifically, they both increased their firing rate when the checkerboard followed the presentation of the face stimulus. During this period stimulation with the face stimulus elicited lower firing rates in both neurons. The averaged firing rate of the neuronal pair during PA and BFS is depicted in the third column.

(D) Scatter plot of z score responses and r_{sc} values of the same neuronal pair during perception of the preferred stimulus in PA and BFS. Subjective perceptual dominance of the preferred pattern in BFS resulted in decorrelated discharges compared to the strongly correlated fluctuations when the same stimulus was perceived without competition in PA.

(E) Scatter plot of z score responses and r_{sc} values of the neuronal pair during perception of the non-preferred stimulus in PA and BFS. The differences in correlation are negligible compared to D. Ellipses in D & E represent 95% confidence intervals of responses. Note

the difference between the ellipses in D where the decorrelation during BFS transforms the ellipse into a circle compared to the large overlap depicted in E.

In total, we recorded from 253 pairs of neurons ($n_{neurons}$ = 300) in the LPFC of 3 macaques (n_{pairs} = 106, 63 and 84 respectively). Each pair comprised units with similar stimulus preference during both PA and BFS. Across this population stimulus preference strength was identical during PA and BFS (*mean* SPI_{PA} = 0.19 ± 0.01 vs. *mean* SPI_{BFS} = 0.177 ± 0.01; Wilcoxon signed rank test p = 0.1). However, for pairs with stronger selectivity ($SPI > 0.2$, n_{pairs} = 52) preference strength was weaker during BFS (*mean* SPI_{PA} = 0.437 ± 0.03 vs. *mean* SPI_{BFS} = 0.355 ± 0.03; Wilcoxon signed rank test $p < 10^{-5}$) in agreement with previous results showing that sensory stimulus preference strength is weaker during BFS [6].

In this population that reflects a reliable neural representation of the content of consciousness, we observed a dramatic decorrelation of discharge fluctuations during subjective perceptual dominance of the preferred stimulus compared to monocular, non-subjective perception of the same pattern (Fig. 3B-C). Specifically, while monocular perception of a preferred stimulus resulted in significant correlations, subjective visibility of the same stimulus during BFS resulted in a significant 42% decrease (*mean* $r_{sc\ PApref}$ = 0.0999 ± 0.016 t-test, $p<10^{-9}$ vs. *mean* $r_{sc\ BFSpref}$ = 0.0584 ± 0.014 t-test, $p=10^{-4}$; Wilcoxon signed rank test p = 0.012). Interestingly, correlations during subjective perceptual dominance were not different from zero assuming a sparse encoding of the content of consciousness by a more selective population exhibiting a particularly strong stimulus preference (*mean* $r_{sc\ BFSpref}$ = 0.0001 ± 0.0312; t-test, $p>0.9$ vs. *mean* $r_{sc\ PApref}$ = 0.1299 ± 0.0358 t-test, $p<10^{-3}$; Wilcoxon signed-rank test $p<10^{-3}$; Fig. 3B). The source of decorrelation can't be ascribed to response strength differences across

conditions [32] since we found no systematic relationship between changes in geometric firing rates and changes in correlations (Fig. S1A-C). Furthermore, the decorrelation effect was mostly observed in pairs exhibiting positive correlations during PA (Fig. 3C) and was also reflected in the reduced number of pairs exhibiting significant (t-test, $p<0.05$) correlations during BFS (n_{pairs} = 34 vs. n_{pairs} = 55 in PA) (Fig. S1D).

The decorrelation during BFS was strongly asymmetric since we found no change in correlations between perceptual suppression and physical absence of the preferred stimulus in BFS and PA, respectively (Fig. 3D). Specifically, correlations were identical during perception of the non-preferred stimulus in PA and BFS (*mean* $r_{sc\ PAnonpref} = 0.0684 \pm 0.0148$; t-test, $p<10^{-5}$; *mean* $r_{sc\ BFSnonpref} = 0.0648 \pm 0.014$; t-test, $p<10^{-5}$; Wilcoxon signed-rank test $p > 0.9$). Although the same was true for pairs exhibiting stronger selectivity (*SPI* > 0.2) correlations during perceptual suppression were also not different from zero ($_{PAnonpref} = 0.059 \pm 0.0269$; t-test, p=0.0469 vs. *mean* $r_{sc\ BFSnonpref} = 0.0519 \pm 0.0304$; t-test, p=0.101; Wilcoxon signed-rank test $p > 0.9$). This asymmetry in decorrelated firing and a trend towards stronger decorrelation during BFS for populations with stronger stimulus selectivity was robustly observed in the LPFC of all 3 macaques (Fig. S2).

The reduction of intrinsic noise was a network-specific effect since we found no difference between PA and BFS in individual variability across the population exhibiting decorrelated discharges (*mean* $F_{PApref} = 3.155 \pm 0.13$ *vs*. *mean* $F_{BFSpref} = 3.118 \pm 0.13$; Wilcoxon signed-rank test $p >0.6$; Fig. 3E). Similarly, individual firing variability was identical during physical removal of the preferred stimulus and perceptual suppression (*mean* $F_{PAnonpref} = 2.63 \pm 0.1$ *vs*. *mean* $F_{BFSnonpref} = 2.67 \pm 0.1$; Wilcoxon signed-rank test $p >0.6$; Fig. 3F). The same results were found for pairs with stronger selectivity (*SPI* >0.2) where individual variability was

identical between monocular perception and subjective perceptual dominance of a preferred stimulus (*mean F* $_{\text{PApref}}$ = 2.817 ± 0.25, *mean F* $_{\text{BFSpref}}$ = 2.921 ± 0.32; Wilcoxon signed-rank test p >0.8; Fig. 3E). Similarly, for these strongly selective pairs no difference was found in the mean Fano factor between physical removal and perceptual suppression of the preferred stimulus (*mean F* $_{\text{PAnonpref}}$ = 2.03 ± 0.12, *mean F* $_{\text{BFSnonpref}}$ = 2.257 ± 0.16; Wilcoxon signed-rank test p >0.3; Fig. 3F).

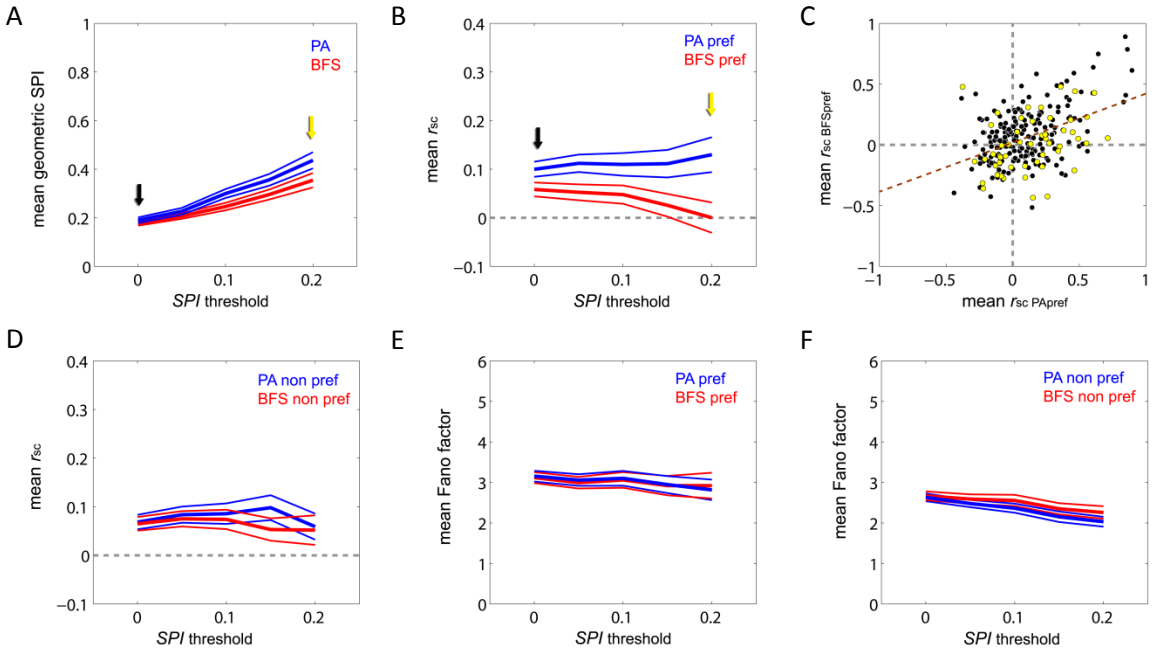

Figure 3

Stimulus preference strength and second-order statistics in PA and BFS

(A) Mean geometric stimulus preference index (SPI) as a function of SPI threshold for pairs with similar stimulus preference during PA (blue) and BFS (red). Populations with strong selectivity in PA show weaker stimulus preference sensitivity during BFS.

(B) Spike count correlations during monocular stimulation with a preferred stimulus in PA (blue) and subjective perceptual dominance of the same stimulus during BFS (red) as a function of *SPI* threshold. The decorrelation during subjective perceptual dominance is observed across the whole selective population (black arrow) and becomes stronger for pairs with stronger preference (yellow arrow).

(C) Scatter plot of noise correlations during monocular perception of the preferred stimulus in PA (x axis) vs. subjective perception of the same stimulus in BFS (y axis). Black and yellow points represent all 253 pairs (black arrows in A and B) while yellow points represent the strongly selective population (yellow arrow in A and B). Red dashed line: linear regression fit.

(D) Spike count correlations during perception of the non-preferred pattern in PA (blue) and BFS (red). In contrast to perception of a preferred pattern in (B) no differences were observed between PA and BFS.

(E) Mean Fano factor for PA and BFS during perception of a preferred pattern. In contrast to the reduction in correlated variability no differences were found in the individual variability for neurons with varying strengths of stimulus preference.

(F) Same as in E during perception of a non-preferred pattern. Fano factor was reduced compared to E but no differences were observed between PA and BFS.

Cross-inhibition is not the source of decorrelation during subjective perception

Decorrelated firing has been associated to a suppression of ongoing fluctuations in excitability [33-35]. However, local cross-inhibition between antagonistic ensembles in BFS could also be a

possible source of decorrelation in our experiments, by increasing inhibition [36]. To resolve the decorrelation mechanism, we considered a biophysically realistic spiking network comprising two selective excitatory neural populations, each one encoding one of the visual stimuli, exhibiting competition through an inhibitory population [37] (Fig. 4A). To disentangle the effect of competition, we considered also the same network without cross-inhibition (Fig. 4B).

The network with competition, for a set of parameters, accounts for the experimental correlations and mean firing rates in PA (Fig. 4C-E). However, simulating BFS with the same parameters results in increased correlations for both dominant and suppressed populations, in contrast to the observed decorrelation. Calculating the excitatory-inhibitory balance at the synapses of neurons we find that this is due to higher excitatory currents, arising from the external input to the suppressed population (Fig 4C-D).

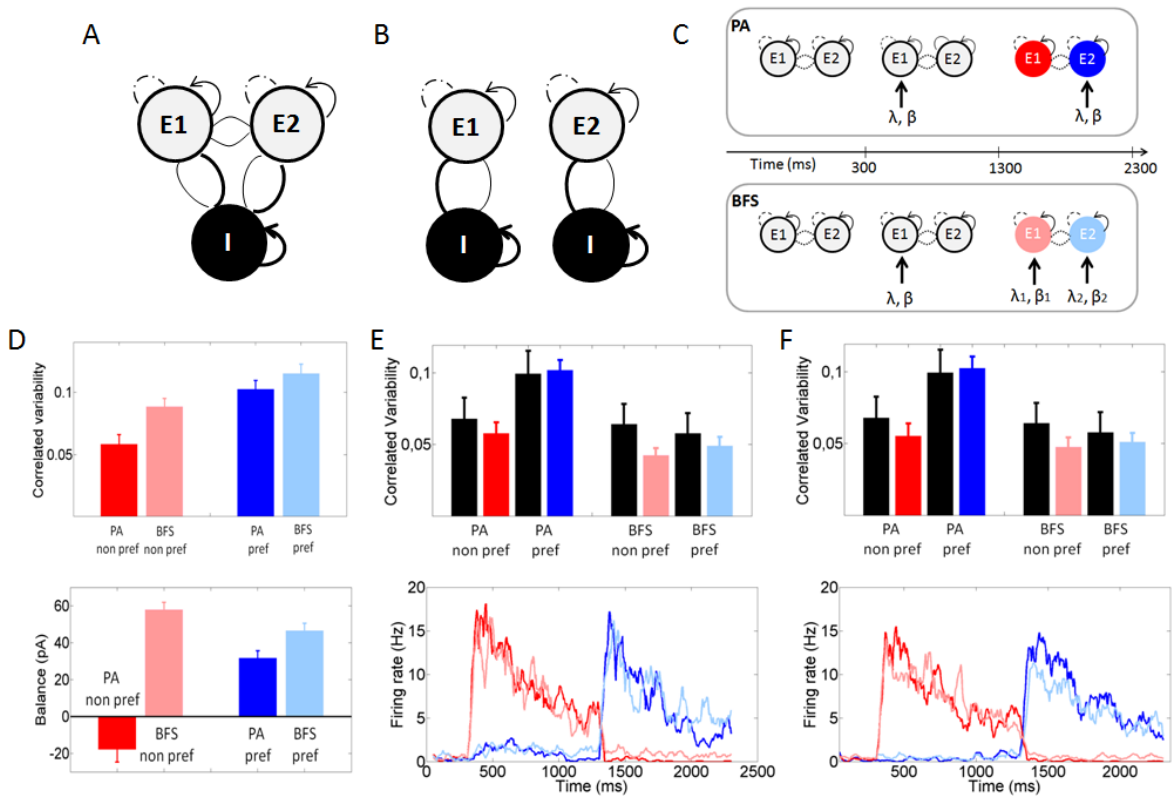

Figure 4

Biophysically realistic spiking networks, stimulation protocols and simulations

A. Network with competition: Two excitatory neuronal populations, E1 and E2, with self-excitation (arrows), neuronal adaptation (dashed lines), connected with each other and with an inhibitory population, I.

B. Network without competition: One excitatory population, E1 (or E2), with self-excitation (arrows), neuronal adaptation (dashed lines), connected with an inhibitory population, I**.** We draw two such networks, for convenience in the description of the simulations and presentation of the results.

C. Stimulation protocol. Physical Alternation (PA): at time 300 ms stimulus of strength λ and variability β is applied to population E1 and at 1300 ms stimulus of same strength and variability is applied to population E2. Binocular Flash Suppression (BFS): at time 300 ms stimulus of strength λ and variability β is applied to population E1 and at 1300 ms stimulus of strength λ_1 and variability β_1 is applied to population E1, while stimulus of strength λ_2 and variability β_2 is applied to population E2. Here, connections between the excitatory populations E1, E2 are drawn with dotted lines, representing the existence of cross inhibition between the excitatory populations (network with competition, Fig. 4A) or its absence (network without competition, Fig. 4). Colors at the last second correspond to the colors used throughout the presentation of the results, for convenience.

D. Network with cross-inhibition. Correlated variability (Up) and excitatory-inhibitory synaptic balance (Down) of the dominant and suppressed neurons in BFS (when there is no input strength or noise modulation: $\beta_1 = \beta_2 = \beta$ and $\lambda_1 = \lambda_2 = \lambda$, Fig. 4C).and of the same neurons in PA.

E. Network with cross-inhibition. Correlated variability (Up) and mean firing rate (Down) of the dominant and suppressed neurons in BFS and of the same neurons in PA. Black bars are the experimental data.

F. Correlated variability and mean firing rates as in Fig. 4E, for the network without cross-inhibitition.

Suppression of input fluctuations decorrelates the perceptually dominant population

We further examined whether input strength and fluctuations could account for the decorrelated activity. For both networks, reducing input strength to the dominant population results in decorrelation (Fig. S3A-B). However, stimulus strength is so weak that the mean firing rate of the dominant population in BFS is significantly smaller than in PA (data not shown) against the empirical observations in LPFC (Fig. S1 and ref. **6**). In contrast, suppression of input fluctuations to the dominant population in both networks results in decorrelation, while the excitatory-inhibitory balance does not change (Fig. 5A-B and Fig. S3A-B). A small stimulus decrease, though, is needed in order to account for the slightly reduced mean firing rate of the dominant population in BFS (Fig. 4E-F).

How does suppression of input fluctuations leads to decorrelated output? Fluctuations of input to neurons of the same ensemble are the same at each time step. Therefore, the external excitatory synaptic currents in pairs of neurons of the same ensemble are correlated across trials (Fig. 5B). Suppression of input fluctuations results in a decorrelation of the external currents while the rest synaptic current correlations in the network cancel each other (Fig. 5B) providing a biophysical mechanism that output (spike count) correlations track input correlations [36]. Furthermore, suppression of input fluctuations to the dominant neurons reduces the variability of

sub-threshold membrane potential fluctuation, while the mean does not change (Fig. 5C-D, Fig. S5). Finally, for the same parameters that result in decorrelation the simulated Fano factor and distribution of correlations match the experimental results (Fig. 5E Fig. S4, S1D).

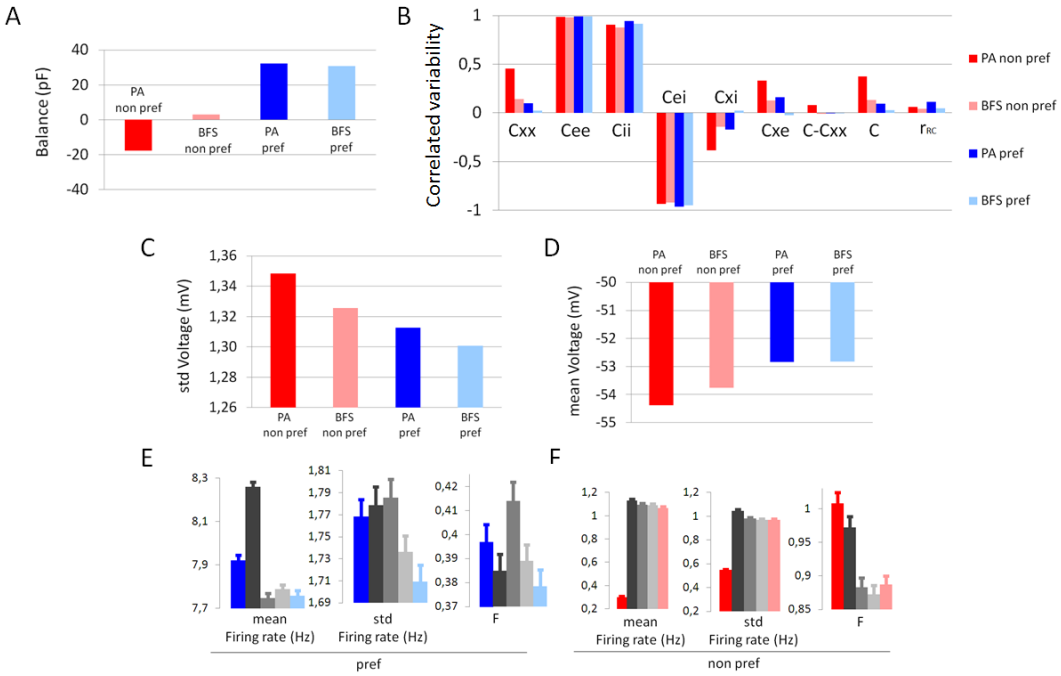

Figure 5

Network with cross-inhibition. Balance, current correlations, membrane voltage, firing rate and fano factor, of each neural ensemble, in each condition

(A) Excitatory-inhibitory balance at the synapses of the dominant and suppressed neurons in PA and of the same neurons in PA.

(B) Trial by trial synaptic current correlations between pairs of excitatory neurons within the same neural ensemble. Correlations Cxx, Cee, Cii are between the external excitatory, recurrent excitatory and recurrent inhibitory post-synaptic currents, respectively. Cei, Cxe, Cxi, are correlations between recurrent excitatory - inhibitory, external excitatory –

recurrent excitatory, external excitatory – recurrent inhibitory post-synaptic currents, respectively. C are the sum of all current correlations (C = Cxx + Cee +Cii + 2Cei + 2Cxe + 2Cxi) and r_{SC} are spike count correlations. Colors correspond to the different neural ensembles and conditions, as previously.

(C) Standard deviation of the membrane voltage of the dominant and suppressed neurons in BFS and of the same neurons in PA.

(D) Mean membrane voltage of the dominant and suppressed neurons in BFS and of the same neurons in PA

(E) Mean firing rate, standard deviation of the mean firing rate and Fano factor of the neurons selective to the image that is presented in PA (blue bars). The Fano factor of the dominant neurons in BFS (cyan bars, $\lambda_1 < \lambda_2 < \lambda$, $\beta_1 > \beta > \beta_2$ in Fig. 4C) is not significantly different than the Fano factor of the same neurons in PA, consistent with the experimental data. This is because the mean firing rate of the dominant neurons in BFS slightly decreases and so does their variance. Decrease of the stimulus to the dominant population (gray bars, $\lambda_1 < \lambda_2 < \lambda$, $\beta_1 = \beta_2 = \beta$ in Fig. 4C) in BFS increases the Fano factor of the neurons. Decrease of the input noise to the dominant population (light gray bars, $\lambda_1 < \lambda_2 < \lambda$, $\beta_1 = \beta > \beta_2$ in Fig. 4C) decreases the Fano factor of the neurons. Both actions result in keeping the Fano factor of the dominant neurons in BFS similar as in PA. Black bars correspond to BFS when $\lambda_1 < \lambda_2 = \lambda$, $\beta_1 = \beta_2 = \beta$ (Fig. 4C). Error bars are deviations of the mean values calculated from 100 sets of 100 trials, where at each set randomly selected neurons from each ensemble were considered.

(F) Mean firing rate, standard deviation of the mean firing rate and Fano factor of the neurons selective to the opposite image than the one presented in PA (red bars). The Fano

factor of the suppressed neurons in BFS (light red bars, $\lambda_1 < \lambda_2 < \lambda$, $\beta_0 > \beta_1 > \beta > \beta_2$ in Fig. 4C, where β_0 is the background input noise in the absence of external stimulus) is not significantly different than the Fano factor of the same neurons in PA, consistent with the experimental data. This is because the mean firing rate of the suppressed neurons slightly increases and so does their variance. The input to the suppressed population, λ_1, in BFS (black bars, $\lambda_1 < \lambda_2 = \lambda$, $\beta_1 = \beta_0 > \beta_2 = \beta$ in Fig. 4C) decreases their Fano factor compared to PA. For smaller input noise (gray bars, $\lambda_1 < \lambda_2 = \lambda$ and $\beta_0 > \beta_1 > \beta_2 = \beta$ in Fig. 4C) the fano factor is even smaller. By increasing, though, the noise of the input rate (light gray bars $\lambda_1 < \lambda_2 = \lambda$ and $\beta_0 > \beta_1 = \beta_2 = \beta$ in Fig. 4C), the Fano factor of the suppressed neurons in BFS increases and approaches the value of their Fano factor in PA. Error bars are deviations of the mean values calculated from 100 sets of 100 trials, where at each set randomly selected neurons from each ensemble where considered).

Reduction of input strength maintains correlations in the perceptually suppressed population

During stimulation with a non-preferred pattern in PA, neurons receive only background input with variability higher than the total input variability that neurons selective to the presented pattern receive [38]. In addition, since there is no external input to neurons selective to the opposite image, than the one presented, they are inhibitory dominated (Fig. 5A). Therefore, despite their higher external current correlations compared to correlations of the neurons selective to the presented image, spike count correlations are smaller (Fig. 5B).

Simulating BFS with the same parameters, the correlated variability of the suppressed neurons is higher than the correlated variability of the same neurons in PA (Figs. 4D, S3C-D).

Suppression of input fluctuation to these neurons would lead to decrease of their spike count correlation, as discussed previously, but the received input strength would lead to a higher mean firing rate than what is experimentally observed. Their spike count correlations are maintained at the same level as in PA, mainly due to input strength decrease (Fig. S3C-4D), so that both their spike count correlation and mean firing rate are replicated by the networks. In addition, slight input noise increase, is also needed to account for the empirically observed maintenance of their Fano factor (Fig. 5F). Input noise increase, also, increases noise correlation, and therefore lower input strength to these neurons is needed in order to account for the empirical noise-correlation and mean firing rate in PA (Figs. 4F, S3C-D). The latter is more apparent in the network without competition (Fig. S3D). In these conditions, their mean voltage approaches the threshold [35] (Figs. 5D, S6), but its standard deviation decreases (Fig. 5C), compared to PA, corresponding to the maintenance of the noise-correlations in both PA and BFS.

Correlation structure during visual consciousness

We also measured correlations in 240 pairs belonging to pools with different stimulus preference, a condition equivalent to neurons having negative signal correlations. These data indicate a direct relationship between functional similarity of neurons and correlations during non-subjective perception, similar to other cortical areas [16, 18-19 24, 39] including the prefrontal cortex [40]. Specifically, in PA functional similarity (*within* pools) resulted in stronger correlations - when correlations for both preferred and non-preferred stimuli were combined - (*mean* $r_{sc\ PAwithin} = 0.0843 \pm 0.01$, t-test, $p = 10^{-14}$) compared to pairs of neurons with opposite (*across* pools) stimulus preference (*mean* $r_{sc\ PAacross} = 0.0048 \pm 0.01$, t-test, $p = 0.637$; two-sample ttest $p = 10^{-7}$; Fig. 6A). The magnitude of limited-range correlation structure was reduced during

subjective visual perception in BFS (*mean* $r_{sc\ BFSwithin}$ = 0.061 ± 0.01 p =10^{-9} *vs*. *mean* $r_{sc\ BFSacross}$ = -0.0006 ± 0.01 p = 0.955, two-sample ttest p = 10^{-5}; Fig. 6A) and almost disappeared for strong stimulus preference (*SPI* > 0.2) (*mean* $r_{sc\ BFSwithin}$ = 0.025 ± 0.03 p =0.26 *vs*. *mean* $r_{sc\ BFSacross}$ = -0.003 ± 0.01 p = 0.88, two-sample ttest p = 0.3). As described previously, this effect was due to an asymmetric decorrelation during subjective perceptual dominance of a preferred stimulus.

For the set of parameters that both networks replicate the correlations within pools of similar stimulus preference, the limited range correlation effects arise naturally, i.e. without using it as a constrain (Fig. 6B). However, correlations between neurons with different preference are closer to the experimental data in the network with competition (Fig. 6BC) suggesting that while cross-inhibition is not effectively relevant for the decorrelation within pools it has an effective role on the measured correlations between pools.

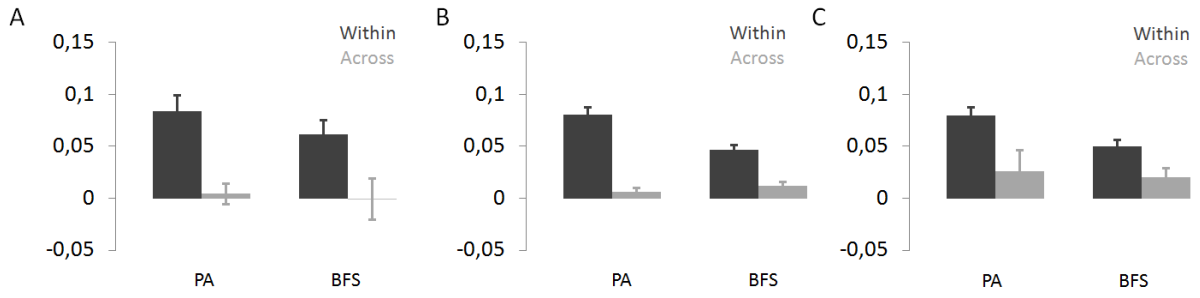

Figure 6

Structure of correlations

(A) A strong limited range structure during PA becomes weaker during BFS, mainly due to an asymmetric decrease of correlations during perception of the preferred stimulus.

(B) The empirical limited-range correlation structure effects emerge in the model with competition for the parameters that simulate correlations within pools of neurons.

(C) The network without competition also reflects a limited range structure. However, without inhibition correlations across pools are higher compared to (A).

DISCUSSION

The direct relationship between the structure of correlated discharges and population coding [10-11, 13, 15, 27] indicates that a detrimental correlation structure during subjective visual perception could cast doubt on the fidelity of conscious representations in association cortical areas [9]. To address this issue we compared the correlated discharge fluctuations of simultaneously recorded pairs of LPFC neurons under conditions of subjective and non-subjective stimulus visibility.

Similar to other visual cortical areas we found a limited range correlation structure in the LPFC during non-subjective perception. It is currently unclear how population coding mechanisms cope with such a detrimental correlation structure during non-subjective perception. However, in non-subjective visibility, discrimination between two simultaneously presented stimuli and their corresponding response distributions is unnecessary. This renders correlated noise less critical compared to rivaling, subjective, perception. We found that in the latter case active decorrelation induces a beneficial cortical state where efficient coding of conscious content could be achieved by averaging neuronal discharges with small or no constraints posed by intrinsic noise.

What is the source of decorrelation? In theoretical models of perceptual bistability, each stable percept is conceived as a stable attractor state, emerging due to cross-inhibition between antagonistic ensembles [36, 41-44]. Cross inhibition could decrease correlations by increasing

inhibition [36]. However, our findings suggest that cross-inhibition is not the source of decorrelation during visual consciousness in the LPFC. Rather, decorrelation seems to be a consequence of the active asymmetric suppression of input fluctuations. In addition, the maintenance of correlations during perceptual suppression in BFS, is due to the smaller iput strength to the suppressed neurons. It has been shown that despite the presence of shared inputs noise correlations are small in recurrent networks, in asynchronous state, due to negative correlations in synaptic currents [36]. This is the case also here (Fig. 6B), and therefore noise correlations in both neural ensembles and conditions are small. However, we are interested in the differences in correlations between two selective populations and between two different stimulation protocols (PA, BFS). The driving force of the decorrelation is the asymmetric suppression of input correlations due to shared input fluctuations originally induced by adding a gaussian process over the poisson generation of spikes. This resembles recent studies showing that input fluctuations are responsible for noise correlations [33-34]. We additionally show that this is the case whether neural ensembles compete with each other via inhibition or when they are not competing, when inhibition is strong enough.

What is the relevance of our findings for the physiological mechanism underlying the emergence of conscious perception during spontaneous perceptual transitions? In theoretical, models transitions between two attractors-percepts have been ascribed to a fine tuning of spiking adaptation and noise with adaptation having a modulatory role and noise being the driving force of alternations [36, 41-44]. Our results suggest weak correlated noise - that is not different from zero assuming sparse coding - during subjective perception. Although our paradigm didn't allow us to study correlations during spontaneous perceptual transitions, simulations indeed show that rivalry transitions can't be induced in a low correlation regime and an increase in correlated

variability could lead to a detrimental state for flash suppression (Fig. 7). Specifically, the level of competition for which the network replicates the experimental data does not lead to perceptual alternations when BR is followed by BFS (Fig. 7A) suggesting that decorrelated activity promotes the stability of perception. Furthermore, for strongly correlated states discharge rates of dominant and suppressed populations are different form the observed patters (Fig. 7B), indicating that a decorrelated state is functionally significant for perceptual stability. We should note that this could be due to the specific choice of parameters. Nevertheless, we derived analytical equations for the second order statistics (Supplementary) and explored all possibilities. We find that even when alternations are observed, mean activity in BFS is different than in PA (Fig. S6-7) in contrast to the empirical data.

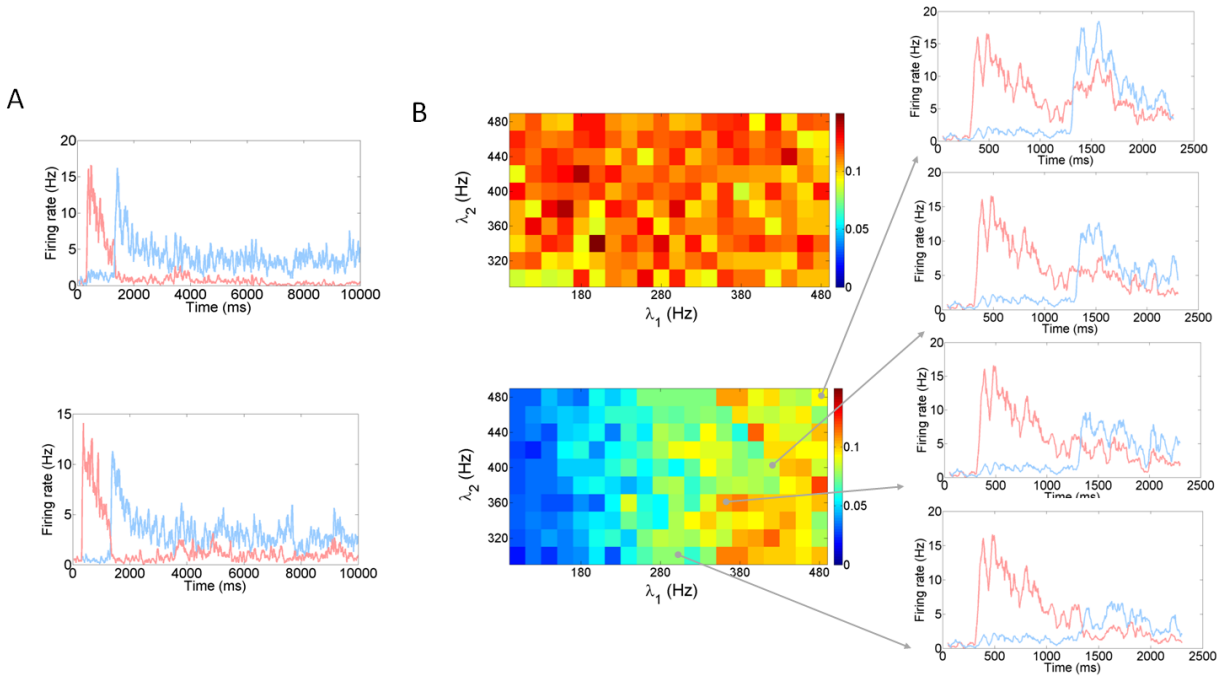

Figure 7

BFS followed by BR and non-detrimental noise correlations

(A) Mean firing rates of the dominant and suppressed neurons in BFS followed by BR, employing the network with competition (Up) and the network without competition (Down). Parameters are the ones for which the networks replicate the experimental noise-correlaitons.

(B) Left: Correlated variability of the E1 (down) and E2 (up) neural ensembles as a function of input strength, when input noise is same as in PA (λ_1, λ_2, $\beta_1 = \beta_2 = \beta$, Fig. 4C). Right: Mean firing rates of both neural ensembles for different sets of λ_1, λ_2, indicated by the arrows.

Furthermore, a decorrelated cortical state is functionally significant for perceptual stability from a theoretical point of view. This is because strong limited range correlations could theoretically constrain the information content and therefore the capacity for stimulus discrimination during rivalry. Therefore, the observation of a decorrelated state during stable perception leads to the testable hypothesis that stronger limited range correlations might be involved in perceptual transitions. Such strong correlations within the competing pools could reflect a common fluctuation component, for example a common process reflected in low-frequency fluctuations that were recently shown to result in increased correlations [33-34]. Such a scenario could be associated to the potential involvement of global, non-specific fluctuations [45-46], in conscious perception. For example, a role for the low-frequency component of LFPs (named the slow cortical potential or SCP) in consciousness was suggested recently [47] but also disputed due to the non-specificity of low frequency cortical signals [48]. Our results may indicate that a non-specific fluctuation like the SCP could indeed be the driving force of perceptual

reorganization by increasing correlations in competing populations and therefore decreasing the information content of rivaling pools.

Interestingly, our finding of decorrelated activity during visual consciousness resembles a similar decorrelation during attention [22-23]. Although visual consciousness and attention can be dissociated [49] a common mechanism has been suggested to underlie the selection of a unique visual attribute and the suppression of competing information [50]. Active decorrelation of interneuronal discharges might thus reflect a canonical computational process in the cortex that effectively gives rise to selection processes in both consciousness and attention by suppressing internal noise under conditions of visual competition [51]. We should note however that while attention appears to result in homogeneous decorrelation [22-23] the decorrelation observed during visual consciousness was strongly asymmetric affecting mainly neurons with similar tuning during perceptual dominance but not suppression.

A better understanding of the functional connectivity dynamics during visual consciousness will require future studies to determine whether active suppression of correlated noise is also observed in early cortical areas where population activity is less representative of subjective perception or it is a phenomenon uniquely observed in association areas where the averaged population activity reflects reliably the content of consciousness.

METHODS

Electrophysiological recordings

We recorded from three adult rhesus monkeys (*macaca mulatta*) weighing between 9 and 17 kg. The cranial head post, scleral eye coil and recording chamber, were implanted under general anesthesia using aseptic and sterile conditions. Briefly, after the subcutaneous injection of

Robinul (0.01 mg/kg) and Ketavet (15 mg/kg), we injected intravenously the analgesic Fentanyl (0.003 mg/kg), the barbiturate anesthetic Trapanal (5 mg/kg) and the paralytic Lysthenon (3 mg/kg). Throughout the duration of the surgery we used balanced anesthesia consisting of 1.3% Isoflurane. The recording chambers (18mm in diameter) were centered stereotaxically above the prefrontal cortex based on high-resolution MR anatomical images collected in a vertical 4.7 T scanner with a 40-cm-diameter bore (Biospec 47/40c; Bruker Medical, Ettlingen, Germany).

In our recordings we used custom-made tetrodes made from Nichrome wire and electroplated with gold to decrease the impedances below 1MΩ. The recorded signal was sampled at 32 kHz, digitized at 32 Hz (12 bits) and stored using the Cheetah data acquisition system (Neuralynx, Tucson, AZ). Multiunit activity was defined as the events detected in the high pass filtered signal (600-6000Hz) that exceeded a predefined threshold (typically 20-30 μV) on any tetrode channel. Single units were identified by employing a spike sorting method using as features the first three principal components of the recorded waveforms (previously described in refs. **31, 38**). Eye movements were monitored on-line using implanted eye coils for D98 and F03 and a high-speed infrared camera for F06. Visual stimuli were displayed using a dedicated graphics workstation (TDZ 2000; Intergraph Systems, Huntsville, AL) with a resolution of 1,280 x 1,024 and a 60 Hz refresh rate, running an OpenGL-based stimulation program. All procedures were approved by the local authorities (Regierungspräsidium Tuebingen) and were in full compliance with the guidelines of the European Community (EUVD 86/609/EEC) for the care and use of laboratory animals.

Estimation of neuronal stimulus preference and assignment to different pools

We assigned simultaneously recorded pairs of neurons in two different pools depending on the stimulus preference index (*SPI*) of the recorded units. The first pool comprised pairs of neurons where both units had a similar stimulus preference during both PA and BFS and we tracked the second order statistics of this population during a) monocular perception of the preferred stimulus in PA, b) monocular perception of the non-preferred stimulus during the physical absence of the preferred pattern in PA, c) subjective perceptual dominance of the preferred stimulus in BFS and d) perception of the non-preferred stimulus inducing perceptual suppression of the preferred one in BFS. The second pool comprised pairs of neurons where the two units had opposite stimulus preference during PA and maintained this opposite preference during BFS and compared their statistics during PA and BFS to examine the effect of visual competition on the functional connectivity of rivaling pools.

We computed the *SPI* for every recorded neuron during PA and BFS as following:

$$SPI = \frac{\overline{x}_{sc_a} - \overline{x}_{sc_b}}{\overline{x}_{sc_a} + \overline{x}_{sc_b}} \qquad \text{Eq. (1)}$$

where $\overline{x}_{sc_a}$ and $\overline{x}_{sc_b}$ are the averaged spike counts (*sc*) across trials during *t* = 1301-2300ms for stimuli *a* (face) and *b* (polar checkerboard), respectively. The range of neuronal *SPI* values is between -1 to 1, indicating a preference for stimulus *a* when positive or a preference for stimulus *b* when negative. Only simultaneously recorded pairs comprising neurons *i* and *j* with an *SPI* in the same direction during both PA and BFS (i.e. either *SPI* > 0 or *SPI* < 0, for both neurons and in both conditions) were included in the first pool, consisting the population encoding the content of subjective perception in BFS. For these neurons an absolute *SPI* value was used for further analysis (Figure 3). Simultaneously recorded pairs comprising neurons with opposite preference (e.g. neuron *i* – preference for stimulus *a*, neuron *j* – preference for stimulus *b* or vice versa) in

the same direction in both PA and BFS were included in the database of neurons from opposite pools. Finally, a pair was discarded from further analysis when at least one of its neurons had a positive *SPI* in PA and a negative one in BFS, or vice versa, indicating instabilities in the stimulus preference across the experimental conditions.

When necessary, in order to obtain the combined discharge response of each neuronal pair comprising units *i* and *j* we estimated the geometric spike count rate ($geo\ \overline{x}_{sc}$) for each trial *k* and each condition separately by computing the square root of the spike count product as following:

$$geo\ \overline{x}_{sc_k} = \sqrt{sc_{k_i}\ sc_{k_j}} \qquad \text{Eq. (2)}$$

and then averaged across trials.

Second-order statistics of neuronal populations

We computed the pair wise spike count correlation coefficient (r_{sc}) during *t* =1301-2300ms similar to ref. **28**. Specifically, for each pair of simultaneously recorded neurons comprising units *i* and *j* and for each of the four conditions - depicted in Figure 1 - separately, we first normalized the total number of spike counts across all trials by converting them into *z*-scores and then for each pair we computed the Pearson correlation coefficient for the two vectors z_i and z_j as following:

$$r_{\mathrm{sc}} = \frac{E[z_i z_j] - Ez_i Ez_j}{\sigma_{z_i}\ \sigma_{z_j}} \qquad \text{Eq. (3)}$$

Where *E* is the expected value and σ is the standard deviation across all trials for a specific condition. Since after normalization of responses $Ez_i = Ez_j = 0$ and $\sigma_{z_i} = \sigma_{z_j} = 1$ Eq. (3) can be written as:

$$r_{sc} = E[z_i z_j] \qquad \text{Eq. (4)}$$

In order to avoid contamination of results from outlier values, we discarded from the analysis pairs with r_{sc} values greater than 3 standard deviations from the mean of each distribution. However, this data manipulation didn't alter the differences between the conditions since they remained significantly different.

For each neuron and for each condition separately we also estimated the individual variability across trials during t = 1301-2300 by computing the Fano factor (F) as following:

$$F = \frac{\sigma_{sc}^2}{\overline{x}_{sc}} \qquad \text{Eq. (5)}$$

where σ_{sc}^2 is the variance and $\overline{x}_{sc}$ the average spike count rate across all trials for each condition.

Simulations

We considered two biophysically realistic networks, with different architectures. One network is consisted of three neuronal populations (two excitatory and one inhibitory) and the other network is consisted of two neuronal populations (one excitatory and one inhibitory). The first network is characterized by cross-inhibition, and hence competition, between the two excitatory neuronal populations. It is an attractor based model, employed for working memory [52], decision making [53], and perceptual bistability [37]. One of the excitatory neuronal populations is consisted of neurons selective to one of the images in PA and BFS, e.g. the face image, and the other excitatory neuronal population is consisted of neurons selective to the other image in PA and BFS, i.e. the polar image. There is all to all connectivity and all neurons are modeled as leaky integrate-and-fire neurons. The second network is similar to the first one, with the difference that there is not cross-inhibition, and hence competition, since there is only one

excitatory neuronal population. The parameters in both networks are the same for the sake of comparison.

We follow the same protocols as in the experiment in order to simulate PA and BFS. In addition, we compute the trial by trial spike count correlations of the simulated neurons the same way as it is computed for the real neurons. Details of the networks, stimulation protocols and analyses can be found in Supplemental Information.

REFERENCES

1. Blake, R. & Logothetis, N.K. Visual competition. *Nat. Rev. Neurosci.* **3**, 13-21 (2002).
2. Crick, F. & Koch, C. A framework for consciousness. *Nat. Neurosci.* **6**, 119-26 (2003).
3. Logothetis, N.K. Single units and conscious vision. *Philos. Trans. R. Soc. Lond. B Biol. Sci.* **353**, 1801–1818 (1998).
4. Leopold, D.A. & Logothetis, N.K. Activity changes in early visual cortex reflect monkeys' percepts during binocular rivalry. *Nature* **379**, 549-53 (1996).
5. Logothetis, N.K. & Schall, J.D. Neuronal correlates of subjective visual perception. *Science* **245**, 761-3 (1989).
6. Panagiotaropoulos, T.I., Deco, G., Kapoor, V. & Logothetis, N.K. Neuronal discharges and gamma oscillations explicitly reflect visual consciousness in the lateral prefrontal cortex. *Neuron* **74**, 924-35 (2012).
7. Sheinberg, D.L. & Logothetis, N.K. The role of temporal cortical areas in perceptual organization. *P. Natl. Acad. Sci. USA* **94**, 3408-13 (1997).

8. Leopold, D.A. Primary visual cortex: awareness and blindsight. *Annu. Rev. Neurosci.* **35**, 91-109 (2012).
9. Panagiotaropoulos, T.I., Kapoor, V. & Logothetis NK. Subjective visual perception: From local processing to emergent phenomena of brain activity. *Philos. Trans. R. Soc. Lond. B Biol. Sci.* **369**, 20130534 (2014).
10. Abbott, L. F. & Dayan, P. The effect of correlated variability on the accuracy of a population code. *Neural Comput.* **11**, 91-101 (1999).
11. Averbeck, B.B., Latham, P.E. & Pouget, A. Neural correlations, population coding and computation. *Nat. Rev. Neurosci.* **7**, 358-66 (2006).
12. Cohen, M.R. & Kohn, A. Measuring and interpreting neuronal correlations. *Nat. Neurosci.* **14**, 811–819 (2011).
13. Sompolinsky, H., Yoon, H., Kang, K. & Shamir M. Population coding in neuronal systems with correlated noise. *Phys. Rev. E Stat. Nonlin. Soft Matter Phys.* **64**, 051904 (2001).
14. Tolhurst, D.J., Movshon, J.A. & Dean, A.F. The statistical reliability of signals in single neurons in cat and monkey visual cortex. *Vision Res.* **23**, 775-85 (1983).
15. Ecker, A.S., Berens, P., Tolias, A.S. & Bethge, M. The effect of noise correlations in populations of diversely tuned neurons. *J. Neurosci.* **31**, 14272-83 (2011).
16. Kohn, A. & Smith, M.A. Stimulus dependence of neuronal correlation in primary visual cortex of the macaque. *J. Neurosci.* **25**, 3661-73 (2005).
17. Gutnisky, D.A. & Dragoi, V. Adaptive coding of visual information in neural populations. *Nature* **452**, 220-224 (2008).
18. Ecker, A.S., Berens, P., Keliris, G.A., Bethge, M., Logothetis, N.K. & Tolias, A.S.

Decorrelated neuronal firing in cortical microcircuits. *Science* **327**, 584-7 (2010).

19. Cotton, R.J., Froudarakis, E., Storer, P., Saggau, P. & Tolias, A.S. Three-dimensional mapping of microcircuit correlation structure. *Front. Neural Circuits* **7**, 151 (2013).
20. Liu, S., Gu, Y., DeAngelis, G.C. & Angelaki, D.E. Choice-related activity and correlated noise in subcortical vestibular neurons. *Nat. Neurosci.* **16**, 89-97 (2013).
21. Romo, R., Hernández, A., Zainos, A. & Salinas, E. Correlated neuronal discharges that increase coding efficiency during perceptual discrimination. *Neuron* **38**, 649-57 (2003).
22. Cohen, M.R. & Maunsell, J.H.R. Attention improves performance primarily by reducing interneuronal correlations. *Nat. Neurosci*. **12**, 1594–1600 (2009).
23. Mitchell, J.F., Sundberg, K.A. & Reynolds, J.H. Spatial attention decorrelates intrinsic activity fluctuations in macaque area V4. *Neuron* **63**, 879-888 (2009).
24. Gu, Y., Liu, S., Fetsch, C.R., Yang, Y., Fok, S., Sunkara, A., DeAngelis, G.C. & Angelaki, D.E. Perceptual learning reduces interneuronal correlations in macaque visual cortex. *Neuron* **71**, 750-61 (2011).
25. Jeanne, J.M., Sharpee, T.O. & Gentner, T.Q. Associative learning enhances population coding by inverting interneuronal correlation patterns. *Neuron* **78**, 352-63 (2013).
26. Cohen, M.R. & Newsome, W.T. Context-dependent changes in functional circuitry in visual area MT. *Neuron* **60**, 162-173 (2008).
27. Zohary, E., Shadlen, M.N. & Newsome, W.T. Correlated neuronal discharge rate and its implications for psychophysical performance. *Nature* **370**, 140–143 (1994).
28. Bair, W., Zohary, E. & Newsome, W.T. Correlated firing in macaque visual area MT: time scales and relationship to behavior. *J. Neurosci.* **21**, 1667-97 (2001).
29. Shadlen, M.N., Britten, K.H., Newsome, W.T. & Movshon, J.A. A computational

analysis of the relationship between neuronal and behavioral responses to visual motion. *J. Neurosci.* **16**, 1486–1510 (1996).

30. Wolfe, J.M. Reversing ocular dominance and suppression in a single flash. Vision Res. *24*, 471-8 (1984).
31. Tolias, A.S, Ecker, A.S., Siapas, A.G., Hoenselaar, A., Keliris, G.A. & Logothetis NK. Recording chronically from the same neurons in awake, behaving primates. *J. Neurophysiol.* **98**, 3780-90 (2007).
32. de la Rocha, J., Doiron, B., Shea-Brown, E., Josic, K. & Reyes, A. Correlation between neural spikes trains increases with firing rate. *Nature* **448**, 802-806 (2007).
33. Ecker, A.S., Berens, P., Cotton, R.J., Subramaniyan, M., Denfield, G.H., Cadwell, C.R., Smirnakis, S.M., Bethge, M. & Tolias, A.S. State dependence of noise correlations in macaque primary visual cortex. *Neuron* **82**, 235-48 (2014).
34. Goris, R.L., Movshon, J.A. & Simoncelli, E.P. Partitioning neuronal variability. *Nat. Neurosci.* [Epub ahead of print] doi: 10.1038/nn.3711 (2014).
35. Tan, A.Y.Y., Chen, Y., Scholl, B., Seidemann, E. & Priebe, N.J. Sensory stimulation shifts visual cortex from synchronous to asynchronous states. *Nature* **509**, 226-229 (2014).
36. Renart, A., de la Rocha, J., Bartho, P., Hollender, L., Parga, N., Reyes, A., & Harris. K.D. The asychronous state in cortical circuits, *Science* **327**, 587-590 (2010).
37. Theodoni, P., Panagiotaropoulos, T.I., Kapoor, V., Logothetis, N.K. & Deco, G. Cortical microcircuit dynamics mediating binocular rivalry: the role of adaptation in inhibition. *Front. Hum. Neurosci*. **5**, 145 (2011).
38. Churchland, M.M., Yu, B.M., Cunningham, J.P., Sugrue, L.P., Cohen, M.R., Corrado,

G.S., Newsome, W.T., Clark, A.M., Hosseini, P., Scott, B.B., Bradley, D.C., Smith, M.A., Kohn, A., Movshon, J.A., Armstrong, K.M., Moore, T., Chang, S.W., Snyder, L.H., Lisberger, S.G., Priebe, N.J., Finn, I.M., Ferster, D., Ryu, S.I., Santhanam, G., Sahani, M. & Shenoy, K.V. Stimulus onset quenches neural variability: a widespread cortical phenomenon. *Nat Neurosci.* **13**, 369-78 (2010).

39. Smith, M.A. & Sommer, M.A. Spatial and temporal scales of neuronal correlation in visual area V4. *J. Neurosci.* **33**, 5422-32 (2013).
40. Constantinidis, C. & Goldman-Rakic, P.S. Correlated discharges among putative pyramidal neurons and interneurons in the primate prefrontal cortex. *J. Neurophysiol.* **88**, 3487-97 (2002).
41. Shpiro, A., Moreno-Bote, R., Rubin, N. & Rinzel, J. Balance between noise and adaptation in competition models of perceptual bistability. *J. Comput. Neurosci.* **27**, 37-54 (2009).
42. Panagiotaropoulos, T.I., Kapoor, V., Logothetis, N.K., & Deco, G. A common neurodynamical mechanism could mediate externally induced and intrinsically generated transitions in visual awareness. *PLoS One* **8**, e53833 (2013).
43. Pastukhov, A., Garcia-Rodriguez, P.E., Haenicke, J., Guillamon, A., Deco, G. & Braun, J. Multi-stable perception balances stability and sensitivity. *Front Comput Neurosci* **7**, 17. (2013).
44. Moreno-Bote, R., Rinzel, J. & Rubin, N. Noise-induced alternations in an attractor network model of perceptual bistability. *J. Neurophysiol.* **98**, 1125–1139 (2007).
45. Arieli, A., Sterkin, A., Grinvald, A., and Aertsen, A. (1999) Dynamics of ongoing activity: explanation of the large variability in evoked cortical responses. Science *273*,

1868-71.

46. Tsodyks, M., Kenet, T., Grinvald, A., and Arieli, A. (1999) Linking spontaneous activity of single cortical neurons and the underlying functional architecture. Science *286*, 1943-6.

47. He, B.J., & Raichle, M.E. The fMRI signal, slow cortical potential and consciousness. *Trends Cogn. Sci.* **13**, 302-9 (2009).

48. Koch, C. The SCP is not specific enough to represent conscious content. *Trends Cogn Sci* **13**, 367 (2009).

49. Koch, C. & Tsuchiya, N. Attention and consciousness: two distinct brain processes. *Trends Cogn. Sci.* **11**, 16-22 (2007).

50. Posner, M.I. Attention: the mechanisms of consciousness. *P. Natl. Acad. Sci. USA* **91**, 7398-403 (1994).

51. Harris, K.D. & Thiele, A. Cortical state and attention. *Nat. Rev. Neurosci* **12**, 509-523 (2011).

52. Brunel, N. & Wang, X.J. Effects of neuromodulation in a cortical network model of object working memory dominated by recurrent inhibition. *J Comput. Neurosci* **11** , 63–68 (2001).

53. Theodoni P, Kovács G, Greenlee MW, and Deco G Neuronal adaptation effects in decision making. J Neurosci 31, 234–246 (2011).

SUPPLEMENTAL INFORMATION

1. SUPPLEMENTAL DATA

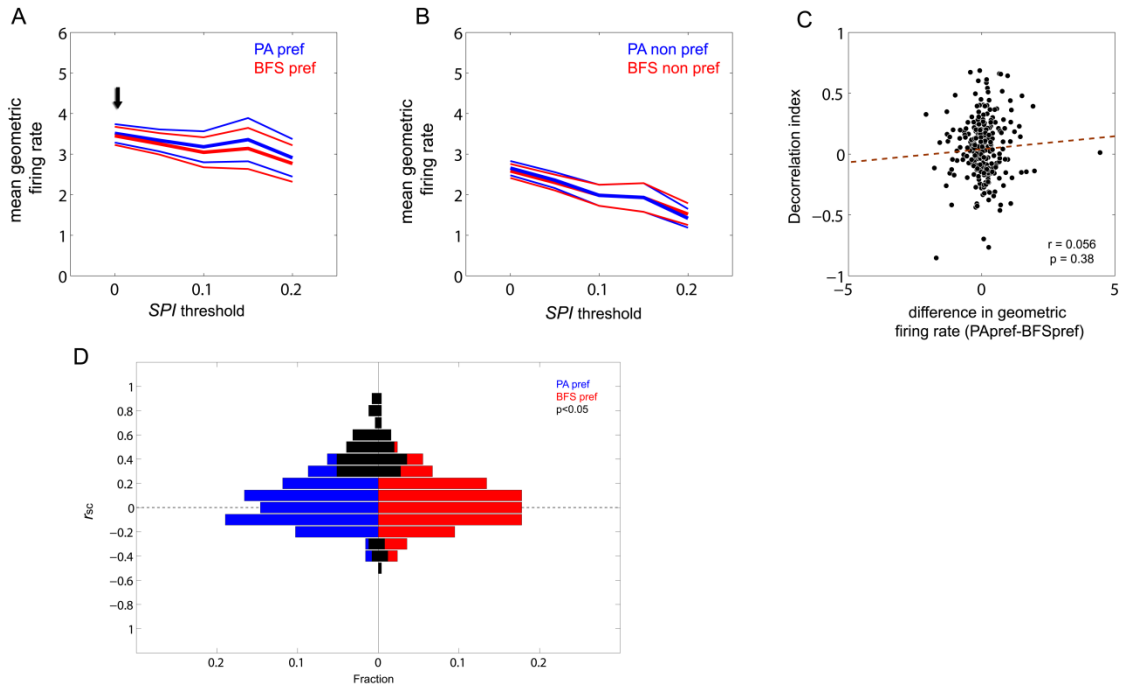

Figure S1

Mean geometric firing rate and distribution of correlations

(A) Mean geometric firing rate as a function of *SPI* threshold during perception of a preferred stimulus. Identical geometric firing rates were observed during monocular stimulation with the preferred pattern in PA (blue) and subjective perceptual dominance of the same pattern in BFS (red).

(B) Mean geometric firing rate as a function of *SPI* threshold during perception of a non-preferred stimulus. Identical geometric firing rates were observed during monocular stimulation with the non-preferred pattern in PA (blue) and subjective perceptual dominance of the same pattern in BFS (red).

(C) Relationship between differences in geometric firing rate and decorrelation index ($r_{scPApref}$ - . $r_{scBFSpref}$) during perception of the preferred pattern in PA and BFS. There was no direct relationship (r=0.056, p=0.38, red line – regression fit) between these two measures suggesting that decorrelation is not associated to the strength of discharge response.

(D) Histograms depicting the distribution of correlations for pairs during perception of the preferred stimulus in PA (blue) and BFS (red). Significant ($p<0.05$) pairs are colored in black. During BFS less pairs were significantly correlated and the distribution of correlations was less positively skewed than in PA.

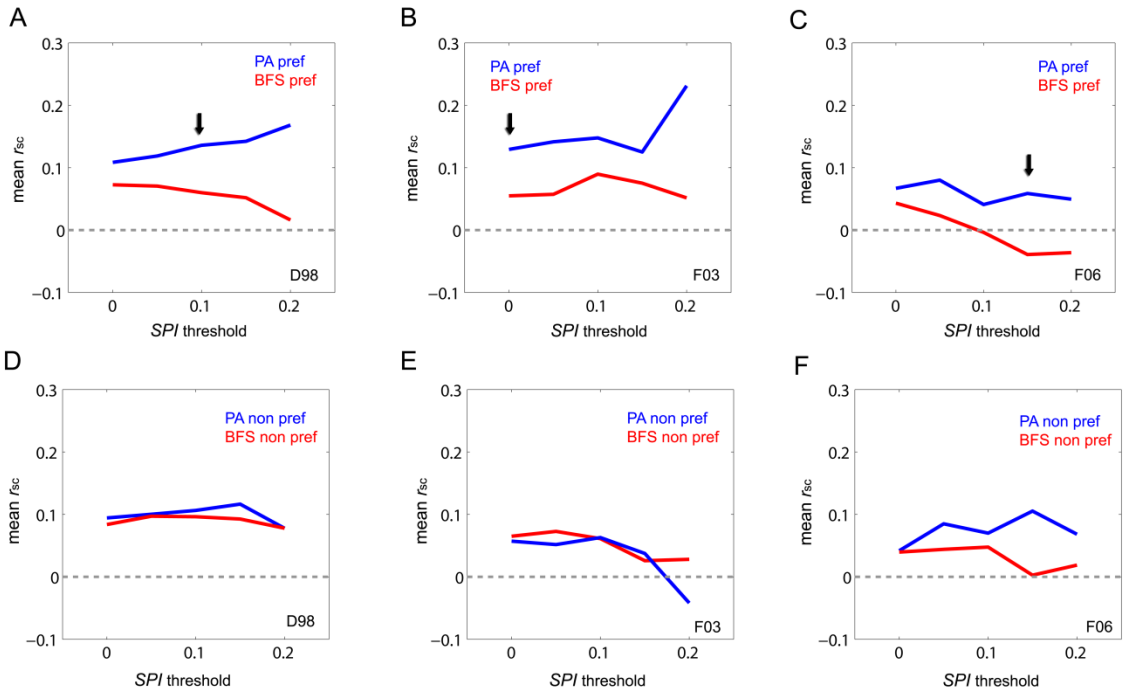

Figure S2

Noise correlations during PA and BFS in the LPFC of three macaques

(A) Spike count correlations during monocular stimulation with a preferred stimulus in PA (blue) and subjective perceptual dominance of the same stimulus during BFS (red) in the LPFC of monkey D98. The decorrelation during subjective perceptual dominance was statistically significant for *SPI*>0.1 (black arrow, $r_{scPApref}$ = 0.136 ± 0.039 t-test, $p<10^{-3}$ vs. $r_{scBFSpref}$ = 0.06 ± 0.026 t-test, p = 0.026; Wilcoxon signed rank test, p=0.038)

(B) Spike count correlations during monocular stimulation with a preferred stimulus in PA (blue) and subjective perceptual dominance of the same stimulus during BFS (red) in the LPFC of monkey F03. The decorrelation during subjective perceptual dominance was statistically significant for *SPI*>0.1 (black arrow, $r_{scPApref}$ = 0.129 ± 0.025 t-test,

$p<10^{-5}$ vs.$r_{scBFSpref}$ = 0.055 ± 0.024 t-test, p = 0.028; Wilcoxon signed rank test, p=0.0196)

(C) Spike count correlations during monocular stimulation with a preferred stimulus in PA (blue) and subjective perceptual dominance of the same stimulus during BFS (red) in the LPFC of monkey F06. The decorrelation during subjective perceptual dominance was statistically significant for *SPI*>0.1 (black arrow, $r_{scPApref}$ = 0.059 ± 0.047 t-test, p=0.22 vs.$r_{scBFSpref}$ = - 0.039 ± 0.047 t-test, p = 0.041; Wilcoxon signed rank test, p=0.038)

(D) Spike count correlations during monocular stimulation with a non-preferred stimulus in PA (blue) and subjective perceptual dominance of the same stimulus during BFS (red) in the LPFC of monkey D98. No significant differences were observed.

(E) Spike count correlations during monocular stimulation with a non-preferred stimulus in PA (blue) and subjective perceptual dominance of the same stimulus during BFS (red) in the LPFC of monkey F03. No significant differences were observed.

(F) Spike count correlations during monocular stimulation with a non-preferred stimulus in PA (blue) and subjective perceptual dominance of the same stimulus during BFS (red) in the LPFC of monkey F06. Despite a decrease during BFS differences were not statistically significant in any point.

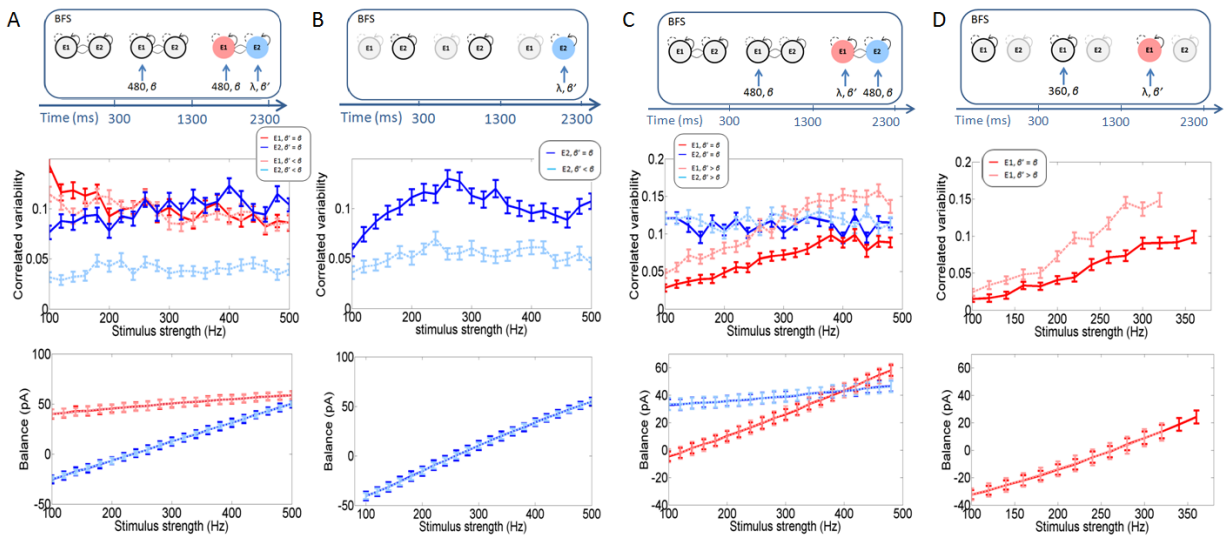

Figure S3

Noise correlations and synaptic balances

(A) Network with competition. Up: Stimulation protocol. Middle: Correlated variability of the suppressed (red), and dominant neurons (blue) in BFS as a function of the input strength to the dominant neurons, when $\beta' \equiv \beta_2 = \beta = 10^{-4}$. Light colors correspond to smaller input variability, $\beta' \equiv \beta_2 = 10^{-5} < \beta$. Down: Excitatory-inhibitory synaptic balance of the dominant and suppressed neurons in BFS for $\beta' = \beta$ and $\beta' < \beta$, respectively.

(B) As in A for the network without competition, for $\beta' \equiv \beta_2 = \beta = 10^{-4}$ and $\beta' \equiv \beta_2 = 5\times10^{-5} < \beta$. Here we do not plot the correlated variability of the suppressed neurons because they are independent from the dominant which receive the input strength and noise modulations.

(C) Network with competition. Up: Stimulation protocol. Middle: Correlated variability of the suppressed (red), and dominant neurons (blue) in BFS as a function of the input strength to the suppressed neurons when $\beta' \equiv \beta_1 = \beta = 10^{-4}$. Light colors correspond

to higher input variability, $\beta' \equiv \beta_1 = 1.1\times10^{-4} > \beta$. Down: Excitatory-inhibitory synaptic balance of the preferred and non neurons in BFS for $\beta' = \beta$ and $\beta' > \beta$, respectively.

(D) As in C for the network without competition, for $\beta' \equiv \beta_1 = \beta = 10^{-4}$ and $\beta' \equiv \beta_1 = 1.5\times10^{-4} > \beta$. Here we do not plot the correlated variability of the dominant neurons because they are independent from the suppressed which receive the input strength and noise modulations.

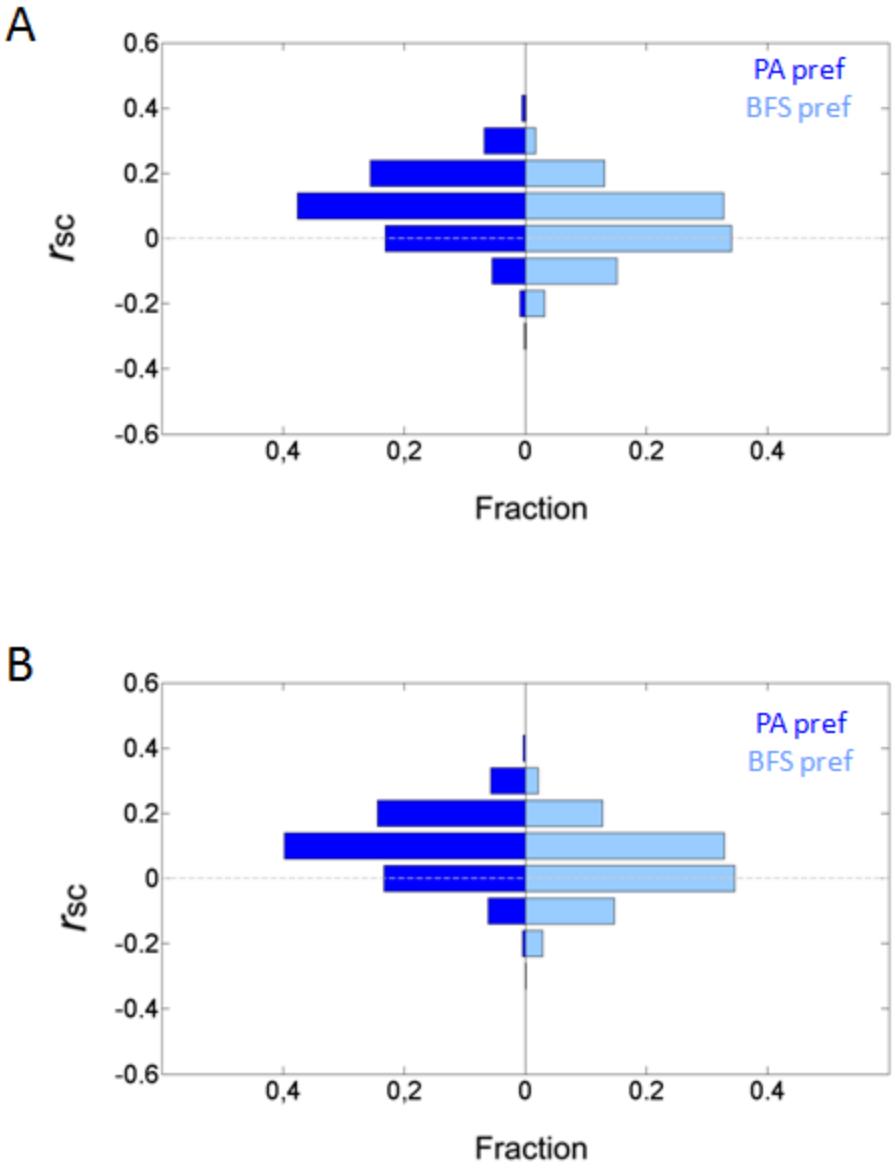

Figure S4

Distribution of spike count correlations

(A) Network with competition. Histogram of the trial by trial spike count correlations of pairs of dominant neurons in BFS (cyan) and of the same neurons in PA (blue).

(B) Same as in A for the network without competition.

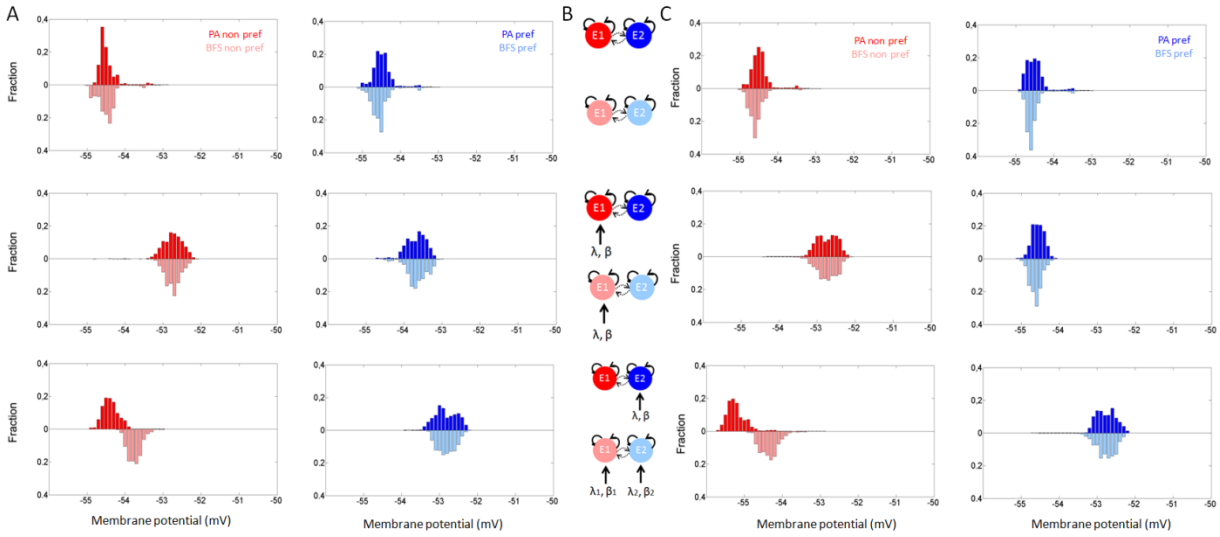

Figure S5.

Distribution of membrane potential

(A) Network with competition. Up: Histogram of the membrane potential of one suppressed (light red) and one dominant (cyan) neuron in BFS, and of the same neurons in PA (red and blue, respectively), during the time interval 1 - 300 ms. Middle: Same as Up for the time interval 300 - 1300 ms. down: Same as Up and Middle for the time interval 1300 - 2300 ms.

(B) Stimulation protocols of neural ensembles in PA (red and blue) and BFS (light red and cyan) at each time interval (Up: 1 - 300 ms, Middle: 300 - 1300 ms, and Down: 1300 - 2300 ms).

(C) Same as in A for the network without competition.

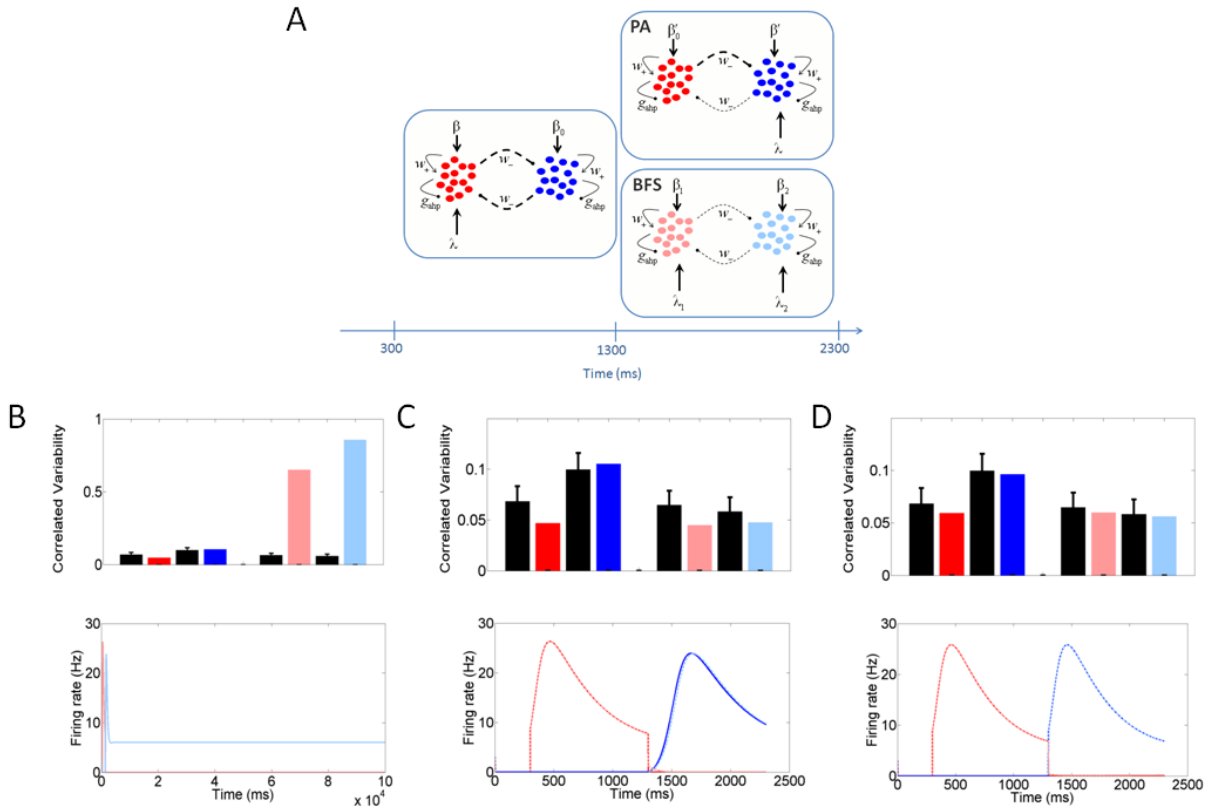

Figure S6.

Analytically derived equations of the second order statistics: Replicating the experimental data

(A) Network and stimulation protocol. Network of two neural ensembles with self-excitation w_+ (arrows) and cross inhibition w_- (dashed lines ending to circles). Each pool is consisted of N neurons selective to the same stimulus. During the first second only one pool is stimulated (e.g. red) with input strength λ. During the 2nd second, in PA, neurons of the other pool (blue) receive external input λ, while in BFS, neurons of pools receive external stimuli, red pool is stimulated by λ_1, and blue by λ_2. β_0, β_0', β', β, β_1, β_2 are the noises of the background and the corresponding inputs.

(B) Network with competition. Up: Correlated variability of the suppressed and dominant neurons in BFS (light red and cyan, respectively) and of the same neurons in PA (red and blue, respectively), when $\lambda_1 = \lambda_2 = \lambda = 90$ Hz and $\beta_1 = \beta_2 = \beta' = \beta_0' = 9$. Black bars are the experimental data. Down: Mean firing activity of the suppressed (light red) and dominant (cyan) neurons in BFS followed by BR, keeping the parameters same as in BFS when the network replicates the experimental data.

(C) Network with competition. Up: Correlated variability of the suppressed and dominant neurons in BFS (light red and cyan, respectively) and of the same neurons in PA (red and blue, respectively), when the network replicates the experimental data (black bars), $g_{AHP} = 2$ nS, $\lambda = 90$ Hz, $\lambda_1 = 60$ Hz, $\lambda_2 = 90$ Hz and $\beta_0' = \beta' = 9$, $\beta_1 = 11$, $\beta_2 = 90$. Down: Mean firing activity of the two neural ensembles for the parameters as in Up.

(D) As in C for the network without competition. Here, the parameters for which the network replicates the experimental data are: $g_{AHP} = 22$ nS, $\lambda = 90$ Hz, $\lambda_1 = 49$ Hz, $\lambda_2 = 90$ Hz, and $\beta_0' = \beta' = 9$, $\beta_1 = 11$, $\beta 2 = 90$.

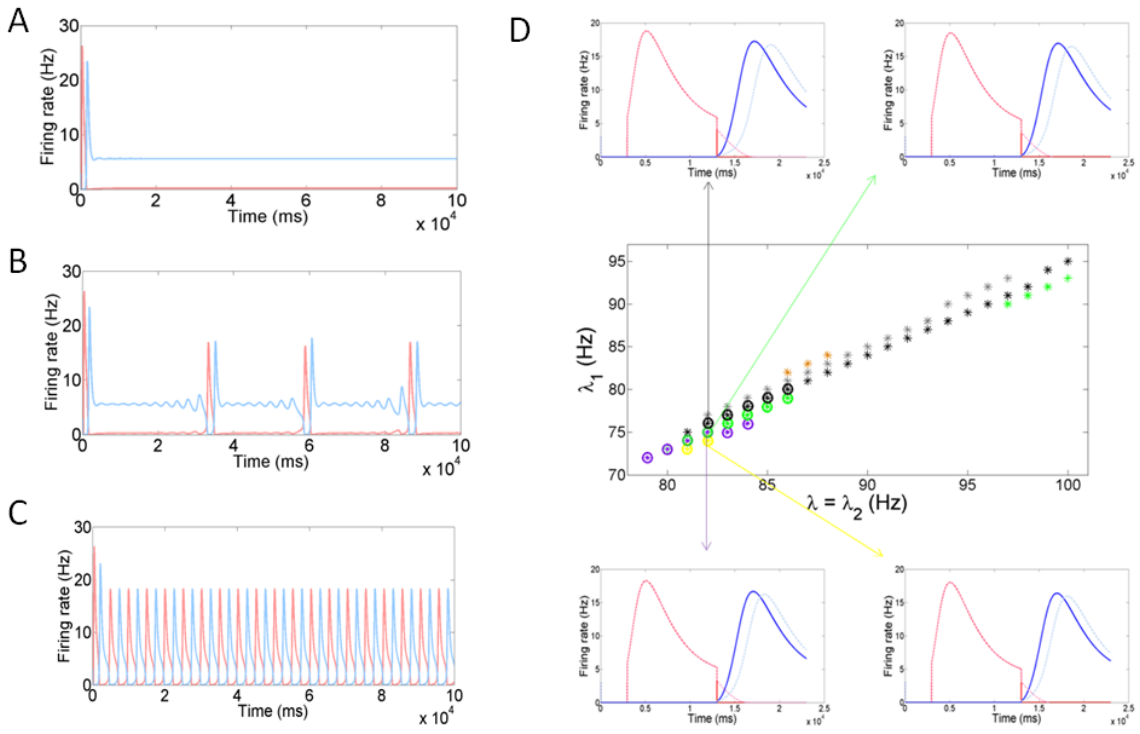

Figure S7.

Analytically derived equations of the second order statistics: BFS followed by BR

(A) Mean firing rate of the two neural ensembles when the system is in the bistability regime (for g_{AHP} = 2 nS, λ = 90 Hz, λ_1 = 83 and λ_2 = 90 Hz).

(B) Same as A in the bifurcation point which separates the bistability from the oscillatory regime (λ_1 = 84 Hz).

(C) Same as A in the oscillatory regime (λ_1 = 90 Hz).

(D) Bifurcation points λ_1, $\lambda = \lambda_2$, g_{AHP} for which the system in BFS followed by long stimulation the system transits to oscillatory regime. Orange points correspond to g_{AHP} = 18 nS, gray to g_{AHP} = 19 nS, black to g_{AHP} = 20 nS, green to g_{AHP} = 21 nS, purple to g_{AHP} =22 nS and yellow to g_{AHP} =23 nS. The λ, g_{AHP} values are taken from the λ - g_{AHP} region for which the model replicates the spike count correlations in PA. Circles correspond to

the bifurcation points for which the system replicates the experimental data in BFS, varying the noise intensities β_1, β_2. In smaller panels we draw the firing rate of the neuronal ensembles in PA (blue, red) and BFS (cyan, magenta) for $\lambda = \lambda_2$. Qualitatively similar is the behavior for the rest of λ_1, $\lambda = \lambda_2$, g_{AHP} points.

2. SUPPLEMENTAL EXPERIMENTAL PROCEDURES

Spiking network model composition

The network with cross-inhibition (Fig. 4A) is an attractor based model, similar to attractor networks employed for working memory [52], decision making [S1, 53], attention [S2], and perceptual bistability [37, 44]. It is biologically realistic and comprised of three neuronal populations of integrate-and-fire neurons, two (E1, E2) consisted of excitatory pyramidal cells and one (I) of inhibitory interneurons. It implements cooperation among excitatory neurons that belong to the same population, due to recurrent synaptic connectivity, and competition between excitatory neurons that belong to different neuronal populations, due to feedback inhibition. The excitatory pyramidal cells of one of the populations, e.g. E1, encode the face image, while the excitatory pyramidal cells of the other population, E_2, encode the polar image. The network without cross-inhibition (Fig. 4B) is comprised of two populations, one (E1 or E2) consisted of excitatory pyramidal cells that are selective to the face (or the polar image) and one (I) consisted of inhibitory interneurons.

In both networks there are $N_E = 0.8N$ excitatory neurons and $N_I = 0.2N$ inhibitory neurons, where N is the total number of neurons ($N = 500$), consistent with the neurophysiological observed proportion of 80% pyramidal cells versus 20% interneurons [S3].

Each of the two selective pools, in the network with cross-inhibition consists of $0.5N_E$ neurons. Neurons belonging to one particular population share the same statistical properties and single-cell parameters, as well as inputs and connectivity.

Connectivity

Both networks have same connectivity, for the sake of comparison. There is all-to-all connectivity, meaning that each neuron receives N_E excitatory and N_I inhibitory synaptic contacts. The recurrent self-excitation within the selective neural populations, the connection strength between the excitatory pools in the network with competition, and the connection between excitatory towards inhibitory neurons is $w_+ = 1$ (thin lines, Fig. 4A-B). Inhibitory neurons connect to each other and to the excitatory neurons with strength $w_I = 2$ (thick lines, Fig. 4A-B).

Dynamics of neurons, synapses and channels

All neurons in the network are modeled as leaky integrate-and-fire neurons. Integrate- and- fire (IF) neurons are point-like elements, meaning that the whole neural membrane is taken as equipotential. The sub threshold dynamics of the membrane potential of excitatory (E) or inhibitory (I) LIF neurons is described by the following dynamics

$$C_m^{E,I}\frac{dV(t)}{dt} = -g_m^{E,I}\left(V(t)-V_L\right)+I_{total}(t) \qquad (1)$$

where $V_L = -70$ mV is the resting potential, $C_m^E = 0.5$ nF, $g_m^E = 25$ nS $\tau_m^E = C_m^E/g_m^E = 20$ ms are the membrane capacitance, leak conductance, and membrane time constant for excitatory neurons respectively, and $C_m^I = 0.2$ nF, $g_m^I = 20$ nS $\tau_m^I = C_m^I/g_m^I = 10$ ms for inhibitory neurons

respectively. The total synaptic current to each neuron is the sum of excitatory postsynaptic currents mediated by AMPA (I_{AMPA}) and NMDA (I_{NMDA}) glutamatergic and $\mathrm{GABA_A}$ (I_{GABA}) gabaergic receptors, an external excitatory postsynaptic current mediated by AMPA receptors ($I_{\mathrm{AMPA,ext}}$) and a slow Ca^{2+}-activated K^+ after-hyperpolarization current (I_{AHP}):

$$I_{\mathrm{total}}(t) = I_{\mathrm{AMPA,ext}}(t) + I_{\mathrm{AMPA}}(t) + I_{\mathrm{NMDA}}(t) + I_{\mathrm{GABA}}(t) + I_{\mathrm{AHP}}(t) \tag{2}$$

Where

$$I_{\mathrm{AMPA,ext}}(t) = -\mathrm{g}^{\mathrm{E,I}}_{\mathrm{AMPA,ext}}\left(V(t) - \mathrm{V_E}\right)\sum_{\mathrm{j}}^{\mathrm{C_{ext}}} S_{\mathrm{j}}^{\mathrm{AMPA,ext}}(t) \tag{3}$$

$$\frac{dS_{\mathrm{j}}^{\mathrm{AMPA,ext}}(t)}{dt} = -\frac{S_{\mathrm{j}}^{\mathrm{AMPA,ext}}(t)}{\tau_{\mathrm{AMPA}}} + \sum_{\mathrm{k}} \delta(t - t_{\mathrm{j}}^{\mathrm{k}}) \tag{4}$$

$$I_{\mathrm{AMPA}}(t) = -\mathrm{g}^{\mathrm{E,I}}_{\mathrm{AMPA}}\left(V(t) - \mathrm{V_E}\right)\sum_{\mathrm{j}}^{\mathrm{C_E}} w_{\mathrm{j}} S_{\mathrm{j}}^{\mathrm{AMPA}}(t) \tag{5}$$

$$\frac{dS_{\mathrm{j}}^{\mathrm{AMPA}}(t)}{dt} = -\frac{S_{\mathrm{j}}^{\mathrm{AMPA}}(t)}{\tau_{\mathrm{AMPA}}} + \sum_{\mathrm{k}} \delta(t - t_{\mathrm{j}}^{\mathrm{k}}) \tag{6}$$

$$I_{\mathrm{NMDA}}(t) = -\frac{\mathrm{g}^{\mathrm{E,I}}_{\mathrm{NMDA}}\left(V(t) - \mathrm{V_E}\right)}{1 + \gamma e^{-\beta V(t)}}\sum_{\mathrm{j}}^{\mathrm{C_E}} w_{\mathrm{j}} S_{\mathrm{j}}^{\mathrm{NMDA}}(t) \tag{7}$$

$$\frac{dS_{\mathrm{j}}^{\mathrm{NMDA}}(t)}{dt} = -\frac{S_{\mathrm{j}}^{\mathrm{NMDA}}(t)}{\tau_{\mathrm{NMDA,decay}}} + \mathrm{a}x_{\mathrm{j}}(t)\left(1 - S_{\mathrm{j}}^{\mathrm{NMDA}}(t)\right) \tag{8}$$

$$\frac{dx_{\mathrm{j}}(t)}{dt} = -\frac{x_{\mathrm{j}}(t)}{\tau_{\mathrm{NMDA,rise}}} + \sum_{\mathrm{k}} \delta(t - t_{\mathrm{j}}^{\mathrm{k}}) \tag{9}$$

$$I_{\mathrm{GABA}}(t) = -\mathrm{g}^{\mathrm{E,I}}_{\mathrm{GABA}}\left(V(t) - \mathrm{V_I}\right)\sum_{\mathrm{j}}^{\mathrm{C_I}} S_{\mathrm{j}}^{\mathrm{GABA}}(t) \tag{10}$$

$$\frac{dS_{\mathrm{j}}^{\mathrm{GABA}}(t)}{dt} = -\frac{S_{\mathrm{j}}^{\mathrm{GABA}}(t)}{\tau_{\mathrm{GABA}}} + \sum_{\mathrm{k}} \delta(t - t_{\mathrm{j}}^{\mathrm{k}}) \tag{11}$$

$$I_{\mathrm{AHP}}(t) = -\mathrm{g}_{\mathrm{AHP}}\mathrm{Ca}(t)\left(V(t) - \mathrm{V}_{\mathrm{K}}\right) \tag{12}$$

$$\frac{d\mathrm{Ca}(t)}{dt} = -\frac{\mathrm{Ca}(t)}{\tau_{\mathrm{Ca}}} + \rho\sum_{\mathrm{i}}\delta(t - t_{\mathrm{i}}) \tag{13}$$

$\mathrm{a} = 0.5\ (\mathrm{ms})^{-1}$, δ(t) is the Dirac delta-function, and S_{j} are the synaptic gating variables (fractions of open channels), where sums over j are over pre-synaptic neurons, sums over k are over spikes emitted by the pre-synaptic neuron j at time $t_{\mathrm{j}}^{\mathrm{k}}$, and the sum over i is over spikes of the same neuron up to time t. w_{j} are the dimensionless connection weights (see Connectivity) between and within the neuronal populations. $\mathrm{V}_{\mathrm{E}} = 0\ \mathrm{mV}$ is the reversal potentials for excitatory postsynaptic currents and for $\mathrm{V}_{\mathrm{I}} = -70\ \mathrm{mV}$ inhibitory postsynaptic currents. The peak conductance for excitatory synapses are $\mathrm{g}^{\mathrm{E}}_{\mathrm{AMPA,ext}} = 2.08\ \mathrm{nS}$, $\mathrm{g}^{\mathrm{E}}_{\mathrm{AMPA}} = 104/N\ \mathrm{nS}$, $\mathrm{g}^{\mathrm{E}}_{\mathrm{NMDA}} = 327/N\ \mathrm{nS}$, $\mathrm{g}^{\mathrm{E}}_{\mathrm{GABA}} = 1250/N\ \mathrm{nS}$, for inhibitory $\mathrm{g}^{\mathrm{I}}_{\mathrm{AMPA,ext}} = 1.62\ \mathrm{nS}$, $\mathrm{g}^{\mathrm{I}}_{\mathrm{AMPA}} = 81/N\ \mathrm{nS}$, $\mathrm{g}^{\mathrm{I}}_{\mathrm{NMDA}} = 258/N\ \mathrm{nS}$, $\mathrm{g}^{\mathrm{I}}_{\mathrm{GABA}} = 973/N\ \mathrm{nS}$, where N is the total number of neurons in the network, and for excitatory or inhibitory $\mathrm{g}_{\mathrm{AHP}} = 30\mathrm{nS}$. The NMDA currents are voltage-dependent, and modulated by intracellular magnesium concentration $\left[\mathrm{Mg}^{2+}\right] = 1\ \mathrm{mM}$, with parameters $\gamma = \left[\mathrm{Mg}^{2+}\right]/3.57$ and $\beta = 0.062\ (\mathrm{mV})^{-1}$. The rise time of the NMDA mediated synaptic current is $\tau_{\mathrm{NMDA,rise}} = 2\ \mathrm{ms}$, while the rise time of AMPA and GABA mediated synaptic currents are neglected for being extremely fast (<1ms). The decay time constants are $\tau_{\mathrm{AMPA}} = 2\ \mathrm{ms}$, $\tau_{\mathrm{NMDA,decay}} = 100\ \mathrm{ms}$, and $\tau_{\mathrm{GABA}} = 10\ \mathrm{ms}$. The reversal potential of the potassium channels is $\mathrm{V}_{\mathrm{K}} = -80\ \mathrm{mV}$.

When the membrane potential of an excitatory or inhibitory neuron reaches a threshold $\mathrm{V}_{\mathrm{thr}} = -50\ \mathrm{mV}$, a spike is emitted and transmitted to other neurons. The membrane potential is

reset to $V_{reset} = -55$ mV after a refractory period, $\tau_{ref}^{E} = 2$ ms for excitatory neurons, and $\tau_{ref}^{I} = 1$ ms for inhibitory neurons. During this period the neuron is unable to produce further spikes. In addition, the gating variable Ca, emulating the cytoplasmic Ca^{2+} concentration, increases by a small amount $\rho = 0.01$, and decays exponentially with a time constant $\tau_{Ca} = 2000$ ms.

Model input and output

All excitatory neurons receive background input, through $C_{ext} = 800$ excitatory connections, each one receiving an independent Poisson spike train with rate λext = 3 Hz, and noise $\beta \cdot g(t)$, where g is being drawing, at each time step, from a Gaussian distribution with mean 0 and standard deviation 1, and β is the level of noise, so called input noise, or input fluctuations. The presentation of an image in the experiment is simulated by additional to the background input Poison spike train of rate λ, and total input noise β, to the excitatory neurons. Inhibitory neurons in all times and all conditions receive background input, through $C_{ext} = 800$ excitatory connections, each one receiving an independent Poisson spike train with rate λext = 3 Hz and noise β = 0.

Physical alternation (PA) stimulation protocol

The first 300 ms all excitatory neurons receive only background input. The next 1000 ms, neurons of one of the selective populations, E1, receive additional external input of rate λand total input noise β, while neurons of E2 receive only background input. The last 1000 ms, neurons of E2 receive additional external input of rate λand total input noise β, while neurons of

E1 receive only background input (PA, Fig. 4C). In Summary, the inputs to the selective populations, v_{E1} and v_{E2} are given by the following equations:

$$\left.\begin{aligned} v_{E1}(t) &= \lambda_{ext} + \beta_{ext} \cdot g(t) \\ v_{E2}(t) &= \lambda_{ext} + \beta_{ext} \cdot g(t) \end{aligned}\right\} \text{for} \quad 0 \le t \le 300\,\text{ms} \tag{14}$$

$$\left.\begin{aligned} v_{E1}(t) &= \lambda_{ext} + \lambda + \beta \cdot g(t) \\ v_{E2}(t) &= \lambda_{ext} + \beta_{ext} \cdot g(t) \end{aligned}\right\} \text{for} \quad 300 < t \le 1300\,\text{ms} \tag{15}$$

$$\left.\begin{aligned} v_{E1}(t) &= \lambda_{ext} + \beta_{ext} \cdot g(t) \\ v_{E2}(t) &= \lambda_{ext} + \lambda + \beta \cdot g(t) \end{aligned}\right\} \text{for } 1300 < t \le 2300\,\text{ms} \tag{16}$$

Considering two networks without cross-inhibition, one where the excitatory population (E1) consists of neurons selective to one of the images, e.g. face image, and excitatory population (E2) of the other consists of neurons selective to the other image, i.e. polar image, we follow the same stimulation protocol as previously (Equations 14 - 16).

Binocular Flash Suppression (BFS) stimulation protocol

The first 300 ms all excitatory neurons receive only background input. For the next 1000 ms, neurons of one of the selective populations (E1) receive additional external input of rate λand noise β. The last 1000 ms, neurons of the same selective population receive additional external input of rate λ_1 and noise β_1 while of the other selective population (E2) receive additional external input of rate λ_2 and noise β_2 (BFS, Fig. 4C). In Summary, the inputs to the selective populations, v_{E1} and v_{E2} are given by the following equations:

$$\left.\begin{aligned} v_{E1}(t) &= \lambda_{ext} + \beta_{ext} \cdot g(t) \\ v_{E2}(t) &= \lambda_{ext} + \beta_{ext} \cdot g(t) \end{aligned}\right\} \text{for} \quad 0 \le t \le 300\,\text{ms} \tag{16}$$

$$\left.\begin{aligned} v_{E1}(t) &= \lambda_{ext} + \lambda + \beta \cdot g(t) \\ v_{E2}(t) &= \lambda_{ext} + \beta_{ext} \cdot g(t) \end{aligned}\right\} \text{for} \quad 300 < t \le 1300\,\text{ms} \tag{17}$$

$$\left.\begin{aligned} v_{E1}(t) &= \lambda_{ext} + \lambda_1 + \beta_1 \cdot g(t) \\ v_{E2}(t) &= \lambda_{ext} + \lambda_2 + \beta_2 \cdot g(t) \end{aligned}\right\} \text{for } 1300 < t \le 2300\,\text{ms} \tag{18}$$

Considering two networks without cross-inhibition, one where the excitatory population (E1) consists of neurons selective to one of the images, e.g. face image, and excitatory population (E2) of the other consists of neurons selective to the other image, i.e. polar image, we follow the same stimulation protocol as previously (Equations 16 - 18).

Parameters for which the networks replicate the experimental data

Theoretical studies have shown that noise correlations are small in neural networks with recurrent [S4] weak connection strengths between excitatory neurons [S5-S6], strong inhibitory feedback [36, S7-S9], heterogeneity in connectivity [S7], and depend on the neural activity [32], network excitatory-inhibitory balance [36, S8-S9], neural adaptation and synaptic depression [S10-S11], network state [S12-S13], and input [36, S14-S16]. In our networks there is homogeneity in connections, but weak recurrent connections and strong inhibitory feedback. These properties maintain noise correlations at low levels in PA and BFS. In this study we were interested in differences between and similarities of the decorrelated variability of neurons in each pool and between conditions. the decorrelation of the dominant neurons in BFS. We found that decorrelation of the preferred neurons in BFS compared to PA, arise from smaller input fluctuations to the dominant pool. The steadiness of the correlated variability of the suppressed neurons, on the other hand, is due to the smaller stimulus strength the suppressed neurons receive in BFS.

The network with cross-inhibition replicates the experimental data in PA and BFS when $\beta_{ext} = 2.5\times10^{-4}$, $\lambda = 480$ Hz, $\beta = 1\times10^{-4}$, $\lambda_1 = 160$ Hz, $\beta_1 = 1.1\times10^{-4}$ and $\lambda_2 = 460$ Hz, $\beta_2 = 1\times10^{-5}$ (Fig.

4E). The network without cross-inhibition replicates the experimental data in PA and BFS when $\beta ext = 3.5\times10^{-4}$, $\lambda = 360$ Hz, $\beta = 1\times10^{-4}$, $\lambda_1 = 160$ Hz, $\beta_1 = 1.5\times10^{-4}$ and $\lambda_2 = 340$ Hz, $\beta_2 = 5.5\times10^{-5}$ (Fig. 4F). The rest of the parameters are the same in both networks. The only difference is the number of the excitatory neurons in each population. The total number of neurons is the same in both networks, thus in the network without cross-inhibition the excitatory population is double in size ($N_{E1orE2} = 400$ neurons) compared with each excitatory population in the network with cross-inhibition ($N_{E1,2} = 200$ neurons).

Simulations

The spiking neural model was programmed with C++ programming and for analyzing the outputs of the spiking simulations, we used Matlab. All scripts are available from the authors upon request. To integrate the system of coupled differential equations that describe the dynamics of all cells and synapses we used a 2nd order Runge-Kutta routine with a time step of 0.02 ms.

Analysis

Mean firing rate: In Figures 4, 6, the mean firing rate of each neuronal population was calculated by dividing the number of spikes emitted in a 50ms window by its number of neurons and by the window size. The time window was sliding with a time step of 5 ms. In Figure 5, at each of 100 trials the spike count is recorded from 200 neurons during the last second of the simulation (1300-2300 ms). Its mean and standard deviation is taken over 100 trials for 50 randomly selected neurons and then the mean and standard deviation of the mean and of the standard deviation is taken over 100 sets of such 100 trials.

Fano factor: At every set of 100 trials we calculate the Fano factor of each neuron, of the 50 randomly selected neurons across the 100 trials and then we average over them. Finally we calculated the mean Fano factor and its standard deviation over 100 sets of such 100 trials.

Spike count correlations: We recorded the spike count of 200 neurons across 100 trials from each excitatory neuronal population of the network with cross-inhibition, and 400 neurons across 100 trials from the excitatory neuronal population of the network without cross-inhibition, in each condition (PA, BFS), during the time interval $1300 < t \leq 2300$. In Figures 4, 5 and S3, we selected randomly 50 neurons, and after converting their spike counts into z-scores, we computed the mean Pearson correlation coefficient for all pairs, as done experimentally, over 100 trials. We followed the same procedure 100 times and finally computed the mean and standard deviation of the mean correlation coefficient. In Figure 5 the mean spike count correlations and in Figure S4 their histogram from one such set of 100 trials are drawn.

Current correlations: For 100 trials from each of 50 neurons from the excitatory selective populations, every 1 ms, we recorded the synaptic currents $I_{\mathrm{AMPA,ext}}$, I_{AMPA}, I_{NMDA}, and I_{GABA} (Eqs. 3,5,7,10). After converting them into z-scores, we computed the mean Pearson correlation coefficient for pairs of external excitatory synaptic currents $I_{\mathrm{AMPA,ext}}$ (Cxx), of recurrent excitatory synaptic currents $I_{\mathrm{AMPA}} + I_{\mathrm{NMDA}}$ (Cee), recurrent inhibitory synaptic currents I_{GABA} (Cii) and all combinations between them (Cei = Cie, Cxe = Cex, and Cxi = Cix) (Fig. 5B).

Excitatory-inhibitory balance. In each trial, every 1 ms, for each excitatory population, we recorded the mean synaptic currents over all its neurons. After summing them, we calculated the mean of over the time, where we add 450 pA [52], and finally we averaged over 100 trials,

$$\mathrm{Balance} = \left\langle \left\langle I_{\mathrm{AMPA,ext}} + I_{\mathrm{AMPA}} + I_{\mathrm{NMDA}} + I_{\mathrm{GABA}} + 450 \right\rangle_{1300 \leq t \leq 2300} \right\rangle_{100\,\mathrm{trials}}$$ (Fig. 4D and Fig. 5A)

Mean and standard deviation of the voltage: At every time step (0.02 ms), during the time interval $1300 < t \leq 2300$ ms, we recorded the voltage of 50 neurons from each excitatory neuronal population, in each condition. We then calculated the mean voltage and its standard deviation, then the mean of them over 100 trials and finally, the mean of them over neurons (Fig. 5C-D). In Figure S5 the histograms of the membrane potential from one neuron, every 0.02 ms time step and from 100 trials, from each neural ensemble and for each condition (PA, BFS) are plotted.

Suppression of input fluctuations decorrelates the dominant population during subjective perception

The spike count correlations of the dominant neurons in BFS are smaller compared to the correlated variability of the same neurons in PA, because the input noise to the neurons of the dominant population in BFS is smaller compared to PA. In Figure S3 we plot the correlated variability of the dominant neurons (blue and cyan lines), in BFS, as a function of stimulus strength λ, for different noises β'. In Figure S3A we consider the network with competition and in Figure S3B, the network without competition. We plot also the correlated variability of the suppressed neurons (red and light red lines) in order to show its dependence on the stimulus strength to the dominant population. We do not show the same for the network without competition (Fig. S3B), because the two populations are independent.

Decrease of input strength maintains correlations in the suppressed population during subjective perception

Both noise and input noise modulations are responsible for the stability of the noise correlation, mean firing rate and Fano factor of the suppressed neurons in BFS, compared to PA. In Figure S3C we plot the correlated variability of the suppressed neurons (red and red light lines), in BFS, as a function of stimulus strength λ, for different noises β′. In Figure S3C we consider the network with competition and in Figure S3C, the network without competition. In Figure S3C we plot also the correlated variability of the dominant neurons (blue and cyan lines) in order to show its dependence on the stimulus strength to the suppressed population. We do not show the same for the network without competition (Fig. S3C), because the two populations are independent.

Analytically derived equations for first- and second- order statistics of the neural activity

We considered a network of two neuronal ensembles; each consisted of *N* neurons modeled as dynamic mean-field based rate models; neural population E1, where neurons are selective to a Face image and neural population E2, where neurons are selective to a Polar image. There is all-to-all connectivity and neurons within each ensemble are connected with self-excitation w_+ (arrows, Fig. S6A), and between ensembles with cross- inhibition w_- (dashed lines ending to circles, Fig. S6A). Each neuron is modeled according to a consistent derivation (Equations 19-21 and ref. 37) from a biophysically realistic network [53] with spike-frequency adapting mechanism based on Ca2+-activated K+ hyperpolarizing currents (lines ending to circles, Fig. S6A, where g_{ahp} is the level of neural adaptation), where, for simplicity, we don't consider AMPA synapses.

Each neuron receives a background input and an external input which represents the presentation of an image during PA and BFS.

We applied the augmented method of moments [S17-S18], in order to derive analytically the equation for the correlation across pairs of neurons within each neuronal ensemble. Dynamics of neuron *i* in a given ensemble *m*, is described by

$$\frac{dx_{ki}^{m}(t)}{dt} = -\frac{x_{ki}^{m}(t)}{\tau_k} + \left(1 - x_{ki}^{m}(t)\right)\gamma\Phi\left(u_i^m\right) + \xi_i \tag{19}$$

$$\frac{dx_{li}^{m}(t)}{dt} = -\frac{x_{li}^{m}(t)}{\tau_l} + \rho\Phi\left(u_i^m\right) \tag{20}$$

where $i = 1, \ldots, N$, m = E1, E2, x^m_{kl} is the synaptic gating variable (fraction of open channels) of the neuron *i* in the ensemble *m* and it is analogous to the firing rate. x^m_{li} is the the gating variable emulating the cytoplasmic Ca^{2+} concentration in neuron *i* of the ensemble *m*. ξ_i denotes additive independent Gaussian white noise source which satisfies $< \xi_i(t) > = 0$ and $< \xi_i(t)\xi_j(t') > = \beta^2\delta(t - t')\delta_{ij}$, where we define β_0 as the level of noise. $\tau = 2$ ms, is the decay time constant of AMPA mediated synaptic currents and $\gamma = 6.41\times10^{-4}$. Φ, is the gain function given by

$$\Phi\left(u_i^m\right) = \frac{cu_i^m - d}{1 - e^{-g(cu_i^m - d)}} \tag{21}$$

where $c = 310$ Hz/nA, $d = 125$ Hz, $g = 0.16$ s and the input to neural population *i* is

$$u_i^m = \frac{w_+}{N_m}\sum_j^{N_m} x_{kj}^m - \frac{w_-}{N_n}\sum_j^{N_n} x_{kj}^n - \lambda x_{lj}^m + I \tag{22}$$

where $I = I_0 + J_{\mathrm{A,ext}}\lambda$, I_0 is the background input, λ is the external input and $J_{\mathrm{A,ext}} = 0.0025$.

Given the local variables x^m_{pi} ($p = k, l$, $m = 1, 2$) we define global variables for each assembly *m* as

$$X_p^m(t) = \frac{1}{N}\sum_i x_{pi}^m(t) \tag{23}$$

their means, variances and covariances are

$$\mu_p^m(t) = \left\langle X_p^m(t) \right\rangle_{trials} = \frac{1}{N_m} \sum_i \left\langle x_{pi}^m(t) \right\rangle_{trials} \tag{24}$$

$$\gamma_{kl}^m(t) = \frac{1}{N_m} \sum_i \left\langle \delta x_{ki}^m(t) \delta x_{li}^m(t) \right\rangle_{trials} \tag{25}$$

$$\rho_{kl}^{mn}(t) = \left\langle \delta X_k^m(t) \delta X_l^n(t) \right\rangle_t = \frac{1}{N_m N_n} \sum_i \sum_j \left\langle \delta x_{ki}^m(t) \delta x_{lj}^n(t) \right\rangle_{trials} \tag{26}$$

where $\delta X_p^m(t) = X_p^m(t) - \mu_p^m(t)$ and $\delta x_{pi}^m(t) = x_{pi}^m(t) - \mu_p^m(t)$.

Assuming that the noise intensity β is small, we express Equation 19 in a Taylor expansion of δx_{ki}^m, and Equation 20 of δx_{li}^m, as

$$\frac{dx_{ki}^m}{dt} = f^{mk}\left(u_m^*\right) + \sum_j^{N_m} \frac{\partial f^{mk}}{\partial x_{kj}^m} \delta x_{kj}^m + \sum_j^{N_n} \frac{\partial f^{mk}}{\partial x_{kj}^n} \delta x_{kj}^n + \frac{\partial f^{mk}}{\partial x_{li}^m} \delta x_{li}^m + \xi_i^m \tag{27}$$

$$\frac{dx_{li}^m}{dt} = f^{ml}\left(u_m^*\right) + \sum_j^{N_m} \frac{\partial f^{ml}}{\partial x_{kj}^m} \delta x_{kj}^m + \sum_j^{N_n} \frac{\partial f^{ml}}{\partial x_{kj}^n} \delta x_{kj}^n + \frac{\partial f^{ml}}{\partial x_{li}^m} \delta x_{li}^m \tag{28}$$

where

$$u_m^* = w_{mm}\mu_k^m - w_{mn}\mu_k^n - \lambda\mu_l^m + I \tag{29}$$

The differential equations (DEs) for the two first order moments are

$$\frac{d\mu_p^m}{dt} = \frac{1}{N_m} \sum_i^{N_m} \frac{d\left\langle x_{pi}^m \right\rangle}{dt} = f^{mp}\left(u_m^*\right) \tag{30}$$

where $p = k, l$. For $p = k$: $d\mu_k^m / dt = -\mu_k^m / \tau_k + \left(1 - \mu_k^m\right)\gamma\Phi\left(u_m^*\right)$ and for $p = l$: $d\mu_l^m / dt = -\mu_l^m / \tau_l + \rho\Phi\left(u_m^*\right)$. From equations 27, 30 and 28, 31 we get DEs for $d\delta x_{ki}^m / dt$ and for $d\delta x_{li}^m / dt$ as

$$\frac{d\delta x_{ki}^{m}}{dt}=\frac{dx_{ki}^{m}}{dt}-\frac{d\mu_{k}^{m}}{dt}=\sum_{j}^{N_m}\frac{\partial f^{mk}}{\partial x_{kj}^{m}}\delta x_{kj}^{m}+\sum_{j}^{N_n}\frac{\partial f^{mk}}{\partial x_{kj}^{n}}\delta x_{kj}^{n}+\frac{\partial f^{mk}}{\partial x_{li}^{m}}\delta x_{li}^{m}+\xi_{ki}^{m} \tag{31}$$

$$\frac{d\delta x_{li}^{m}}{dt}=\frac{dx_{li}^{m}}{dt}-\frac{d\mu_{l}^{m}}{dt}=\sum_{j}^{N_m}\frac{\partial f^{ml}}{\partial x_{kj}^{m}}\delta x_{kj}^{m}+\sum_{j}^{N_n}\frac{\partial f^{ml}}{\partial x_{kj}^{n}}\delta x_{kj}^{n}+\frac{\partial f^{ml}}{\partial x_{li}^{m}}\delta x_{li}^{m} \tag{32}$$

From Equations 25 and 32, 33 we get DEs for $d\gamma_{kl}^{m}/dt$ as

$$\begin{aligned}\frac{d\gamma_{kl}^{m}}{dt}&=\frac{1}{N_m}\sum_{i}^{N_m}\left\langle\frac{d\delta x_{ki}^{m}}{dt}\delta x_{li}^{m}\right\rangle+\frac{1}{N_m}\sum_{i}^{N_m}\left\langle\delta x_{ki}^{m}\frac{d\delta x_{li}^{m}}{dt}\right\rangle\\&=\gamma_{k\neq l,l}^{m}\frac{\partial f^{mki}}{\partial x_{k\neq l,i}^{m}}+\left(N_m\rho_{k\neq l,l}^{mm}-\gamma_{k\neq l,l}^{m}\right)\frac{\partial f^{mki}}{\partial x_{k\neq l,j}^{m}}+N_{p\neq m}\rho_{k\neq l,l}^{p\neq m,m}\frac{\partial f^{mki}}{\partial x_{k\neq l,j}^{p\neq m}}+\gamma_{l\neq k,l}^{m}\frac{\partial f^{mki}}{\partial x_{l\neq k,i}^{m}}\\&\quad+\gamma_{k,k\neq l}^{m}\frac{\partial f^{mli}}{\partial x_{k\neq l,i}^{m}}+\left(N_m\rho_{k,k\neq l}^{mm}-\gamma_{k,k\neq l}^{m}\right)\frac{\partial f^{mli}}{\partial x_{k\neq l,j}^{m}}+N_{p\neq m}\rho_{k,k\neq l}^{m,p\neq m}\frac{\partial f^{mli}}{\partial x_{k\neq l,j}^{p\neq m}}+\gamma_{k,l\neq k}^{m}\frac{\partial f^{mli}}{\partial x_{l\neq k,i}^{m}}\\&\quad+\delta_{k\neq l,l}\beta^{2}\end{aligned} \tag{33}$$

From Equations 26 and 32, 33 we get DEs for $d\rho_{kl}^{mn}/dt$ as

$$\begin{aligned}\frac{d\rho_{kl}^{mn}}{dt}&=\frac{1}{N_mN_n}\sum_{i}^{N_m}\sum_{j}^{N_n}\left\langle\frac{d\delta x_{ki}^{m}}{dt}\delta x_{li}^{n}\right\rangle+\frac{1}{N^{2}}\sum_{i}^{N_m}\sum_{j}^{N_n}\left\langle\delta x_{ki}^{m}\frac{d\delta x_{li}^{n}}{dt}\right\rangle\\&=\rho_{k\neq l,l}^{mn}\frac{\partial f^{mki}}{\partial x_{k\neq l,i}^{m}}+\left(N_m-1\right)\rho_{k\neq l,l}^{mn}\frac{\partial f^{mki}}{\partial x_{k\neq l,j}^{m}}+N_{p\neq m}\rho_{k\neq l,l}^{p\neq m,n}\frac{\partial f^{mki}}{\partial x_{k\neq l,j}^{p\neq m}}+\rho_{k\neq l,l}^{mn}\frac{\partial f^{mki}}{\partial x_{l\neq k,i}^{m}}\\&\quad+\rho_{k,k\neq l}^{mn}\frac{\partial f^{nli}}{\partial x_{k\neq l,i}^{n}}+\left(N_n-1\right)\rho_{k,k\neq l}^{mn}\frac{\partial f^{nli}}{\partial x_{k\neq l,j}^{n}}+N_{p\neq n}\rho_{k,k\neq l}^{m,p\neq n}\frac{\partial f^{nli}}{\partial x_{k\neq l,j}^{p\neq m}}+\rho_{k,l\neq k}^{mn}\frac{\partial f^{nli}}{\partial x_{l\neq k,i}^{n}}\\&\quad+\delta_{k\neq l,l}^{mn}\frac{\beta^{2}}{N_m}\end{aligned} \tag{34}$$

Equations 29, 30, 33 and 34 is a system of 29 coupled equations; four equations for means ($\mu^{m}{}_{1}$, $\mu^{m}{}_{2}$, $\mu^{n}{}_{1}$, $\mu^{n}{}_{2}$), eight equations for variances ($\gamma^{m}{}_{11}$, $\gamma^{m}{}_{12}$, $\gamma^{m}{}_{22}$, $\gamma^{m}{}_{21}$, $\gamma^{n}{}_{11}$, $\gamma^{n}{}_{12}$, $\gamma^{n}{}_{22}$, $\gamma^{n}{}_{21}$) and sixteen equations for covariances ($\rho^{mm}{}_{11}$, $\rho^{mm}{}_{12}$, $\rho^{mm}{}_{22}$, $\rho^{mm}{}_{21}$, $\rho^{nn}{}_{11}$, $\rho^{nn}{}_{12}$, $\rho^{nn}{}_{22}$, $\rho^{nn}{}_{21}$, $\rho^{mn}{}_{11}$, $\rho^{mn}{}_{12}$, $\rho^{mn}{}_{22}$, $\rho^{mn}{}_{21}$, $\rho^{nm}{}_{11}$, $\rho^{nm}{}_{12}$, $\rho^{nm}{}_{22}$, $\rho^{nm}{}_{21}$). The correlation variability is calculated as

When there is no competition ($w_- = 0$, Fig. 6A) , and the system of equations is consisted of eleven equations for each population; two equations for means (μ^m_1, μ^m_2), four equations for variances (γ^m_{11}, γ^m_{12}, γ^m_{22}, γ^m_{21}) and four equations for covariances (ρ^{mm}_{11}, ρ^{mm}_{12}, ρ^{mm}_{22}, ρ^{mm}_{21}). Finally, the correlated variability of the neural activity inside an ensemble, m, is given by

$$S^m_{kk}(t) = \frac{N\rho^{mm}_{kk} / \gamma^m_{kk} - 1}{N-1} \tag{39}$$

which is 0 for completely asynchronous state and 1 for completely synchronous [S17-S18, S12].

We solved the system of the DEs with Euler method and time step dt = 0.1 ms. Noise intensities β_0, β, β_0', β', β_1 and β_2 in the followings are integers for simplicity, since results do not change when all are multiplied by the same factor.

Using the augmented method of moments described above, we simulated PA and BFS (Fig. S6C-D) and replicated the experimental correlated variability, employing both networks, with and without competition. We, hence, conclude that competition is not the driving force for the noise-correlation reduction during rivalrous visual stimulations. Instead, the noise-correlation reduction is due to stimulus and noise modulation coming from previous stages. Therefore, we conclude the same result that we found by employing the biophysically realistic networks.

More specifically, we first consider the case when there is not cross-inhibition between the two neuronal ensembles ($w_- = 0$), i.e. when there is not competition. We simulated PA for a given level of adaptation, g_{AHP}, and stimulus strength, λ, and found the region in the β_0'- β space where the correlated variability of both ensembles is similar to the experimental data. Then, for a set of noise intensities taken from this region we found the region in the g_{AHP} - λ space where the simulated correlated variability of both ensembles is similar to the experimental data. Then, for a set of a level of adaptation g_{AHP} and stimulus strength, λ, from this region, and for a given set of λ_1, λ_2, we simulated BFS and found the region in the β_1 - β_2 space where the simulated correlated

variability of both ensembles is similar to the experimental ones. Finally, for a set of β_1, β_2 from this region, we find the region in the λ_1 - λ_2 space where the simulated correlated variability of both ensembles in BFS is similar to the experimental ones. From this region some sets of λ_1, λ_2 should be excluded because the firing rate of the ensembles are not similar with the experimental, when $\lambda_1 > \lambda_2$ and $\lambda_2 <$ 87 Hz. For a set of λ_1, λ_2 from the final region in the λ_1 - λ_2 space, we plot the mean firing rates in PA and BFS and the correlated variabilities together with the experimental ones (Fig. S6D). In addition, as expected, when we stimulate both pools for longer period of time, no alternations are observed, since there is no competition.

We follow the same procedure employing the network with competition ($w_- \neq 0$, Figure S6A). For the parameters for which we replicate the experimental data, if we stimulated both pools for longer period of time we find no alternations, even in the case when there is competition in the network (Fig. S6B), as we found with the biophysically realistic spiking network (Fig. 7A). Therefore we conclude that competition is not resolved in LPFC, rather neurons in LPFC are driven by previous procession stages or top-down activity.

We find that only with competition, i.e. when $\lambda_1 = \lambda_2 = \lambda$ and $\beta_1 = \beta_2 = \beta' = \beta_0'$, the experimental results in BFS are not satisfied (Fig. 6B), meaning, that competition is not enough in order to replicate the experimental data. Manipulating the noise intensities, still it is not possible to replicate the experimental data (data not shown).

We conclude that LPFC is driven by previous processing stages or top-down activity, because of the stimulus manipulation needed in order to account for the experimental results, but also because, as we show, if we stimulate longer both pools there are no alternations of their firing rates. This is expected for the network without competition but it is not trivial for the network with competition. In Figure S6C we present the results of one set of λ_1, λ_2. Nevertheless, higher

λ_1 lead to alternations (Figures S7A-C). We calculated the correlated variability of both ensembles, in BFS, for different values of λ_2, especially near the bifurcation. We find that the experimental data are not satisfied in the oscillatory regime.

Our results come from a given set of g_{AHP}, λ. Therefore, for the sake of robustness, we calculated the correlated variability at the bifurcation points for all sets of g_{AHP}, λ that replicate the PA data. For these values we then computed the correlated variability as a function of β_1, β_2, and found if and when the model replicates the BFS data. There are some cases when the model with competition can replicate the experimental trial by trial spike count correlations in the oscillatory regime (circles, Figure S7D). Nevertheless, the firing rate of the dominant population in BFS when the model is in the oscillatory regime, is not similar to PA (Figure S7D). As λ_1 increases the diferrence between the firing rate of the dominant pool in BFS compared to PA is increasing. We therefore, conclude that both the spiking and the rate model operate in the non-oscillatory regime, in order to replicate the experimental data.

3. SUPPLEMENTAL REFERENCES

S1. Wang XJ (2002) Probabilistic decision making by slow reverberation in cortical circuits.Neuron 36, 955–968.

S2. Deco G, and Rolls ET (2005) Neurodynamics of biased competition and cooperation for attention: a model with spiking neurons. Journal of Neurophysioogy 94, 295–313.

S3. Abeles A (1991) Corticonics. New York: Cambridge UP.

S4. Helias M, Tetzlaff T, and Diesmann M (2014), The correlation structure of local neuronal networks intrinsically results from recurrent dynamics, PLoS Computational Biology, 10(1): e1003428.

S5. Bernacchia A, and Amit DJ (2007) Impact of spatiotemporally correlated images on the structure of memory. Proc. Natl. Acad. Sci. USA, 104, 3544–3549.

S6. Ginzburg I, and Sompolinski H (1994). Theory of correlations in stochastic neural networks. Phys Rev. E, 50, 3171–3191.

S7. Bernacchia, A., and Wang, X.J. (2013). Decorrelation by recurrent inhibition in heterogeneous neural circuits, Neural Comput. *25*, 1732-67.

S8. Tetzlaff T, Helias M, Einevoll GT, and Diezman M (2012) Decorrelation of Neural-Network Activity by Inhibitory Feedback, PloS Comp. Biol. 8, 8, e1002596, 1-29

S9. Helias M, Tetzlaff T, and Diesmann M (2013), Echoes in correlated neural systems, New Journal of Physics 15, 023002, 1-24

S10. Cortes JM, Marinazzo D, Series P, Oram MW, Sejnowski TJ, and van Rossum MCW (2011), The effect of neural adaptation on population coding accuracy, Journal of Computational Neuroscience 32, 3, 387-402

S11. Rosenbaum R, Rubin JE, and Doiron B (2012) Short-term synaptic depression and stochastic vesicle dynamics reduce and shape neuronal correlations, Journal of Neurophysiology 109:475-484

S12. Ponce-Alvarez A., Thiele A., Albright TD, Stoner GR, and Deco G (2013) Stimulus-dependent variability and noise correlations in cortical MT neurons. PNAS 110, 32, 13162–13167

S13. Trousdale, J., Hu, Y., Shea-Brown, E., and Josic, K. (2012) Impact of network structure and cellular response on spike time correlations, PLoSComput. Biol. *8*, e1002408.

S14. Josić, K., Shea-Brown, E., Doiron, B., and de la Rocha, J. (2009) Stimulus-dependent correlations and population codes.Neural Comput. *21*, 2774-804.

S15. Litwin-Kumar A, Oswald AMM, Urban NN, and Doiron B (2011), Balanced synaptic input shapes the correlation between neural spike trains, PloS Computational Biology 7, 12, e1002305, 1-14

S16. Moreno, R., de la Rocha, J.,Renart, A., and Parga, N. (2002). Response of spiking neurons to correlated inputs. Phys. Rev. Lett. *89*, 288101.

S17. Hasegawa H (2004) Augmented moment method for stochastic ensembles with delayed couplings. I. Langevin model. Physical Review E, 70, 021911.

S18**.** Hasegawa H (2004) Augmented moment method for stochastic ensembles with delayed couplings. II. FitzHugh-Nagumo model. Physical Review E, 70, 021912.

A.4 Is the frontal lobe involved in conscious perception?

"No longer need one spend time attempting to understand the far-fetched speculation of physicists, nor endure the tedium of philosophers perpetually disagreeing with each other. Consciousness is now largely a scientific problem."

Francis Crick, "Visual perception: rivalry and consciousness"

frontiers in PSYCHOLOGY

OPINION ARTICLE
published: 19 September 2014
doi: 10.3389/fpsyg.2014.01063

Is the frontal lobe involved in conscious perception?

Shervin Safavi[1,2†], Vishal Kapoor[1,2†], Nikos K. Logothetis[1,3] and Theofanis I. Panagiotaropoulos[1]*

[1] Department Physiology of Cognitive Processes, Max Planck Institute for Biological Cybernetics, Tübingen, Germany
[2] International Max Planck Research School for Cognitive and Systems Neuroscience, University of Tübingen, Tübingen, Germany
[3] Department of Imaging Science and Biomedical Engineering, University of Manchester, Manchester, UK
*Correspondence: theofanis.panagiotaropoulos@tuebingen.mpg.de

† These authors have contributed equally to this work.

Edited by:
Jaan Aru, University of Tartu, Estonia

Reviewed by:
Wolfgang Einhauser, Philipps-Universität Marburg, Germany
Jaan Aru, University of Tartu, Estonia

Keywords: prefrontal cortex, conscious visual perception, frontal lobe, binocular rivalry, perceptual suppression

When studying the neural mechanisms underlying conscious perception we should be careful not to misinterpret evidence, and delineate these mechanisms from activity which could reflect the prerequisites or consequences of conscious experiences (Aru et al., 2012; De Graaf et al., 2012). However, at the same time, we need to be careful not to exclude any relevant evidence about the phenomenon.

Recently, novel paradigms have attempted to dissociate activity related to conscious perception from activity reflecting its prerequisites and consequences. In particular, one of these studies focused on resolving the role of frontal lobe in conscious perception (Frässle et al., 2014). Through a clever experimental design that contrasted blood-oxygen-level-dependent (BOLD) activity elicited during binocular rivalry with and without behavioral reports, Frässle et al. (2014) suggested that frontal lobe, or a large part of it, may not be necessary for conscious perception *per se*. Rather frontal areas are involved in processing the consequences of conscious perception like monitoring the perceptual content in order to elicit the appropriate report of the subjective experience. In particular, Frässle et al. showed that behavioral reports of conscious experiences resulted in increased and more widespread activity of the frontal lobe compared to a condition without behavioral reports, where spontaneous transitions in the content of consciousness were estimated through the objective measures like optokinetic nystagmus (OKN) and pupil dilation. The authors of this study concluded that "*frontal areas are associated with active report and introspection rather than with rivalry per se.*" Therefore, activity in prefrontal regions could be considered as a consequence rather than a direct neural correlate of conscious experience.

However, a previous study (Panagiotaropoulos et al., 2012) that measured directly neural activity in the macaque lateral prefrontal cortex (LPFC) using extracellular electrophysiological recordings could help to narrow down the role of frontal activity in conscious perception and exclude the contribution of cognitive or motor consequences in prefrontal neural activity during visual awareness. Specifically, the activity of feature selective neurons in the macaque LFPC was shown to be modulated in accordance with the content of subjective perception, without any confound from motor action (i.e., behavioral reports). Using binocular flash suppression (BFS), a paradigm of robust, externally induced perceptual suppression and without any requirement of behavioral reports, neurons in the LPFC were found to increase or decrease their discharge activity when their preferred stimulus was perceptually dominant or suppressed, respectively. Therefore, since neuronal discharges in the LPFC follow the content of conscious perception even without any motor action, the conclusion of Frässle et al. (2014) about the role of frontal lobe activity in rivalrous perception needs to be refined. Prefrontal activity can indeed reflect the content of conscious perception under conditions of rivalrous stimulation and this activity should not be necessarily considered as the result of a motor action or self-monitoring required for active report. Moreover, the results obtained by Frässle et al. (2014) do not anatomically preclude the entire prefrontal cortex from having a role in conscious perception. Specifically, the BOLD activity related to rivalry in their experiment is still present in the right inferior frontal lobe and right superior frontal lobe (Zaretskaya and Narinyan, 2014). Further, activation of dorso- LPFC in conscious perception of Mooney images was also reported in a study that explicitly controlled for activity elicited by motor action (Imamoglu et al., 2012).

It is true that the BFS-related prefrontal activity cannot conclude on a mechanistic, causal involvement of prefrontal activity in driving spontaneous transitions in conscious perception. This is because BFS is a paradigm of externally induced perceptual suppression and is therefore not directly informative about the role of recorded activity in spontaneous transitions. Therefore, the possibility remains open that the kind of prefrontal activity observed in the macaque LPFC during BFS is not a causal factor for conscious perception but rather reflects some other aspects of monitoring that are not directly related to motor action. For example, prefrontal activity could just reflect a read-out from other areas like the inferior temporal cortex (Sheinberg and Logothetis, 1997) that also reliably reflects the content of conscious perception. However, if this is the case, it triggers the question why this activity that closely follows the content of subjective perception is observed in the LPFC even in the absence of any behavioral report. Overall, it motivates further investigation to understand whether prefrontal activity

has a mechanistic role in conscious perception or it might underlie some monitoring functions that are not necessarily bound to motor action.

Similar to this debate on the role of LPFC in visual awareness, the last decade witnessed disagreement on whether activity in primary visual cortex reflects subjective perception as monitored with electrophysiology and fMRI (Leopold and Logothetis, 1996; Tong, 2003; Maier et al., 2008; Keliris et al., 2010; Leopold, 2012). Measuring both electrophysiological activity and the BOLD signal in the same macaques engaged in an identical task of perceptual suppression finally provided the solution (Maier et al., 2008; Leopold, 2012). Therefore, in order to investigate and resolve the role of PFC in visual perception, one must take a similar approach that utilizes multiple measurement techniques simultaneously or in the same animal along with a careful experimental design. The experimental tasks should not only segregate the effect of various cognitive processes such as attention or introspection in comparison to awareness (Watanabe et al., 2011; Frässle et al., 2014), but also use an objective criterion to decode the content of conscious experience (Frässle et al., 2014), therefore separating perception-related activities from the subsequent behavioral report. Such an approach could therefore robustly delineate the prerequisites and consequences of conscious experience and reveal the true correlates of conscious perception.

Lastly, although such a multimodal approach could provide us substantial insights into the activity underlying the representation of conscious content, whether or not this activity has a causal role in mediating perception remains to be understood. Although a number of studies indeed point to a causal involvement of prefrontal cortex in conscious perception (reviewed in Dehaene and Changeux, 2011), a systematic study which directly interferes with prefrontal activity during a task of subjective perception is currently, to the best of our knowledge, missing. While utilizing objective criteria as indicators of perceptual transitions, systematic perturbation of the PFC (such as cooling, transcranial magnetic stimulation, microstimulation, or optogenetics) and observing concomitant changes in the temporal dynamics of perceptual transitions could reveal its causal contribution. Indeed, patients with frontal lesions are impaired in their ability to switch from one subjective view of an ambiguous figure to the other (for example see Ricci and Blundo, 1990, but also see a different case study from Valle-Inclán and Gallego, 2006).

We would like to conclude that in formulating our conclusions related to prerequisites, consequences and true correlates of conscious experiences, we need to have an *integrative view* on the available evidence. Our investigations and conclusions about the neural correlates of consciousness must not only entail better-designed experiments but also diverse experimental techniques (e.g., BOLD fMRI, electrophysiology) that could measure brain activity on different spatial and temporal scales (Panagiotaropoulos et al., 2014). Such a multi-modal approach holds great promise in refining our current understanding of conscious processing.

ACKNOWLEDGMENT

This work was supported by the Max Planck Society and the International Max Planck Research School for Cognitive and Systems Neuroscience, University of Tübingen, Germany.

REFERENCES

Aru, J., Bachmann, T., Singer, W., and Melloni, L. (2012). Distilling the neural correlates of consciousness. *Neurosci. Biobehav. Rev.* 36, 737–746. doi: 10.1016/j.neubiorev.2011.12.003

De Graaf, T. A., Hsieh, P. J., and Sack, A. T. (2012). The "correlates" in neural correlates of consciousness. *Neurosci. Biobehav. Rev.* 36, 191–197. doi: 10.1016/j.neubiorev.2011.05.012

Dehaene, S., and Changeux, J. P. (2011). Experimental and theoretical approaches to conscious processing. *Neuron* 70, 200–227. doi: 10.1016/j.neuron.2011.03.018

Frässle, S., Sommer, J., Jansen, A., Naber, M., and Einhauser, W. (2014). Binocular rivalry: frontal activity relates to introspection and action but not to perception. *J. Neurosci.* 34, 1738–1747. doi: 10.1523/JNEUROSCI.4403-13.2014

Imamoglu, F., Kahnt, T., Koch, C., and Haynes, J. D. (2012). Changes in functional connectivity support conscious object recognition. *Neuroimage* 63, 1909–1917. doi: 10.1016/j.neuroimage.2012.07.056

Keliris, G. A., Logothetis, N. K., and Tolias, A. S. (2010). The role of the primary visual cortex in perceptual suppression of salient visual stimuli. *J. Neurosci.* 30, 12353–12365. doi: 10.1523/JNEUROSCI.0677-10.2010

Leopold, D. A. (2012). Primary visual cortex: awareness and blindsight. *Annu. Rev. Neurosci.* 35, 91–109. doi: 10.1146/annurev-neuro-062111-150356

Leopold, D. A., and Logothetis, N. K. (1996). Activity changes in early visual cortex reflect monkeys' percepts during binocular rivalry. *Nature* 379, 549–553. doi: 10.1038/379549a0

Maier, A., Wilke, M., Aura, C., Zhu, C., Ye, F. Q., and Leopold, D. A. (2008). Divergence of fMRI and neural signals in V1 during perceptual suppression in the awake monkey. *Nat. Neurosci.* 11, 1193–1200. doi: 10.1038/nn.2173

Panagiotaropoulos, T. I., Deco, G., Kapoor, V., and Logothetis, N. K. (2012). Neuronal discharges and gamma oscillations explicitly reflect visual consciousness in the lateral prefrontal cortex. *Neuron* 74, 924–935. doi: 10.1016/j.neuron.2012.04.013

Panagiotaropoulos, T. I., Kapoor, V., and Logothetis, N. K. (2014). Subjective visual perception: from local processing to emergent phenomena of brain activity. *Philos. Trans. R. Soc. Lond. B. Biol. Sci.* 369:20130534. doi: 10.1098/rstb.2013.0534

Ricci, C., and Blundo, C. (1990). Perception of ambiguous figures after focal brain lesions. *Neuropsychologia* 28, 1163–1173. doi: 10.1016/0028-3932(90)90052-P

Sheinberg, D. L., and Logothetis, N. K. (1997). The role of temporal cortical areas in perceptual organization. *Proc. Natl. Acad. Sci. U.S.A.* 94, 3408–3413. doi: 10.1073/pnas.94.7.3408

Tong, F. (2003). Primary visual cortex and visual awareness. *Nat. Rev. Neurosci.* 4, 219–229. doi: 10.1038/nrn1055

Valle-Inclán, F., and Gallego, E. (2006). Chapter 13 Bilateral frontal leucotomy does not alter perceptual alternation during binocular rivalry. *Prog. Brain Res.* 155, 235–239. doi: 10.1016/S0079-6123(06)55013-7

Watanabe, M., Cheng, K., Murayama, Y., Ueno, K., Asamizuya, T., Tanaka, K., et al. (2011). Attention but not awareness modulates the BOLD signal in the human V1 during binocular suppression. *Science* 334, 829–831. doi: 10.1126/science.1203161

Zaretskaya, N., and Narinyan, M. (2014). Introspection, attention or awareness? The role of the frontal lobe in binocular rivalry. *Front. Hum. Neurosci.* 8:527. doi: 10.3389/fnhum.2014.00527

Conflict of Interest Statement: The authors declare that the research was conducted in the absence of any commercial or financial relationships that could be construed as a potential conflict of interest.

Received: 30 July 2014; accepted: 04 September 2014; published online: 19 September 2014.

*Citation: Safavi S, Kapoor V, Logothetis NK and Panagiotaropoulos TI (2014) Is the frontal lobe involved in conscious perception? Front. Psychol. **5**:1063. doi: 10.3389/fpsyg.2014.01063*

This article was submitted to Consciousness Research, a section of the journal Frontiers in Psychology.

A.5 Desynchronization and rebound of beta oscillations during conscious and unconscious local neuronal processing in the macaque lateral prefrontal cortex.

"We believe that there are questions of such philosophical import that they deserve being pursued without any consideration of utility. One of them refers to the nature of thought processes, or more generally, of complex behavior."

Valentino Braitenberg, "Manifesto of Brain Science"

frontiers in PSYCHOLOGY

ORIGINAL RESEARCH ARTICLE
published: 11 September 2013
doi: 10.3389/fpsyg.2013.00603

Desynchronization and rebound of beta oscillations during conscious and unconscious local neuronal processing in the macaque lateral prefrontal cortex

Theofanis I. Panagiotaropoulos[1]*, Vishal Kapoor[1] and Nikos K. Logothetis[1,2]

[1] *Department of Physiology of Cognitive Processes, Max-Planck-Institute for Biological Cybernetics, Tübingen, Germany*
[2] *Division of Imaging Science and Biomedical Engineering, University of Manchester, Manchester, UK*

Edited by:
Ezequiel Morsella, San Francisco State University and University of California, USA

Reviewed by:
Ezequiel Morsella, San Francisco State University and University of California, USA
Bernhard Hommel, Leiden University, Netherlands

****Correspondence:***
Theofanis I. Panagiotaropoulos, Department of Physiology of Cognitive Processes, Max-Planck-Institute for Biological Cybernetics, Spemanstrasse 38, 72076 Tübingen, Germany
e-mail: theofanis.panagiotaropoulos@tuebingen.mpg.de

Accumulating evidence indicates that control mechanisms are not tightly bound to conscious perception since both conscious and unconscious information can trigger control processes, probably through the activation of higher-order association areas like the prefrontal cortex. Studying the modulation of control-related prefrontal signals in a microscopic, neuronal level during conscious and unconscious neuronal processing, and under control-free conditions could provide an elementary understanding of these interactions. Here we performed extracellular electrophysiological recordings in the macaque lateral prefrontal cortex (LPFC) during monocular physical alternation (PA) and binocular flash suppression (BFS) and studied the local scale relationship between beta (15–30 Hz) oscillations, a rhythmic signal believed to reflect the current sensory, motor, or cognitive state (status-quo), and conscious or unconscious neuronal processing. First, we show that beta oscillations are observed in the LPFC during resting state. Both PA and BFS had a strong impact on the power of this spontaneous rhythm with the modulation pattern of beta power being identical across these two conditions. Specifically, both perceptual dominance and suppression of local neuronal populations in BFS were accompanied by a transient beta desynchronization followed by beta activity rebound, a pattern also observed when perception occurred without any underlying visual competition in PA. These results indicate that under control-free conditions, at least one rhythmic signal known to reflect control processes in the LPFC (i.e., beta oscillations) is not obstructed by local neuronal, and accordingly perceptual, suppression, thus being independent from temporally co-existing conscious and unconscious local neuronal representations. Future studies could reveal the additive effects of motor or cognitive control demands on prefrontal beta oscillations during conscious and unconscious processing.

Keywords: beta oscillations, control, prefrontal cortex, consciousness

INTRODUCTION

According to a traditionally held view suggesting that control functions are bound to consciousness (Norman and Shallice, 1986), it is reasonable to assume that conscious perception of sensory cues is a prerequisite for their integration into a control function. However, more recently, there is accumulating evidence that control of action is functionally distinct from consciousness since it can be affected by subliminal, unconscious information processing of masked stimuli. Specifically, control functions like response inhibition (van Gaal et al., 2008, 2010), task-set preparation, conflict detection, motivation, and error detection can be initiated by unconscious stimuli (for a thorough review see van Gaal and Lamme, 2012; van Gaal et al., 2012). Although in general, the impact of these subliminal stimuli in control is rather small compared to conscious signals, the observed effects suggest that control processes are not strictly conscious but can be detected across a wide spectrum of conscious and unconscious processing. These observations suggest that control and consciousness are, to a considerable degree, separable functions (Hommel, 2007, 2013; van Gaal et al., 2012) and therefore a similar dissociation should be expected for their respective neuronal correlates.

In this context, it was recently examined whether physiological signals related to control are observed not only when a visual stimulus is consciously perceived but also during its visual masking, a manipulation that renders the stimulus invisible. Indeed, electroencephalography (EEG) signals associated to inhibitory control like the N2 event-related potential (ERP) component were detected for both masked and unmasked stop stimuli, suggesting that the neural mechanism of inhibitory control can be dissociated from consciousness (van Gaal et al., 2010). The source of the N2 ERP component has a frontal origin (van Gaal et al., 2008) which is in accordance with the activation of inferior frontal gyrus during unconscious inhibitory control and other control-related tasks affected by unconscious information as determined by functional magnetic resonance imaging (fMRI) or intracranial EEG

(Berns et al., 1997; Stephan et al., 2002; Lau and Passingham, 2007; van Gaal et al., 2010).

Another electrophysiological signal strongly associated to control functions is oscillatory synchronization in the beta frequency range (∼15–40 Hz). In particular, beta oscillations in the somatosensory, motor, and frontal cortices reflect different aspects of sensory, motor, and cognitive processing and control. Specifically, processing of visual cues as well as different phases of a motor sequence have been shown to exert a strong impact on the power of beta oscillations in the frontal, premotor, motor, and sensory cortex (for a review see Kilavik et al., 2013). The most striking effect is an initial beta desynchronization (i.e., decrease in beta power) following stimulus onset or voluntary motor behavior that is followed by a beta activity rebound during unchanged stimulus input or steady contractions and holding periods (Sanes and Donoghue, 1993; Pfurtscheller et al., 1996; Donoghue et al., 1998; Baker et al., 1999; Gilbertson et al., 2005; Jurkiewicz et al., 2006; O'Leary and Hatsopoulos, 2006; Baker, 2007; Siegel et al., 2009; Engel and Fries, 2010; Puig and Miller, 2012; Kilavik et al., 2013). Although the functional significance of these stereotypical modulations remains largely elusive, the dominance of beta band activity during such "no-change," resting state-like periods led recently to the suggestion that beta oscillations could reflect an active process that supports the maintenance of the current sensory, motor, or cognitive set (Gilbertson et al., 2005; Pogosyan et al., 2009; Swann et al., 2009; Engel and Fries, 2010). Interestingly, this hypothesis is supported by clinical observations showing that the power of beta oscillations is abnormally high in cortical and subcortical structures of patients suffering from Parkinson's disease (PD; Marsden et al., 2001; Brown, 2007; Chen et al., 2007; Hammond et al., 2007). The accompanying disruption of motor function and control observed in PD suggests that pathologically enhanced beta oscillations could mediate reduced flexibility and a pathological maintenance of the current sensory and motor state. These results combined with findings directly involving prefrontal beta activity in cognitive control (Buschman and Miller, 2007, 2009; Buschman et al., 2012) indicate that beta oscillations could be related to both basic and higher-order control processes across sensory, cognitive, and motor domains (Engel and Fries, 2010).

Despite the wealth of information on the role of beta oscillations on control it is currently unknown how beta is affected by conscious or unconscious processing, particularly in cortical areas like the prefrontal cortex which is heavily involved in control. To resolve this issue, we examined the temporal dynamics of beta oscillatory power in the lateral prefrontal cortex (LPFC) during conscious and unconscious stimulus processing using binocular flash suppression (BFS), a paradigm of rivalrous visual stimulation that dissociates conscious perception from purely sensory stimulation, and compared it with the respective dynamics during monocular physical alternation (PA) of the same visual patterns. In a previous study, we demonstrated that local spiking activity in the LPFC correlates with conscious and unconscious processing (Panagiotaropoulos et al., 2012). That is, neuronal discharges increase when a preferred stimulus is consciously perceived and decrease when the preferred stimulus is perceptually suppressed. Here, we examined in detail the modulation of beta oscillations in these prefrontal sites where locally recorded spiking activity reflects conscious or unconscious processing.

Our results show that the power modulation of beta oscillations under control-free conditions follows the same temporal dynamics during monocular, purely sensory stimulus transitions (i.e., without any underlying stimulus competition) and perceptual transitions involving rivalry that result in the suppression of a competing stimulus. Therefore, the temporal dynamics of prefrontal beta oscillatory power following perceptual transitions appear not to be influenced by the presence of a competing but perceptually suppressed stimulus. Most interestingly, in prefrontal sites where spiking activity followed the perceptual dominance or suppression of a preferred stimulus, beta power was modulated in a non-specific manner regardless of dominance or suppression.

These findings indicate that the stimulus-induced modulation of beta oscillatory power in the LPFC under control-free conditions could reflect a general purpose process, not bound to neuronal—and therefore perceptual—dominance or suppression, but rather indicating transitions in visual perception. We suggest that prefrontal beta oscillations could reflect an elementary process that represents the maintenance or change in the current visual sensory state, independent of stimulus awareness.

MATERIALS AND METHODS

ELECTROPHYSIOLOGICAL DATA COLLECTION AND STIMULUS PRESENTATION

The cranial headpost, scleral eye coil, and recording chambers were implanted in two monkeys under general anesthesia using aseptic and sterile conditions. The recording chambers (18 mm in diameter) were centered stereotaxically above the LPFC (covering mainly the ventrolateral inferior convexity of the LPFC) based on high-resolution MR anatomical images collected in a vertical 4.7 T scanner with a 40-cm-diameter bore (Biospec 47/40c; Bruker Medical, Ettlingen, Germany).

We used custom-made tetrodes made from Nichrome wire and electroplated with gold with impedances below 1 MΩ. Local field potential (LFP) signals were recorded by analog band pass filtering of the raw voltage signal (high-pass at 1 Hz and low-pass at 475 Hz) and digitized at 2 kHz (12 bits). Multi-unit spiking activity (MUA) was defined as the events detected in the high-pass analog filtered signal (0.6–6 kHz) that exceeded a predefined threshold (typically, 25 μV) on any tetrode channel. The 0.6–6 kHz recorded signal was sampled at 32 kHz and digitized at 32 kHz (12 bits). The recorded signals were stored using the Cheetah data acquisition system (Neuralynx, Tucson, AZ, USA). Eye movements were monitored online and stored for offline analysis using the QNX-based acquisition system (QNX Software Systems Ltd.) and Neuralynx. Visual stimuli were displayed using a dedicated graphics workstation (TDZ 2000; Intergraph Systems, Huntsville, AL, USA) with a resolution of 1280 × 1024 and a 60 Hz refresh rate, running an OpenGL-based stimulation program. All procedures were approved by the local authorities (Regierungspräsidium Tübingen, Tübingen, Germany) and were in full compliance with the guidelines of the European Community (EUVD 86/609/EEC) for the care and use of laboratory animals.

BEHAVIORAL TASK AND LFP ANALYSIS

We performed extracellular electrophysiological recordings in the LPFC of 2 macaque monkeys during (a) monocular PA and (b) BFS, a well-controlled version of rivalrous visual stimulation that allowed us to induce robust perceptual dominance and suppression for a duration of 1000 ms. Although the task used in this study had no behavioral conditions in which control was explicitly examined it nevertheless allowed us to observe the local cortical interactions between distinct neurophysiological signals related to control and consciousness, during conditions that elicited subjective perceptual dominance and suppression. Specifically, in a previous study we identified LPFC sites where the summed neuronal discharges and gamma oscillations followed the perceptual dominance or suppression of a preferred stimulus (Panagiotaropoulos et al., 2012). Here we reexamined the temporal modulation of LFPs from the same recording sites to determine the influence of conscious perception on oscillatory activity with a special focus on beta frequency range (15–30 Hz), the frequency band that is involved in the maintenance or disruption of sensory or motor status quo (Engel and Fries, 2010) and cognitive control (Buschman et al., 2012).

Before the beginning of each recorded data set, a battery of visual stimuli was presented, and, based on the MUA response, a preferred stimulus that could drive local neuronal activity better was contrasted to a non-preferred stimulus that induced less robust responses. Visual stimuli were foveally presented with a typical size of 2–3°. In both BFS and PA trials, a fixation spot (size, 0.2°; fixation window, ±1°) was presented for 300 ms (t = 0–300 ms), followed by the same visual pattern to one eye (t = 301–1300 ms). In BFS trials (**Figures 1C,D** "BFS"), 1 s after stimulus onset, a disparate visual pattern was suddenly flashed to the corresponding part of the contralateral eye. The flashed stimulus remained on for 1000 ms (t = 1301–2300 ms), robustly suppressing the perception of the contralateraly presented visual pattern, which was still physically present. In the PA trials (**Figures 1A,B** "PA"), the same visual patterns were physically alternating between the two eyes, resulting in a visual percept identical to the perceptual condition but this time without any underlying visual competition. At the end of each trial and after a brief, stimulus free, fixation period (100–300 ms), a drop of juice was used as a reward for maintaining fixation. The efficiency of BFS to induce perceptual suppression, was tested in a different monkey that was trained to report PA and BFS by pulling levers for the two different stimuli used in our recordings (Panagiotaropoulos et al., 2012). PA and BFS conditions were pseudorandomized and allowed us to record from perceptually dominant and suppressed populations by changing the order of presentation of the two disparate stimuli (**Figure 1**). Binocular stimulation was achieved through the use of a stereoscope.

The baseline preference of MUA activity was determined in the control, PA trials, where perception of a preferred or a non-preferred pattern occurred without any underlying stimulus competition (**Figures 1A,B**). In BFS, a monocularly presented preferred or non-preferred stimulus was perceptually suppressed by the presentation ("flash") of a disparate visual pattern in the contralateral eye for at least 1000 milliseconds (Wolfe, 1984;

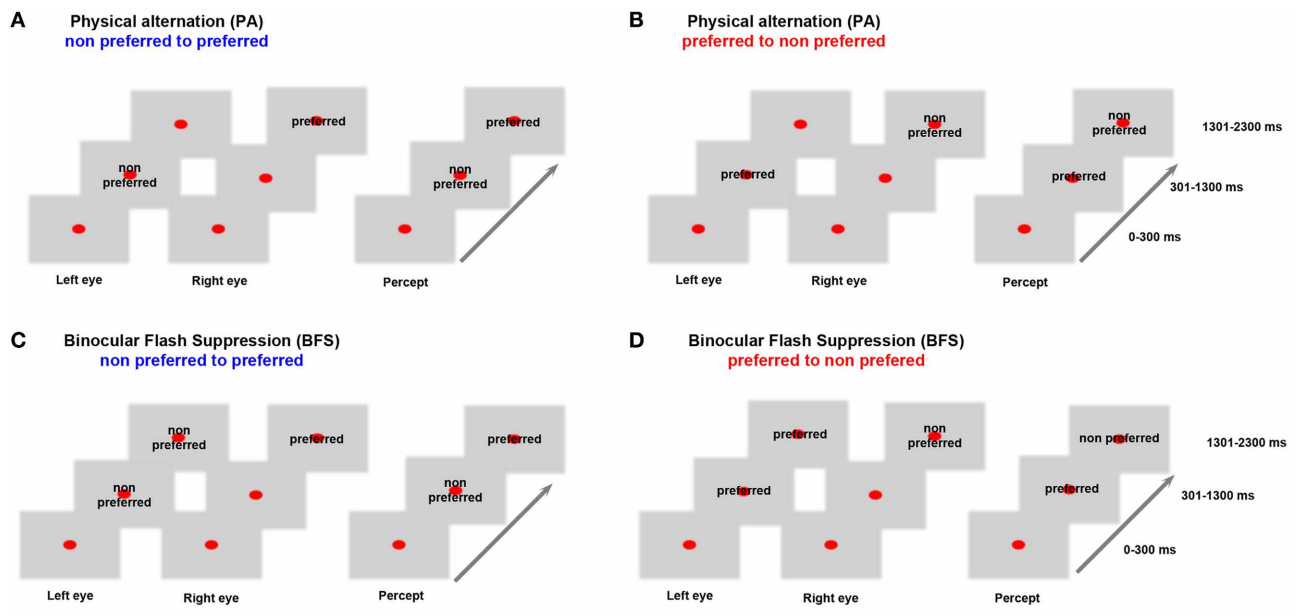

FIGURE 1 | Behavioral task. In **(A)** monocular stimulation with a non-preferred pattern is followed by stimulation of the contralateral eye with a preferred visual stimulus. In **(B)** the order of visual stimulation is reversed. These PA conditions allowed us to study neurophysiological responses during purely sensory stimulation without any underlying competition. In **(C)** the non-preferred stimulus is suppressed by the presentation of a preferred visual pattern while in **(D)** the preferred pattern is suppressed due to a flash of the non-preferred. These BFS conditions that introduced visual competition allowed recordings during perceptual dominance and suppression of a local population. Therefore, BFS allowed us to study conscious and unconscious processing of a visual stimulus. Stimulus preference was determined by comparing the local population discharge response to the two stimuli used in **(A)** and **(B)** between t = 1301–2300 ms (see also Panagiotaropoulos et al., 2012).

Panagiotaropoulos et al., 2012). By changing the order of visual stimulus presentation in half of the trials, it was possible to discern between the perceptual suppression of a preferred and a non-preferred visual stimulus (**Figures 1C,D**). A contrastive analysis that compared neuronal activity during BFS (where visual rivalry occurred) with the respective activity during PA (thus without any underlying competition) was used to distill the consciousness-related neuronal correlates (Panagiotaropoulos et al., 2012).

In this study we analyzed LFP signals from sites where we recorded spontaneous, resting-state, activity as well as from local prefrontal sites that exhibited significant stimulus preference (Panagiotaropoulos et al., 2012). We binned the long spontaneous activity recordings (lasting approximately 10–30 min) in windows of 1000 ms duration. The PSD of the raw LFP signals for long, spontaneous activity recordings (**Figure 2**), was estimated using the multitaper method (Thomson, 1982) for narrow frequency bins of 1 Hz and for each 1000 ms window. This method uses linear or non-linear combinations of modified periodograms to estimate the PSD. These periodograms are computed using a sequence of orthogonal tapers (windows in the frequency domain) specified from the discrete prolate spheroidal sequences. For each dataset we averaged the spectra across all time windows. Time frequency analysis during PA and BFS (**Figure 5**) was performed by computing a spectrogram of the power spectral density in each trial using overlapping (94%) 256 ms windows and then averaged across all trials for the same condition. In **Figure 6** a Hilbert transform of the beta band limited signal in each trial was used to extract the band-limited LFP envelope between 15 and 30 Hz. The mean envelope was averaged across trials and across conditions for each dataset. Digital filters were constructed via the Parks–McClellan optimal equiripple FIR filter design to obtain the beta (15–30 Hz) band-limited LFP signal. The LFP data presented here are from the same sites where local spiking activity was previously found to exhibit significant selectivity during PA (Panagiotaropoulos et al., 2012).

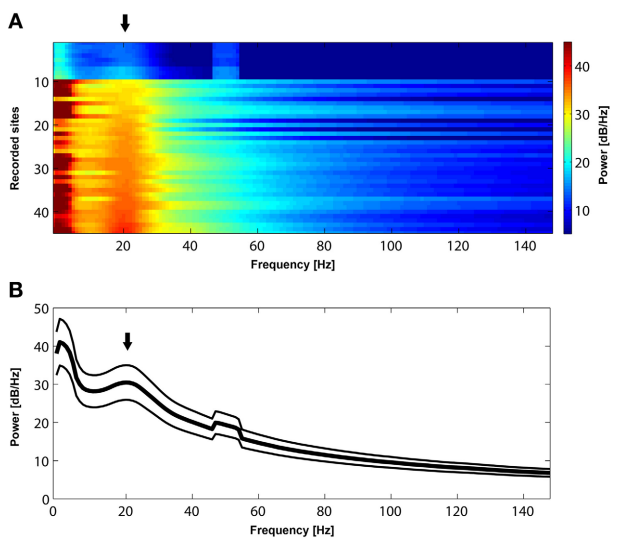

FIGURE 2 | (A) Power spectrum of resting-state activity in 45 recorded sites sorted according to the power magnitude at 22 Hz. All sites exhibit a prominent peak (black arrow) in the beta frequency range (approximately between 15 and 30 Hz). **(B)**. Mean power spectrum ± s.e.m during resting state activity across the 45 recorded sites presented in **(A)**. Note a bump (black arrow) in the mean power spectrum in the beta range. The peak in 50 Hz is due to power line noise.

RESULTS

Initially, we established that beta oscillations reflect a dominant oscillatory rhythm in the LPFC during resting state. We recorded long (approximately 10–30 min) periods of spontaneous, resting state activity during which the awake macaques could keep their eyes open or closed. As depicted in **Figure 2**, the mean power spectrum of spontaneous oscillatory activity in all ($n = 45$) LPFC recorded sites is characterized by a prominent peak in the beta frequency range, between 15 and 30 Hz. Since such peaks or bumps in the LFP power spectrum are indicative of dominant, frequency-specific, intrinsic rhythmic activity, these results show that beta oscillations represent a dominant resting-state rhythm in the LPFC.

We analyzed how the power of this spontaneously occurring prefrontal rhythm is modulated during purely sensory visual stimulation in PA, in recorded sites where spiking activity showed a significant preference for one of the two stimuli used in each dataset. In our previous study (Panagiotaropoulos et al., 2012) we found that despite significant spiking selectivity the power of low frequency oscillations averaged over 1 s of visual stimulation in the same local sites was not selective, showing no stimulus preference. However, when we reexamined our LFP data we observed that high amplitude low frequency oscillations detected in the broadband LFP signal were consistently modulated across trials, exhibiting signs of desynchronization (i.e., reduction in power) and rebound activity during the presence of visual stimulation (example trials from a typical LPFC recording site are depicted in **Figure 3**). We performed a Hilbert transform in the recorded LFP signal for each trial and extracted the band-limited oscillations in the beta frequency range (15–30Hz). For all conditions we observed periods of abrupt desynchronization following both initial visual stimulation ($t = 301$–1300 ms) or a change in the visual input ($t = 1301$–2300 ms) that were replaced by a rebound of oscillatory activity (**Figure 4**). We captured a qualitative representation of beta modulation across conditions by computing the time-frequency spectrogram for each trial and then averaged across trials for each recording site and finally across sites for each condition. The averaged spectrograms show that beta oscillations were dynamically modulated during visual stimulation regardless of the co-existing stimulus preference exhibited by the averaged spiking activity (**Figure 5**). Specifically, in PA trials where visual stimulation started with the presentation of a non-preferred (by the local spiking activity) pattern that was followed by a preferred one (**Figure 5A**), beta oscillations were desynchronized immediately after the initiation of fixation and then a rebound of synchronous activity was observed until the first, non-preferred, stimulus was presented ($t = 0$–300 ms). The presentation of the non-preferred stimulus resulted in a new decrease in beta power until ∼400 ms following the onset of visual stimulation where a rebound in the power of beta oscillatory activity appeared ($t = 301$–1300 ms). Following a monocular stimulus alternation (i.e., removal of the first stimulus and stimulation

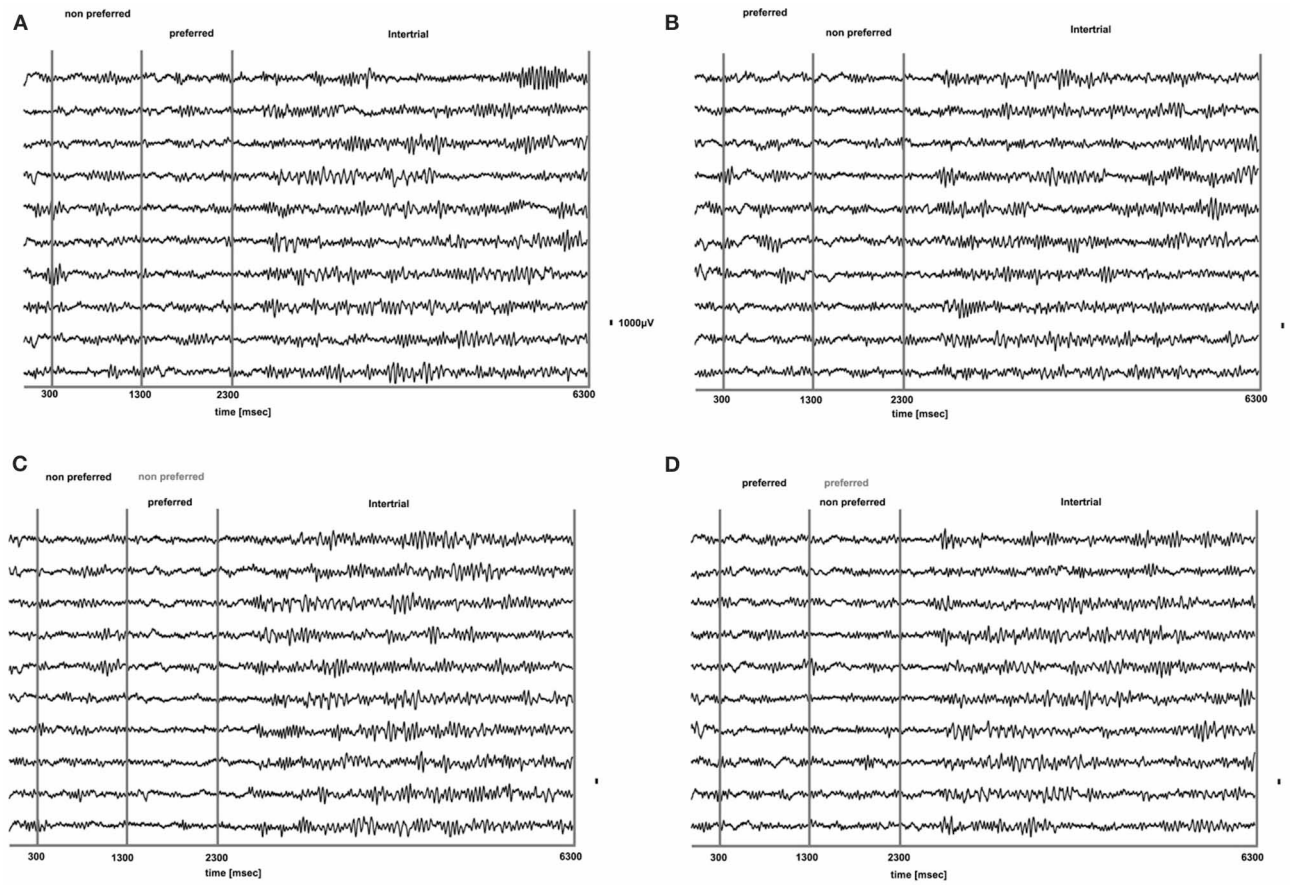

FIGURE 3 | Raw LFP traces (1–475 Hz) during PA (A,B) and BFS (C,D) for 10 trials from a typical prefrontal recording site. In **(A)**, a non-preferred stimulus is presented in one eye and after 1 s is removed and a disparate pattern is presented in the contralateral eye. Using as a criterion the discharge response of the locally recorded population we determined that the second stimulus was the "preferred." In **(B)** the order of visual stimulation is reversed and the preferred stimulus is followed by the presentation of the non-preferred. In **(C,D)** for BFS the order of stimulation is the same as in **(A,B),** respectively. However, in these trials the stimulus presented first is not removed but remains on and is suppressed by the stimulus presented between $t = 1301$–2300 ms (dominant stimulus-black, suppressed stimulus-gray). In both PA and BFS and for all conditions we can observe that the onset or change of visual stimulation results in a remarkable suppression of low frequency-high amplitude LFP components that rebound later when the stimulus remains on. These components are particularly dominant during the inter-trial period ($t = 1301$–2300).

of the contralateral eye with a disparate pattern), beta oscillations were modulated again ($t = 1301$–2300 ms). Specifically, the presentation of the preferred (as determined by spiking activity) stimulus in the contralateral eye resulted in a new round of desynchronization followed by beta rebound activity after ∼400 ms. As expected, due to the absence of any obvious selectivity in beta power, the same pattern of beta power modulation was also observed in the PA condition when a non-preferred (by the spiking activity) pattern followed the monocular presentation of a preferred pattern (**Figure 5B**). The initial desynchronization following the first stimulus presentation and monocular switch was followed by a beta power rebound. This result demonstrates that in a local prefrontal level, in sites where spiking activity exhibits stimulus preference, beta oscillations are dynamically modulated regardless of stimulus preference when perception occurs without any underlying visual competition.

However, the PA condition provides no information about the modulation of beta oscillations when local spiking activity reflects conscious perception or perceptual suppression. Therefore, we determined the influence of conscious perception or perceptual suppression in beta power modulation during BFS trials that involved visual competition. As depicted in the averaged time-frequency plot in **Figure 5C**, when a preferred stimulus suppressed the initially presented non preferred visual pattern ($t = 1301$–2300 ms) the power of beta oscillations showed the same modulation pattern (initial desynchronization followed by a beta rebound) as when a preferred stimulus was perceived without competition in PA (**Figure 5A**). Most interestingly, the same desynchronization followed by beta activity rebound was also observed when the local population signaling the preferred stimulus was suppressed by the presence of a non-preferred visual pattern (**Figure 5D**). This result indicates that beta oscillations are visually modulated regardless of the simultaneously recorded local spiking activity that may be dominant or suppressed. Finally, in both PA and BFS trials, the inter-trial period, during which eye movements were free and the animals were allowed to fixate

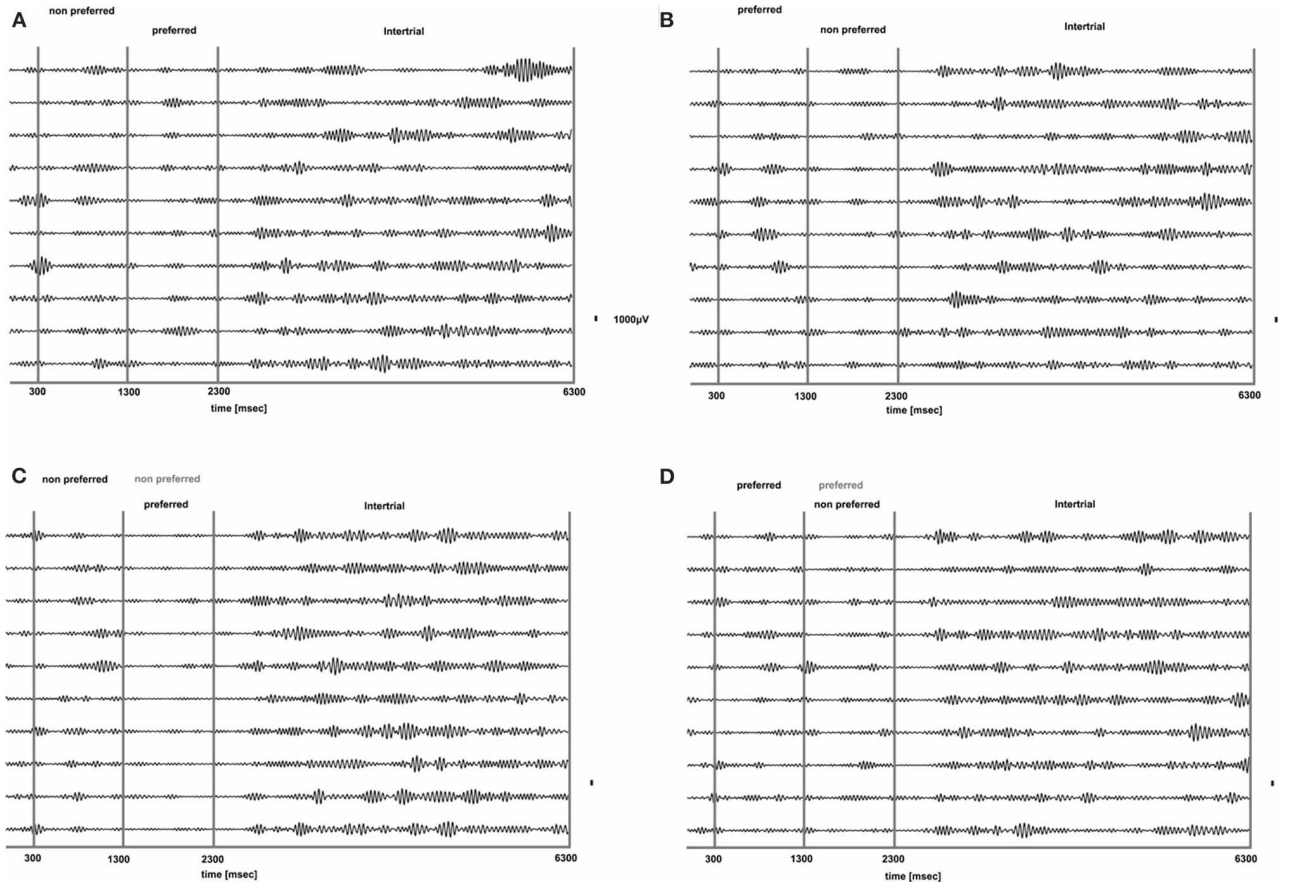

FIGURE 4 | Band-limited LFP signal (15–30 HZ) of the raw LFP signals presented in Figure 3. Beta oscillations are suppressed for all conditions during visual stimulation without any obvious relationship to stimulus preference for both PA (**A** and **B**) and BFS (**C** and **D**). Beta oscillations are particularly prominent during the inter-trial period.

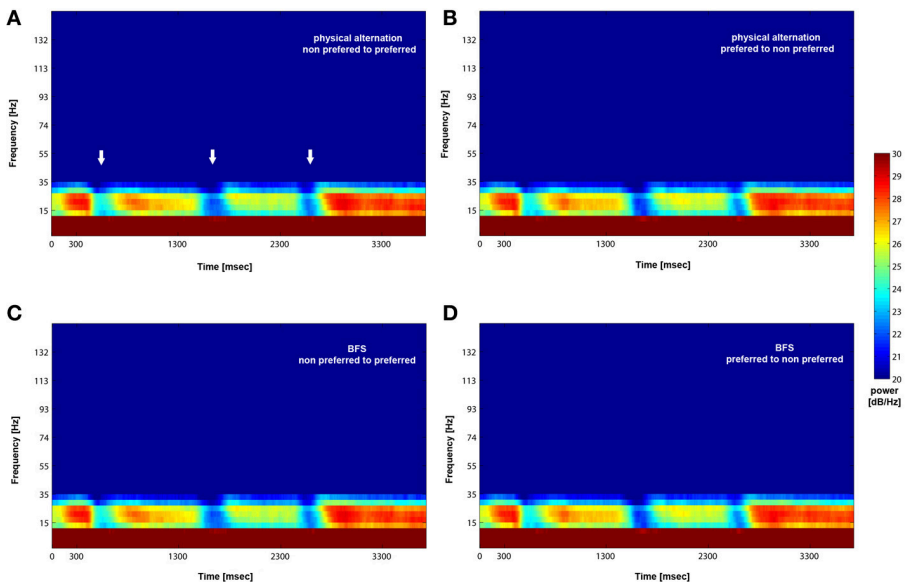

FIGURE 5 | Mean (across trials and recorded sites) time-frequency plot for PA and BFS. Following visual stimulation beta power exhibits desynchronization (white arrows in **A**) followed by a rebound of activity regardless of stimulus preference for both PA (**A** and **B**) and BFS (**C** and **D**). The frequency band is between 15 and 30 Hz.

anywhere or have their eyes closed, resulted in the reestablishment of beta oscillations and high beta power, similar to the activity detected during long, resting-state activity recordings.

We quantified the effects qualitatively described in the time frequency plots by plotting the mean envelope of the beta band (15–30 Hz)-filtered signal in PA and BFS. In **Figure 6A**, visual stimulation without perceptual competition (PA) initially results in beta power reduction followed by a rebound of oscillatory activity regardless of neuronal stimulus preference. Exactly the same pattern can be observed in **Figure 6B** for BFS. In this condition that employs visual rivalry between a preferred and a non-preferred stimulus during $t = 1301$–2300 ms, beta oscillations recorded when the spiking activity of local neuronal populations is suppressed exhibit the same desynchronization and rebound effect that is observed when the same population is dominant. During the inter-trial period the power of beta oscillations is significantly higher compared to the period of visual stimulation.

These results indicate that visual competition (during BFS) has no effect on the modulation pattern of beta oscillations in the LPFC observed during purely sensory stimulation (during PA). Most importantly, based on the absence of any indication of stimulus selectivity in the power of beta oscillations in sites where spiking activity is selective during visual rivalry, we can infer that at least two neurophysiological signals related to consciousness (local spiking activity) and control (beta oscillations) follow discrete modulation patterns in a local prefrontal level. Even when a preferred stimulus becomes suppressed during rivalrous stimulation and the local neuronal populations are not responsive, beta oscillations recorded from the same non-responsive area undergo the same desynchronization and rebound of activity as when the local population becomes perceptually dominant. These results establish a baseline condition for the modulation of beta oscillations during conscious and unconscious processing that could be exploited by future studies in which both conscious perception and control demands are modulated during a task. We show that a control related signal (i.e., beta oscillations) is non-specifically modulated by visual stimulation and, most importantly, this modulation is not influenced by the dominance or suppression of spiking activity during rivalrous visual stimulation. Therefore, beta oscillatory power in the LPFC could reflect a general purpose mechanism that is not related to conscious perception *per se* but rather indicates transitions and stability in visual perception.

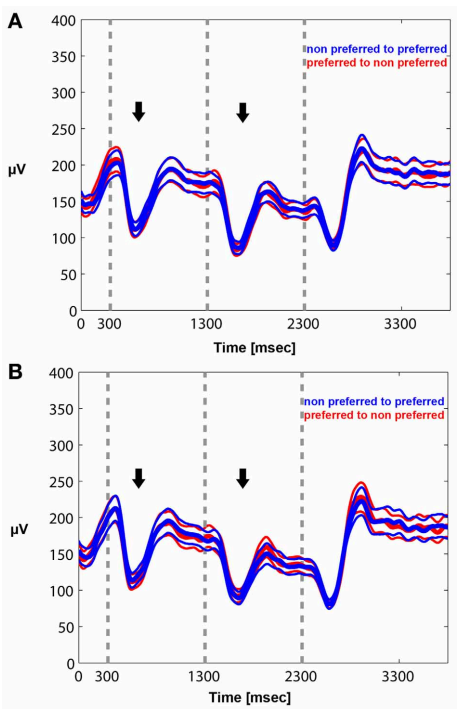

FIGURE 6 | Mean envelope (15–30 Hz) across trials and recorded sites for PA (A) and BFS (B). In PA there is no difference in the modulation of beta power between a switch from a preferred to a non-preferred (red curve) and a switch from a non-preferred to a preferred (blue curve) visual stimulus. Stimulus-induced desynchronization (black arrows) followed by a beta rebound is observed in both cases. The same pattern is observed during BFS **(B)**. Note that in BFS from $t = 1301$–2300 there are no differences in beta power when the recorded neuronal population as well as the preferred pattern is dominant (blue) or suppressed (red).

DISCUSSION

CONTROL AND CONSCIOUSNESS IN THE PFC

Executive or cognitive control functions define a large set of higher-order mental operations that organize, initiate, monitor, and act on goal-directed behavior in a flexible manner. Historically, the dependence of these executive operations on perceptual awareness generated a great deal of philosophical debate since resolving the details of this intricate relationship could provide significant insights into the functional role of consciousness and constrain theoretical concepts of free will (Mayr, 2004; Hommel, 2007). More recently, experimental investigations revealed that—contrary to common belief—both elementary and higher order, cognitive, control processes have access to subliminal, unconscious information (Eimer and Schlaghecken, 1998; Eimer, 1999; Lau and Passingham, 2007; van Gaal et al., 2008, 2010, 2012).

It is possible to eavesdrop on some aspects of the relationship between consciousness and control by studying the local interactions of the respective neuronal correlates in the neocortex. The current body of evidence suggests that part of the neuronal correlates of both conscious perception (Lumer et al., 1998; Sterzer and Kleinschmidt, 2007; Gaillard et al., 2009; Dehaene and Changeux, 2011; Libedinsky and Livingstone, 2011; Panagiotaropoulos et al., 2012) and cognitive control (Luria, 1969; Goldman-Rakic et al., 1992; Miller, 1999, 2000; White and Wise, 1999; Miller and Cohen, 2001; Wallis et al., 2001; Tanji and Hoshi, 2008; Swann et al., 2009; Buschman et al., 2012) are co-localized in the prefrontal cortex (PFC). However, although these two parallel streams of research led to significant insights into the neuronal correlates of conscious perception and executive functions, the progress was, until recently, to a large extent independent and as a consequence little is known about the interactions of these two neuronal representations in the PFC, at least in the fine spatiotemporal scale offered by extracellular electrophysiological recordings. For example, an elementary

but not yet addressed issue is to what extent control-related neurophysiological signals in the PFC, like beta oscillations, are influenced by the perceptual dominance or suppression of a preferred stimulus during rivalrous stimulation, under control-free conditions. Such information could reveal the baseline impact of conscious processing and perceptual suppression on the state of intrinsic signals related to control, before control is learned or applied.

BETA OSCILLATIONS DURING CONSCIOUS AND UNCONSCIOUS PROCESSING IN THE LPFC

In this study we determined the extent to which the visual, sensory-induced, modulation of beta (15–30 Hz) oscillations depends on conscious neuronal processing in a local prefrontal cortical level. Our task didn't involve any motor or cognitive control demands and therefore our results are not informative about the role of beta oscillations on cognitive or motor control during conscious or unconscious processing. However, we were able to discern the effect of conscious and unconscious processing as a result of visual competition on beta oscillations.

The results presented in this study reveal that intrinsically generated beta oscillations in the LPFC are non-specifically modulated by visual sensory input in local sites where spiking activity exhibits preference for stimulus features. The pattern of purely sensory-induced beta power modulation is characterized by an initial stimulus-induced desynchronization followed by a beta rebound, as shown in the PA condition. This desynchronization-rebound pattern has been reported in the past in the context of other electrophysiological studies, as a result of visual input in the prefrontal cortex (Siegel et al., 2009; Puig and Miller, 2012). However, PA or purely sensory input is not adequate to dissociate the effect of conscious visual perception from sensory stimulation. This was achieved during BFS which allowed us to elicit visual competition between two stimuli and study the modulation of beta oscillations in local prefrontal sites during periods that a preferred stimulus was perceptually dominant (thus consciously perceived) or suppressed (i.e., without access to awareness). Our results show that local processing of consciously perceived or perceptually suppressed information, as determined by the dominance or suppression of spiking activity in the BFS condition, is not a limiting factor for the modulation of beta oscillations by visual input. In particular, beta oscillatory activity recorded from sites where spiking activity becomes suppressed exhibits the same desynchronization-rebound pattern recorded from the same sites when spiking activity is dominant.

The absence of any stimulus preference in the power of beta (15–30 Hz) oscillations during monocular PA, in sites where local spiking activity is selective for one of the two stimuli used, is not surprising. It is known that even high-frequency, gamma, LFP's which are more likely to have a similar tuning to spikes than beta oscillations don't exhibit the same robust tuning as spiking activity in the visual cortex (Frien et al., 2000; Henrie and Shapley, 2005; Liu and Newsome, 2006; Berens et al., 2008; Panagiotaropoulos et al., 2012). Poor feature selectivity has been ascribed to different factors, some of them being that gamma activity is generated by neuronal ensembles larger than the local neuronal populations contributing to multi-unit activity recorded from the same electrode. Particularly for the beta LFP band, the impressive absence of any stimulus selectivity has been suggested to reflect the dominant influence of diffuse neuromodulatory input (Belitski et al., 2008; Magri et al., 2012). It is therefore likely that the non-specific modulation of beta oscillations during PA reflects a common source of input in the LPFC. Most importantly, our findings could suggest that this input is not affected by visual competition since the magnitude of non-specific modulation is similar during both PA and BFS. We can therefore conclude that under baseline, control-free conditions, the modulation of beta oscillations is independent of conscious or unconscious stimulus processing in the LPFC.

IMPLICATIONS FOR CONTROL FUNCTIONS AND CONSCIOUSNESS

Although in this study we didn't use a control task our findings are of importance for future studies that will explicitly manipulate both consciousness and control functions. We suggest that our results point to a functional independence between the sensory modulation of oscillatory signals that are employed by control processes (beta oscillations) and conscious processing in the prefrontal cortex under baseline, control-free conditions. Furthermore, it is likely that beta oscillations could reflect an intrinsic mechanism of elementary control due to the pattern of modulation observed as a result of sensory input. Apart from higher-order processes, control functions can apparently engulf more basic functions that satisfy the criterion of disturbance compensation (Hommel, 2007). Our results suggest that visual sensory input represents a disturbance to the cortical network interactions responsible for generating the intrinsic prefrontal beta rhythm. This sensory disturbance results in the initial desynchronization of beta oscillations as reflected in the beta power reduction. During that period the network interactions responsible for beta become destabilized and result in a reduction/desynchronization of beta power but soon control over this disturbance is achieved by the underlying network as reflected in the rebound of beta activity ∼400 ms following a change in visual input. The similarity of this effect for PA and BFS, perceptual dominance and suppression, points to an independence of this elementary mechanism from the coexisting neuronal networks underlying conscious perception.

Our findings are also in line with previous studies that detected physiological signals reflecting control processes during both conscious and unconscious information processing, especially in the prefrontal cortex which appears to have a crucial role in control functions (Berns et al., 1997; Stephan et al., 2002; Lau and Passingham, 2007; van Gaal et al., 2008, 2010). The extracellular electrophysiological recordings in the LPFC used in our study offered the additional advantage of high spatial resolution compared to fMRI or EEG recordings. The limited spatial resolution of these methods prevents the detection of local sites involved in the conscious processing of a particular visual stimulus. However, this can be achieved using local extracellular electrophysiological recordings (Logothetis and Schall, 1989; Leopold and Logothetis, 1996; Sheinberg and Logothetis, 1997; Kreiman et al., 2002;

Gail et al., 2004; Keliris et al., 2010; Panagiotaropoulos et al., 2012). For the first time, we were able to record control-related signals (i.e., beta oscillations) from prefrontal sites where spiking activity reflected perceptual dominance or suppression during control-free conditions and our findings may support the conclusions of physiological studies suggesting that control and consciousness are probably independent, but also overlapping, functions. Future studies that combine intracortical recordings of electrophysiological signals during conscious perception or perceptual suppression and control within the same task could further elucidate the relationship between these two higher-order cognitive functions.

AUTHOR CONTRIBUTIONS

Conceived and designed the experiments: Theofanis I. Panagiotaropoulos. Performed the experiments: Theofanis I. Panagiotaropoulos, Vishal Kapoor. Analyzed the data: Theofanis I. Panagiotaropoulos. Contributed reagents/materials/analysis tools: Theofanis I. Panagiotaropoulos, Nikos K. Logothetis. Wrote the paper: Theofanis I. Panagiotaropoulos.

ACKNOWLEDGEMENTS

This work was supported by the Max Planck Society. We thank Joachim Werner and Axel Oeltermann for excellent technical help.

REFERENCES

Baker, S. N., Kilner, J. M., Pinches, E. M., and Lemon, R. N. (1999). The role of synchrony and oscillations in the motor output. *Exp. Brain Res.* 128, 109–117. doi: 10.1007/s002210050825

Baker, S. N. (2007). Oscillatory interactions between sensorimotor cortex and the periphery. *Curr. Opin. Neurobiol.* 17, 649–655. doi: 10.1016/j.conb.2008.01.007

Berens, P. Keliris, G. A., Ecker, A. S., Logothetis, N. K., Tolias, A. S. (2008). Comparing the feature selectivity of the gamma-band of the local field potential and the underlying spiking activity in primate visual cortex. *Front. Syst. Neurosci.* 2:2. doi: 10.3389/neuro.06.002.2008

Belitski, A., Gretton, A., Magri, A., Murayama, Y., Montemurro, M. A., Logothetis, N. K., et al. (2008). Low-frequency local field potentials and spikes in primary visual cortex convey independent visual information. *J. Neurosci.* 28, 5696–5709. doi: 10.1523/JNEUROSCI.0009-08.2008

Berns, G. S., Cohen, J. D., and Mintun, M. A. (1997). Brain regions responsive to novelty in the absence of awareness. *Science* 276, 1272–1275. doi: 10.1126/science.276.5316.1272

Brown, P. (2007). Abnormal oscillatory synchronization in the motor system leads to impaired movement. *Curr. Opin. Neurobiol.* 17, 656–664. doi: 10.1016/j.conb.2007.12.001

Buschman, T. J., and Miller, E. K. (2007). Top-down versus bottom-up control of attention in the prefrontal and posterior parietal cortices. *Science* 315, 1860–1862. doi: 10.1126/science.1138071

Buschman, T. J., and Miller, E. K. (2009). Serial, covert shifts of attention during visual search are reflected by the frontal eye fields and correlated with population oscillations. *Neuron* 63, 386–396. doi: 10.1016/j.neuron.2009.06.020

Buschman, T. J., Denovellis, E. L., Diogo, C., Bullock, D., and Miller, E. K. (2012). Synchronous oscillatory neural ensembles for rules in the prefrontal cortex. *Neuron* 76, 838–846. doi: 10.1016/j.neuron.2012.09.029

Chen, C. C., Litvak, V., Gilbertson, T., Kühn, A., Lu, C. S., Lee, S. T., et al. (2007). Excessive synchronization of basal ganglia neurons at 20 Hz slows movement in Parkinson's disease. *Exp. Neurol.* 205, 214–221. doi: 10.1016/j.expneurol.2007.01.027

Dehaene, S., and Changeux, J. P. (2011). Experimental and theoretical approaches to conscious processing. *Neuron* 70, 200–227. doi: 10.1016/j.neuron.2011.03.018

Donoghue, J. P., Sanes, J. N., Hatsopoulos, N. G., and Gaál, G. (1998). Neural discharge and local field potential oscillations in primate motor cortex during voluntary movements. *J. Neurophysiol.* 79, 159–173.

Eimer, M. (1999). Facilitatory and inhibitory effects of masked prime stimuli on motor activation and behavioural performance. *Acta Psychol. (Amst.)* 101, 293–313. doi: 10.1016/S0001-6918(99)00009-8

Eimer, M., and Schlaghecken, F. (1998). Effects of masked stimuli on motor activation: behavioral and electrophysiological evidence. *J. Exp. Psychol. Hum. Percept. Perform.* 24, 1737–1747. doi: 10.1037/0096-1523.24.6.1737

Engel, A. K., and Fries, P. (2010). Beta-band oscillations–signalling the status quo? *Curr. Opin. Neurobiol.* 20, 156–165. doi: 10.1016/j.conb.2010.02.015

Frien, A., Eckhorn, R., Bauer, R., Woelbern, T., and Gabriel, A. (2000). Fast oscillations display sharper orientation tuning than slower components of the same recordings in striate cortex of the awake monkey. *Eur. J. Neurosci.* 12, 1453–1465. doi: 10.1046/j.1460-9568.2000.00025.x

Gail, A., Brinksmeyer, H. J., and Eckhorn, R. (2004). Perception-related modulations of local field potential power and coherence in primary visual cortex of awake monkey during binocular rivalry. *Cereb. Cortex* 14, 300–313. doi: 10.1093/cercor/bhg129

Gaillard, R., Dehaene, S., Adam, C., Clémenceau, S., Hasboun, D., Baulac, M., et al. (2009). Converging intracranial markers of conscious access. *PLoS Biol.* 7:e1000061. doi: 10.1371/journal.pbio.1000061

Gilbertson, T., Lalo, E., Doyle, L., Di Lazzaro, V., Cioni, B., and Brown, P. (2005). Existing motor state is favored at the expense of new movement during 13-35 Hz oscillatory synchrony in the human corticospinal system. *J. Neurosci.* 25, 7771–7779. doi: 10.1523/JNEUROSCI.1762-05.2005

Goldman-Rakic, P. S., Bates, J. F., and Chafee, M. V. (1992). The prefrontal cortex and internally generated motor acts. *Curr. Opin. Neurobiol.* 2, 830–835. doi: 10.1016/0959-4388(92)90141-7

Hammond, C., Bergman, H., and Brown, P. (2007). Pathological synchronization in Parkinson's disease: networks, models and treatments. *Trends Neurosci.* 30, 357–364. doi: 10.1016/j.tins.2007.05.004

Henrie, J. A., and Shapley, R. (2005). LFP power spectra in V1 cortex: the graded effect of stimulus contrast. *J. Neurophysiol.* 94, 479–490. doi: 10.1152/jn.00919.2004

Hommel, B. (2007). Consciousness and control. Not identical twins. *J. Conscious. Stud.* 14, 155–176.

Hommel, B. (2013). Dancing in the dark: no role for consciousness in action control. *Front. Psychol.* 4:380. doi: 10.3389/fpsyg.2013.00380

Jurkiewicz, M. T., Gaetz, W. C., Bostan, A. C., and Cheyne, D. (2006). Post- movement beta rebound is generated in motor cortex: evidence from neuromagnetic recordings. *Neuroimage* 32, 1281–1289. doi: 10.1016/j.neuroimage.2006.06.005

Keliris, G. A., Logothetis, N. K., and Tolias, A. S. (2010). The role of the primary visual cortex in perceptual suppression of salient visual stimuli. *J. Neurosci.* 30, 12353–12365. doi: 10.1523/JNEUROSCI.0677-10.2010

Kilavik, B. E., Zaepffel, M., Brovelli, A., Mackay, W. A., and Riehle, A. (2013). The ups and downs of beta oscillations in sensorimotor cortex. *Exp. Neurol.* 245, 15–26. doi: 10.1016/j.expneurol.2012.09.014

Kreiman, G., Fried, I., and Koch, C. (2002). Single-neuron correlates of subjective vision in the human medial temporal lobe. *Proc. Natl. Acad. Sci. U.S.A.* 99, 8378–8383. doi: 10.1073/pnas.072194099

Lau, H. C., and Passingham, R. E. (2007). Unconscious activation of the cognitive control system in the human prefrontal cortex. *J. Neurosci.* 27, 5805–5811. doi: 10.1523/JNEUROSCI.4335-06.2007

Leopold, D. A., and Logothetis, N. K. (1996). Activity changes in early visual cortex reflect monkeys' percepts during binocular rivalry. *Nature* 379, 549–553. doi: 10.1038/379549a0

Libedinsky, C., and Livingstone, M. (2011). Role of prefrontal cortex in conscious visual perception. *J. Neurosci.* 31, 64–69. doi: 10.1523/JNEUROSCI.3620-10.2011

Liu, J., and Newsome, W. T. (2006). Local field potential in cortical area MT: stimulus tuning and behavioral correlations. *J. Neurosci.* 26, 7779–7790. doi: 10.1523/JNEUROSCI.5052-05.2006

Logothetis, N. K., and Schall, J. D. (1989). Neuronal correlates of subjective visual perception. *Science* 245, 761–763. doi: 10.1126/science.2772635

Lumer, E. D., Friston, K. J., and Rees, G. (1998). Neural correlates of perceptual rivalry in the human brain. *Science* 280, 1930–1934. doi: 10.1126/science.280.5371.1930

Luria, A. R. (1969). "Frontal lobe syndromes," in *Handbook of Clinical Neurology,* Vol. 2, eds P. J. Vinken and G. W. Bruyn (New York, NY: Elsevier), 725–757.

Magri, C., Schridde, U., Murayama, Y., Panzeri, S., and Logothetis, N. K. (2012). The amplitude and timing of the BOLD signal reflects the relationship between local field potential power at different frequencies. *J. Neurosci.* 32, 1395–1407. doi: 10.1523/JNEUROSCI.3985-11.2012

Marsden, J. F., Limousin-Dowsey, J. F., Ashby, P., Pollak, P., and Brown, P. (2001). Subthalamic nucleus, sensorimotor cortex and muscle interrelationships in Parkinson's disease. *Brain* 124, 378–388. doi: 10.1093/brain/124.2.378

Mayr, U. (2004). Conflict, consciousness, and control. *Trends Cogn. Sci.* 8, 145–148. doi: 10.1016/j.tics.2004.02.006

Miller, E. K. (1999). The prefrontal cortex: complex neural properties for complex behavior. *Neuron* 22, 15–17. doi: 10.1016/S0896-6273(00)80673-X

Miller, E. K., and Cohen, J. D. (2001). An integrative theory of prefrontal cortex function. *Annu. Rev. Neurosci.* 24, 167–202. doi: 10.1146/annurev.neuro.24.1.167

Miller, E. K. (2000). The prefrontal cortex and cognitive control. *Nat. Rev. Neurosci.* 1, 59–65. doi: 10.1038/35036228

Norman, D. A., and Shallice, T. (1986). "Attention to action: willed and automatic control of behavior," in *Consciousness and Self-Regulation,* Vol. 4, eds R. J. Davidson, G. E. Schwartz and D. Shapiro (New York, NY: Plenum Press), 1–14.

O'Leary, J. G., and Hatsopoulos, N. G. (2006). Early visuomotor representations revealed from evoked local field potentials in motor and premotor cortical areas. *J. Neurophysiol.* 96, 1492–1506. doi: 10.1152/jn.00106.2006

Panagiotaropoulos, T. I., Deco, G., Kapoor, V., and Logothetis, N. K. (2012). Neuronal discharges and gamma oscillations explicitly reflect visual consciousness in the lateral prefrontal cortex. *Neuron* 74, 924–935. doi: 10.1016/j.neuron.2012.04.013

Pfurtscheller, G., Stancák, A. Jr, and Neuper, C. (1996). Post-movement beta synchronization. A correlate of an idling motor area? *Electroencephalogr. Clin. Neurophysiol.* 98, 281–293. doi: 10.1016/0013-4694(95)00258-8

Pogosyan, A., Gaynor, L. D., Eusebio, A., and Brown, P. (2009). Boosting cortical activity at beta-band frequencies slows movement in humans *Curr. Biol.* 19, 1637–1641. doi: 10.1016/j.cub.2009.07.074

Puig, M. V., and Miller, E. K. (2012). The role of prefrontal dopamine D1 receptors in the neural mechanisms of associative learning. *Neuron* 74, 874–886. doi: 10.1016/j.neuron.2012.04.018

Sanes, J. N., and Donoghue, J. P. (1993). Oscillations in local field potentials of the primate motor cortex during voluntary movement. *Proc. Natl. Acad. Sci. U.S.A.* 90, 4470–4474. doi: 10.1073/pnas.90.10.4470

Sheinberg, D. L., and Logothetis, N. K. (1997). The role of temporal cortical areas in perceptual organization. *Proc. Natl. Acad. Sci. U.S.A.* 94, 3408–3413. doi: 10.1073/pnas.94.7.3408

Siegel, M., Warden, M. R., and Miller, E. K. (2009). Phase-dependent neuronal coding of objects in short-term memory. *Proc. Natl. Acad. Sci. U.S.A.* 106, 21341–21346. doi: 10.1073/pnas.0908193106

Stephan, K. M., Thaut, M. H., Wunderlich, G., Schicks, W., Tian, B., Tellmann, L., et al. (2002). Conscious and subconscious sensorimotor synchronization–prefrontal cortex and the influence of awareness. *Neuroimage* 15, 345–352. doi: 10.1006/nimg.2001.0929

Sterzer, P., and Kleinschmidt, A. (2007). A neural basis for inference in perceptual ambiguity. *Proc. Natl. Acad. Sci. U.S.A.* 104, 323–328. doi: 10.1073/pnas.0609006104

Swann, N., Tandon, N., Canolty, R., Ellmore, T. M., McEvoy, L. K., Dreyer, S., et al. (2009). Intracranial EEG reveals a time- and frequency-specific role for the right inferior frontal gyrus and primary motor cortex in stopping initiated responses. *J. Neurosci.* 29, 12675–12685. doi: 10.1523/JNEUROSCI.3359-09.2009

Tanji, J., and Hoshi, E. (2008). Role of the lateral prefrontal cortex in executive behavioral control. *Physiol. Rev.* 88, 37–57. doi: 10.1152/physrev.00014.2007

Thomson, D. J. (1982). Spectrum estimation and harmonic-analysis. *Proc. IEEE* 70, 1055–1096. doi: 10.1109/PROC.1982.12433

van Gaal, S., de Lange, F. P., and Cohen, M. X. (2012). The role of consciousness in cognitive control and decision making. *Front. Hum. Neurosci.* 6:121. doi: 10.3389/fnhum.2012.00121

van Gaal, S., Ridderinkhof, K. R., Fahrenfort, J. J., Scholte, H. S., and Lamme, V. A. (2008). Frontal cortex mediates unconsciously triggered inhibitory control. *J. Neurosci.* 28, 8053–8062. doi: 10.1523/JNEUROSCI.1278-08.2008

van Gaal, S., Ridderinkhof, K. R., Scholte, H. S., and Lamme, V. A. (2010). Unconscious activation of the prefrontal no-go network. *J. Neurosci.* 30, 4143–4150. doi: 10.1523/JNEUROSCI.2992-09.2010

van Gaal, and S., Lamme, V. A. (2012). Unconscious high-level information processing: implication for neurobiological theories of consciousness. *Neuroscientist* 18, 287–301. doi: 10.1177/1073858411404079

Wallis, J. D., Anderson, K. C., and Miller, E. K.,(2001). Single neurons in prefrontal cortex encode abstract rules. *Nature* 411, 953–956. doi: 10.1038/35082081

White, I. M., and Wise, S. P. (1999). Rule-dependent neuronal activity in the prefrontal cortex. *Exp. Brain Res.* 126, 315–335. doi: 10.1007/s002210050740

Wolfe, J. M. (1984). Reversing ocular dominance and suppression in a single flash. *Vision Res.* 24, 471–478. doi: 10.1016/0042-6989(84)90044-0

Conflict of Interest Statement: The authors declare that the research was conducted in the absence of any commercial or financial relationships that could be construed as a potential conflict of interest.

Received: 21 June 2013; accepted: 19 August 2013; published online: 11 September 2013.

*Citation: Panagiotaropoulos TI, Kapoor V and Logothetis NK (2013) Desynchronization and rebound of beta oscillations during conscious and unconscious local neuronal processing in the macaque lateral prefrontal cortex. Front. Psychol. **4**:603. doi: 10.3389/fpsyg.2013.00603*

This article was submitted to Cognition, a section of the journal Frontiers in Psychology.

A.6 Sequential neuronal activity in the lateral prefrontal cortex during binocular flash suppression.

"Time present and time past
Are both perhaps present in time future,
And time future contained in time past.
If all time is eternally present,
All time is unredeemable."

T.S. Eliot, "Four Quartets"

Sequential neuronal activity in the lateral prefrontal cortex during the task of binocular flash suppression

Vishal Kapoor [1, 2], Michel Besserve[1,3], Nikos K. Logothetis[1, 4], Theofanis I. Panagiotaropoulos[1,5, 6]

1. Department of Physiology of Cognitive Processes, Max Planck Institute for Biological Cybernetics, 72076 Tübingen, Germany
2. Graduate School of Neural and Behavioral Sciences, International Max Planck Research School, Eberhard-Karls University of Tübingen, 72074 Tübingen, Germany.
3. Department of Empirical Inference, Max Planck Institute for Intelligent Systems, 72076 Tübingen, Germany
4. Imaging Science and Biomedical Engineering, University of Manchester, Manchester M13 9PL, UK.
5. Centre for Systems Neuroscience, University of Leicester, Great Britain
6. Institute of Psychiatry, Psychology and Neuroscience, King's College London, Great Britain.

Keywords: prefrontal cortex, sequential activity, binocular flash suppression, noise correlations

ABSTRACT

Neurons in the lateral prefrontal cortex (LPFC) exhibit a huge diversity of activity patterns underlying various cognitive functions ranging from working memory to serial order and even visual awareness. In a previous study, we showed that perceptual content is robustly represented in the neuronal activity recorded from the LPFC utilizing an ambiguous visual stimulation paradigm called the binocular flash suppression. However, we found that only a minority of neurons displayed feature selective neuronal responses. In order to characterize any other dominant patterns in the neuronal activity, we used the non negative factorization procedure to decompose the matrix of peristimulus time histograms of units recorded during the task. We identified five dominant patterns whose peak amplitude was distributed across different temporal phases of a trial. Moreover, a majority of the units with firing profiles similar to a given response pattern did not exhibit significant difference in their responses during the monocular and binocular conditions of the task, thus suggesting that their firing was unaffected by ambiguous visual input. Interestingly, an assessment of the effective functional connectivity across the pairs of neurons with profiles similar to different patterns revealed that such correlated variability was highest among units which were temporally coincident. However, we observed successive decorrelation as the pairs of units were chosen from temporally separated populations. Moreover, this tendency was observed during both monocular and ambiguous stimulation, suggesting that such a correlation structure is independent of visual ambiguity. Finally, this tendency of decorrelation was present among positive correlations but, surprisingly, the negative negative correlations displayed a uniform distribution across the different populations. This suggests a computational network principle mediating a representation of sequential patterns of activity in the LPFC.

INTRODUCTION

A major role attributed to the lateral prefrontal cortex (LPFC) of the primate is the temporal organization of behavior (Rao, Rainer et al. 1997, Fuster 2001, Miller and Cohen 2001, Fuster 2008). Such a function entails integration of convergent sensory input (Chavis and Pandya 1976, Miller and Cohen 2001, Romanski 2012) and its subsequent retention for executing a goal directed motor act (Tanji and Hoshi 2008). The organization of cortical connectivity of LPFC with posterior association cortices (Barbas and Mesulam 1985, Petrides and Pandya 1999, Romanski, Tian et al. 1999, Petrides and Pandya 2002) and higher motor areas (Bates and Goldman-Rakic 1993, Lu, Preston et al. 1994, Takada, Nambu et al. 2004) provides the essential anatomical substrate to serve this role.

We have come to ascribe this role to LPFC through a large number of neurophysiological studies involving non human primates performing a visuo-motor task. Vision, being the dominant sensory modality among primates has been exploited in many neurophysiological investigations aimed at understanding this function of LPFC. First studies aimed at understanding the electrical activity in the LPFC found cells responsive to simple as well as complex visual stimuli such as faces (Pigarev, Rizzolatti et al. 1979, Rosenkilde, Bauer et al. 1981). Later studies not only indicated an areal segregation of these neuronal discharges between those responding to object identity in the ventrolateral prefrontal cortex (VLPFC) and those responding to spatial location in the dorsolateral prefrontal cortex (DLPFC) (Wilson, Scalaidhe et al. 1993) (but also see (Rao, Rainer et al. 1997, Rainer, Asaad et al. 1998) and (Meyer, Qi et al. 2011)), but also identified a localized region wherein, neural activity was highly selective to visual face stimuli (SP, Wilson et al. 1997, Scalaidhe, Wilson et al. 1999). In a recent study, we exploited this sensory selectivity in the LPFC in order to understand its role in visual awareness.

By using a task called binocular flash suppression (BFS) (Lansing 1964, Wolfe 1984), which allows the successful dissociation of sensory input from phenomenal awareness, it was found that a majority of cells (60-90% depending upon the strength of selectivity) that display preference to a visual stimulus also respond when the same stimulus is perceived during ambiguous stimulation (Panagiotaropoulos, Deco et al. 2012). It was therefore concluded that the LPFC robustly represents the current contents in visual awareness.

Besides the representation of current perceptual contents, the LPFC also participates in the execution of context dependent task specific cognitive behavior (Mante, Sussillo et al. 2013). The neurons in the region encode in their activity varied signals relevant to the current task; not just the sensory input as discussed above but also the cognitive processes responsible for successful behavior (Duncan 2001, Miller and Cohen 2001, Tanji and Hoshi 2008). Modulation in the responses of neurons in the LPFC has been observed in several different paradigms such as those probing the neural correlates of decision making, working memory, temporal sequencing of sensory input or motor action, reward expectation to mention a few (Tanji and Hoshi 2008). Thus, there is a huge diversity of functional properties related to various psychological processes relevant to a task reflected in the neuronal activity recorded in the LPFC.

Our electrophysiological investigation of this region probing its role in visual perception revealed that only about 12 percent of the recorded neurons displayed visual responses which significantly differentiated between the visual stimuli used for the study (Panagiotaropoulos, Deco et al. 2012). Cognizant of this region's role in mediating various aspects of behavior, we wondered about the existence of any other task related activity, if any among the remaining majority of single units. We therefore clustered the peristimulus time histograms of the neurons in order to elucidate and understand any other dominant patterns of activity relevant to the task.

This led us to characterize the major response profiles present among neurons in the LPFC during a simple visual fixation paradigm of BFS. In addition, we investigated the modulation of the neurons clustered similar to these patterns during different task conditions. Finally, we assessed the effective functional connectivity across the different populations of neurons in order to understand the network principles underlying sequential neuronal activity.

MATERIALS AND METHODS

Behavioral Task and Stimulus Presentation

The task has been described in detail in an earlier publication (Panagiotaropoulos, Deco et al. 2012). Briefly, there were two stimulus conditions, namely, physical alternation (PA) and flash suppression (FS), which were pseudo randomly interleaved. Each trial in both conditions started with the presentation of a fixation spot (foveal presentation, size: 0.2°). 300 milliseconds later, a monocular visual stimulus (size: 2°-3°) was presented (overlaid by the fixation spot) for 1000 milliseconds. In PA trials, 1000 milliseconds after the presentation of the first stimulus, a second visual stimulus in the corresponding location of the other eye was presented. During FS trials, the disparate visual stimulus was presented without the removal of the first visual stimulus. This results in the robust perceptual suppression of the first visual stimulus (Lansing 1964, Wolfe 1984, Keliris, Logothetis et al. 2010, Panagiotaropoulos, Deco et al. 2012). Therefore the two different trial conditions were identical perceptually but differed in the concomitant sensory input during the second half of a trial. The stimulus order and eye (in which the first stimulus was presented) was pseudo randomized and balanced across trials in a single dataset. Animals were trained to limit their fixation within a fixation window (±1°) for the entire duration of a trial

and following successful fixation were given a juice reward. Eye movements were monitored throughout the behavioral and electrophysiological recording and stored offline for further analysis. All the visual stimuli were presented with the help of a stereoscope and displayed at a resolution of 1,280×1,024 on the monitors (running at a 60 Hz refresh rate) using a dedicated graphics workstation (TDZ 2000; Integraph Systems, Huntsvilli, AL, USA). Animals sat in an animal restraining chair during the behavioral training and electrophysiological recordings.

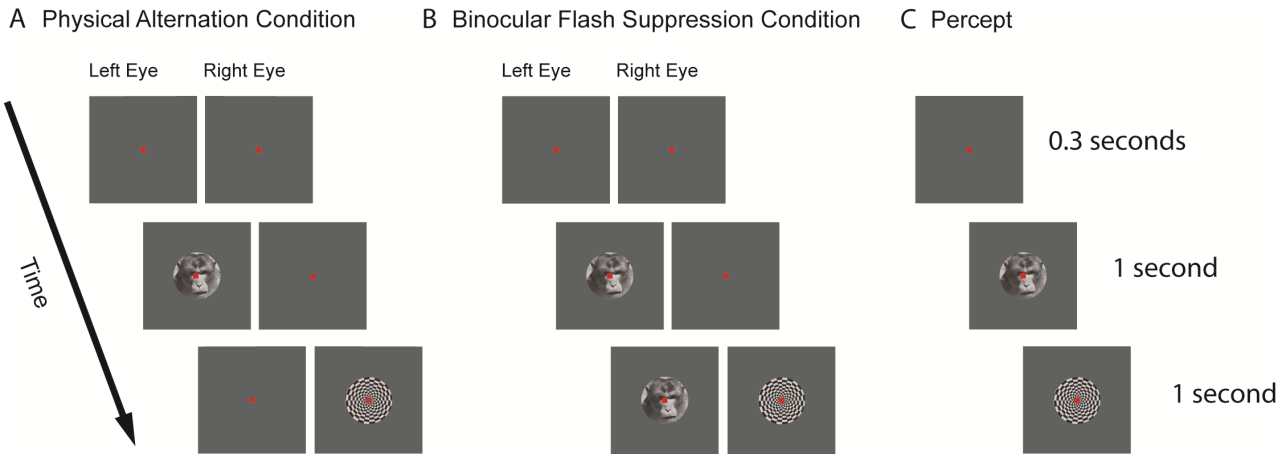

Figure 1: Time line of the psychophysical paradigm used for investigation, namely (A) Physical Alternation and (B) Binocular Flash Suppression. The percept is shown in (C). Note that although the sensory stimulation is different across the two conditions, the percept is the same. (Refer to the text for details.)

Electrophysiological Recordings

Three healthy adult rhesus monkeys (Macaca mullatta), D'98, F'03 and F'06, participated in electrophysiological recordings. All experiments were approved by the local authorities (Regierungspraesidium) and were in full compliance with the applicable guidelines of the

European community (EUVD 86/609/EEC) for the care and use of laboratory animals. The cranial headpost and recording chamber were custom designed for each animal based on the high resolution MR scans collected using a 4.7 tesla scanner (Biospec 47/40c; Bruker Medical), while the animal was under general anesthesia. The MR scan was also used for localizing the region of interest and the chambers were implanted over the LPFC. Implantation of the recording procedures was carried out under aseptic conditions as reported previously (Logothetis, Merkle et al. 2002). Additionally, a scleral eye coil was also implanted for measuring eye movements.

Custom made nichrome wire tetrodes (electroplated with gold for reducing impedance) were loaded on a custom designed microdrive for recording the neural activity in the LPFC. Cheetah data acquisition system (Neuralynx, Tuscon, AZ) was used to acquire, amplify, filter and store the signal recorded with the tetrodes. Local field potential (LFP) signal was obtained by filtering the raw voltage signal with an analog band pass filter (1- 475 Hz). The signal recorded in the 0.6-6 kHz which exceeded a predefined threshold (typically 25 μV) was classified as multi-unit activity (MUA). The sampling rate of the signal was 32 kHz and digitized (12 bits). Spike sorting for single units was done offline using custom algorithms, which utilized the first three principal components of the spike waveforms as features (Tolias, Ecker et al. 2007). Cluster cutting was performed using Klusters (Lynn Hazan, Buzsáki lab, Rutgers, Newark NJ).

NNMF based clustering of Single Unit

Neural data was recorded from 1285 neurons. 151 units (~ 12 % of the total), which displayed sensory selectivity were removed from this dataset thus leaving a total of 1134 neurons. We aimed to cluster this neuronal activity with a Non Negative Matrix Factorization

(NNMF) method (Paatero and Tapper 1994, Lee and Seung 1999). The data which was input to the algorithm was preprocessed in the following way. First, the trial averaged peri stimulus time histogram (PSTH) (Time duration - 0 (First stimulus on) to 2000 milliseconds (Stimulus off), smoothed using a gaussian kernel of standard deviation - 40 milliseconds) was estimated for each single unit recorded. Next, the four PSTH's per neuron/site for four different conditions (The order of the conditions was as follows, a. Flash Suppression (Polar stimulus first and Face stimulus second), b. Physical Alternation (the same order as in a.), c. Flash Suppression (Face stimulus first and polar stimulus second) and d. Physical Alternation (the same order as in c.)) thus obtained were concatenated one after the other giving in all 1004 (251 per condition) data points per neuron. We removed from this matrix, all units with very low spiking activity (leading to the removal of units with an average of less than 1.26 spikes per concatenated trial). Finally this unit response matrix **R** with dimensions (1083 (number of units) x 1004) was clustered with NNMF in order to ascertain the dominant neuronal response patterns. Since we assume that the recorded units can not only exhibit firing patterns encoding a particular aspect of the tasks, but could also be a mixture of these patterns, we assume that the unit activity can be described as a linear combination of a few typical temporal response components. As a consequence, we assume that R can be decomposed as a matrix product:

$$\mathbf{R} \approx \mathbf{HW}$$

where, **W** is the (K x 1004) matrix gathering the dominant K temporal response patterns observed in the data, and **H** is a (number of units x K) weight matrix gathering the weights associated to the contribution of the K dominant response patterns to each unit response. The factorization was initialized by drawing dominant responses at random using coefficients uniformly distributed on the unit interval, and the corresponding time contributions were

initialized using least square regression. Since the solution of this minimization problem is not guaranteed to be non-negative, we then kept only the positive part of each entry to build the initialization matrix. The NNMF decomposition was then optimized using the multiplicative update algorithm (Sra and Dhillon 2005) and the stability of the solution was enforced using an iterative bootstrap approach to find a good initialization of the components. We ran 50 bootstrap iterations as follows. Starting from the initialized matrices, we partition the columns of the matrix **R** in two subsets of equal length by random permutation of the columns, the **R**/2 first columns being assigned to the first subset and the rest to the second.

The NNMF optimization is then run separately on the two matrices built from the columns of the respective subsets resulting in two sets of dominant components. Solutions should in principle reach similar values assuming the number of samples is large enough and the solution of the NNMF being stable for this number of components. However, the two sets of components thus obtained might be similar but sorted in a different order. We thus assessed similarity by first reordering the components so that they match together. The ordering of the components was done by computing the kernel principal component analysis (KPCA) of all columns of both the matrices pooled together. Then the components of each sub-matrix were reordered according to the value of their projection on the first KPCA component. Once the components are reordered, pairs of columns from each matrix are matched together according to this order and members of a given pair are compared according to a cosine similarity measure.

For pairs exceeding the similarity threshold of .5, the corresponding columns were retained for the initialization of the next bootstrap iteration, while the remaining columns would be simply re-initialized again using random responses as described previously. After 50 bootstrap iterations, we store the spectral components found in the last 15 iterations. Firstly, the

average of these components (across iterations) is used to build the final initialization matrix, and the NNMF algorithm is run on the full response matrix **R** to generate the final solution. Secondly, the variance across the last 15 bootstrap iterations is used for quantifying the stability of the NNMF solution and is defined as the *component variability*. More precisely, the component variability is the ratio of component variance across the last 15 iterations of the NMF algorithm to the component mean square across trials (both quantities being averaged across time).

We determined an optimal number of NNMF components K by running the previous procedure in 10 batches of 100 runs each for K varying between 2 and 10, and thereafter evaluated for each run and each K, the average across components or component variability ratio defined above. We selected the optimal K as the largest number of components achieving a median component variability across runs inferior to 5% and for this value of K the NNMF solution achieving minimum residual error among all runs, defined as the entry wise sum of squares

$$\sum_{u \in \text{units}} \sum_{t \in \text{time samples}} \left(\mathbf{R} - \mathbf{HW}\right)^2_{u,t} ,$$

was selected as the optimal one (Supplementary Figure 1).

Noise Correlation Analysis

The spike count correlation coefficient (r_{sc}) was calculated for pairs of neurons during the time window of visual stimulation (Temporal duration – 2 seconds) as follows. First, we normalized the total number of spike counts by converting the spike count of each of the pair of neurons (i and j) separately for the four conditions across trials by converting them into z-scores. Thereafter, the z-scores across conditions were concatenated to obtain two vectors respectively

for the pair of units. Next, the Pearson's correlation coefficient was computed for the two vectors z_i and z_j using the corr function in matlab.

It's known that the magnitude of spike count correlation could be biased because of spike sorting errors (Cohen and Kohn 2011). We therefore performed the noise correlation analysis only with pairs of well isolated single units. The single unit isolation quality was judged using a method reported previously (Tolias, Ecker et al. 2007) which has been utilized for a reliable estimate of noise correlation (Ecker, Berens et al. 2010).

RESULTS

Neuronal responses in the LPFC during BFS

Electrophysiological activity was recorded from 1285 single units with wire tetrodes in the LPFC of three monkeys engaged in the task of BFS. Figure 2 shows response profiles and raster plots of example neurons recorded during the task of BFS. The neuronal activity displayed different patterns as exemplified by the neurons in Figure 2. These included a ramping up or a ramping down nature of activity as well as a more transient neuronal response limited to the first or the second half of the trial. Three observations can be made from the nature of the response profiles. Firstly, there is an enormous heterogeneity among single unit responses in the LPFC. Second, the discharges of these neurons were usually temporally restricted to different and specific phases of the trial. Finally, the neuronal response profiles are very similar across the four different stimulus conditions (see the methods section for a description of the stimulus conditions).

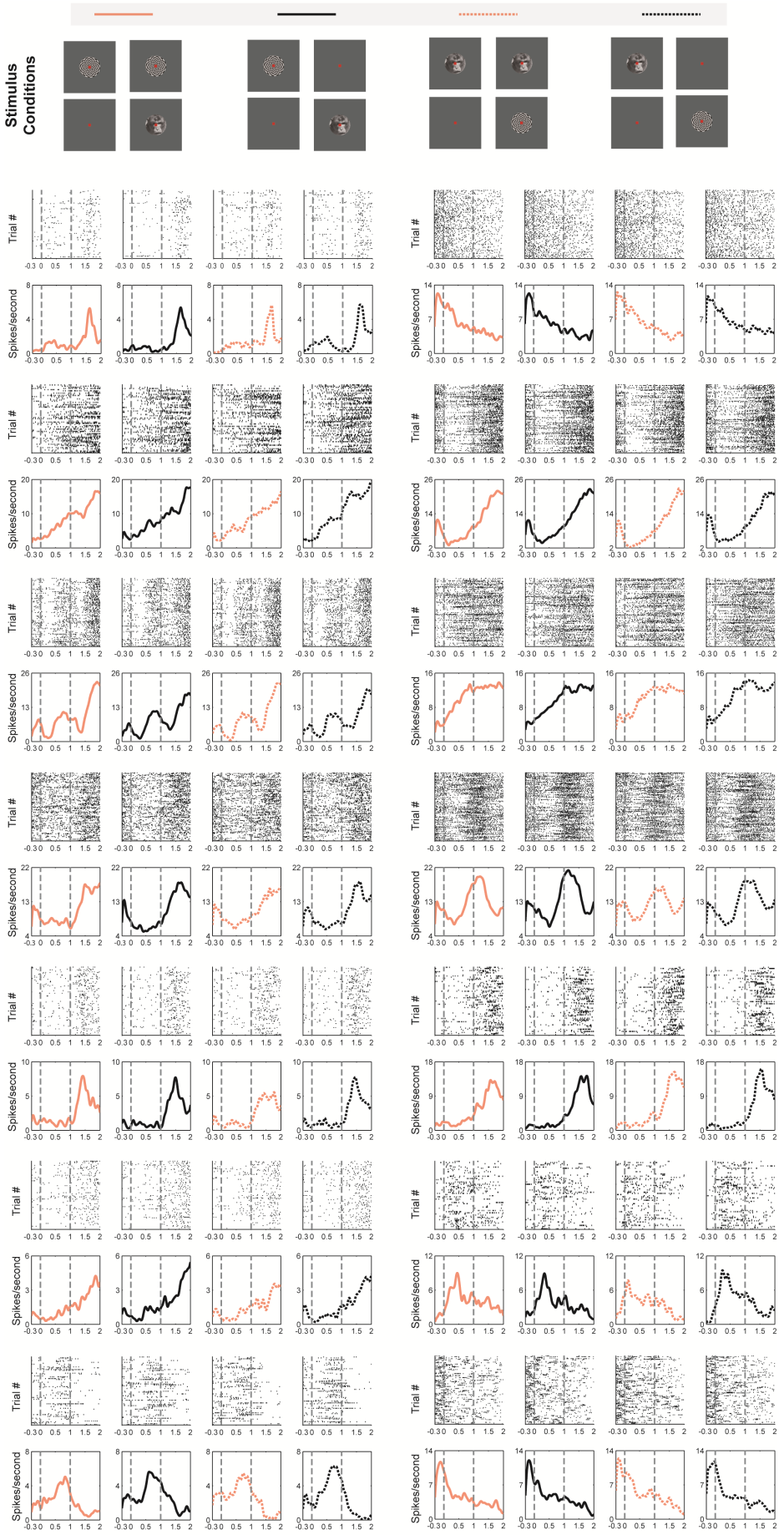
Stimulus Conditions
Trial #
Spikes/second
Time

Figure 2: Example single unit responses of different neurons recorded during PA (black) and FS (orange). Each neurons single trial response is shown using raster plots. Below the raster plots, is the peristimulus time histogram of each neuron. Plotted with solid lines are the neuronal responses when checkerboard pattern is presented first followed by the face stimulus. Neuronal response when the face is presented first followed by the checkerboard pattern is plotted with dotted lines. The stimulus conditions are also displayed in the uppermost panel. Some cells tend to fire in an earlier phase of the trial and some later. Neurons also display a huge heterogeneity in their response pattern.

Neuronal Response Patterns identified with NNMF

In order to better identify and differentiate between the diverse patterns of responses observed among the recorded single units, an NNMF (Paatero and Tapper 1994, Lee and Seung 1999) based clustering of neuronal response profiles was performed (see methods for details and Supplementary Figure 2). With this method, we identified five dominant components which summarized the recorded single units. These components and the respective stimulus conditions are displayed in Figure 3. Two of these components exhibited a gradual ramping up or a ramping down profile. Another two represented peaks in their amplitude after the first or the second presented stimulus. In addition, one component displayed a response pattern, which increased its activity towards the expected stimulus switch and then decreased thereafter. Moreover, the component profile across the different stimulus conditions was virtually identical, therefore signifying the similarity of responses across the various conditions.

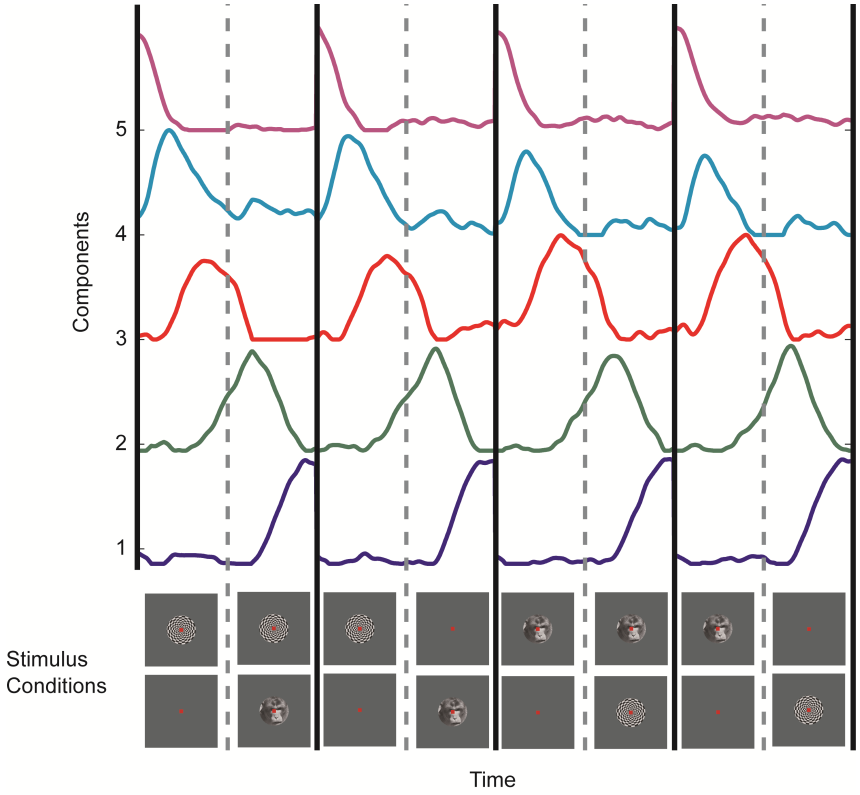

Figure 3: Dominant components obtained by clustering the single units, with non-negative matrix factorization (NNMF) (Refer to text for the details of the clustering procedure). Five components were obtained, displaying a transient increase during a specific phase of the trial or a monotonous rise or decay pattern. Additionally, a component displayed an increase in amplitude around the time, when the stimulus changes from the first to the second one. The lower panel displays the stimulus presentation conditions, demarcated by black lines.

Electrical activity of neurons belonging to a single component

Cosine similarity measure was utilized for comparing each single unit's activity profiles to the patterns obtained after nnmf based factorization. Each unit was thus sorted to one of the five patterns judged on the basis of maximum similarity to one of them (cosine similarity measure, see method section). The number of units belonging to each component was as follows:

component 1 – 356, component 2 – 182, component 3 – 148, component 4 – 181, component 5 - 216). Although the individual components displayed a similar pattern across the different stimulus conditions (Figure 3), we wanted to assess if the single unit sorted to each component displayed any differences in activity during monocular stimulation in comparison to when incongruent visual stimuli were presented to the two eyes. Plotting the average single unit activity revealed a very similar pattern of activity across the two conditions (Figure 4A). A scatter plot of the average firing rates (time period – 1001 milliseconds to 2000 milliseconds) of single units belonging to the same cluster is shown in Figure 4B. Most of the units lie on the diagonal further exemplifying the similarity in their response across the physical alternation and binocular flash suppression condition. Indeed, a majority of units (~89 percent) were not selective in either of the two conditions, when their activity was compared during the second half of the trial (rank sum test).

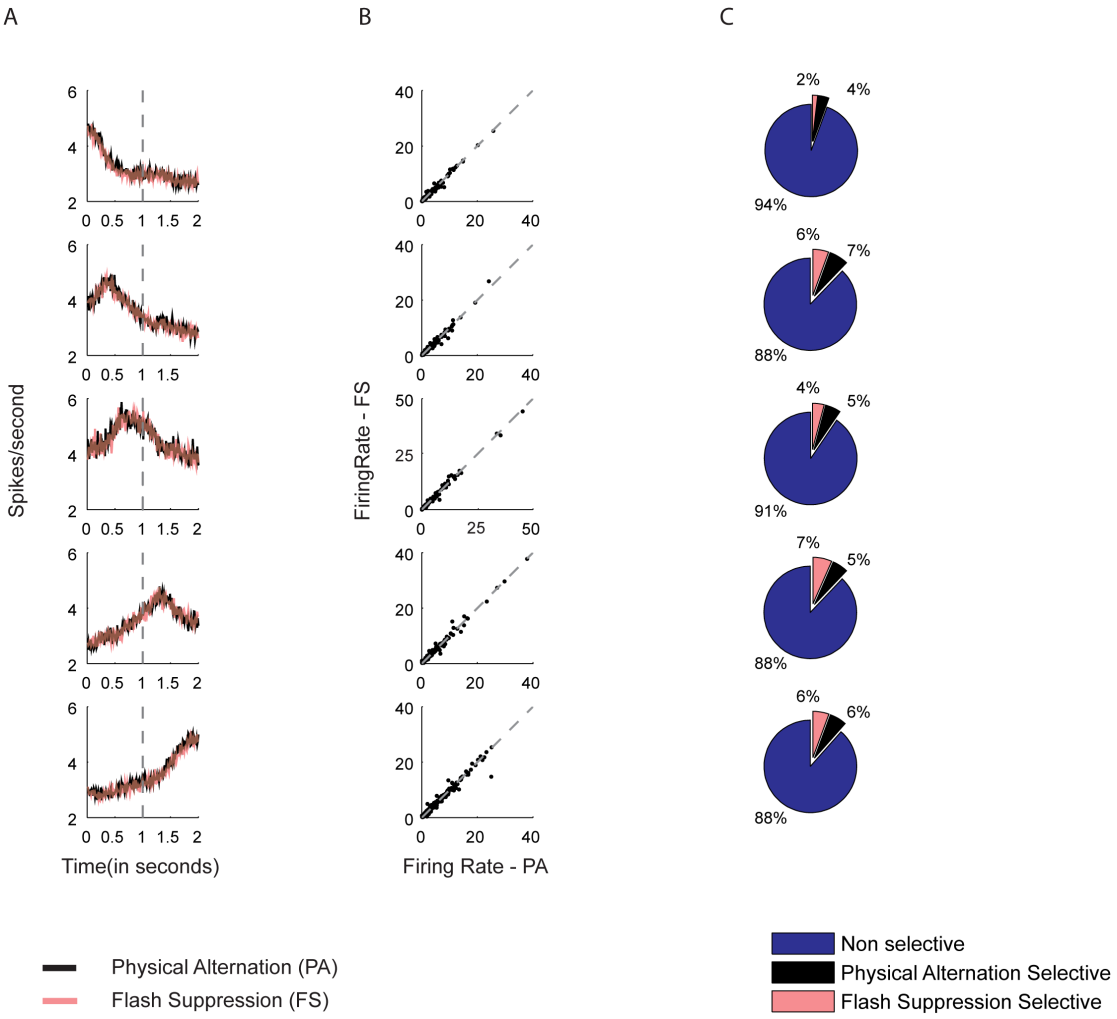

Figure 4: Single unit population activity.

(A) Average population activity across all single units belonging to a single component shown in Figure 3, during the condition of physical alternation (black) and flash suppression (orange). Note that the average activity is similar across the two conditions.

(B) Scatter plot of the average firing rate of each single unit in the same cluster during the second part of the trial (1001 - 2000 milliseconds).

(C) Percentage of units which fired significantly higher in the physical alternation (black) or flash suppression (orange) condition. A majority of the units did not fire significantly different in either of the stimulus conditions.

Sequential single unit activity spans the trial duration

Having observed that the five components spanned the entire duration of the trial, we wanted to characterize and visualize if the individual single unit activity also displayed such a sequential nature. Such successive neuronal activity has been typically observed among the rodent hippocampal cells signaling time and is known to be distributed across the entire duration under observation (Eichenbaum 2014). Since, we had four different stimulus conditions, we first averaged the psth of each neuron (N = 1083) across the four different stimulus conditions, to obtain one activity profile per unit. The neurons were then sorted according to the latency of the peak of this average psth. Figure 5 shows the average psth activity (displayed as normalized firing rate) for each neuron according to the new sorting order in the four different conditions. The peak of neuronal responses was distributed through the entire duration of the trial signifying the sequential nature of the activity. Further, qualitative inspection of the activity revealed that it was very similar across the different stimulus conditions.

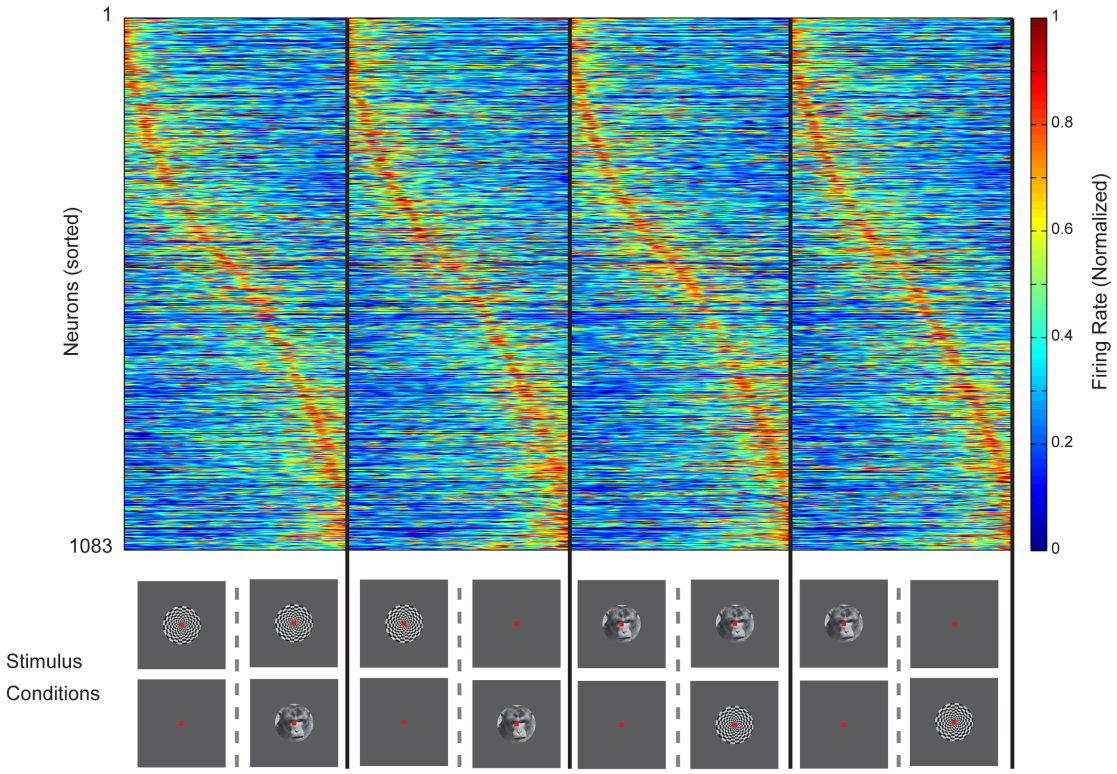

Figure 5: Shown in the four panels is the neuronal activity in the different stimulus conditions (shown in the lower panel) sorted according to the latency of the peak amplitude. For determining the sorting order, the average PSTH across the four conditions was calculated, peak latency for the resultant PSTH was determined and neurons were sorted accordingly. Neurons tend to peak around the same time across the four stimulus conditions. Moreover the peaks are distributed across the entire duration of the trial.

Correlation Structure of Neurons

Since correlated variability between pairs of neurons is thought to reflect direct or indirect synaptic connectivity, or a shared common input, it has been utilized as a tool to assess

functional connectivity between neuronal populations. We wondered if the population of cells, whose activity profiles were similar to the individual patterns demonstrated such a functional segregation as judged by their correlated variability. Therefore, we calculated the trial by trial, spike count correlation across pairs of simultaneously recorded neurons (N = 538 pairs). The two neurons constituting a pair could have a response profile alike either to the same or different patterns. Additionally, in order to understand, if temporality played a role in structure of these correlations, we sorted the patterns according to their peak latency and sampled the neurons to each response profile accordingly. The matrix displayed in Figure 6A depicts the average spike count correlations obtained across the various combinations of units belonging to the five different clusters. The principal diagonal includes all the neuronal pairs, wherein, the constituent units are clustered to the same pattern (this category could be referred to as one with a temporal distance (t.d.) of zero, or units clustered to the same component). Consecutive diagonals lateral to the main diagonal display correlations, obtained from pairs of units classified to successive, temporally separated patterns (t.d. of one, or two and more refers respectively to the first, or the second and the rest of the neighboring diagonals to the main diagonal). Interestingly, the correlations tend to be higher along the principal diagonal and decreased in successively lateral diagonals. (Histograms of the correlation coefficients obtained are shown in Supplementary Figure 3). Specifically, the spike count correlation between pairs of units with similar patterns was significantly stronger (*mean* r_{sc} (temporal distance 0) = 0.1206 ± 0.0194) than when the constituent units were from groups which were temporally divergent (*mean* r_{sc} (t.d. 1) = 0.0716 ± 0.0140, *mean* r_{sc} (t.d. 2 and more) = 0.0205 ± 0.0092; t-test (t.d.0 vs t.d. 1), $p < 0.05$; t-test (t.d.(0) vs t.d. (2 and more)), $p < 0.001$; t-test (t.d.(1) vs t.d. (2 and more), $p < 0.01$). Therefore, the average noise correlation displayed a decrement when the units were from components which

were temporally distant. These results are summarized in figure 6B showing average noise correlation among neurons as a function of the temporal distance. Such a trend was also observed when correlations were computed for individual conditions physical alternation (PA) and flash suppression (FS) separately (*mean* r_{scPA} (t.d. 0) = 0.1243 ± 0.0205, *mean* r_{scPA} (t.d. 1) = 0. 0.0751 ± 0. 0154, *mean* r_{scPA} (t.d. 2 and more) = 0.0204 ± 0.0103; t-test (t.d.0 vs t.d. 1), $p = 0.0547$; t-test (t.d.(0) vs t.d. 2 or more), $p < 0.001$; t-test (t.d. 1 vs t.d. 2 and more), $p < 0.01$; *mean* r_{scFS} (t.d. 0) = 0.1167 ± 0.0199, *mean* r_{scFS} (t.d. 1) = 0. 0.0693 ± 0. 0146, *mean* r_{scFS} (t.d. 2 and more) = 0.0218 ± 0.0105; t-test (t.d.0 vs t.d. 1), $p = 0.0541$; t-test (t.d.0 vs t.d. 2 and more), $p < 0.001$; t-test (t.d.(1) vs t.d. (2 and more), $p < 0.01$; see supplementary Figure 3). Moreover, no significant difference was observed when the correlations obtained in physical alternation were compared with flash suppression at respective temporal distances (for all three t.d. (0, 1 and 2 and more) comparisons, t-test, $p > 0.05$), thus displaying that such functional connectivity is maintained irrespective of whether the visual input is monocular or ambiguous.

Next, we investigated the positive ($r_{sc\text{-}pos}$) and negative correlations ($r_{sc\text{-}neg}$) in order to understand their distribution across the population as a function of temporal distance. The positive correlations exhibited a trend very similar to the average correlation in that they displayed progressive decorrelation as a function of temporal distance (*mean* $r_{sc\text{-}pos}$ (t.d. 0) = 0. 2109 ± 0.0213, *mean* $r_{sc\text{-}pos}$ (t.d. 1) = 0.1441 ± 0. 0156, *mean* $r_{sc\text{-}pos}$ (t.d. 2 and more) = 0.1137 ± 0.0093; t-test (t.d. 0 vs t.d. 1), $p < 0.05$; t-test (t.d.0 vs t.d. 2 and more), $p < 0.001$; t-test (t.d. 1 vs t.d. 2 and more, $p = 0.0788$). Surprisingly, the negative correlations were uniformly distributed across temporal distance (*mean* $r_{sc\text{-}neg}$ (t.d. 0) = - 0. 0924 ± 0.0135, *mean* $r_{sc\text{-}neg}$ (t.d. 1) = - 0.0778 ± 0. 0110, *mean* $r_{sc\text{-}neg}$ (t.d. 2 or more) = - 0.0915 ± 0.0091; t-test (t.d.0 vs t.d. 1), $p = 0.4018$; t-test (t.d. 0 vs t.d. 2 and more), $p = 0.9583$; t-test (t.d. 1 vs t.d. 2 and more), $p = 0.3873$).

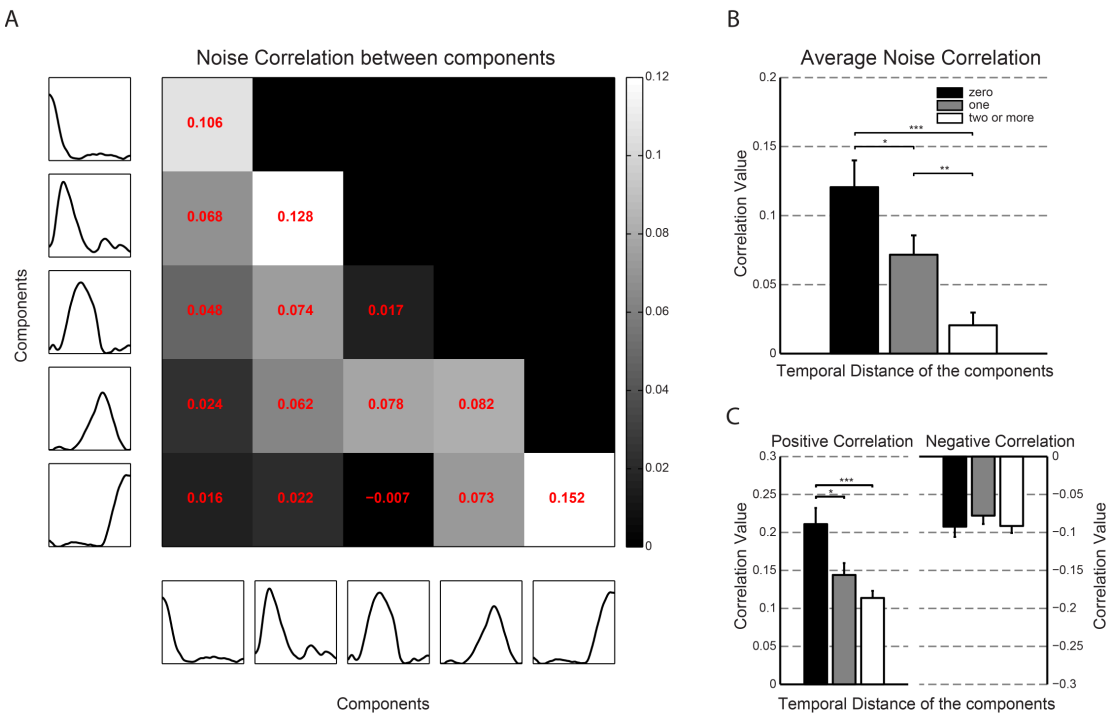

Figure 6: Noise correlation matrix and average correlations as a function of temporal distance.

(A) Correlations were calculated across various combinations of neurons belonging to the sequential components (arranged chronologically with earliest on the top and latest on the bottom along the x and earliest at the left most position and latest on the right most position on the y axis). The brightness of the individual pixels depicts the strength of the correlation according to the colorbar on the right, with white and black depicting high and low correlations respectively. Strong correlations were observed between neurons lying on the major diagonal, which constitutes units of similar response types. And the correlations seem to decrease as depicted from the intensity of pixels across successive diagonals lateral to the main diagonal.

(B) Average correlations decreased with an increase in the temporal distance between the components to which the constituent single units were clustered to.

(C) Positive correlations displayed a trend very similar to the average correlations. However the negative correlations were not significantly modulated by temporal distance.

DISCUSSION

The present study investigated the nature of neuronal responses in the LPFC during a simple fixation paradigm of BFS. We find different patterns of responses dependent on the temporal phase of a trial. We aimed to detect and describe the various kinds of responses and the effect of visual competition on the nature of these responses. To this end, we used a novel classification method of neuronal response patterns. We first discuss the novelty of the methodology used for detecting the different patterns of responses and thereafter the findings related to temporally contingent neuronal activity.

NNMF as a method for clustering of neuronal response patterns

Firstly, we present a novel method for classifying patterns of neuronal activity. To the best of our knowledge, it is the first time that nnmf based classification approach (Paatero and Tapper 1994, Lee and Seung 1999, Sra and Dhillon 2005) has been utilized for clustering patterns of neuronal peri stimulus time histograms. A key advantage of this methodology with respect to another kind of linear decomposition such as PCA is the interpretability of the resulting dominant components as typical neuronal responses. This interpretability is ensured by enforcing non-negativity of the components, thus preserving a key property of the original unit

responses. In addition, such a methodology permits the isolation of strikingly different response patterns present in the data, thus allowing us to infer deductions that are not necessarily plausible based merely upon visualization of the population activity. Besides, as the electrophysiological methods advance and become viable for recording the electrical activity simultaneously from several hundred neurons or sites with multi electrode arrays (Pine 2006, Miller and Wilson 2008), it necessitates the need for development of automated algorithms for visualization, classification and presentation of neuronal responses. The computational approach presented here could therefore be utilized for offline and potentially for online classification and visualization of data collected from large number of cells or sites. Such a clustering methodology has already been utilized for detection of neural events from the LFP signal recorded in the hippocampus (Logothetis, Eschenko et al. 2012). Finally, a method for detecting neural events could theoretically be used to manipulate an external prosthetic device or as an online trigger for electrical/optical stimulation of the brain or the delivery of a drug.

Individual Components and sequential activity in the LPFC

Utilizing this clustering methodology revealed five dominant neuronal response patterns of temporally contingent neuronal activity in the LPFC during the task of BFS. Two of the five patterns, were restricted to the first or the second half of the trial, possibly signifying temporal order of the stimuli being presented. Tuning of LPFC neurons to temporal order of events has been previously reported. This has been in the context of a task, wherein the presented sensory input dictated the requisite and sequential motor act (Ninokura, Mushiake et al. 2003, Ninokura, Mushiake et al. 2004, Inoue and Mikami 2006, Berdyyeva and Olson 2010). These tasks have ranged from requiring the memorization of a sequence of images (Ninokura, Mushiake et al.

2003, Ninokura, Mushiake et al. 2004), to making serial movements for drawing geometrical shapes using a joystick (Averbeck, Chafee et al. 2002, Averbeck, Chafee et al. 2003). All these examples of rank selectivity among neurons have been discovered while animals performed serial order tasks. Similarly, we have observed neurons which signify serial order by increasing their firing amplitude during the first or the second part of the trial. Interestingly, the task only required animals to passively fixate and did not require carrying out a serial motor action, but did require monitoring of the ongoing behavior (that is the act of fixation), a key role attributed to the lateral prefrontal cortex (Tanji and Hoshi 2008). Moreover, this activity remained unchanged during ambiguous stimulation signifying its dependence on the temporal phase of the trial rather than on visual competition. This further illustrates that such activity possibly sub serves a more general role of monitoring irrespective of the nature of the visual input.

The other three patterns of activity displayed ramping up or ramping down activity and increased activity in the middle of the trial. The temporally contingent neuronal activity which had a ramping up pattern could also possibly be related to anticipation of reward or the passage of elapsed time. Cellular activity in the lateral prefrontal cortex has been reported to be modulated by reward expectation (Watanabe 1996, Leon and Shadlen 1999, Roesch and Olson 2003). The activity of the same neurons signifying rank in serial order tasks has also been shown to partially correlate with both reward expectation and elapsed time (Berdyyeva and Olson 2011). This is expected, as a serial order task is accompanied by both the passage of time as the trial progresses as well as an anticipation of an upcoming reward.

Taken together, the serial activity patterns observed in our data could specify the phase or progress of the trial. Single neurons whose activity tracks the progress of task have been reported in the LPFC, when the animals carried out a self-ordered task (Hasegawa, Blitz et al. 2004), as

well as when the task required keeping track of the progression of successively presented sensory stimuli (Saga, Iba et al. 2011). Similarly, monkeys with lesions in the LPFC show deficits in tasks which require remembering the temporal order of stimuli (Petrides 1995). Further, all the components obtained with clustering could together signify the various phases of a trial in a continuum. Again, like discussed previously, we observe the development of these patterns of activity without any explicit demands on the animal to keep track of the stimuli being presented. However, the successful completion of the task was dependent on continuous fixation and thus the animal monitoring his own behavior.

Together, the different sequential patterns of activity are related to the various temporally organized variables in the task. Future studies could be directed towards delineating the contributions of these different variables and understanding their relative contributions to the generation of such sequential patterns.

Correlation structure of sequential neuronal activity

Trial to trial variability as measured with spike count correlation provides a measure for judging effective functional connectivity across neuronal populations (Bair, Zohary et al. 2001, Cohen and Kohn 2011). Our results revealed that neurons with similar temporal profiles displayed the strongest correlations. It has been suggested previously that the effective connectivity among prefrontal cortex neurons could depend on their temporal correlation (Constantinidis, Franowicz et al. 2001) and such a relationship might be present even before task training (Qi and Constantinidis 2012). Further, cells with similar 'time tuning' in the hippocampal CA1 region of the rodent display strong correlated variability as compared to random cell pairs and the structure of correlations is modulated with learning on a trace

conditioning paradigm (Modi, Dhawale et al. 2014). Interestingly, similar modulation of the magnitude of correlations as a function of temporal preference has also been observed in the posterior parietal cortex during a virtual navigation decision task with a memory component (Harvey, Coen et al. 2012). We observe this however without any memory demands among the neurons recorded in the lateral prefrontal cortex. Further, none of these studies investigated the nature of these correlations in a task which dissociates visual perception from sensory input as we did here. Presumably, such a temporal dependency in correlation structure could rely on the chronological structure of perceptual content, for determining the timing of events. Therefore, in a region of the brain, where the current percept is unambiguously represented (Panagiotaropoulos, Deco et al. 2012); one would expect that such temporal correlations would not be affected by ambiguous input. This is also what we find when the two task conditions were compared. Firstly, in both conditions, we observed a decorrelation as a function of temporal distance and secondly, the magnitudes of correlations for individual temporal distances were almost identical when compared to each other.

Next, we investigated the distribution of positive and negative correlations in our results. Although the positive correlations displayed a decrease akin to the average correlations, the negative correlations were uniformly distributed as a function of temporal distance. In a recent study, a similar dichotomy was observed between positive and negative correlations in the visual cortex as a function of orientation difference (Chelaru and Dragoi 2014). The authors modeled the correlations and adjudged that an increase in the negative noise correlations improved the population signal to noise ratio and network accuracy. It is rather surprising that a common correlation structure is observed among neuronal populations in different regions of the brain and

involved in divergent neural processes. Perhaps, one could speculate that such a network principle might be a more general way of representation in the brain.

Sequential Activity patterns in the various regions of the brain

Interestingly, similar sequential patterns of activity have been observed in various regions of the brain. These include the hippocampus (Eichenbaum 2014) of the rodent and in the temporal lobe of the macaque (Sakon, Naya et al. 2014) attributed to the flow of time, in the olfactory system involved in encoding of the identity of odor stimuli (Laurent, Wehr et al. 1996, Wehr and Laurent 1996, Laurent 2002), during decision making (Harvey, Coen et al. 2012) and object construction task (Crowe, Averbeck et al. 2010) in the parietal cortex, and in the medial prefrontal cortex during memory guided saccade paradigm (Campos, Breznen et al. 2010). Although such sequential patterns of activity are observed in many different regions of the brain in diverse neural processes, it remains to be seen, if the structure of neuronal discharge fluctuations also displays similarity across different paradigms and various areas in the brain. If such a ubiquitous network encoding principle exists, it could provide a common ground for the sequential responses found so pervasive among neurons in the brain.

ACKNOWLEDGMENTS

This study was supported by the Max Planck Society. We would like to thank Joachim Werner and Axel Oeltermann for their excellent technical help and Shervin Safavi for discussions on the noise correlation analysis.

REFERENCES

Averbeck, B. B., M. V. Chafee, D. A. Crowe and A. P. Georgopoulos (2002). "Parallel processing of serial movements in prefrontal cortex." Proc Natl Acad Sci U S A **99**(20): 13172-13177.

Averbeck, B. B., M. V. Chafee, D. A. Crowe and A. P. Georgopoulos (2003). "Neural activity in prefrontal cortex during copying geometrical shapes. I. Single cells encode shape, sequence, and metric parameters." Exp Brain Res **150**(2): 127-141.

Bair, W., E. Zohary and W. T. Newsome (2001). "Correlated firing in macaque visual area MT: time scales and relationship to behavior." J Neurosci **21**(5): 1676-1697.

Barbas, H. and M. M. Mesulam (1985). "Cortical afferent input to the principals region of the rhesus monkey." Neuroscience **15**(3): 619-637.

Bates, J. F. and P. S. Goldman-Rakic (1993). "Prefrontal connections of medial motor areas in the rhesus monkey." J Comp Neurol **336**(2): 211-228.

Berdyyeva, T. K. and C. R. Olson (2010). "Rank signals in four areas of macaque frontal cortex during selection of actions and objects in serial order." J Neurophysiol **104**(1): 141-159.

Berdyyeva, T. K. and C. R. Olson (2011). "Relation of ordinal position signals to the expectation of reward and passage of time in four areas of the macaque frontal cortex." J Neurophysiol **105**(5): 2547-2559.

Campos, M., B. Breznen and R. A. Andersen (2010). "A neural representation of sequential states within an instructed task." J Neurophysiol **104**(5): 2831-2849.

Chavis, D. A. and D. N. Pandya (1976). "Further observations on corticofrontal connections in the rhesus monkey." Brain Res **117**(3): 369-386.

Chelaru, M. I. and V. Dragoi (2014). "Negative Correlations in Visual Cortical Networks." Cereb Cortex.

Cohen, M. R. and A. Kohn (2011). "Measuring and interpreting neuronal correlations." Nat Neurosci **14**(7): 811-819.

Constantinidis, C., M. N. Franowicz and P. S. Goldman-Rakic (2001). "Coding specificity in cortical microcircuits: a multiple-electrode analysis of primate prefrontal cortex." J Neurosci **21**(10): 3646-3655.

Crowe, D. A., B. B. Averbeck and M. V. Chafee (2010). "Rapid sequences of population activity patterns dynamically encode task-critical spatial information in parietal cortex." J Neurosci **30**(35): 11640-11653.

Duncan, J. (2001). "An adaptive coding model of neural function in prefrontal cortex." Nat Rev Neurosci **2**(11): 820-829.

Ecker, A. S., P. Berens, G. A. Keliris, M. Bethge, N. K. Logothetis and A. S. Tolias (2010). "Decorrelated neuronal firing in cortical microcircuits." Science **327**(5965): 584-587.

Eichenbaum, H. (2014). "Time cells in the hippocampus: a new dimension for mapping memories." Nat Rev Neurosci **15**(11): 732-744.

Fuster, J. M. (2001). "The prefrontal cortex--an update: time is of the essence." Neuron **30**(2): 319-333.

Fuster, J. M. (2008). Chapter 8 - Overview of Prefrontal Functions: The Temporal Organization of Action. The Prefrontal Cortex (Fourth Edition). J. M. Fuster. San Diego, Academic Press**:** 333-385.

Harvey, C. D., P. Coen and D. W. Tank (2012). "Choice-specific sequences in parietal cortex during a virtual-navigation decision task." Nature **484**(7392): 62-68.

Hasegawa, R. P., A. M. Blitz and M. E. Goldberg (2004). "Neurons in monkey prefrontal cortex whose activity tracks the progress of a three-step self-ordered task." J Neurophysiol **92**(3): 1524-1535.

Inoue, M. and A. Mikami (2006). "Prefrontal activity during serial probe reproduction task: encoding, mnemonic, and retrieval processes." J Neurophysiol **95**(2): 1008-1041.

Keliris, G. A., N. K. Logothetis and A. S. Tolias (2010). "The role of the primary visual cortex in perceptual suppression of salient visual stimuli." J Neurosci **30**(37): 12353-12365.

Lansing, R. W. (1964). "Electroencephalographic Correlates of Binocular Rivalry in Man." Science **146**(3649): 1325-1327.

Laurent, G. (2002). "Olfactory network dynamics and the coding of multidimensional signals." Nat Rev Neurosci **3**(11): 884-895.

Laurent, G., M. Wehr and H. Davidowitz (1996). "Temporal representations of odors in an olfactory network." J Neurosci **16**(12): 3837-3847.

Lee, D. D. and H. S. Seung (1999). "Learning the parts of objects by non-negative matrix factorization." Nature **401**(6755): 788-791.

Leon, M. I. and M. N. Shadlen (1999). "Effect of expected reward magnitude on the response of neurons in the dorsolateral prefrontal cortex of the macaque." Neuron **24**(2): 415-425.

Logothetis, N., H. Merkle, M. Augath, T. Trinath and K. Ugurbil (2002). "Ultra high-resolution fMRI in monkeys with implanted RF coils." Neuron **35**(2): 227-242.

Logothetis, N. K., O. Eschenko, Y. Murayama, M. Augath, T. Steudel, H. C. Evrard, M. Besserve and A. Oeltermann (2012). "Hippocampal-cortical interaction during periods of subcortical silence." Nature **491**(7425): 547-553.

Lu, M. T., J. B. Preston and P. L. Strick (1994). "Interconnections between the prefrontal cortex and the premotor areas in the frontal lobe." J Comp Neurol **341**(3): 375-392.

Mante, V., D. Sussillo, K. V. Shenoy and W. T. Newsome (2013). "Context-dependent computation by recurrent dynamics in prefrontal cortex." Nature **503**(7474): 78-84.

Meyer, T., X. L. Qi, T. R. Stanford and C. Constantinidis (2011). "Stimulus selectivity in dorsal and ventral prefrontal cortex after training in working memory tasks." J Neurosci **31**(17): 6266-6276.

Miller, E. K. and J. D. Cohen (2001). "An integrative theory of prefrontal cortex function." Annu Rev Neurosci **24**: 167-202.

Miller, E. K. and M. A. Wilson (2008). "All My Circuits: Using Multiple Electrodes to Understand Functioning Neural Networks." Neuron **60**(3): 483-488.

Modi, M. N., A. K. Dhawale and U. S. Bhalla (2014). "CA1 cell activity sequences emerge after reorganization of network correlation structure during associative learning." Elife **3**: e01982.

Ninokura, Y., H. Mushiake and J. Tanji (2003). "Representation of the temporal order of visual objects in the primate lateral prefrontal cortex." J Neurophysiol **89**(5): 2868-2873.

Ninokura, Y., H. Mushiake and J. Tanji (2004). "Integration of temporal order and object information in the monkey lateral prefrontal cortex." J Neurophysiol **91**(1): 555-560.

Paatero, P. and U. Tapper (1994). "Positive Matrix Factorization - a Nonnegative Factor Model with Optimal Utilization of Error-Estimates of Data Values." Environmetrics **5**(2): 111-126.

Panagiotaropoulos, T. I., G. Deco, V. Kapoor and N. K. Logothetis (2012). "Neuronal discharges and gamma oscillations explicitly reflect visual consciousness in the lateral prefrontal cortex." Neuron **74**(5): 924-935.

Petrides, M. (1995). "Impairments on nonspatial self-ordered and externally ordered working memory tasks after lesions of the mid-dorsal part of the lateral frontal cortex in the monkey." J Neurosci **15**(1 Pt 1): 359-375.

Petrides, M. and D. N. Pandya (1999). "Dorsolateral prefrontal cortex: comparative cytoarchitectonic analysis in the human and the macaque brain and corticocortical connection patterns." Eur J Neurosci **11**(3): 1011-1036.

Petrides, M. and D. N. Pandya (2002). "Comparative cytoarchitectonic analysis of the human and the macaque ventrolateral prefrontal cortex and corticocortical connection patterns in the monkey." Eur J Neurosci **16**(2): 291-310.

Pigarev, I. N., G. Rizzolatti and C. Scandolara (1979). "Neurons responding to visual stimuli in the frontal lobe of macaque monkeys." Neurosci Lett **12**(2-3): 207-212.

Pine, J. (2006). A History of MEA Development

Advances in Network Electrophysiology. M. Taketani and M. Baudry, Springer US**:** 3-23.

Qi, X. L. and C. Constantinidis (2012). "Correlated discharges in the primate prefrontal cortex before and after working memory training." Eur J Neurosci **36**(11): 3538-3548.

Rainer, G., W. F. Asaad and E. K. Miller (1998). "Memory fields of neurons in the primate prefrontal cortex." Proc Natl Acad Sci U S A **95**(25): 15008-15013.

Rao, S. C., G. Rainer and E. K. Miller (1997). "Integration of what and where in the primate prefrontal cortex." Science **276**(5313): 821-824.

Roesch, M. R. and C. R. Olson (2003). "Impact of expected reward on neuronal activity in prefrontal cortex, frontal and supplementary eye fields and premotor cortex." J Neurophysiol **90**(3): 1766-1789.

Romanski, L. M. (2012). Convergence of Auditory, Visual, and Somatosensory Information in Ventral Prefrontal Cortex. The Neural Bases of Multisensory Processes. M. M. Murray and M. T. Wallace. Boca Raton (FL).

Romanski, L. M., B. Tian, J. Fritz, M. Mishkin, P. S. Goldman-Rakic and J. P. Rauschecker (1999). "Dual streams of auditory afferents target multiple domains in the primate prefrontal cortex." Nat Neurosci **2**(12): 1131-1136.

Rosenkilde, C. E., R. H. Bauer and J. M. Fuster (1981). "Single cell activity in ventral prefrontal cortex of behaving monkeys." Brain Res **209**(2): 375-394.

Saga, Y., M. Iba, J. Tanji and E. Hoshi (2011). "Development of multidimensional representations of task phases in the lateral prefrontal cortex." J Neurosci **31**(29): 10648-10665.

Sakon, J. J., Y. Naya, S. Wirth and W. A. Suzuki (2014). "Context-dependent incremental timing cells in the primate hippocampus." Proc Natl Acad Sci U S A **111**(51): 18351-18356.

Scalaidhe, S. P., F. A. Wilson and P. S. Goldman-Rakic (1999). "Face-selective neurons during passive viewing and working memory performance of rhesus monkeys: evidence for intrinsic specialization of neuronal coding." Cereb Cortex **9**(5): 459-475.

SP, O. S., F. A. Wilson and P. S. Goldman-Rakic (1997). "Areal segregation of face-processing neurons in prefrontal cortex." Science **278**(5340): 1135-1138.

Sra, S. and I. S. Dhillon (2005). Generalized nonnegative matrix approximations with Bregman divergences. Advances in neural information processing systems.

Takada, M., A. Nambu, N. Hatanaka, Y. Tachibana, S. Miyachi, M. Taira and M. Inase (2004). "Organization of prefrontal outflow toward frontal motor-related areas in macaque monkeys." Eur J Neurosci **19**(12): 3328-3342.

Tanji, J. and E. Hoshi (2008). "Role of the lateral prefrontal cortex in executive behavioral control." Physiol Rev **88**(1): 37-57.

Tolias, A. S., A. S. Ecker, A. G. Siapas, A. Hoenselaar, G. A. Keliris and N. K. Logothetis (2007). "Recording chronically from the same neurons in awake, behaving primates." J Neurophysiol **98**(6): 3780-3790.

Watanabe, M. (1996). "Reward expectancy in primate prefrontal neurons." Nature **382**(6592): 629-632.

Wehr, M. and G. Laurent (1996). "Odour encoding by temporal sequences of firing in oscillating neural assemblies." Nature **384**(6605): 162-166.

Wilson, F. A., S. P. Scalaidhe and P. S. Goldman-Rakic (1993). "Dissociation of object and spatial processing domains in primate prefrontal cortex." Science **260**(5116): 1955-1958.

Wolfe, J. M. (1984). "Reversing ocular dominance and suppression in a single flash." Vision Res **24**(5): 471-478.

SUPPLEMENTARY INFORMATION

Supplementary Figures

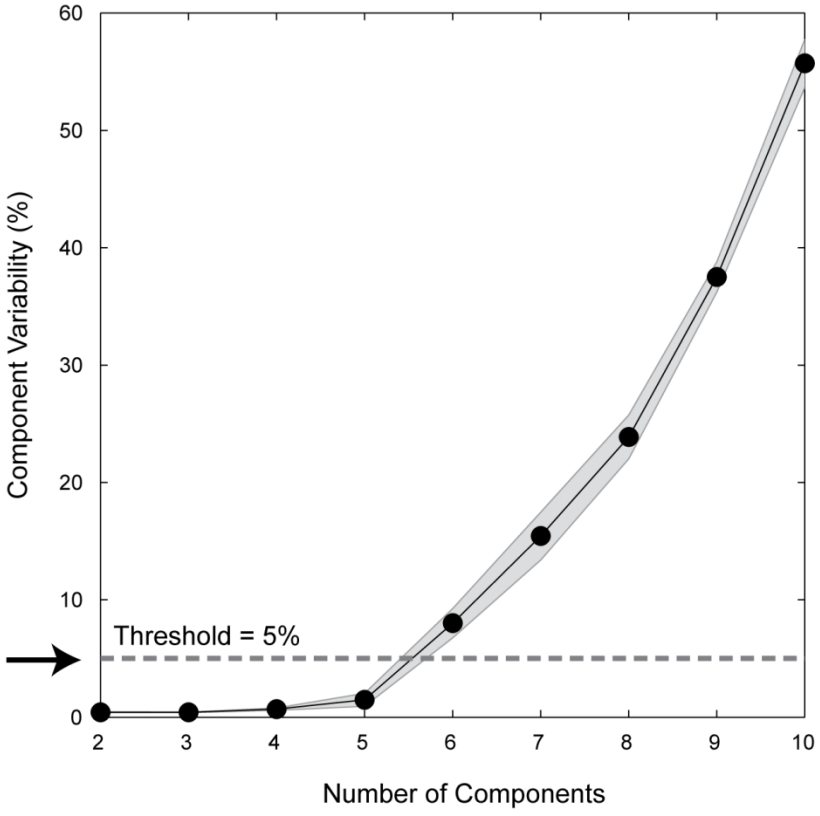

Figure 1: Variance estimate utilized for the choice of components. Component Variability is plotted as a function of the number of components chosen for the nnmf procedure. The standard deviation is across 10 different runs. The threshold is set at 5 percent, which directed our final choice for the number of components.

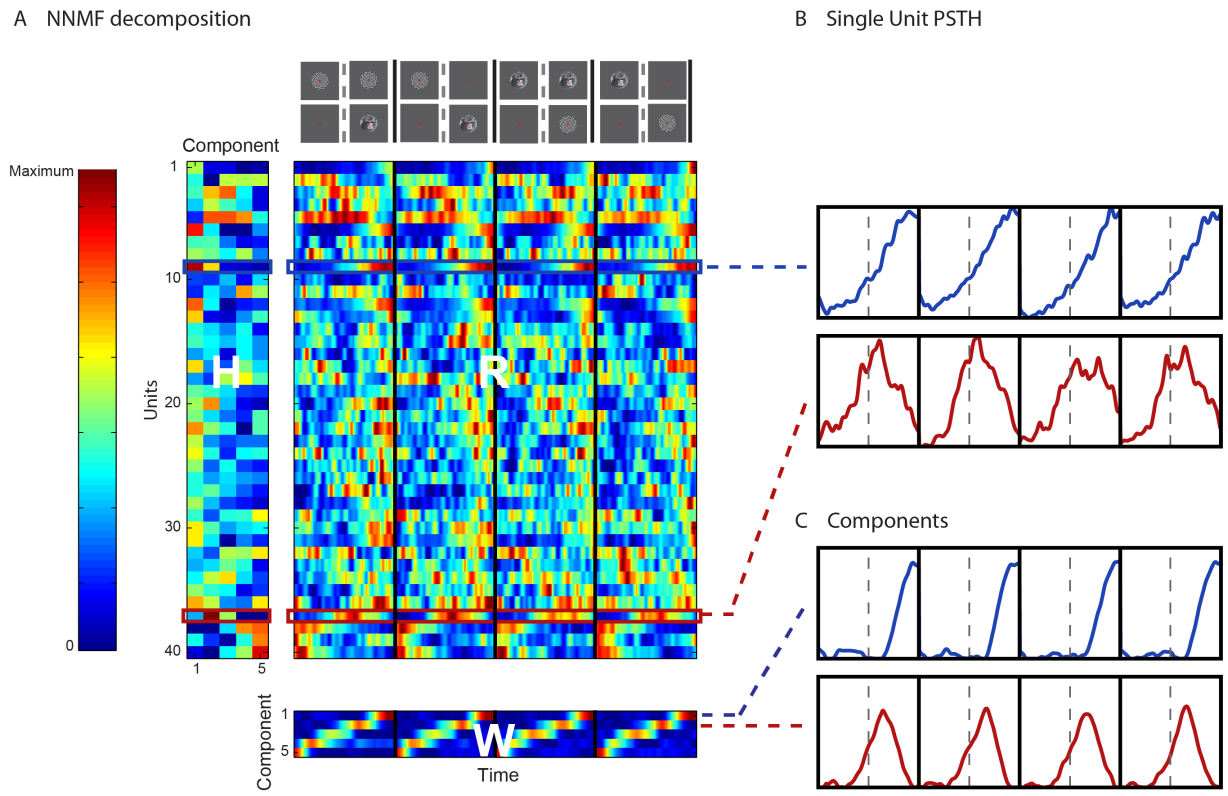

Figure 2: Principle of the NNMF decomposition**.** (A) The matrix of single unit average response (center) is decomposed into the product of two non-negative matrices: W the matrix of the time varying response of each component (left hand side) representing typical response patterns for phase preferring units, and H the matrix gathering the contribution of each component to a given unit response. (B) Two example phase preferring single unit responses (in blue and green), each of them has a dominant coefficient in the corresponding row of the matrix H in panel A, corresponding to component 1 and 3 respectively. (C) Time course of the two components corresponding to the dominant response pattern of the respective single unit responses shown in panel B.

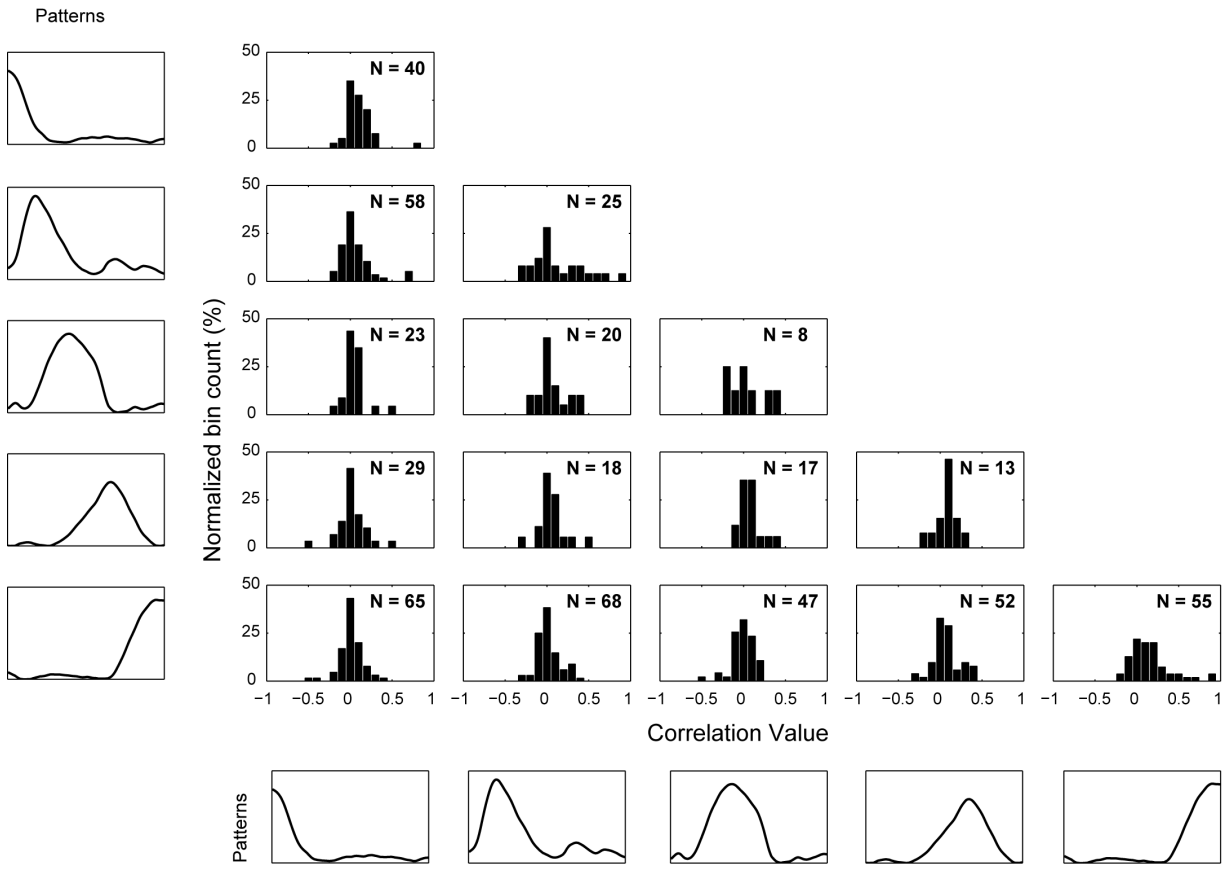

Figure 3: Displayed are histograms which contribute to the average correlations in the noise correlation matrix shown in figure 6 in the main text. Upon a closer inspection of the histogram, one can observe its gradual bias towards zero from positive side, when one compares the principal diagonal to the lateral diagonals of the matrix.

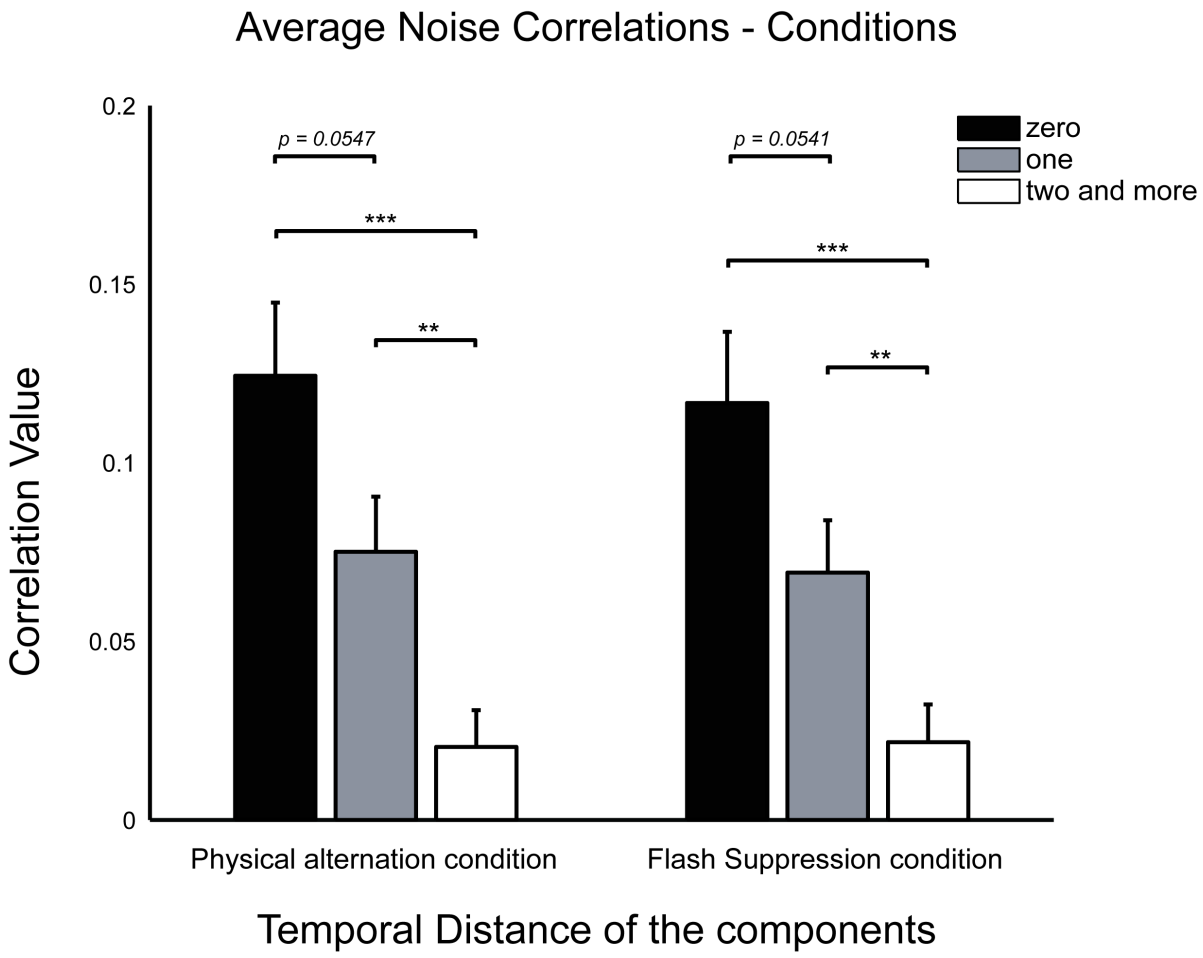

Figure 4: Noise Correlation for different stimulus conditions. Average noise correlations as a function of temporal distance displayed a decrease as a function of temporal distance for both the flash suppression as well as the physical alternation conditions.

A.7 Development of tube tetrodes and a multi-tetrode drive for deep structure electrophysiological recordings in the macaque brain.

"If you want to build a ship, don't herd people together to collect wood, and don't assign them tasks and work, but teach them to long for the endless immensity of the sea."

Antoine de Saint-Exupery, "Wisdom of the Sands"

Journal of Neuroscience Methods 216 (2013) 43–48

Contents lists available at SciVerse ScienceDirect

Journal of Neuroscience Methods

journal homepage: www.elsevier.com/locate/jneumeth

Basic Neuroscience

Development of tube tetrodes and a multi-tetrode drive for deep structure electrophysiological recordings in the macaque brain

Vishal Kapoor[a,*], Eduard Krampe[a], Axel Klug[a], Nikos K. Logothetis[a,b], Theofanis I. Panagiotaropoulos[a,**]

[a] Max-Planck-Institute for Biological Cybernetics, Department of Physiology of Cognitive Processes, Spemannstrasse 38, 72076 Tübingen, Germany
[b] Division of Imaging Science and Biomedical Engineering, University of Manchester, Manchester M13 9PT, UK

HIGHLIGHTS

- Developed new stiffer tube tetrodes for deep brain electrophysiology.
- Protocol for constructing tube tetrodes with standard laboratory tools.
- Developed a microdrive for advancing these tube tetrodes in macaque brain.
- Conducted electrophysiology with tube tetrodes in the inferotemporal cortex.
- Multiple single units can be recorded with tube tetrodes.

ARTICLE INFO

Article history:
Received 17 December 2012
Received in revised form 14 March 2013
Accepted 22 March 2013

Keywords:
Electrophysiology
Tube tetrodes
Macaque
Inferotemporal cortex
Microdrive
Population recordings

ABSTRACT

Understanding the principles that underlie information processing by neuronal networks requires simultaneous recordings from large populations of well isolated single units. Twisted wire tetrodes (TWTs), typically made by winding together four ultrathin wires (diameter: 12–25 μm), are ideally suited for such population recordings. They are advantageous over single electrodes; both with respect to quality of isolation as well as the number of single units isolated and have therefore been used extensively for superficial cortical recordings. However, their limited tensile strength poses a difficulty to their use for recordings in deep brain areas. We therefore developed a method to overcome this limitation and utilize tetrodes for electrophysiological recordings in the inferotemporal cortex of rhesus macaque. We fabricated a novel, stiff tetrode called the tube tetrode (TuTe) and developed a multi-tetrode driving system for advancing up to 5 TuTes through a ball and socket chamber to precise locations in the temporal lobe of a rhesus macaque. The signal quality acquired with TuTes was comparable to conventional TWTs and allowed excellent isolation of multiple single units. We describe here a simple method for constructing TuTes, which requires only standard laboratory equipment. Further, our TuTes can be easily adapted to work with other microdrives commonly used for electrophysiological investigation in the macaque brain and produce minimal damage to the cortex along its path because of their ultrathin diameter. The tetrode development described here could allow studying neuronal populations in deep lying brain structures previously difficult to reach with the current technology.

1. Introduction

Since Galvani's discovery of 'animal electricity', electrophysiology has been instrumental in understanding and unraveling brain function (Galvani, 1791; Scanziani and Hausser, 2009). From the recording of the first action potential in the giant squid axon (Hodgkin and Huxley, 1939), the technique has recently evolved to utilize multi-electrode arrays which facilitate recording the activity of several neurons simultaneously (Pine, 2006). As a result, the initial approach of linking the activity of single neurons to sensory input or behavior (Barlow, 1972; Evarts, 1968) has progressed toward understanding information processing at the level of neuronal ensembles or populations (Deadwyler and Hampson, 1995; Quian Quiroga and Panzeri, 2009). However, this requires ascertaining the origin of spikes recorded on the tip of a microelectrode to single neurons with high reliability. To resolve this issue, parallel advances have been made in

* Corresponding author at: Max Planck Institute for Biological Cybernetics, Spemannstrasse 38, 72076, Tübingen, Germany. Tel.: +49 7071 601697, fax: +49 7071 601652.
** Corresponding author at: Max Planck Institute for Biological Cybernetics, Spemannstrasse 38, 72076, Tübingen, Germany. Tel.: +49 7071 601655, fax: +49 7071 601652.
E-mail addresses: vishal.kapoor@tuebingen.mpg.de (V. Kapoor), theofanis.panagiotaropoulos@tuebingen.mpg.de (T.I. Panagiotaropoulos).

0165-0270/$ – see front matter © 2013 Elsevier B.V. All rights reserved.
http://dx.doi.org/10.1016/j.jneumeth.2013.03.017

microelectrode technology as well as spike sorting algorithms (Buzsaki, 2004).

The advances in microelectrode technology, aimed at better isolation of single neurons from the recorded data started with the invention of the stereotrode, consisting of two wires twisted together (McNaughton et al., 1983). The paper describing it, already indicated the possible inception of its successor, the twisted wire tetrode (TWT), "*a closely spaced tetrahedral array of recording electrodes with tips sufficiently close together to record signals from overlapping population of neurons*". They theorized, that such an electrode "*should permit the unique identification of all neuronal spikes which exceed the noise level*". This was shown in a later study (Gray et al., 1995) which not only indicated that the number of isolated single neurons with a tetrode were more than single electrodes or stereotrodes, but also demonstrated their reliability over its peers. Their unique advantage stems from having four tips, close together so that they could all record the spikes from the same neuron. The spike amplitude, however being inversely proportional to the distance from each one of them, can be distinct on each tip which allows triangulating the signal source to a single neuron (Gray et al., 1995; Harris et al., 2000; Henze et al., 2000). Tetrodes have, therefore been used extensively for extracellular electrophysiological recordings of neuronal populations (Buzsaki, 2004). Such large ensemble recordings have been instrumental for understanding population coding of sensory input in the macaque brain (Ecker et al., 2011; Ohiorhenuan et al., 2010).

A limitation, however of TWTs is their weak tensile strength which has impeded their use for recordings in deep brain structures. Further, splaying of the tetrode tips has been a valid concern during chronic implantation (Jog et al., 2002). Because of these constraints, their use for electrophysiological recordings in primates in deep structures has been relatively sparse and just recently reported (Erickson and Desimone, 1999; Erickson et al., 2000; Feingold et al., 2012; Santos et al., 2012; Skaggs et al., 2007; Thome et al., 2012). Among these, earlier studies employed tetrodes for electrical recording in the perirhinal cortex of the macaque using a telescoping guide tube system with twisted wire tetrodes glued inside 30 gauge stainless steel tubes (Erickson and Desimone, 1999; Erickson et al., 2000). More recently, they have been used within a chronically implanted 'hyperdrive', which permitted recordings at depths of 30–50 mm below the brain surface, in the hippocampus (Skaggs et al., 2007; Thome et al., 2012). However, the spatial position of these tetrodes in such a configuration is fixed at the time of implantation and can only be manipulated in depth, thus allowing only a limited area of the brain to be sampled. Therefore, the ethical and resource limitations for primate use require that a method be developed for neurophysiological recordings with tetrodes in the primate brain at depths difficult to reach with conventional twisted wire tetrodes and able to sample from a large area in the same animal. A method for extracellular electrophysiological recordings with many twisted wire tetrodes in deep structures would allow us to sample activity of several single units simultaneously, allowing extensive functional characterization of neuronal activity in these areas, where the details of neuronal interactions remain largely unknown. Further, it shall significantly reduce the number of experiments and animals required for acquiring comparable amounts of electrophysiological data.

Two further recent reports have demonstrated the ability to target several brain structures, both superficial and deep, simultaneously by developing novel microdrives (Feingold et al., 2012; Santos et al., 2012). The main limitation of the reported techniques is the larger cannulae holding the electrodes rather than the electrode itself, since both would enter the brain tissue. These cannulae ranged from 27 gauge (outer diameter (OD): 0.016 in.) (Feingold et al., 2012) to 30 gauge (OD: 0.012 in.) (Santos et al., 2012), and would cause more tissue damage in their path as compared to the probe they enclose, which is smaller in diameter (~0.12 mm, Feingold et al., 2012; ~0.07 mm, Skaggs et al., 2007; ~0.06 to 0.08 mm, Santos et al., 2012). These cannulae, however are essential in order to reach the distance the tetrode needs to travel in the brain without bending. A suitable way to overcome this limitation would be to develop a technique for conferring stiffness to the tetrodes, but at the same time keeping the tetrode-cannula diameter as small as possible. This should allow exploiting the already demonstrated superior features of twisted wire tetrodes with respect to yield and reliability of the isolated single units (Gray et al., 1995) while extending its applicability to deeper structures in the macaque brain. To this end, we strengthened the twisted wire tetrodes by developing a simple laboratory technique of inserting them inside 35 gauge stainless steel tubes (OD: 0.005 in., inner diameter (ID): 0.002 in.). A custom drive, for holding and advancing up to 5 tetrodes independently was also developed. These novel TuTes are in size about 10–20% of that of the cannulae, which have been used in the most recent studies (Erickson and Desimone, 1999; Erickson et al., 2000; Feingold et al., 2012; Santos et al., 2012; Skaggs et al., 2007; Thome et al., 2012).

2. Materials and methods

2.1. Tube tetrode fabrication

Standard methods were used for fabricating long TWTs (Nguyen et al., 2009). They are mentioned here briefly. First, an 85 cm long piece of insulated NiCr wire (OD: 0.0005 in., RO-800, Sandvik Wire and Heating Technology, Moerfelden-Walldorf, Germany) was cut out from a roll. The two ends of the wire were brought together and then gently stroked throughout the length by holding and passing the wires between the thumb and index finger. The wire was then placed around a horizontal bar so that equal length hanged on both sides. The lower ends of the wires (four ends altogether) were then clamped with a crocodile clip (modified with a metallic bar running through its lower end). The wires were then rotated clockwise using a magnetic rotator placed below the crocodile clip for about 50 turns. Next, a heat gun was used to melt the insulation by moving the gun from the bottom to the top and at a distance of about 2 cm from the wire with two exceptions. First, the heat gun was stopped just before the loop on the top, since this part shall be later used to pull the tetrode inside the 35 gauge tube. Second, no heat was applied for a length of ~1.5 cm at a distance 1 cm from the bottom, since these ends shall be later separated. The motion was repeated downwards and this entire procedure (bottom-top-bottom motion) was repeated twice. The tetrode was then removed from the bar and pushed through a 12 cm long polyimide tubing (OD: 0.0055 in., MinVasive Components, GA, USA) by holding either of them with carbofib tweezers (Accu-Tek 304, Aven Inc., MI, USA). Finally, the tetrode and polyimide assembly was threaded through an 11 cm long, 30 gauge stainless steel tube (OD: 0.012 in., Small Parts Inc., FL, USA). After this, the non loopy end was cut with the help of scissors and the non heated ends at the bottom were separated. This, we call the 'loopy tetrode'. The different parts are shown in Fig. S1A.

All further operations were carried with an aid of a regular light microscope. Deburred, cleaned and ~2–4 cm long, 35 gauge stainless steel tubes (304SS, welded and drawn, hard temper, Vita Needle, MA, USA) were first beveled by grinding them with a sharpening stone (Sharpening Stone – Triangle, Fine Science Tools, Heidelberg, Germany). A piece of stainless steel wire (Diameter: 0.00078 in., 304, California Fine Wire Company, CA, USA), with a length of 5–7 cm was threaded inside the ultrathin 35 gauge tubes through the non-beveled round end. The wire was then passed through the loop of the 'loopy tetrode' and back inside the tube

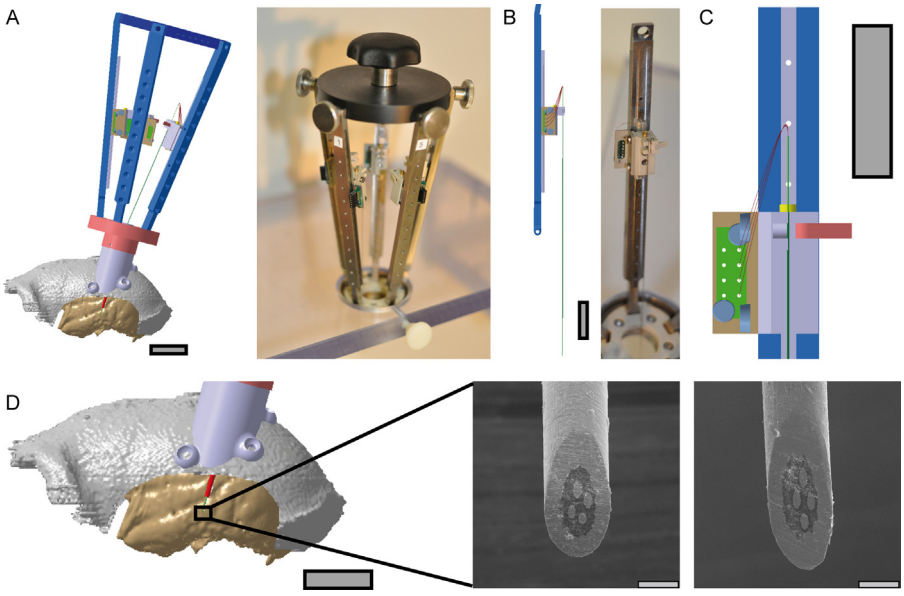

Fig. 1. Custom designed multi-tube tetrode drive and tube tetrodes. (A) Computer-aided design (CAD) model of the multi-tube tetrode (TuTe) drive is shown sitting on top of a ball and socket chamber. The chamber sits on a model of the skull extracted from the MRI scan of a macaque. The skull has been stripped to expose the temporal lobe. Adjacent to it is shown an actual photograph of the drive on a plexiglass stand. (B) Single leg of the multi-TuTe drive, holding a TuTe, shown as a CAD model and an actual photograph. (C) Magnified view from a single leg exemplifying the TuTe's connection to the electrode interface board (EIB). The TuTe's wires make contact and are held in position by inserting a gold pin through the holes of the EIB. Also seen is the red clip that can be closed in order to hold the TuTe in place. (D) Cropped and magnified from (A) to show the TuTe's placement in the temporal lobe. Adjacent are shown the scanning electron micrograph images of the TuTe. The four tips of the TuTe can be clearly seen embedded within the epoxy glue inside a 35 guage stainless steel tube. Scale bars for all the CAD images: Length: 20 mm and width: 5 mm. Scale bar for the electron micrographs: 80 μm. (For interpretation of the references to color in this figure legend, the reader is referred to the web version of the article.)

for 1–1.5 cm. The free end of the wire toward the beveled end of the tube was then pulled with a pair of metallic forceps (Inox Super Fine Tip, Fine Science Tools, Heidelberg, Germany). Once the wires were through, polyimide was pulled over the tetrode wires until the tip of the 35 gauge tube. Following this, the 35 gauge tube was pushed inside the 30 gauge holding tubes. Epoxy glue (EPO TEK 353 NDT – Epoxy Technology Inc., MA, USA) was then applied to the tip and the joint where the 35 gauge tube entered the 30 gauge holding tube. After the glue was dry, which typically took about 12–24 h; the wires were cut using a pair of sharp scissors (Vannas Spring Scissors – Straight (4 mm blade), Fine Science Tools, Heidelberg, Germany) carefully and close to the tip. Finally the tip was grinded and excess glue removed with a grinding stone (Sharpening Stone – Triangle, Fine Science Tools, Heidelberg, Germany), until the four tips were clearly visible under the microscope. (All current procedures are schematically shown in Fig. S1B.)

The finished TuTes were then loaded on to the electrode holders mounted onto a custom built drive (Fig. 1A). The electrode holders (Fig. 1C) were specially designed with a clipping mechanism for holding 30 gauge stainless steel tubes. Each of the four TuTe wires was then connected to custom built Electrode Interface Boards, mounted next to the electrode holder by inserting them into holes and the connection was enforced by inserting a gold pin (EIB Pins, Large, Neuralynx, AZ, USA) through them. Finally, the TuTe impedance was lowered below 1 MΩ by electroplating the tip of each channel with gold. Every TuTe holder could be moved

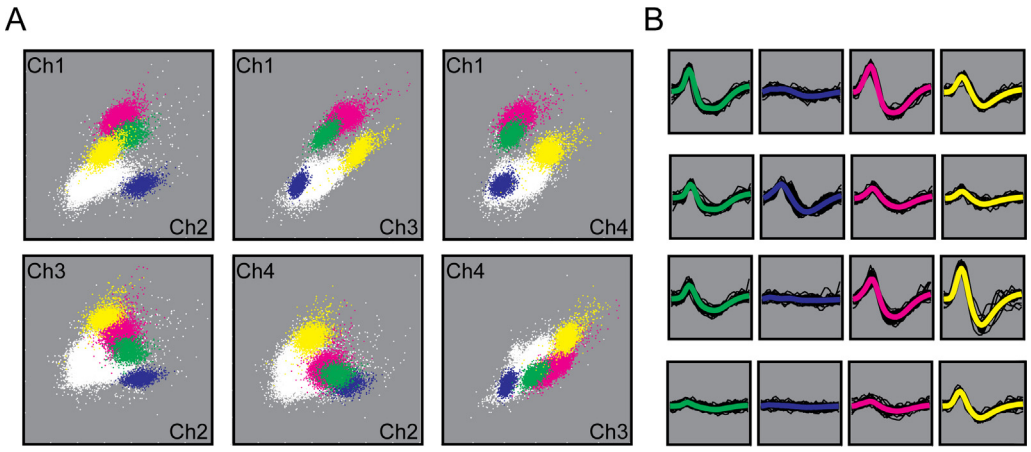

Fig. 2. Cluster isolation using PCA based spike sorting and Klusters. (A) Waveforms are projected onto the first principal component axis of each channel. Four distinct clusters can be seen. (B) Waveforms of the single units corresponding to different clusters. Shown are average waveform (same color as the cluster) overlaid on sample waveforms (in black) of the four different clusters recorded on the four TuTe channels. Also see Fig. S4 for the stability of isolated clusters across time in the electrophysiological recordings obtained with TuTes.

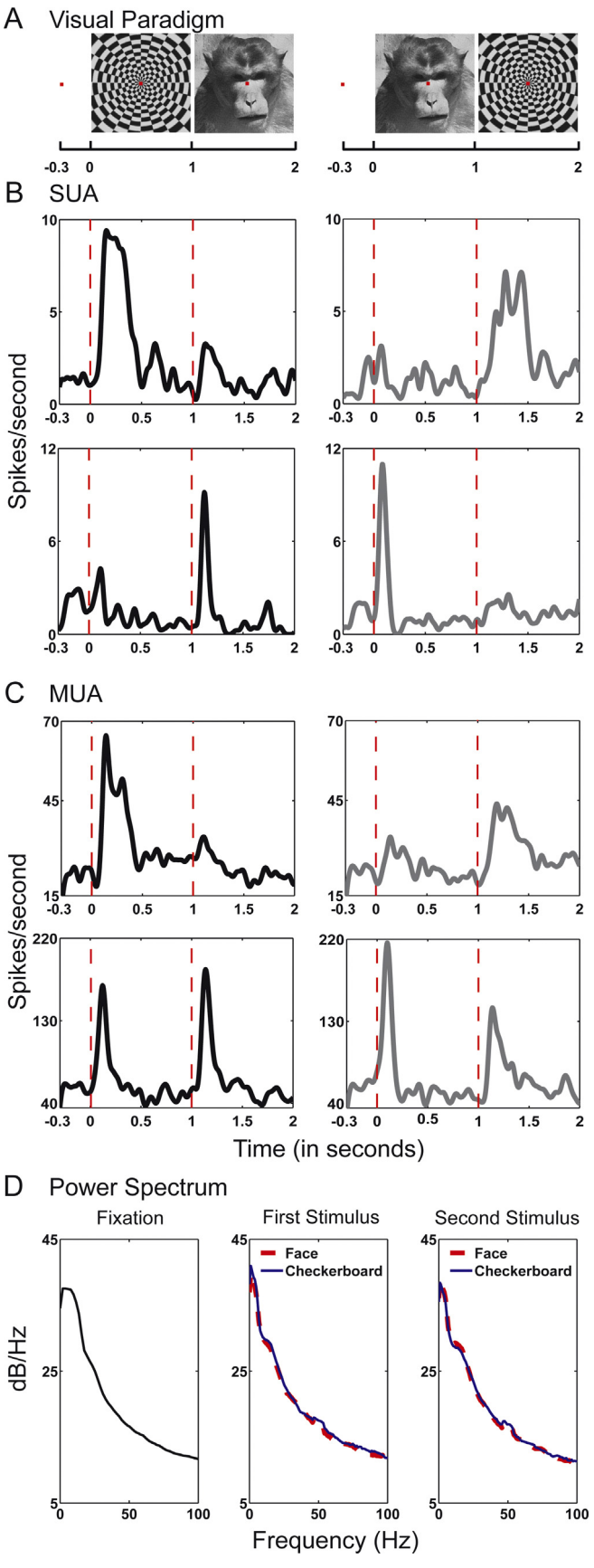

Fig. 3. Visual paradigm and neuronal discharges recorded with tube tetrodes. (A) The visual paradigm. Trial started with a fixation spot displayed in the center of the screen for duration of 300 ms following which either a checkerboard stimulus or a monkey face stimulus was presented monocularly for 1 s. After this, a second disparate stimulus was presented in the other eye for duration of 1 s. The monkey was awarded with juice following the successful fixation for the entire duration of the trial. (B) Example single unit activity (SUA) recorded from the temporal lobe. The first panel shows a cell which shows preference in activity to the checkerboard while in the second panel is a cell showing a preference for the monkey face. (C) Example multi unit activity (MUA) recorded in the temporal lobe. The first panel shows MUA which shows preference to the checkerboard stimulus. The second example (lower panel) has unspecific, albeit strong visual responses. (D) Spectral power as calculated from the local field potential recorded with the TuTe from a single site in the temporal lobe. The three columns from left to right correspond to the power spectrum calculated during three windows, namely, the fixation period (combined across the two conditions), the first stimulus (time period: 0–1000 ms) and the second stimulus (time period: 1001–2000 ms) presentation.

via its connection to a flexible shaft, which was driven by a motor, controlled through a custom written computer program in Matlab (Mathworks Inc., MA, USA).

2.2. Tube tetrode tip examination with electron microscopy

A scanning electron microscope (SEM) photograph of the TuTe tip was made after the grinding procedure. The tips are shown in Fig. 1D and exemplify the typical tip geometries that were produced. All four channels of the TuTe observable in the micrograph have similar diameter and their integrity is preserved.

2.3. Electrophysiological recordings with tube tetrodes

One healthy adult male rhesus monkey (Macaca mullatta) participated in electrophysiological recordings. All experiments were approved by the local authorities (Regierungspraesidium) and were in full compliance with the applicable guidelines of the European community (EUVD 86/609/EEC) for the care and use of laboratory animals. The region of interest was localized based on the high resolution MR scans collected using a vertical 4.7 T scanner (Biospec 47/40c; Bruker BioSpin, Ettlingen, Germany) with the animal under general anesthesia. Following this, a cranial head post and a ball and socket recording chamber (first developed by Schiller and Koerner, 1971; modified versions were used for the electrophysiological investigation of the inferotemporal cortex by Leopold et al., 2006; Logothetis et al., 1995; Sheinberg and Logothetis, 1997; Sigala et al., 2011) with a 17 gauge stainless steel tube passing through its center, custom designed to fit the skull of the animal were manufactured (Logothetis et al., 2002). The surgical procedures for the implants were carried out in aseptic conditions under general anesthesia and have been reported previously (Logothetis et al., 2002). The ball and socket chamber was implanted on the left hemisphere, with the aid of stereotactic coordinates with the center of the chamber at AP (anterior–posterior): 7 mm, ML (mediolateral): 21 mm. The well of the chamber was tilted with an angle of 15° posteriorly.

Neural activity was recorded using the custom designed TuTes placed in a microdrive, where each of these tetrodes could be driven independently through the guide tube of the ball and socket chamber. Activity recorded by the tetrodes was acquired, amplified, filtered and stored using the Cheetah data acquisition system (Neuralynx, AZ, USA). Local field potential (LFP) was acquired by analog band pass filtering (1–475 Hz) the raw voltage signal. Events detected in the high pass analog filtered signal (0.6–6 kHz) typically crossing the threshold of 25 μV were classified as multiunit spiking activity (MUA). The sampling rate of this signal was 32 kHz and digitized at 12 bits. Single units were sorted offline from the high frequency thresholded signal using customized algorithms, which used the first three components of the recorded waveforms as features (the details of spike sorting methods have been previously reported, Tolias et al., 2007). Visual inspection of the resulting clusters was performed using Klusters (Lynn Hazan, Buzsáki Lab, Rutgers, Newark, NJ). Fig. 2 exemplifies the excellent

cluster isolation achieved with TuTes. Additionally, the stability of the recordings with TuTes across time is demonstrated in Fig. S4.

3. Results

3.1. Visually responsive spiking activity in the temporal lobe

We conducted electrophysiological recordings using the TuTes driven to the temporal lobe of the rhesus macaque with the custom built microdrive, positioned on a ball and socket chamber. The animal was trained to maintain eye position on a red fixation spot (size: 0.2°) within a ±1.5° fixation window, while visual stimuli (size: 2–3°) were presented monocularly through a stereoscope. Specifically, the task started with a fixation spot presented binocularly for 300 ms. Following this, randomly on half of the trials, a visual stimulus, such as a checkerboard pattern was presented monocularly, for 1000 ms followed by a monkey face stimulus in the other eye for 1000 ms (Fig. 3A). In the rest half of the trials, the order of the stimuli was reversed. Following the second stimulus, the animals had to maintain fixation on the fixation spot for 100–300 ms. The trial was successfully completed, when the animal maintained fixation during the entire duration of 2400–2600 ms. Fig. 3B shows responses of two example single units when these stimuli were presented. The first single unit responded more to the checkerboard stimulus, while the second one increased its activity more in response to the monkey face. Two examples of MUA are shown in Fig. 3C. The MUA in the upper panel shows that the activity was higher when the checkerboard stimulus was presented. MUA in the lower example shows a strong unspecific visual response.

3.2. Power spectral density of the local field potential signal

We estimated the spectral power of the LFP signal recorded from the temporal lobe with the TuTe. The spectrum was calculated during three different periods (Fig. 3D), the first being during the presentation of the fixation spot, lasting 300 ms. We further calculated the spectral power during the presentation of the first and the second stimulus for the two different visual stimuli, the face and the checkerboard. The power followed a similar trend for the two different stimuli presented. As expected, most of the power was concentrated in the lower frequencies (1–4 Hz). The amplitude of the LFP power had an inverse relationship with temporal frequency, thus, following the power law, a typical feature of the LFP signal (Bédard et al., 2006).

4. Discussion

We have developed a novel electrode-fabrication technique for constructing a new kind of tetrode, namely the TuTe, using standard laboratory equipment. These TuTes are particularly advantageous for recordings in deep brain structures due to their rigidity and stiffness in comparison to conventional TWTs. Further, the diameter of these tetrodes is ~0.127 mm and their lengths customizable up to 40 mm; thus, being the thinnest lab manufactured tetrodes of such lengths and reasonable rigidity. Santos et al. (2012) have recently reported using tetrodes with probe diameter of ~0.06–0.08 mm. However, the guide cannula holding these probes is ~0.3 mm in diameter which also enters the brain tissue. These tubes are thus about 5.5 times larger in size than the TuTes we report and so would be the damage caused to the brain tissue above the region of interest. Further, our tetrodes are completely customizable to microdrives recently reported for deep structure recordings in primates (Feingold et al., 2012; Santos et al., 2012; Skaggs et al., 2007) and can therefore be easily integrated. In addition, to the best of our knowledge, we are the first to report a tetrode microdrive for advancing them through a ball and socket chamber for recording in the inferior temporal cortex of a rhesus macaque. Recording with a ball and socket chamber permits a unique advantage with respect to electrophysiological investigation of a large area since several deep brain regions (like subdivisions of the temporal lobe, Sheinberg and Logothetis, 1997; Sigala et al., 2011) can be explored using the same implant.

This technology is timely and needed as modern neuroscience rapidly progresses toward multielectrode electrophysiological recordings in order to better understand representation of information at the level of neuronal populations during diverse cognitive phenomena. In the past, tetrodes have aided extensively in pursuing such research directions with primates, because of their advantages over conventional electrodes in the number and isolation quality of single units recorded (Gray et al., 1995; Tolias et al., 2007). However, mostly recently, but sparsely, TWTs have been used for recordings in deeper structures of the macaque brain (Erickson and Desimone, 1999; Erickson et al., 2000; Santos et al., 2012; Skaggs et al., 2007; Thome et al., 2012). The TuTes reported here are ideal for such a purpose, since, not only do they overcome any limitations of depth recordings with tetrodes, but also provide a solution with minimal amount of tissue damage along the electrode path. Moreover, the glue, within which the wires of the TuTe are embedded at the tip, ensures that no splaying can occur, a caveat that has been previously reported (Jog et al., 2002).

TuTes shall aid in extending the current methodologies of multielectrode electrophysiological recording from the easily accessible superficial cortex to subcortical areas as well as cortical areas, lying deep within the brain (e.g. sulci). While other groups have tried to address this need by building microdrives suited for driving tetrodes to multiple cortical and subcortical areas at the same time, the tissue damage resulting from the cannulae used has been a valid and ethical issue. Chronically implanted microdrives with tetrodes have also been utilized in the past for deep brain electrophysiology (Skaggs et al., 2007; Thome et al., 2012). A difficult parameter to judge is whether, the daily insertion of several smaller TuTes would cause less or more damage as compared to a one time implantation of a thicker guide tube enclosing a tetrode. The chronic preparation does provide the advantage of limiting the damage to precise tracks, where these guide tubes pass through, albeit larger than the TuTes at a specific location. However, such a chronic preparation limits the recording locations to the sites of the implanted guide tubes, while allowing neurophysiological exploration at variable depths. With a routine of daily insertion of TuTes, the neural tissue damage shall occur at a new location everyday, while allowing the possibility of recording from several target locations during the course of the experiment. The experimental demands, therefore shall dictate the methodology of choice. Our tetrodes with adequate rigidity and ultra small diameter provide the possibility of achieving this goal with minimal tissue damage in the electrode track. Moreover, a simple protocol requiring only simple lab tools for their construction makes them a cost effective solution. Finally, the modularity of the TuTe, should make it theoretically, easily adaptable for use with other commercially available as well as custom microdrives.

Acknowledgements

We would like to thank Juergen Berger for help with acquiring the electron micrographs and Michael Beyerlein for the ex vivo anatomy. We would also like to thank Axel Oeltermann, Marina Fridman and Carina Immer for their excellent technical help. This study was supported by the Max Planck Society.

Appendix A. Supplementary data

Supplementary data associated with this article can be found, in the online version, at http://dx.doi.org/10.1016/j.jneumeth.2013.03.017.

References

Barlow HB. Single units and sensation: a neuron doctrine for perceptual psychology. Perception 1972;1:371–94.

Bédard C, Kröger H, Destexhe A. Does the 1/*f* frequency scaling of brain signals reflect self-organized critical states? Physical Review Letters 2006;97:118102.

Buzsaki G. Large-scale recording of neuronal ensembles. Nat Neurosci 2004;7:446–51.

Deadwyler SA, Hampson RE. Ensemble activity and behavior: what's the code. Science 1995;270:1316–8.

Ecker AS, Berens P, Tolias AS, Bethge M. The effect of noise correlations in populations of diversely tuned neurons. J Neurosci 2011;31:14272–83.

Erickson CA, Desimone R. Responses of macaque perirhinal neurons during and after visual stimulus association learning. J Neurosci 1999;19:10404–16.

Erickson CA, Jagadeesh B, Desimone R. Clustering of perirhinal neurons with similar properties following visual experience in adult monkeys. Nat Neurosci 2000;3:1143–8.

Evarts EV. A technique for recording activity of subcortical neurons in moving animals. Electroencephalogr Clin Neurophysiol 1968;24:83–6.

Feingold J, Desrochers TM, Fujii N, Harlan R, Tierney PL, Shimazu H, Amemori K, Graybiel AM. A system for recording neural activity chronically and simultaneously from multiple cortical and subcortical regions in nonhuman primates. J Neurophysiol 2012;107:1979–95.

Galvani L. Aloysii Galvani De viribus electricitatis in motu musculari commentarius. Ex Typographia Instituti Scientiarum: Bononiae; 1791.

Gray CM, Maldonado PE, Wilson M, McNaughton B. Tetrodes markedly improve the reliability and yield of multiple single-unit isolation from multi-unit recordings in cat striate cortex. J Neurosci Methods 1995;63:43–54.

Harris KD, Henze DA, Csicsvari J, Hirase H, Buzsaki G. Accuracy of tetrode spike separation as determined by simultaneous intracellular and extracellular measurements. J Neurophysiol 2000;84:401–14.

Henze DA, Borhegyi Z, Csicsvari J, Mamiya A, Harris KD, Buzsaki G. Intracellular features predicted by extracellular recordings in the hippocampus in vivo. J Neurophysiol 2000;84:390–400.

Hodgkin AL, Huxley AF. Action potentials recorded from inside a nerve fibre. Nature 1939;144:710–1.

Jog MS, Connolly CI, Kubota Y, Iyengar DR, Garrido L, Harlan R, Graybiel AM. Tetrode technology: advances in implantable hardware, neuroimaging, and data analysis techniques. J Neurosci Methods 2002;117:141–52.

Leopold DA, Bondar IV, Giese MA. Norm-based face encoding by single neurons in the monkey inferotemporal cortex. Nature 2006;442:572–5.

Logothetis N, Merkle H, Augath M, Trinath T, Ugurbil K. Ultra high-resolution fMRI in monkeys with implanted RF coils. Neuron 2002;35:227–42.

Logothetis NK, Pauls J, Poggio T. Shape representation in the inferior temporal cortex of monkeys. Curr Biol 1995;5:552–63.

McNaughton BL, O'Keefe J, Barnes CA. The stereotrode: a new technique for simultaneous isolation of several single units in the central nervous system from multiple unit records. J Neurosci Methods 1983;8:391–7.

Nguyen DP, Layton SP, Hale G, Gomperts SN, Davidson TJ, Kloosterman F, Wilson MA. Micro-drive array for chronic in vivo recording: tetrode assembly. J Vis Exp 2009:26.

Ohiorhenuan IE, Mechler F, Purpura KP, Schmid AM, Hu Q, Victor JD. Sparse coding and high-order correlations in fine-scale cortical networks. Nature 2010;466:617–21.

Pine J. In: Taketani M, Baudry M, editors. A history of MEA development advances in network electrophysiology. US: Springer; 2006. p. 3–23.

Quian Quiroga R, Panzeri S. Extracting information from neuronal populations: information theory and decoding approaches. Nat Rev Neurosci 2009;10:173–85.

Santos L, Opris I, Fuqua J, Hampson RE, Deadwyler SA. A novel tetrode microdrive for simultaneous multi-neuron recording from different regions of primate brain. J Neurosci Methods 2012;205:368–74.

Scanziani M, Hausser M. Electrophysiology in the age of light. Nature 2009;461:930–9.

Schiller PH, Koerner F. Discharge characteristics of single units in superior colliculus of the alert rhesus monkey. J Neurophysiol 1971;34:920–36.

Sheinberg DL, Logothetis NK. The role of temporal cortical areas in perceptual organization. Proc Natl Acad Sci USA 1997;94:3408–13.

Sigala R, Logothetis NK, Rainer G. Own-species bias in the representations of monkey and human face categories in the primate temporal lobe. J Neurophysiol 2011;105:2740–52.

Skaggs WE, McNaughton BL, Permenter M, Archibeque M, Vogt J, Amaral DG, Barnes CA. EEG sharp waves and sparse ensemble unit activity in the macaque hippocampus. J Neurophysiol 2007;98:898–910.

Thome A, Erickson CA, Lipa P, Barnes CA. Differential effects of experience on tuning properties of macaque MTL neurons in a passive viewing task. Hippocampus 2012;22:2000–11.

Tolias AS, Ecker AS, Siapas AG, Hoenselaar A, Keliris GA, Logothetis NK. Recording chronically from the same neurons in awake, behaving primates. J Neurophysiol 2007;98:3780–90.

Development of Tube Tetrodes and a Multi-Tetrode Drive for deep structure electrophysiological recordings in the macaque brain

Vishal Kapoor [a], Eduard Krampe[a], Axel Klug[a], Nikos K. Logothetis[a,b], Theofanis I. Panagiotaropoulos[a]

a. Max-Planck-Institute for Biological Cybernetics, Department of Physiology of Cognitive Processes, Spemannstrasse 38, 72076, Tübingen, Germany.
b. Imaging Science and Biomedical Engineering, University of Manchester, Manchester M13 9PL, UK.

Supplementary Information

Relative Strength of the Tube Tetrodes Compared to Twisted Wire Tetrodes

We tested and compared the stiffness of TuTe with conventional TWTs. Since we wanted to draw an as accurate as possible comparison across the two kinds of tetrodes, the TWTs used for this procedure, were encased inside polyimide tubing as well as a stainless steel guide tube. Therefore, they looked identical to the loopy tetrodes except that they were without a loop, instead of which a straight TWT came out of the polyimide. Additionally, the tetrode was glued to the polyimide and the different components of the tetrode assembly were adjusted such that only the TWT looked out of the stainless steel guide tube for a length comparable to the TuTes. In a simple procedure, we measured the weight exerted by either of these tetrodes, when normally pushed against a weighing balance, before it started bending. The bending was visualized in two ways. Firstly, we observed by eye, the deflection with respect to a millimeter paper placed right behind the tetrode. Second, it was confirmed by observing the bending with the aid of a microscope camera (DigiMicro Profi, dnt GmbH, Germany), the output of

which could be seen on a computer screen. The procedure was carried out for 5 TuTes and 5 TWTs. On average, the weight exerted by TuTes (4.52 ± 1.02 g (mean ± standard deviation), n = 5) was more than 100 times of that exerted by the TWTs (0.04 ± 0.01 g (mean ± standard deviation), n = 5) before they started to bend.

Supplementary Figure 1:

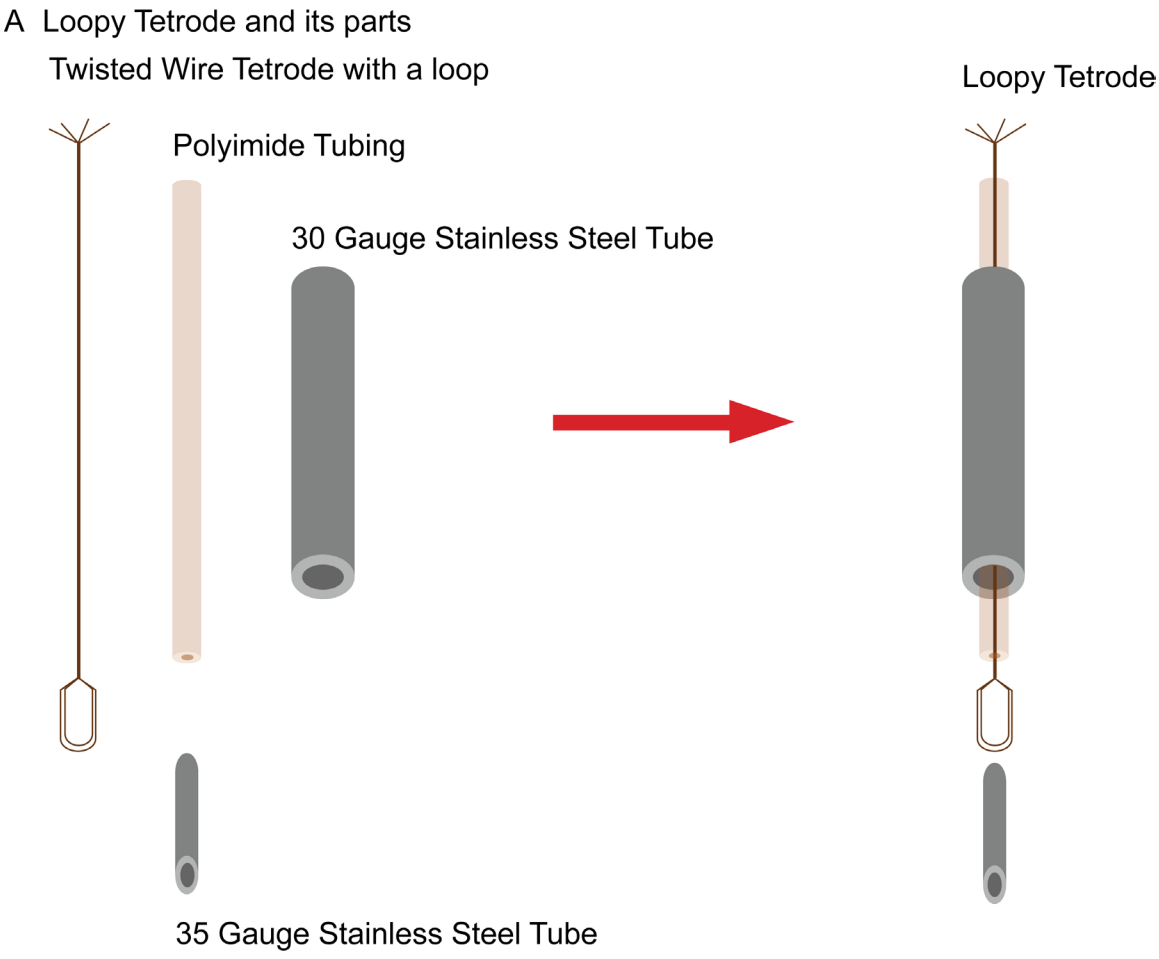

B Protocol for building Tube Tetrodes

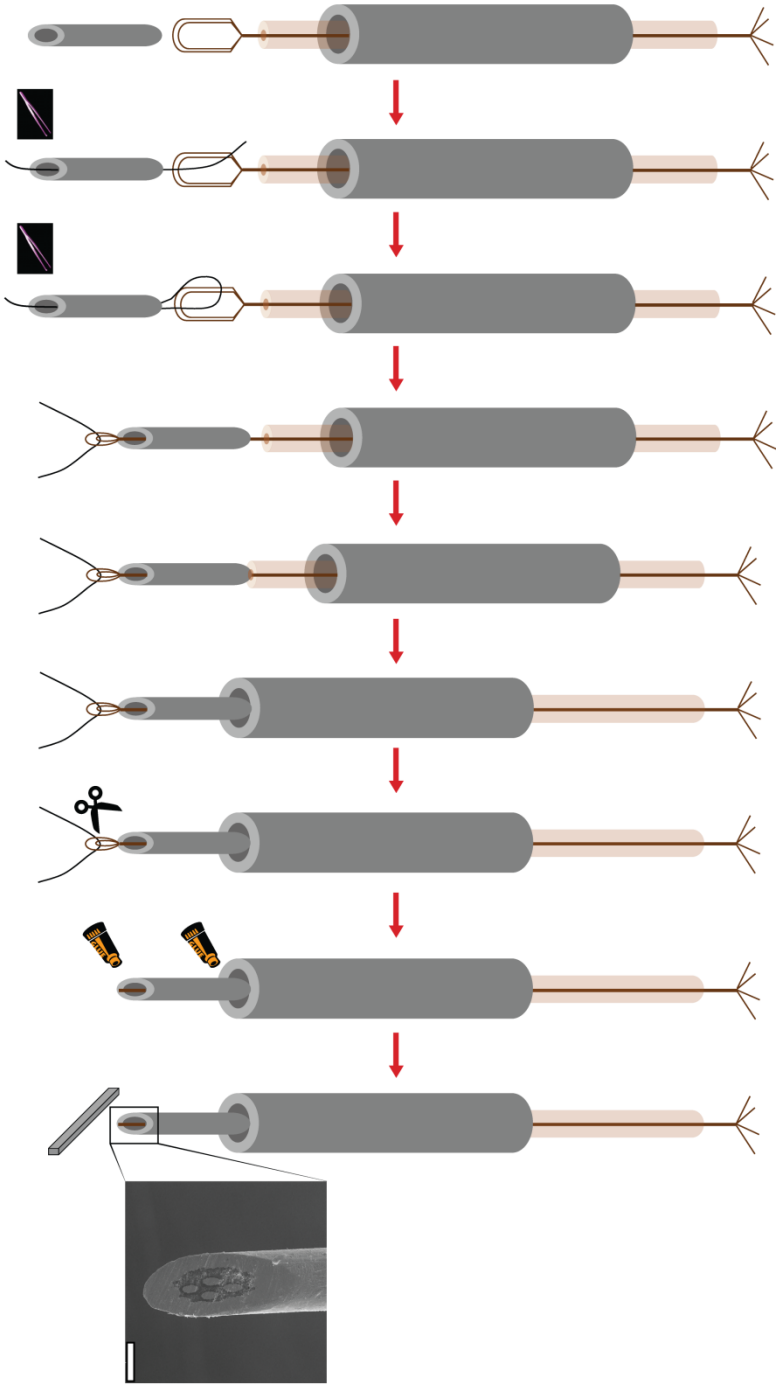

Loopy tetrode and the Tube Tetrode Construction Procedure

(A) Schematic showing different parts of the loopy tetrode. The 35 Gauge Tube is also shown.

(B) Schematic explaining the protocol for constructing the TuTe. Refer to the section 2.1 of the paper for details. Scale bar for the Electron Micrograph – 80 Microns.

Supplementary Figure 2:

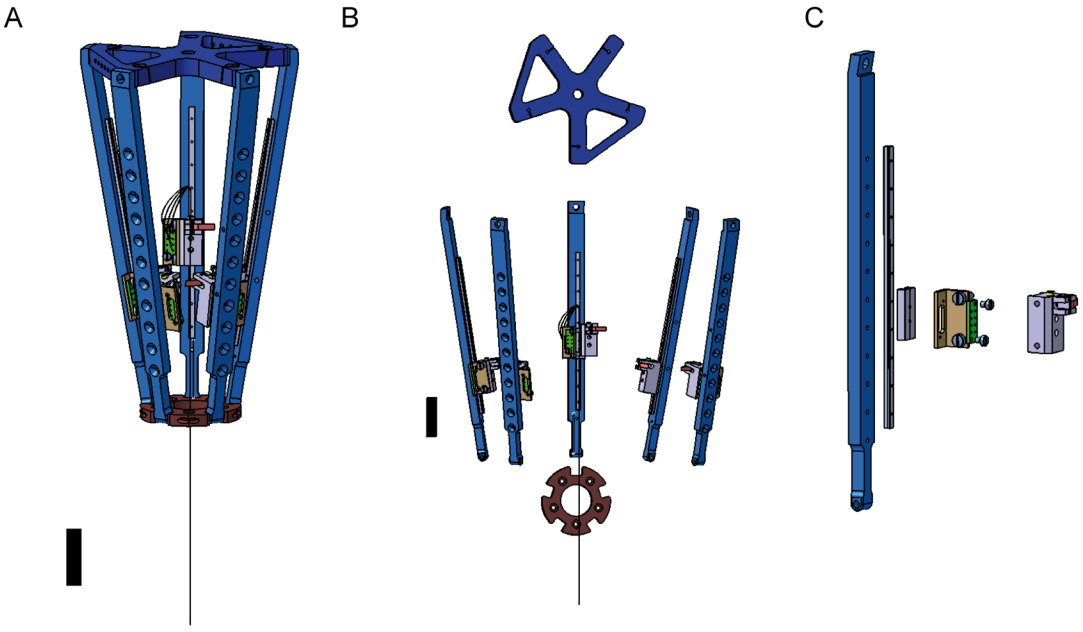

Exploded View of the Multi – Tube Tetrode Drive

The computer aided design (CAD) model of the drive is displayed in a disassembled form in order to display its constituent parts.

(A) The whole drive holding a single TuTe.

(B) The five legs of the drive are shown along with the head and the base part of the drive.

(C) Expanded view of different parts that constitute a single leg. The constituents as we go from left to right 1) base plate, 2) Guidance rail, 3) Slider, 4) Guide Slide, 5) TuTe interface board holder, 6) TuTe interface board 7) TuTe clamper.

Scale bars shown besides the CAD images: Length - 20mm and width - 5mm.

Supplementary Figure 3:

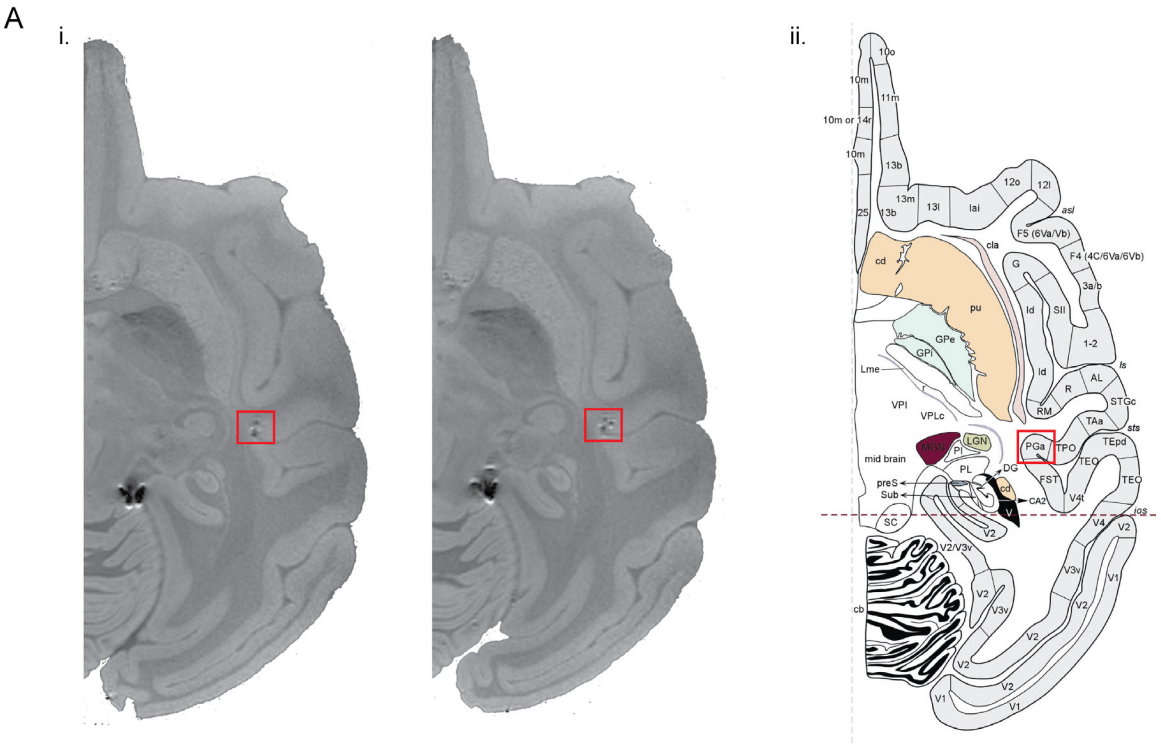

Location of the Tube Tetrodes as Judged from MRI Scan

The recording locations with TuTes were assessed postmortem with an ex vivo high resolution structural MRI scan. The anatomy was acquired using a 3D rapid acquisition

with relaxation enhancement (RARE) sequence (TR/TE = 500/13ms, RARE factor = 2, Field Of View: 90x64x70mm, Matrix: 360x256x280). Two closely spaced slices in the transverse plane are shown in (i). The location of the TuTe penetrations (bounded by a red square) as judged from the displayed slice (and compared with the (ii) anatomical atlas (Saleem and Logothetis, 2007)) were in the area PGa, a multimodal region of the temporal lobe, which has been reported to have cells that predominantly respond to visual stimuli (Baylis et al., 1987). Likewise, as is evident from the responses, we find visually modulated cells in the region (Figure 3).

Supplementary Figure 4:

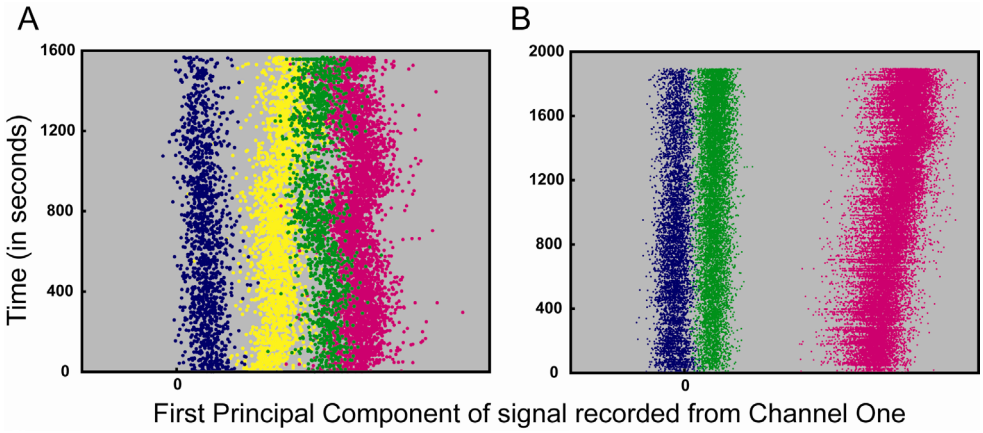

Stability of Recorded units across Time

The first principal component of the electrophysiological signal recorded from the first channel of a TuTe is plotted as a function of time in order to demonstrate the relatively good stability of single units during a single experimental session. (A) and (B) are two different experimental sessions and each single unit is represented by a different color. In

(B), a drift in the first principal component of the red cluster is observed. However due to the large amplitude of the spikes from this unit and the stability of the two other clusters (green and blue), unit isolation is not dramatically affected. Plotted in (A) are the same clusters as shown in Figure 2.

Supplementary References

Baylis GC, Rolls ET, Leonard CM. Functional subdivisions of the temporal lobe neocortex. J Neurosci, 1987; 7: 330-42.

Saleem KS, Logothetis N. A combined MRI and histology atlas of the rhesus monkey brain in stereotaxic coordinates. Academic: London ; Burlington, MA, 2007.